

6-1-1954

A Mathematical and Experimental Investigation of the Application of Air Spring to Shock Testing Machines

Eric E. Ungar

Follow this and additional works at: https://digitalrepository.unm.edu/me_etds



Part of the [Mechanical Engineering Commons](#)

Recommended Citation

Ungar, Eric E.. "A Mathematical and Experimental Investigation of the Application of Air Spring to Shock Testing Machines." (1954).
https://digitalrepository.unm.edu/me_etds/149

This Thesis is brought to you for free and open access by the Engineering ETDs at UNM Digital Repository. It has been accepted for inclusion in Mechanical Engineering ETDs by an authorized administrator of UNM Digital Repository. For more information, please contact disc@unm.edu.

UNIVERSITY OF NEW MEXICO-UNIVERSITY LIBRARIES



A14429 089684

UNGAR

INVESTIGATION
OF THE
APPLICATION
OF
AIR SPRINGS
TO SHOCK
TESTING
MACHINES

378.789

Un 3 Ou

1954

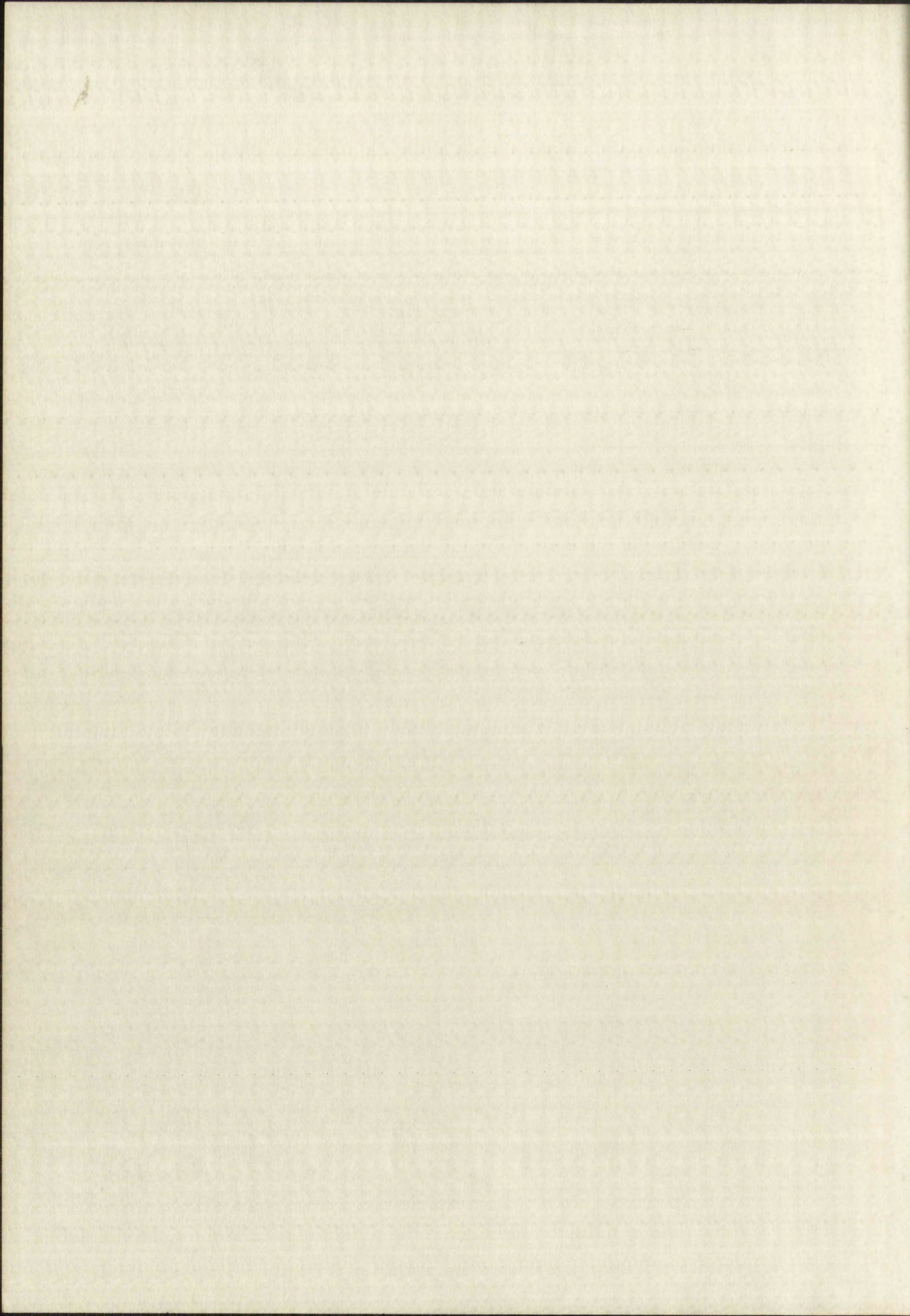
cop. 2

THE LIBRARY
UNIVERSITY OF NEW MEXICO



Call No.
378.789
Un3Ou
1954
cop.2

Accession
Number
196860



UNIVERSITY OF NEW MEXICO LIBRARY

MANUSCRIPT THESES

Unpublished theses submitted for the Master's and Doctor's degrees and deposited in the University of New Mexico Library are open for inspection, but are to be used only with due regard to the rights of the authors. Bibliographical references may be noted, but passages may be copied only with the permission of the authors, and proper credit must be given in subsequent written or published work. Extensive copying or publication of the thesis in whole or in part requires also the consent of the Dean of the Graduate School of the University of New Mexico.

This thesis by Eric E. Ungar.....
has been used by the following persons, whose signatures attest their acceptance of the above restrictions.

A Library which borrows this thesis for use by its patrons is expected to secure the signature of each user.

NAME AND ADDRESS

DATE

NAME (PRINT)

Unpublished theses submitted to the University of New Mexico are deposited in the University of New Mexico Library and are open for inspection by the public. The University of New Mexico Library reserves the right of the author to withdraw the thesis from the library at any time. The University of New Mexico Library reserves the right to make copies of the thesis for the purpose of making a permanent record of the thesis. The University of New Mexico Library reserves the right to make copies of the thesis for the purpose of making a permanent record of the thesis. The University of New Mexico Library reserves the right to make copies of the thesis for the purpose of making a permanent record of the thesis.

This thesis by _____ has been used by the University of New Mexico Library for the purpose of making a permanent record of the thesis.

A library which borrows this thesis for its own use is expected to return the thesis to the University of New Mexico Library.

DATE

NAME (PRINT)

A MATHEMATICAL AND EXPERIMENTAL
INVESTIGATION OF THE APPLICATION OF AIR
SPRINGS TO SHOCK TESTING MACHINES

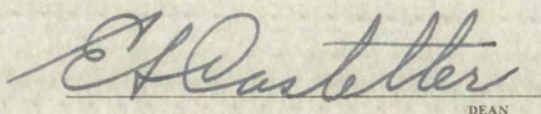
By
Eric E. Ungar

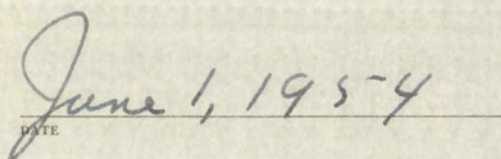
A Thesis
In partial fulfillment of the
Requirements for the Degree of
Master of Science in Mechanical Engineering

The University of New Mexico
1954

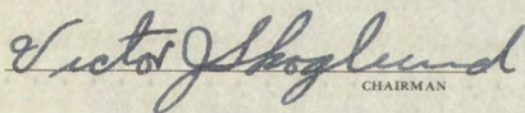
This thesis, directed and approved by the candidate's committee, has been accepted by the Graduate Committee of the University of New Mexico in partial fulfillment of the requirements for the degree of

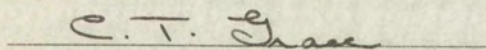
MASTER OF SCIENCE

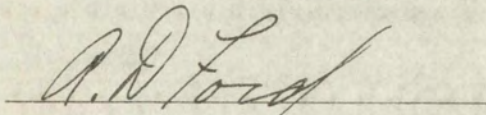

DEAN


DATE

Thesis committee


CHAIRMAN





378.789

Un30u

1954

cop. 2

TABLE OF CONTENTS

CHAPTER	PAGE
I. INTRODUCTION	1
ORIGIN OF INVESTIGATION	2
The Problem.	2
Transient acceleration test machines.	2
Superiority of the air spring.	5
PURPOSE OF THIS INVESTIGATION	6
ORGANIZATION OF INVESTIGATION	6
II. PRELIMINARY INVESTIGATIONS	8
REVIEW OF THE LITERATURE	8
Literature on air springs.	8
Literature on mathematical methods applicable to the solution of the differential equations of the air spring.	10
MATHEMATICAL METHODS	12
Analytical solution.	12
Analytical approximation methods.	13
Numerical solutions.	14
Graphical Solution Methods.	22
Evaluation and comparison of methods of solution.	27
III. THEORETICAL INVESTIGATION OF AN AIR SPRING	34
THE DIFFERENTIAL EQUATION OF THE AIR SPRING	34
Definitions of symbols and assumptions.	34
The restoring force	35

196860

I.	INTRODUCTION	1
1		1
2		2
3		3
4		4
5		5
6		6
7		7
8		8
9		9
10		10

II.	PRELIMINARY INVESTIGATION	11
11		11
12		12
13		13
14		14
15		15
16		16
17		17
18		18
19		19
20		20
21		21
22		22
23		23
24		24
25		25
26		26
27		27

III.	THEORETICAL INVESTIGATION	28
28		28
29		29
30		30
31		31
32		32

CHAPTER	PAGE
CHARACTERISTICS OF A FRICTIONLESS AIR SPRING	44
Some properties of a frictionless air spring.	45
Acceleration and acceleration build-up time of a frictionless air spring.	55
Utilization of characteristics of frictionless air springs in shock testing.	55
IV. INVESTIGATION OF AN EXPERIMENTAL AIR SPRING	63
APPARATUS	63
The air spring.	63
Instrumentation.	68
PROCEDURE	69
Calibration.	69
Preliminary adjustments and readings.	70
Measurement of friction.	70
Measurements of air spring action.	71
DATA REDUCTION	72
Friction.	72
Air Spring Action.	73
EXPERIMENTAL RESULTS	84
Friction.	84
Air spring action.	84
MATHEMATICAL TREATMENT OF THE EXPERIMENTAL AIR SPRING	93
EVALUATION OF RESULTS OBTAINED FOR EXPERIMENTAL AIR SPRING	97
Accuracies of experimental measurements.	97

44	CHARACTERISTICS OF A FRICTIONLESS AIR SPRING
45	Some properties of a frictionless air spring.
46	Accelerated and decelerated build-up time of a frictionless air spring.
47	Utilization of observations of frictionless air springs in shock testing.
48	IV. INVESTIGATION OF AN EXPERIMENTAL AIR SPRING
49	APPARATUS
50	The air spring.
51	Instrumentation.
52	PROCEDURE
53	Calibration.
54	Preliminary adjustments and readings.
55	Measurement of friction.
56	Measurements of air spring action.
57	DATA REDUCTION
58	Friction.
59	Air Spring Action.
60	EXPERIMENTAL RESULTS
61	Friction.
62	Air spring action.
63	MATHEMATICAL TREATMENT OF THE EXPERIMENTAL AIR SPRING
64	EVALUATION OF RESULTS OBTAINED FOR EXPERIMENTAL AIR SPRING
65	Assessment of experimental measurements.

	111
CHAPTER	PAGE
Reproducibility of experimental measurements.	106
Accuracies of calculations.	106
Comparison of experimental and calculated results.	107
Discussion of results.	109
V. CONCLUSIONS AND RECOMMENDATIONS	118
FEASIBILITY OF USING AIR SPRING AS TESTING MACHINE	118
PREDICTION OF AIR SPRING ACTION BY MATHEMATICAL ANALYSIS	119
IMPROVEMENTS IN APPARATUS	119
FURTHER DEVELOPMENTS	121
VI. ACKNOWLEDGEMENTS	123
BIBLIOGRAPHY	124
APPENDIX A - SAMPLE SOLUTION OF DIFFERENTIAL EQUATION FOR LINEAR SPRING BY NUMERICAL INTEGRATION	127
APPENDIX B - SAMPLE SOLUTION OF DIFFERENTIAL EQUATION FOR FRICTIONLESS AIR SPRING BY NUMERICAL INTEGRATION	136
APPENDIX C - SAMPLE APPLICATIONS OF JACOBSEN'S GRAPHICAL METHOD	145
SOLUTION OF THE DIFFERENTIAL EQUATION OF THE LINEAR SPRING	145
SOLUTION OF THE DIFFERENTIAL EQUATION OF THE FRICTIONLESS AIR SPRING	149
APPENDIX D - APPLICATION OF JACOBSEN'S GRAPHICAL METHOD TO THE EXPERIMENTAL AIR SPRING	155

PAGE	CHAPTER
106	Reproducibility of experimental measurements.
106	Assessment of deviations.
107	Comparison of experimental and calculated results.
109	Discussion of results.
110	V. CONCLUSIONS AND RECOMMENDATIONS
112	FEASIBILITY OF USING AIR SPRING AS TESTING MACHINE
113	PREDICTION OF AIR SPRING ACTION BY MATHEMATICAL ANALYSIS
113	IMPROVEMENTS IN APPARATUS
121	FURTHER DEVELOPMENTS
123	VI. ACKNOWLEDGMENTS
124	BIBLIOGRAPHY
127	APPENDIX A - SAMPLE SOLUTION OF DIFFERENTIAL EQUATION FOR LINEAR SPRING BY NUMERICAL INTEGRATION
133	APPENDIX B - SAMPLE SOLUTION OF DIFFERENTIAL EQUATION FOR FRIGIDNESS AIR SPRING BY NUMERICAL INTEGRATION
143	APPENDIX C - SAMPLE APPLICATION OF JACOBI'S GRAPHICAL METHOD
143	SOLUTION OF THE DIFFERENTIAL EQUATION OF THE LINEAR SPRING
143	SOLUTION OF THE DIFFERENTIAL EQUATION OF THE FRIGIDNESS AIR SPRING
153	APPENDIX D - APPLICATION OF JACOBI'S GRAPHICAL METHOD TO THE EXPERIMENTAL AIR SPRING

LIST OF GRAPHS

GRAPH NUMBER	TITLE	PAGE
1	\bar{V} -X Relation For Undamped Air Spring (Evaluation of Methods of Computation)	32
2	X- \bar{V} Relation, Undamped Air Spring (Comparison of Methods of Computation)	33
3	Variation of Restoring Force With Non- Dimensional Displacement	39
4	Variation of Restoring Force With Non- Dimensional Displacement (For Positive Displacement)	40
5	Variation of Restoring Force With Non- Dimensional Displacement (For Negative Displacement)	41
6	Variation of Energy Function, $q(X)$, with X	46
7	X- \bar{V} Curves, (Phase Trajectories), Undamped Air Spring	48
8	Some X- \bar{V} Relations For Undamped Air Spring	50
9	Some X- \bar{V} Relations For Undamped Air Spring	51
10	Relation Between Extreme Positive and Negative Values of Displacement of Undamped Air Spring	53
11	Variation of Period of Vibration of Undamped Air Spring with Initial Position, Starting from Rest	54
12	Variation of Maximum Non-Dimensional Acceleration with Initial Displacement (Undamped Air Spring)	56
13	Variation of Time Taken for Build-Up from Zero to Maximum Acceleration with Initial Position, Starting from Rest (Undamped Air Spring)	57
14	Relation of Build-Up Time and Maximum Acceleration in Non-Dimensional Variables (Undamped Air Spring)	59

LIST OF GRAPHS

GRAPH NUMBER	TITLE	PAGE
1	V-X Relation for Undamped Air Spring (Variation of Methods of Computation)	39
2	X-Y Relation, Undamped Air Spring (Variation of Methods of Computation)	33
3	Variation of Restoring Force With Non- Dimensional Displacement	32
4	Variation of Restoring Force With Non- Dimensional Displacement (For Positive Displacement)	40
5	Variation of Restoring Force With Non- Dimensional Displacement (For Negative Displacement)	41
6	Variation of Energy Function, $g(X)$, with X	40
7	X-V Curves, (Phase Trajectories), Undamped Air Spring	48
8	Same X-Y Relation for Undamped Air Spring	30
9	Same X-Y Relation for Undamped Air Spring	31
10	Relation Between Extreme Positive and Negative Values of Displacement of Undamped Air Spring	32
11	Variation of Period of Vibration of Undamped Air Spring with Initial Position, Starting from Rest	34
12	Variation of Maximum Non-Dimensional Acceleration with Initial Displacement (Undamped Air Spring)	35
13	Variation of Time Taken for Build-Up from Zero to Maximum Acceleration with Initial Position, Starting from Rest (Undamped Air Spring)	37
14	Relation of Build-Up Time and Maximum Acceleration in Non-Dimensional Variables (Undamped Air Spring)	38

GRAPH NUMBER	TITLE	PAGE
15	Sample Calculation of Variation of Friction with Velocity, from Oscillograph Record (16.5 lb. Piston)	74
16	Sample Reduction of Oscillograph Data, Air Spring Vibration	75
17	Variation of Friction with Velocity (Experimental Results)	85
18	Variation of Friction Coefficient with Zn/p Factor, For Full Bearings	86
19	Experimental Results, $\beta = 14.98$	87
20	Experimental Results, $\beta = 9.04$	88
21	Experimental Results, $\beta = 6.72$	89
22	Experimental Results, $\beta = 5.12$	90
23	Experimental Results, $\beta = 4.06$	91
24	Experimental Results, Summary of Mean Curves	92
25	Extrapolated Friction vs. Velocity Curve	98
26	Calculated Results, $\beta = 14.98$	99
27	Calculated Results, $\beta = 9.04$	100
28	Calculated Results, $\beta = 6.72$	101
29	Calculated Results, $\beta = 5.12$	102
30	Calculated Results, $\beta = 4.06$	103
31	Variation of Friction with Velocity Calculated from Air Spring Data	114
32	Graphic Solution - Linear Spring	147
33	Variation of δ with X for Undamped Air Spring ($X > 0$)	151
34	Variation of δ with X for Undamped Air Spring ($X < 0$)	152

12	Graphic of the variation of the air pressure at the station during the month of January 1911
13	Graphic of the variation of the air pressure at the station during the month of February 1911
14	Graphic of the variation of the air pressure at the station during the month of March 1911
15	Graphic of the variation of the air pressure at the station during the month of April 1911
16	Graphic of the variation of the air pressure at the station during the month of May 1911
17	Graphic of the variation of the air pressure at the station during the month of June 1911
18	Graphic of the variation of the air pressure at the station during the month of July 1911
19	Graphic of the variation of the air pressure at the station during the month of August 1911
20	Graphic of the variation of the air pressure at the station during the month of September 1911
21	Graphic of the variation of the air pressure at the station during the month of October 1911
22	Graphic of the variation of the air pressure at the station during the month of November 1911
23	Graphic of the variation of the air pressure at the station during the month of December 1911
24	Graphic of the variation of the air pressure at the station during the month of January 1912
25	Graphic of the variation of the air pressure at the station during the month of February 1912
26	Graphic of the variation of the air pressure at the station during the month of March 1912
27	Graphic of the variation of the air pressure at the station during the month of April 1912
28	Graphic of the variation of the air pressure at the station during the month of May 1912
29	Graphic of the variation of the air pressure at the station during the month of June 1912
30	Graphic of the variation of the air pressure at the station during the month of July 1912
31	Graphic of the variation of the air pressure at the station during the month of August 1912
32	Graphic of the variation of the air pressure at the station during the month of September 1912
33	Graphic of the variation of the air pressure at the station during the month of October 1912
34	Graphic of the variation of the air pressure at the station during the month of November 1912
35	Graphic of the variation of the air pressure at the station during the month of December 1912

GRAPH NUMBER	TITLE	PAGE
35	Graphical Solution, Undamped Air Spring	153
36	Graphical Solution, Experimental Air Spring	162

PAGE	TITLE	GRAPH NUMBER
185	Graphical Solution, Standard Air Working	35
186	Graphical Solution, Experimental Air Working	36

LIST OF FIGURES

FIGURE NUMBER	TITLE	PAGE
1	The Basic Construction of Jacobsen's Method	25
2	Geometry of Differentials in Jacobsen's Method	25
3	Schematic Sketch of Horizontal Air Spring	36
4	Schematic Sketch of Vertical Air Spring, Piston on Top	36
5	Experimental Air Spring	64
6	Overall View of Experimental Setup	65
7	Piston Assembly on Guide Rods	66

LIST OF FIGURES

FIGURE	TITLE	PAGE
1	The Basic Construction of Jacobson's Method	25
2	Geometry of Differential in Jacobson's Method	33
3	Schematic Sketch of Horizontal Air Spring	36
4	Schematic Sketch of Vertical Air Spring, Piston on Top	38
5	Experimental Air Spring	44
6	Overall View of Experimental Setup	55
7	Piston Assembly on Guide Rods	56

LIST OF TABLES

TABLE NUMBER	TITLE	PAGE
I	Properties of Shock Test Devices	4
II	Comparison of Exact Values and Values Found by Numerical Integration for Linear Spring	29
III	Data and Results for Test of Experimental Air Spring	76
IV	Calculation of Friction from Air Spring Data	115
V	X- τ Relation for Frictionless Air Spring (From Graphic Solution)	148
VI	Calculations for Jacobsen's Construction as Applied to Experimental Air Spring	163

LIST OF TABLES

TABLE NUMBER	TITLE	PAGE
I	Preparation of Shock Tube Devices	1
II	Comparison of Knudsen Values and Values Based on Numerical Integration for Blunt Bodies	22
III	Data and Results for Test of Experimental Air Spring	28
IV	Calculation of Position from Air Spring Data	113
V	X-7 Relation for Positionless Air Spring (Two Gasoline Springs)	148
VI	Calculation for Johnson's Construction as Applied to Experimental Air Spring	167

LIST OF SYMBOLS

A	Area of piston or cross-section of air column
B	$AP_0 + W$ for experimental air spring. See p. 32
C	A constant
E	Restoring Force
K	Stiffness of spring
L	Length of air column when piston is in equilibrium
P	Pressure within confined air column
P_0	Ambient pressure
T_0	Period of small oscillations of frictionless piston
V	$\frac{dX}{dY}$
V_0	Initial value of V
\bar{V}	$\frac{V}{P}$
W	Weight of piston
X	$\frac{x}{L}$
X_0	Initial value of X
X_m	Maximum value of X
X_n	Minimum value of X
a	Acceleration, $\frac{d^2 x}{dt^2}$
g	Acceleration of gravity
p	$\frac{2\pi}{T}$

LIST OF SYMBOLS

A	Area of piston or cross-section of air column
A_0	Area of piston or cross-section of air column for experimental air column
A	Amplitude
R	Restoring force
K	Stiffness of spring
L	Length of air column when piston is in equilibrium
P	Pressure within confined air column
P_0	Atmospheric pressure
T_0	Period of small oscillations of pistonless system
V	Volume of air column
V_0	Initial value of V
\bar{V}	Mean value of V
W	Weight of piston
X	Displacement of piston
X_0	Initial value of X
X_m	Maximum value of X
X_n	Minimum value of X
a	Acceleration, $\frac{d^2 X}{dt^2}$
g	Acceleration of gravity, $\frac{g}{g}$

q	Potential energy stored in air spring
r	Radial polar coordinate
s	Arc length
t	Time
t_B	Acceleration build-up time
v	Velocity, $\frac{dx}{dt}$
x	Displacement of piston from equilibrium position

α	A constant
β	B/W
γ	Ratio of specific heats of air
δ	X-coordinate of center of curvature of $X-\bar{V}$ curve
ϵ	A constant
θ	Angular polar coordinate
ϕ	Friction force function
ϕ_0	$-\frac{\phi}{B}$
τ	t/T_0
τ_B	t_B/T_0

ϕ	Potential energy stored in air spring
r	Radial polar coordinate
e	Arm length
t	Time
\ddot{x}	Acceleration (inches/sec ²)
v	Velocity, $\frac{dx}{dt}$
x	Displacement of piston from equilibrium position
α	A constant
β	β/α
γ	Ratio of specific heats of air
δ	X-coordinate of center of curvature of X-V curve
ϵ	A constant
θ	Angular polar coordinate
ϕ	Friction torque function
$\phi - \frac{\phi}{\epsilon}$	
τ	τ/α
τ	τ/α

CHAPTER I

INTRODUCTION

The applications of many modern devices require them to be able to perform their functions satisfactorily after having been subjected to transient accelerations of considerable magnitude. Some devices are required to operate even during the period of the acceleration.

Since failure of components or sub-assemblies during the actual operation of the entire assembly would in general be extremely undesirable and costly (for example, failure of instrumentation in a high-speed aircraft or guided missile might lead to loss of the entire vehicle), it is necessary to test the components and sub-assemblies in order to determine whether they may be expected to perform adequately during or after being exposed to accelerations equivalent to those to which they will be subjected when used in their intended application.

Currently available transient acceleration testing machines lack flexibility of adjustment and generally are expensive. A more flexible and economical device which could be used to study the behavior of machines subject to specified transient accelerations would be of immediate value.

INTRODUCTION

The application of many modern devices requires that

be able to perform their functions satisfactorily when

having been subjected to transient accelerations of considerable

magnitudes. Some devices are required to operate even during

the onset of the acceleration.

Since failure of components or sub-assemblies during

the actual operation of the entire assembly would in general

be extremely undesirable and costly (for example, failure

of instrumentation in a high-speed aircraft or guided missile

might lead to loss of the entire vehicle), it is necessary

to test the components and sub-assemblies in order to determine

also whether they may be expected to perform adequately

during or after being exposed to acceleration conditions to

those to which they will be subjected when used in their

intended applications.

Currently available transient acceleration testing

techniques lack flexibility of adjustment and generally are

expensive. A more flexible and economical device which would

be used to study the behavior of machines subject to specified

transient accelerations would be of immediate value.

I. ORIGIN OF INVESTIGATION

The Problem. In general the effect of a transient acceleration on a structure depends mainly on two quantities: the maximum acceleration and the acceleration build-up time. The latter is the time taken for the acceleration to increase from zero to its maximum value. Thus, a desirable transient acceleration test machine must have provisions for adjustment of these two primary variables and must be economical. The basic problem consists of finding a principle of operation upon which such a machine may be based.

Transient acceleration test machines. At present a number of different devices are employed for subjecting objects to be tested to specified transient accelerations. A summary of properties of these devices and an air spring appears in Table I; a brief description follows.

A vibration table is a machine for subjecting objects to sinusoidal vibration. Frequency and amplitude of this oscillation are usually independently adjustable, so that maximum acceleration and rise time may be controlled. Since a vibration table always subjects the test objects to many cycles of acceleration it may not be called strictly a transient acceleration test device. However, vibration tables have been employed for this type of test by approximating the

1. THEORY OF VIBRATION

The Problem. In general the effect of a sinusoidal acceleration on a structure depends mainly on two quantities: the maximum acceleration and the acceleration built-up time. The latter is the time taken for the acceleration to increase from zero to the maximum value. Thus, a desirable transient acceleration test machine must have provision for adjustment of these two primary variables and must be economical. The basic problem consists of finding a principle of operation that which such a machine may be based.

Transient acceleration test machines. At present a number of different devices are employed for subjecting objects to be tested to specified transient accelerations. A summary of properties of these devices and an attempt to compare in Table I, a brief description follows.

A vibration table is a machine for subjecting objects to sinusoidal vibration. Frequency and magnitude of this acceleration are usually independently adjustable, so that maximum acceleration and rise time may be controlled. Since a vibration table always subjects the test objects to many cycles of acceleration it may not be called strictly a transient acceleration test device. However, vibration tables have been employed for this type of test by superimposing the

specified transient acceleration by each cycle of the vibration table.

A centrifuge whirls the items to be tested about a fixed center, subjecting them to centrifugal acceleration. No adequate control of rise time is available at present.

An impact table or a drop tower makes use of a platform, called drop stage, on which the items to be tested are mounted. The drop stage is permitted to drop into a restraining device, the nature of which, together with the distance the stage drops, determine the maximum acceleration and rise time obtained.

A rocket sled or rocket car is a vehicle, usually confined to travel along a track, which is accelerated by rockets and decelerated by some retarding device. The rocket thrust and retarding device gives control over acceleration in two opposite directions, and some control over rise time.

A linear spring may be used as an acceleration testing machine of limited flexibility. Maximum acceleration and rise time may be controlled by adjustment of the active length of the spring, the initial displacement, the damping device, and the mass on which the spring acts. However, adjustment of active length and damping is usually mechanically complex

specified constant acceleration by each cycle of the vibration table.

A controller within the frame is provided which, under control, regulates the constant acceleration. No separate control of the time is available at present.

An input table or a drop tower may use a platform, called drop stage, on which the item to be tested is mounted. The drop stage is permitted to drop into a receiving device, the nature of which, together with the distance the stage drops, determines the maximum acceleration and rise time obtained.

A rocket sled or rocket car is a vehicle, usually confined to travel along a track, which is accelerated by rockets and decelerated by some retarding device. The rocket thrust and retarding device gives control over acceleration in two opposite directions, and some control over the time.

A linear spring may be used as an accelerator in testing machine of limited flexibility. External acceleration and rise time may be controlled by adjustment of the active length of the spring, the initial displacement, the driving device, and the mass on which the spring acts. However, adjustment of active length and driving is usually mechanically complex.

TABLE I

PROPERTIES OF SHOCK TEST DEVICES

DEVICE							
PROPERTY		VIBRATION TABLE	CENTRIFUGE	IMPACT TABLE DROP TOWER	ROCKET SLED OR CAR	LINEAR SPRING	AIR SPRING
Reproducibility of Maximum Acceleration		Good	Good	Limited	Limited	Good	Good
Range of Available Acceleration		Wide	Wide	Limited	Limited	Small	Fair
Reproducibility of Rise Times		Good	Poor	Fair	Limited	Good	Fair
Range of Available Rise Times		Wide	Not Controlled	Limited	Limited	Small	Wide
Adaptability to Uni- directional Loading		None	Good	Good	Good	None	Fair
Mechanical Complexity		High	Depends on Size & Controls	Not high	Not high	Low	Low
Cost of Device		High	Medium	Low	Medium	Low	Low
Cost of Operation		Low	Medium	Medium	High	Low	Low

TABLE I

RECORDS OF THE BUREAU OF REVENUE

DATE	NAME	RESIDENCE	OCCUPATION	REMARKS	REMARKS
1900	John Smith	123 Main St.	Farmer	Good	Good
1901	John Smith	123 Main St.	Farmer	Good	Good
1902	John Smith	123 Main St.	Farmer	Good	Good
1903	John Smith	123 Main St.	Farmer	Good	Good
1904	John Smith	123 Main St.	Farmer	Good	Good
1905	John Smith	123 Main St.	Farmer	Good	Good
1906	John Smith	123 Main St.	Farmer	Good	Good
1907	John Smith	123 Main St.	Farmer	Good	Good
1908	John Smith	123 Main St.	Farmer	Good	Good
1909	John Smith	123 Main St.	Farmer	Good	Good
1910	John Smith	123 Main St.	Farmer	Good	Good

and difficult, and independent adjustment of maximum acceleration and rise time is very difficult.

An air spring is a device which utilizes the resilience of a confined column of air. As conceived here, it consists essentially of a cylinder closed at one end with a piston inserted at the other. The objects to be tested are mounted on the piston. For testing, the length of the air column is adjusted to a calculated value, and the piston is withdrawn a predetermined amount and then released.

Superiority of the Air Spring. As apparent from Table I, an air spring seems to be a possible solution to the problem of obtaining an economical and flexible transient acceleration test machine. The air spring is not mechanically complex, hence could be constructed with relatively little expense. It requires no expenditure of fuel and needs no complicated control devices, so that operating costs are low. The air spring promises to make available a fairly extensive range of maximum accelerations and rise times, with reasonable reproducibility and accuracy. Unlike the linear spring or vibration table, the air spring permits subjecting an object to a much larger acceleration in one direction than in the opposite direction.

However, the air spring can not be made to give the precise results and repeatability of these results available

with a vibration table. Also, it is expected that an air spring will not be able to give accelerations as large as those that can be obtained with a drop tower. The main limitation of an air spring device probably will be the limitation imposed on the size and weight of a test object; these are less critical in nearly all of the other devices. Nevertheless, the air spring seems to hold a good deal of promise of success within its own domain.

II. PURPOSE OF THIS INVESTIGATION

The object of this investigation was to determine the feasibility of using an air spring in a testing machine in which both maximum acceleration and the acceleration build-up time can be adjusted, and to develop and validate experimentally a mathematical method for predicting the performance of a given air spring.

III. ORGANIZATION OF INVESTIGATION

The main portion of this thesis consists of three major parts. At first, a mathematical analysis of an ideal air spring is undertaken in order to determine the properties of this ideal spring and also to establish concepts and mathematical methods applicable to a real air spring. Secondly, the characteristics of a real air spring are

with a vibration table. Also, it is expected that an air spring will not be able to give accelerations as large as those that can be obtained with a steel spring. The main limitation of an air spring device probably will be the limitation imposed on the size and weight of a rear spring; these are less critical in nearly all of the other joints. Nevertheless, the air spring seems to hold a good deal of promise of success within its own domain.

II. PURPOSE OF THIS INVESTIGATION

The object of this investigation was to determine the feasibility of using an air spring in a springing machine in which both maximum acceleration and the acceleration limits can be adjusted, and to develop and evaluate experimentally a mathematical method for predicting the performance of a given air spring.

III. ORGANIZATION OF INVESTIGATION

The main portion of this thesis consists of three major parts. At first, a mathematical analysis of an ideal air spring is undertaken in order to determine the properties of this ideal spring and also to establish certain mathematical methods applicable to a real air spring. Secondly, the characteristics of a real air spring are

measured; and finally, the experimentally obtained results are compared with those obtained by mathematical methods.

In the treatment of the real air spring isentropic compression of the air is assumed. The effect of wall friction on the piston is considered, but all other dissipative effects, such as leakage, heat transfer, and pressure waves, are neglected. In the preliminary investigation of the ideal air spring, all dissipative effects, including wall friction, are neglected.

... and finally, the experimentally obtained results.

and compared with those obtained by calculation.

In the treatment of the real air-water interface

oscillation of the air is assumed. The effect of wall friction

on the piston is considered, but of other dissipative effects

such as friction, heat conduction, and viscosity, no account

is taken. In the preliminary investigation of the ideal air

surface, all dissipative effects, including wall friction,

are neglected.

CHAPTER II

PRELIMINARY INVESTIGATIONS

I. REVIEW OF THE LITERATURE

Although in recent years a good deal of work has been done on mathematical analysis of problems in non-linear vibrations, only a very small portion of this work was found to be directly applicable to the air spring. Reference to indexes of technical literature ¹ revealed only a few articles concerned with air springs.

Literature on air springs. B. Sussholz's article, "Forced and Free Motion of a Mass on an Air Spring", ² and the subsequently published discussions of this article ³ were most directly applicable to this thesis. In the above mentioned article the motion of a horizontal air spring is subjected to detailed analysis, and dimensionless variables

¹ Science Abstracts, Physics Section, and Engineering Index. Library search included literature from 1953 back until 1920.

² B. Sussholz, "Forced and Free Motion of a Mass on an Air Spring," Journal of Applied Mechanics, XI, No. 2, June, 1944, pp. A-101 to A-107.

³ Discussion of paper by B. Sussholz, "Forced and Free Motion of a Mass on an Air Spring", Journal of Applied Mechanics, XII, January, 1945, pp. A-175 to A-180.

CHAPTER II

PRELIMINARY REMARKS

1. REVIEW OF THE LITERATURE

Although in recent years a good deal of work has been done on mathematical analysis of vibrations, only a very small portion of this work can be directly applicable to the air transport industry. The literature of technical literature is covered only in a cursory manner with air transport.

2. LITERATURE ON AIR TRANSPORT

Forced and Free Motion of a Mass on an Elastic Support, V. and the subsequent published literature on this subject were more directly applicable to the transport industry. The literature mentioned above the motion of a pendulum, the motion of a mass on an elastic support, and the motion of a mass on a spring.

¹ Science Abstracts, Physics Section, and Engineering Index. Library search included literature from 1920 to 1930. Until 1930.

² E. B. Mathews, "Forced and Free Motion of a Mass on an Elastic Support," *Journal of Applied Physics*, Vol. 1, No. 2, June, 1930, pp. 1-10.

³ Discussion of paper by E. B. Mathews, "Forced and Free Motion of a Mass on an Elastic Support," *Journal of Applied Physics*, Vol. 1, No. 2, June, 1930, pp. 1-10.

for the air spring are developed. The application of air springs to measure transient pressures is discussed and graphical methods for solving non-linear differential equations are mentioned.

Other methods of solution are suggested in the discussion of the article, and, in reply to some of the discussions, B. Sussholz was able to show that if pressure waves are not neglected only a very small correction results.⁴

Various adaptations of air springs are at present being used or considered for use in automobile suspension systems. Tests of such a system embodying the essentials of an air spring indicate that low spring rates with attendant comfort to passengers may be realized.⁵ A form of air spring is actually being used in the newest General Motors Corporation buses⁶, but the air spring used there is only remotely related to the application proposed in this paper.

⁴ idem, p. A-178

⁵ R. W. Brown, "Air Springs - Tomorrow's Ride", Journal of the Society of Automotive Engineers, XXXVIII, No. 4, April, 1936, pp. 126-32.

⁶ "Compressed Air Cuts Bounce". Business Week, October 18, 1952, pp. 78.

For the air engine are developed. The conditions of the engine to measure transient pressure in the engine. The methods for solving non-linear differential equations are mentioned.

Other methods of solution are suggested in the discussion of the analysis, and, in order to know of the discussion, E. G. Gusev was able to show that the results are not neglected only a very small part of the results.

Various adaptations of air engine are presented. Being used or considered for use in aircraft engine systems. Tests of such a system involving the design of an air engine indicate that low engine rates of air engine control to passengers may be realized. A test of air engine is actually being used in the new design of aircraft engine. The air engine used here is actually related to the application proposed in this paper.

1. E. G. Gusev, "Air engine - design and construction," Journal of the Society of Automotive Engineers, Vol. 4, April, 1958, pp. 128-32.

2. "Generalized Air Engine," Engineering News-Record, October 18, 1952, pp. 78.

Literature on mathematical methods applicable to the solution of the differential equations of the air spring.

Analytical solutions of differential equations are discussed in any standard text on differential equations. Probably the most complete index to the types of equations for which solutions are known is found in Differentialgleichungen by E. Kamke.⁷

Analytical approximation methods are discussed in texts on non-linear vibrations, such as Theory of Oscillations by A. A. Andronow and G. E. Chaikin,⁸ Nonlinear Vibrations in Mechanical and Electrical Systems by J. J. Stoker,⁹ Introduction to Nonlinear Mechanics by N. Minorsky¹⁰, and

⁷ E. Kamke, Differentialgleichungen, Lösungs-methoden und Lösungen, Vol I Gewöhnliche Differentialgleichungen, 2nd Ed. (Leipzig: Becker & Erler Kom - Ges., 1943).

⁸ A. A. Andronow and G. E. Chaikin, Theory of Oscillations, English Translation edited by Solomon Lefschetz (Princeton, New Jersey: Princeton University Press, 1949) - Method of van der Pol, pp. 302-315, Method of Poincare, pp. 315-330.

⁹ J. J. Stoker, Nonlinear Vibrations in Mechanical and Electrical Systems (New York: Interscience Publishers, Inc., 1950).

¹⁰ N. Minorsky, Introduction to Non-linear Mechanics (Ann Arbor, Michigan: Edwards Brothers, Inc., 1947).

others listed in the bibliography. No analytical solution of the air spring equation was found in the literature. The analytical approximation methods were found to necessitate numerical integrations and were for the most part very tedious and good only for a small range of the independent variables.

Numerical methods of integration of the air spring equation seemed more feasible. Such methods are well known and may be found in standard texts on numerical analysis, such as that by Scarborough¹¹ or that by Levy and Baggott.¹²

Of the many graphical methods that have been developed, a number of which are mentioned in the bibliography, the simplest, most general, and most directly applicable is one by L. S. Jacobsen.¹³ This method is discussed in detail subsequently.

¹¹ F. B. Scarborough, Numerical Mathematical Analysis (Baltimore: The Johns Hopkins Press, 1930).

¹² H. Levy and E. A. Baggott, Numerical Solutions of Differential Equations, (New York: Dover Publications, Inc., 1950).

¹³ L. S. Jacobsen, On A General Method of Solving Second-Order Ordinary Differential Equations by Phase Plane Displacements. Paper No. 52 -- A-1. Presented at meeting of the American Society of Mechanical Engineers, November 30 - December 5, 1952.

others listed in the bibliography. No general conclusion
of the spin-orbit coupling in the nucleus. The
analytical approximation method was found to be suitable
numerical investigations and were in the first part very
regions and good only for a small range of the independent
variables.

Generalized method of separation of the spin-orbit
equation seemed very suitable. The results are well known
and may be found in standard texts on nuclear physics.
such as that by Bethe and Bacher. It is that of Bethe and Bacher.
Of the many general methods that have been developed,
a number of which are mentioned in the bibliography, the
simplest, most general, and most directly applicable to one
by L. S. Jacobsen. This method is discussed in detail
extensively.

11. L. S. Jacobsen, Generalized Separation Method
(Baltimore: The Johns Hopkins Press, 1957).

12. H. Levy and F. A. Harwood, Nuclear Physics
Differential Equations, New York: Dover Publications, Inc.,
1957.

13. L. S. Jacobsen, A Generalized Separation Method
Second-Order Partial Differential Equations, Ph.D. thesis,
University of Maryland, 1957. Also in: Proceedings of the
The American Society of Mathematical Physicists, December 30 -
December 31, 1957.

II. MATHEMATICAL METHODS

The differential equation applicable to the air spring is derived in Chapter III. It may be written as

$$(1) \quad \frac{d^2X}{d\gamma^2} + \frac{4\pi^2}{\gamma} \phi_0 \left(\frac{dX}{d\gamma} \right) + \frac{4\pi^2}{\gamma} \left[(1-X)^{-\gamma} - 1 \right] = 0$$

Since in the present section only the mathematics are of concern, the meaning of the symbols is not discussed here. It is sufficient to know that X is the dependent, and γ the independent variable, that ϕ_0 is a function of $\frac{dX}{d\gamma}$, and that γ is a constant.

Analytical Solution. No general analytical solution for equation (1) could be found. However, if $\phi_0 \equiv 0$, the substitution of $V = \frac{dX}{d\gamma}$, whence $\frac{d^2X}{d\gamma^2} = \frac{dV}{d\gamma} = \frac{dV}{dX} \frac{dX}{d\gamma} = V \frac{dV}{dX}$, changes equation (1) to

$$(2) \quad V \frac{dV}{dX} + \frac{4\pi^2}{\gamma} \left[(1-X)^{-\gamma} - 1 \right] = 0.$$

This new equation may be integrated once by separation of variables, with the result

$$(3) \quad \frac{1}{2} (V^2 - V_0^2) = \frac{4\pi^2}{\gamma} \left[X - X_0 + \frac{(1-X)^{1-\gamma} - (1-X_0)^{1-\gamma}}{1-\gamma} \right]$$

where X_0 and V_0 respectively denote the values of X and $\frac{dX}{d\tau}$ at $\tau=0$. Equation (3) may now be solved for $V = \frac{dX}{d\tau}$, yielding

$$(4) \quad \frac{dX}{d\tau} = \sqrt{\frac{8\pi^2}{\gamma} \left[X - X_0 + \frac{(1-X)^{1-\gamma} - (1-X_0)^{1-\gamma}}{1-\gamma} \right] + V_0^2},$$

an expression which may once more be integrated by separation of variables. However, no integral for the expression

$\left[X + \alpha (1-X)^{1-\epsilon} \right]^{-\frac{1}{\epsilon}} dX$, where α and ϵ denote constants, could be found. Hence, numerical methods must be used for integration of equation (4).

Although analytic performance of the second integration is not possible, the exact solution (3) was put to good use in evaluating the accuracy of the approximation methods to be considered.

Analytical Approximation Methods. Of the many methods of this type available in the literature nearly all apply only to non-linear equations of certain types.¹⁴ Equation (1), unfortunately does not fall directly into any of the categories considered. The methods which are sufficiently general so that they could be applied to equation (1), however, are complicated, mathematically

¹⁴ N. Minorsky, op. cit., pp. 135

where X_0 and V_0 respectively denote the values of X and

$\frac{dX}{dt}$ at $t=0$. Equation (3) may now be solved for $V = \frac{dX}{dt}$

yielding

$$(4) \quad \frac{dX}{dt} = \left[\frac{aX^2}{Y} \right] \left[X - X_0 + \frac{(1 - X_0^{1-\delta} - 1) - (1 - X^{1-\delta})}{1-\delta} \right] + V_0$$

an expression which may now be integrated by separation

of variables. However, no integral for the expression

$$\left[X - X_0 + \frac{(1 - X_0^{1-\delta} - 1) - (1 - X^{1-\delta})}{1-\delta} \right]^{-1} dX$$

can be found. Hence, numerical methods must be

used for integration of equation (4).

Although analytic determination of the second integration

is not possible, the error relation (3) was put to good use

in evaluating the accuracy of the approximation method so

as to be considered.

Analysis of the results of the many

methods of this type available in the literature nearly all

apply only to non-linear systems of certain types.

Equation (1), unfortunately does not fall directly into any

of the categories considered. The methods which are

analytically general so that they could be applied to

equation (1), however, are complicated, mathematically

intricate, apply only over a limited range of the variables, and require that successive functions can be integrated analytically.¹⁵ However, analytic integration of these functions for the air spring can not be performed, so that numerical integration becomes necessary.¹⁶ thus, analytical approximation methods have no advantage over a direct numerical integration of equation (1) in the first place.

Numerical Solutions.

Equation (1) lends itself to solution by numerical methods without much difficulty. While the general theory of calculation by finite differences is beyond the scope of the present discussion, it is of advantage here to discuss in some detail the method which may be employed in the solution of equation (1). Except for minor variations, this method is well established and accepted. Proof of its validity

¹⁵For instance, the "Perturbation Method", J. J. Stoker, op. cit., pp. 223-33; the "Method of Small Parameters" of Poincare, discussed by N. Minorsky, op. cit., pp. 135-ff; the Method of van der Pol, discussed by J. J. Stoker, op. cit., pp. 149-ff; and by N. Minorsky, op. cit., pp. 167-81; and the "Method of Equivalent Linearization" of Kryloff and Bogoliuboff, discussed by N. Minorsky, op. cit., pp. 183-246.

¹⁶ Author's closure, Discussion of "Forced and Free Motion of a Mass on an Air Spring." B. Sussholz, Journal of Applied Mechanics, XII, No. 3, (September, 1945) pp. A-179.

may be found in the book by Scarborough ¹⁷, but the following method was taken from the work of Levy and Baggott. ¹⁸

The method of numerical solution which is most recommended by the aforementioned texts consists of a primary and a secondary stage. The primary stage is rather tedious and only fairly accurate unless extremely laborious methods are employed. Hence the method of the primary stage is used only as long as necessary until the less tedious, more accurate, self-checking, method of the secondary stage can be applied.

Equation (1) may be written as

$$(5) \quad \frac{d^2X}{d\tau^2} = f(X, \tau, \frac{dX}{d\tau}).$$

By letting $V = \frac{dX}{d\tau}$, (5) may be transformed into the simultaneous equations

$$(6) \quad \begin{aligned} V &= \frac{dX}{d\tau} \\ \frac{dV}{d\tau} &= f(X, \tau, V). \end{aligned}$$

¹⁷ F. B. Scarborough, op. cit., pp. 117-70.

¹⁸ H. Levy and E. A. Baggott, op. cit., pp. 92-96, 141-181.

may be found in the book by H. A. Heston, Jr., and the following method was taken from the work of Levy and Heston, Jr.

The method of numerical solution which is most recommended by the aforementioned texts consists of a primary and a secondary stage. The primary stage is rather tedious and only fairly accurate unless extremely laborious methods are employed. Hence the method of the primary stage is used only as long as necessary until the two stages are accurate, self-correcting, method of the secondary stage can be applied.

Equation (1) may be written as

$$(2) \quad \frac{d^2 X}{dt^2} = f(X, T, \frac{dX}{dt})$$

By letting $V = \frac{dX}{dt}$, (2) may be transformed into the simultaneous equations

$$(3) \quad \frac{dV}{dt} = f(X, T, V)$$

$$\frac{dX}{dt} = V$$

17. F. H. Schott, Jr., op. cit., pp. 117-120.

18. H. Levy and H. A. Heston, Jr., op. cit., pp. 117-120.

From the initial conditions ($X=X_0$, $V=V_0$ at $\tau=\tau_0$) $f_0 = f(X_0, \tau_0, V_0)$ may be evaluated and the primary stage of the integration may be undertaken by the following method of Euler.¹⁹ For the sake of convenience, the convention of denoting the number of an approximation by a subscript outside parentheses is adopted. For example, $(f_1)_3$ means the third approximation to f_1 . A convenient small interval of τ , $\Delta\tau$, is chosen. The first approximation to the change in V corresponding to this $\Delta\tau$, $(\Delta V_1)_1$, is found by application of the second of equations (6):

$$(\Delta V_1)_1 = f_0 \Delta\tau$$

The first approximation to V_1 , the value of V at $\tau_1 = \tau_0 + \Delta\tau$, is determined from

$$(V_1)_1 = V_0 + (\Delta V_1)_1$$

From the first of equations (6), ΔX may also be approximated by

$$(\Delta X_1)_1 = V_0 \Delta\tau$$

and $(X_1)_1$ may be found from

$$(X_1)_1 = X_0 + (\Delta X_1)_1.$$

¹⁹ H. Levy and E. A. Baggott, op. cit., pp. 93-96.

from the initial condition $X = X_0$, $V = V_0$, $U = U_0$.
 $t_0 = 0$ (X_0, V_0, U_0) was determined and the initial
 stage of the investigation was carried out by the following
 method of Euler. For the sake of convenience, the com-
 putations of the numerical solution of the system of the
 equations outside the interval t_0 to t_1 were carried out.
 $(X_1)_1$ means the first approximation to X_1 . A convenient
 small interval of t , Δt , is chosen. The first
 approximation to the change in V corresponding to this Δt

$(\Delta V)_1$, is found by solution of the second of equations (6):

$$(\Delta V)_1 = V_0 \Delta t$$

The first approximation to V_1 , the value of V at $t_1 = t_0 + \Delta t$,
 is determined from

$$(V_1)_1 = V_0 + (\Delta V)_1$$

from the first of equations (6), ΔX may also be determined by

$$(\Delta X)_1 = V_0 \Delta t$$

and $(X_1)_1$ may be found from

$$(X_1)_1 = X_0 + (\Delta X)_1$$

The newly found first approximations to the values of X and V at τ_1 , may now be utilized in computing a first approximation to f_1 :

$$(f_1)_1 = f \left[(X_1)_1, \tau_1, (V_1)_1 \right]$$

Now, better approximations to X_1 , V_1 , and f_1 , may be obtained by application of the following formulas:

$$(\Delta V_1)_2 = \frac{1}{2} \left[f_0 + (f_1)_1 \right] \Delta \tau$$

$$(V_1)_2 = V_0 + (\Delta V_1)_2$$

$$(\Delta X_1)_2 = \frac{1}{2} \left[V_0 + (V_1)_2 \right] \Delta \tau$$

$$(X_1)_2 = X_0 + (\Delta X_1)_2$$

$$(f_1)_2 = f \left[(X_1)_2, \tau_2, (V_1)_2 \right]$$

These approximations may now be improved, and the process continued until no further change within the desired accuracy is obtained in the next round, by use of the following generalized formulas corresponding to the above:

$$(\Delta V_1)_{n+1} = \frac{1}{2} \left[f_0 + (f_1)_n \right] \Delta \tau$$

$$(V_1)_{n+1} = V_0 + (\Delta V_1)_{n+1}$$

$$(\Delta X_1)_{n+1} = \frac{1}{2} \left[V_0 + (V_1)_{n+1} \right] \Delta \tau$$

The newly found first approximations to the values of X and

V at T_1 may now be utilized in computing a third

approximation to T_1 :

$$\left[\begin{array}{c} (T_1)_2 \\ (X_1)_2 \\ (V_1)_2 \end{array} \right] = \left[\begin{array}{c} (T_1)_1 \\ (X_1)_1 \\ (V_1)_1 \end{array} \right]$$

Now, better approximations to T_1 , V_1 , and X_1 may be

obtained by application of the following formulas:

$$(T_1)_2 = (T_0)_1 + (T_1)_1 \Delta T$$

$$(V_1)_2 = (V_0)_1 + (V_1)_1 \Delta V$$

$$(X_1)_2 = (X_0)_1 + (X_1)_1 \Delta X$$

$$(T_1)_2 = (T_0)_1 + (T_1)_1 \Delta T$$

$$\left[\begin{array}{c} (T_1)_2 \\ (X_1)_2 \\ (V_1)_2 \end{array} \right] = \left[\begin{array}{c} (T_1)_1 \\ (X_1)_1 \\ (V_1)_1 \end{array} \right]$$

These approximations may now be improved, and the process

continued until no further change within the desired accuracy

is obtained in the next round, by use of the following

generalized formulas corresponding to the above:

$$(T_{n+1})_2 = (T_n)_1 + (T_{n+1})_1 \Delta T$$

$$(V_{n+1})_2 = (V_n)_1 + (V_{n+1})_1 \Delta V$$

$$(X_{n+1})_2 = (X_n)_1 + (X_{n+1})_1 \Delta X$$

$$(X_1)_{n+1} = X_0 + (\Delta X_1)_{n+1}$$

$$(f_1)_{n+1} = f \left[(X_1)_{n+1}, \tau_1, (V_1)_{n+1} \right]$$

After X and V have been found to the desired degree of accuracy, X_2 and V_2 may be found by a method similar to the above, and the process may be continued until X_4 and V_4 have been found. The procedure may be summarized by the equations

$$(7a) \quad (\Delta V_{m+1})_1 = f_m \Delta \tau$$

$$(7b) \quad (V_{m+1})_1 = V_m + (\Delta V_{m+1})_1$$

$$(7c) \quad (\Delta X_{m+1})_1 = V_m \Delta \tau$$

$$(7d) \quad (X_{m+1})_1 = X_m + (\Delta X_{m+1})_1$$

$$(7e) \quad (f_{m+1})_1 = f \left[(X_{m+1})_1, \tau_{m+1}, (V_{m+1})_1 \right]$$

and

$$(8a) \quad (\Delta V_{m+1})_{n+1} = \frac{1}{2} \left[f_m + (f_{m+1})_n \right] \Delta \tau$$

$$(8b) \quad (V_{m+1})_{n+1} = V_m + (\Delta V_{m+1})_{n+1}$$

$$(8c) \quad (\Delta X_{m+1})_{n+1} = \frac{1}{2} \left[V_m + (V_{m+1})_{n+1} \right] \Delta \tau$$

$$(8d) \quad (X_{m+1})_{n+1} = X_m + (\Delta X_{m+1})_{n+1}$$

$$X_{n+1} = X_n + \Delta X_n$$

$$Y_{n+1} = Y_n + \Delta Y_n$$

where X and Y have been found to the desired degree of accuracy. X_n and Y_n may be found by a method similar to the above, and the process may be continued until X and Y have been found. The process may be continued until the desired accuracy is reached.

$$(7a) \quad \Delta V_{n+1} = V_n \Delta T$$

$$(7b) \quad V_{n+1} = V_n + \Delta V_{n+1}$$

$$(7c) \quad \Delta X_{n+1} = V_n \Delta T$$

$$(7d) \quad X_{n+1} = X_n + \Delta X_{n+1}$$

$$(7e) \quad \Delta Y_{n+1} = V_n \Delta T$$

and

$$(8a) \quad \Delta V_{n+1} = V_n \Delta T$$

$$(8b) \quad V_{n+1} = V_n + \Delta V_{n+1}$$

$$(8c) \quad \Delta X_{n+1} = V_n \Delta T$$

$$(8d) \quad X_{n+1} = X_n + \Delta X_{n+1}$$

$$(8e) \quad (f_{m+1})_{n+1} = f \left[(x_{m+1})_{n+1}, \tau_{m+1}, (v_{m+1})_{n+1} \right]$$

$$\text{where} \quad \tau_{m+1} = \tau_m + \Delta\tau = \tau_0 + m\Delta\tau.$$

The values of x_m, v_m , where $m = 1, 2, 3, 4$, must be checked and corrected before the second stage of the integration can be started. This is done by means of the following steps;²⁰ the bar over a symbol denoting the corrected value of that quantity, and Δ having the meaning given by:

$$(9) \quad \Delta^p x_r = \Delta^{(p-1)} x_{r+1} - \Delta^{(p-1)} x_r, \quad p=1, 2, 3, \dots$$

$$\Delta^0 x_r = x_r$$

This means, for example, that $\Delta^3 f_6 = \Delta^2 f_7 - \Delta^2 f_6$, or

$$\Delta v_2 = v_3 - v_2.$$

Step 1. x_1 is corrected by

$$(10a) \quad \bar{x}_1 = x_0 + \Delta\tau \left[v_0 + \frac{1}{2} \Delta v_0 - \frac{1}{12} \Delta^2 v_0 + \frac{1}{24} \Delta^3 v_0 - \frac{1}{40} \Delta^4 v_0 \right],$$

$$\text{Error} \leq \frac{1}{720} \Delta^4 v_0 \Delta\tau.$$

²⁰ H. Levy and E. A. Baggott, op. cit., pp. 158.

$$(92) \quad \left[\frac{(x_{n+1})^{p-1}}{(x_n)^{p-1}} - 1 \right] \frac{1}{p-1} = \frac{1}{p-1} \left[\frac{(x_{n+1})^p}{(x_n)^p} - 1 \right] \frac{1}{p} + \dots$$

$$\text{where } \frac{1}{p-1} = \frac{1}{p} + \Delta \frac{1}{p-1} = \frac{1}{p} + \Delta \frac{1}{p-1}.$$

The values of x_n , y_n , where $n = 1, 2, 3, \dots$, must be checked and corrected before the second stage of the investigation can be started. This is done by means of the following steps:

the bar over a symbol denoting the corrected value of the quantity, and Δ having the meaning given by:

$$(93) \quad \Delta^p x_n = x_{n+p} - x_n, \quad p=1, 2, 3, \dots$$

$$\Delta^0 x_n = x_n$$

This means, for example, that $\Delta^2 x_n = \Delta^2 x_{n+1} - \Delta^2 x_n$, or

$$\Delta^2 x_n = x_{n+2} - 2x_{n+1} + x_n.$$

Step 1. x_1 is corrected by

$$(102) \quad \bar{x}_1 = x_0 + \Delta x_0 - \frac{1}{12} \Delta^2 x_0 + \frac{1}{24} \Delta^3 x_0 - \frac{1}{40} \Delta^4 x_0 + \dots$$

$$- \frac{1}{40} \Delta^4 x_0 + \dots$$

$$\text{Error} \leq \frac{1}{720} \Delta^5 x_0$$

Step 2. V_1 is corrected from the formula

$$(10b) \quad \bar{V}_1 = V_0 + \Delta T \left[f_0 + \frac{1}{2} \Delta f_0 - \frac{1}{12} \Delta^2 f_0 + \frac{1}{24} \Delta^3 f_0 - \frac{1}{40} \Delta^4 f_0 \right]$$

$$\text{Error} \leq \frac{1}{720} \Delta^4 f_0 \Delta T .$$

Step 3. The corrected value of f_1 is calculated from

$$(10c) \quad \bar{F}_1 = f(\bar{X}_1, T_1, \bar{V}_1)$$

Step 4. V_2 is corrected by the formula

$$(10d) \quad \bar{V}_2 = V_0 + \Delta T \left[2 \bar{F}_1 + \frac{1}{3} \Delta^2 f_0 \right]$$

$$\text{Error} \leq \frac{1}{90} \Delta^4 f_0 \Delta T .$$

Step 5. X_2 is now corrected from the formula

$$(10e) \quad \bar{X}_2 = X_0 + \Delta T \left[2 \bar{V}_1 + \frac{1}{3} \Delta^2 V_2 \right]$$

$$\text{Error} \leq \frac{1}{90} \Delta^4 V_0 \Delta T .$$

Step 6. Then \bar{F}_2 may be found

$$(10f) \quad \bar{F}_2 = f(\bar{X}_2, T_2, \bar{V}_2) .$$

Steps 4, 5, and 6 may now be repeated, with all subscripts raised by 1, in order to determine the corrected values of

Step 2. \bar{V}_1 is corrected from the formula

$$(10b) \quad \bar{V}_1 = V_0 + \Delta T \left[\bar{V}_0 + \frac{1}{2} \Delta T_0 - \frac{1}{12} \Delta^2 T_0 + \frac{1}{24} \Delta^3 T_0 \right]$$

$$- \frac{1}{48} \Delta^4 T_0 \left[\right]$$

$$\text{Error} \leq \frac{1}{720} \Delta^5 T_0 \Delta T$$

Step 3. The corrected value of \bar{V}_1 is calculated from

$$(10c) \quad \bar{V}_1 = \bar{V}_1 + \bar{V}_1 \Delta T_1$$

Step 4. \bar{V}_2 is corrected by the formula

$$(10d) \quad \bar{V}_2 = V_0 + \Delta T \left[2\bar{V}_1 + \frac{1}{2} \Delta^2 T_1 - \frac{1}{6} \Delta^3 T_1 \right]$$

$$\text{Error} \leq \frac{1}{360} \Delta^5 T_1 \Delta T$$

Step 5. \bar{V}_3 is now corrected from the formula

$$(10e) \quad \bar{V}_3 = V_0 + \Delta T \left[2\bar{V}_2 + \frac{1}{2} \Delta^2 T_2 - \frac{1}{6} \Delta^3 T_2 \right]$$

$$\text{Error} \leq \frac{1}{360} \Delta^5 T_2 \Delta T$$

Step 6. Then \bar{V}_3 may be found

$$(10f) \quad \bar{V}_3 = \bar{V}_3 + \bar{V}_3 \Delta T_2$$

Steps 4, 5, and 6 may now be repeated, with all subscripts raised by 1, in order to determine the corrected value of

X_3, V_3, f_3 . Then, corrected values of X_4, V_4, f_4 are found in a similar manner, but with all subscripts increased by 2.

After completion of the first stage, the second stage of the integration may be undertaken. This second stage consists of application of the following steps. For the first cycle of calculations the index n is taken as $n = 5$. For each subsequent cycle, n is increased by 1.

Step 1. $(V_n)_1$ is calculated by the equation

$$(11a) \quad (V_n)_1 = V_{n-2} + \left[2 f_{n-1} + \frac{1}{3} \Delta^2 f_{n-5} + \Delta^3 f_{n-4} \right] \Delta \tau,$$

$$\text{Error} \leq \frac{1}{90} \Delta^4 f_{n-2} \Delta \tau - \frac{31}{90} \Delta^5 f_{n-2} \Delta \tau$$

Step 2. $(X_n)_1$ is determined from

$$(11b) \quad (X_n)_1 = X_{n-2} + \left[2 V_{n-1} + \frac{1}{3} \Delta^2 V_{n-2} \right] \Delta \tau$$

$$\text{Error} \leq \frac{1}{90} \Delta^4 V_{n-2} \Delta \tau - \frac{31}{90} \Delta^5 V_{n-2} \Delta \tau$$

Step 3. $(f_n)_1$ is calculated by

$$(11c) \quad (f_n)_1 = f \left[(X_n)_1, \tau_n, (V_n)_1 \right]$$

Step 1. $(V_n)_I$ is calculated by the equation

After completion of the first stage, the second stage of the integration may be undertaken. This second stage consists of application of the following steps. For the first cycle of calculations the index n is taken as $n = 2$. For each subsequent cycle, n is increased by 1.

Step 1. $(V_n)_I$ is calculated by the equation

$$(11a) \quad (V_n)_I = V_{n-2} - \left[2V_{n-1} - \frac{1}{2} \Delta^2 V_{n-2} + \Delta^2 V_{n-1} \right] \Delta t$$

$$\text{Error} \leq \frac{1}{30} \Delta^4 V_{n-2} \Delta t - \frac{5}{90} \Delta^4 V_{n-1} \Delta t$$

Step 2. $(X_n)_I$ is determined from

$$(11b) \quad (X_n)_I = X_{n-2} + \left[2V_{n-1} + \frac{1}{2} \Delta^2 V_{n-2} \right] \Delta t$$

$$\text{Error} \leq \frac{1}{30} \Delta^4 V_{n-2} \Delta t - \frac{5}{90} \Delta^4 V_{n-1} \Delta t$$

Step 3. $(V_n)_I$ is calculated by

$$(11c) \quad (V_n)_I = V_{n-1} - \left[(X_n)_I - (X_{n-1})_I \right] \Delta t$$

Step 4. V_n is corrected by the formula

$$(11d) \quad (v_n)_2 = v_{n-2} + \left[2 f_{n-1} + \frac{1}{3} \Delta^2 f_{n-2} \right] \Delta \tau$$

Step 5. X_n is corrected from

$$(11e) \quad (x_n)_2 = (x_n)_1 + \frac{1}{3} \left[(v_n)_2 - (v_n)_1 \right] \Delta \tau$$

Step 6. The accuracy of the following relation is tested, as a check to insure the accuracy of the foregoing work:

$$(11f) \quad \Delta^2 x_{n-1} \approx (\Delta \tau)^2 \left[f_n + \frac{1}{2} \Delta^2 f_{n-1} \right]$$

In some cases, when increased accuracy is desired, additional steps may be inserted. However, this was found to be not necessary here.

The entire foregoing procedure appears difficult when expressed in general form, but is relatively simple in its actual use. Appendix A is an example of its application to the solution of the differential equation for an undamped linear spring. Appendix B is an illustration of its application to the solution of the air spring equation with $\phi_0 = 0$.

Graphical Solution Methods. A number of methods have been proposed for the solution of second order ordinary

Step 4. V_n is corrected by the formula

$$(11a) \quad (V_n)_S = (V_{n-1})_S + \frac{1}{2} \Delta^2 (V_{n-1})_S + \frac{1}{6} \Delta^3 (V_{n-1})_S$$

Step 5. V_n is corrected from

$$(11b) \quad (V_n)_S = (V_{n-1})_S + \frac{1}{2} \Delta^2 (V_{n-1})_S + \frac{1}{6} \Delta^3 (V_{n-1})_S$$

Step 6. The accuracy of the following relation is tested

as a check to insure the accuracy of the foregoing work:

$$(11c) \quad \Delta^2 (V_{n-1})_S = \Delta^2 (V_{n-1})_S + \frac{1}{2} \Delta^3 (V_{n-1})_S$$

In some cases, when increased accuracy is desired,

additional steps may be inserted. However, this was not

so as not necessarily done.

The entire foregoing procedure becomes extremely efficient

when expressed in general form, but is relatively simple in

its actual use. Appendix A is an example of the application

to the solution of the differential equation for an undamped

linear spring. Appendix B is an illustration of the application

to the solution of the air spring equation with $\phi = 0$.

Graphical Solution Methods. A number of methods

have been proposed for the solution of second order ordinary

differential equations by graphical means. Of these, the majority is applicable only to equations of a special type,²¹ and hence not to the air spring equation, because of its unusual form. Some of the graphical methods, on the other hand, may be employed in the solution of the above mentioned type of equation, regardless of the functions involved. Of the several graphical methods surveyed for purposes of this study,²² the method recently published by L. S. Jacobsen²³ combines relative simplicity, accuracy, and lack of restrictions as to use. This method is explained here in some detail, since Jacobsen's paper may not be readily available to the reader.

Jacobsen's method is based on writing the differential equations in the form

$$(12) \quad \frac{d^2x}{d\tau^2} + p^2 (x + \delta) = 0$$

where p is a constant and δ is a function of x , τ , and $\frac{dx}{d\tau}$.

²¹ For instance, Lienard's construction, as discussed by J. J. Stoker, op. cit., pp. 31-36.

²² V. G. Bruce, "A Graphical Method for Solving Vibration Problems of a Single Degree of Freedom", Bulletin of the Seismological Society of America, XII, April 1951, pp. 101-109, H. O. Fuchs, "Spiral Diagrams to Solve Vibration Problems", Product Engineering, VII, 1936, pp. 294-96.

²³ Loc. cit.

differentiation is essential in the study of the
 subject is essential only in the study of the
 and hence not to the air or the water of the
 human form. Some of the physical methods of the
 hand, may be applied in the solution of the above mentioned
 type of equation, particularly of the Laplace equation.
 the several physical methods surveyed for purposes of this
 study, the method recently published by L. E. Jackson
 contains relative simplicity, economy, and lack of re-
 sults as by now. This method is explained here in some
 detail, since Jackson's paper may not be readily available
 to the reader.

Jackson's method is based on writing the differential

equation in the form

$$(1) \quad \frac{d^2x}{dt^2} + p \frac{dx}{dt} + q(x + z) = 0$$

where p is a constant and z is a function of x , t , and $\frac{dx}{dt}$.

For instance, Jackson's equation, as
 discussed by J. E. Jackson, op. cit., pp. 31-32.

V. G. Ginzburg, "A Physical Method for Solving
 the Problem of a Particle in a Magnetic Field," *Journal of
 the International Academy of Sciences*, XII, April 1951, pp.
 101-102. R. D. Field, "Physical Methods for Solving Problems
 in Physics," *Physical Review*, VII, 1952, pp. 694-69.

23 loc. cit.

The "phase plane coordinates", X and \bar{V} , are defined as

$$(13) \quad X = x, \quad \bar{V} = \frac{1}{p} \frac{dx}{d\tau}.$$

with this definition of \bar{V} ,

$$\frac{d^2x}{d\tau^2} = p \frac{d\bar{V}}{d\tau} = p^2 \bar{V} \frac{d\bar{V}}{dX}$$

By substitution of the foregoing into (12),

$$(14) \quad \bar{V} \frac{d\bar{V}}{dX} + X + \delta = 0$$

This may be solved for $\frac{dX}{d\bar{V}}$, with the result

$$(15) \quad \frac{dX}{d\bar{V}} = - \frac{\bar{V}}{X + \delta}.$$

If the $X - \bar{V}$ plane is drawn as shown in Figure 1, with the X - axis vertical and the \bar{V} - axis horizontal, the geometric meaning of (15) can be readily interpreted. If a short circular arc is drawn through the point $P (X_0, \bar{V}_0)$, with the center of the circle at $Q (-\delta, 0)$, the slope of the radius PQ is $\frac{1}{\bar{V}_0} (X_0 + \delta)$. Hence, the slope of the circular arc at P is $-\frac{\bar{V}_0}{X_0 + \delta}$. Thus, the differential equation of the normal to PQ is identical to (15), and the particular $X - \bar{V}$ curve of the motion defined by (12) which passes through P is also normal to PQ . Since an approximation method

the plane plane parallel to X and Y is the following:

$$(13) \quad X = Y = Z = \frac{1}{2} \quad \text{with this condition of } Y$$

$$\frac{\partial^2}{\partial X^2} = \frac{\partial^2}{\partial Y^2} = \frac{\partial^2}{\partial Z^2} = 0$$

By substitution of the condition (13),

$$(14) \quad \frac{\partial^2}{\partial X^2} + \frac{\partial^2}{\partial Y^2} + \frac{\partial^2}{\partial Z^2} = 0$$

This may be solved for $\frac{\partial^2}{\partial X^2}$, with the result

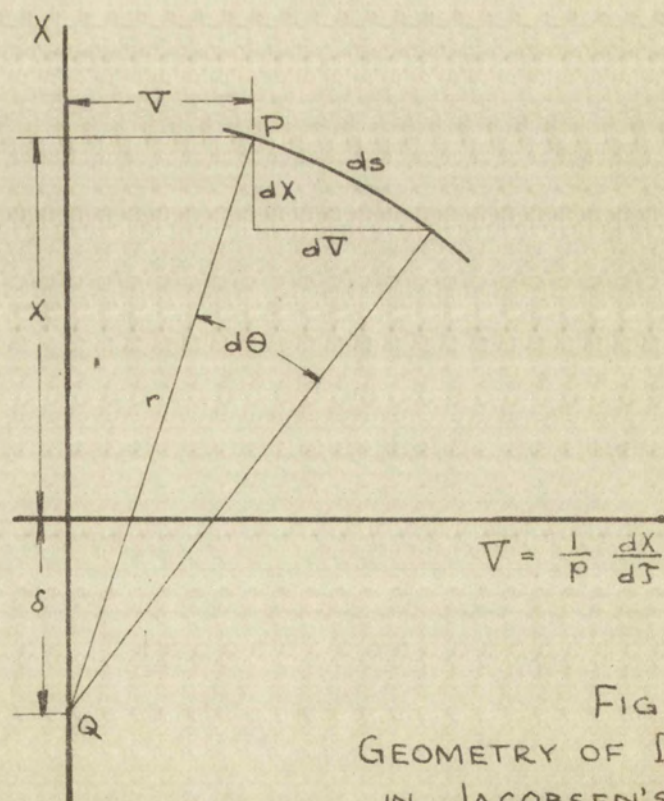
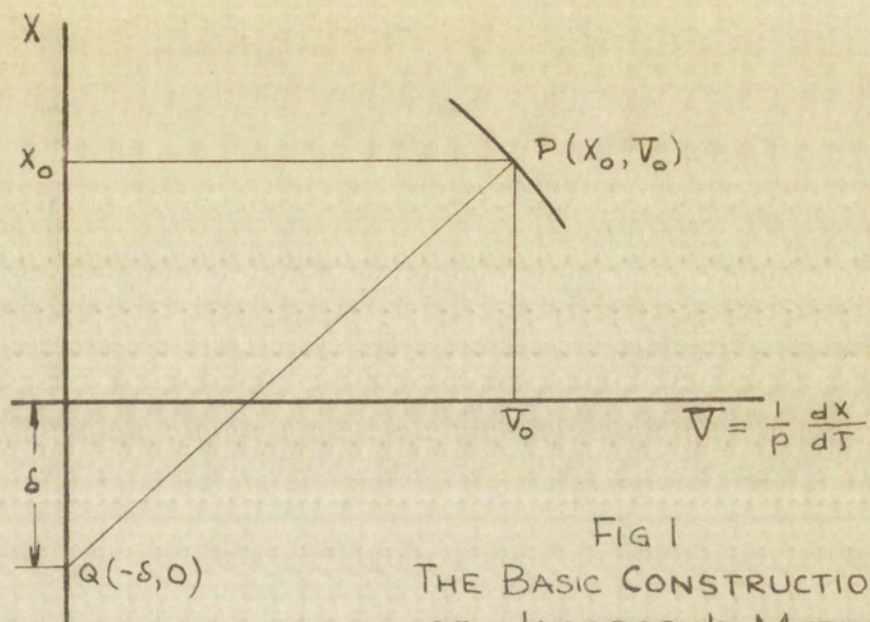
$$(15) \quad \frac{\partial^2}{\partial X^2} = - \frac{\partial^2}{\partial Y^2} - \frac{\partial^2}{\partial Z^2}$$

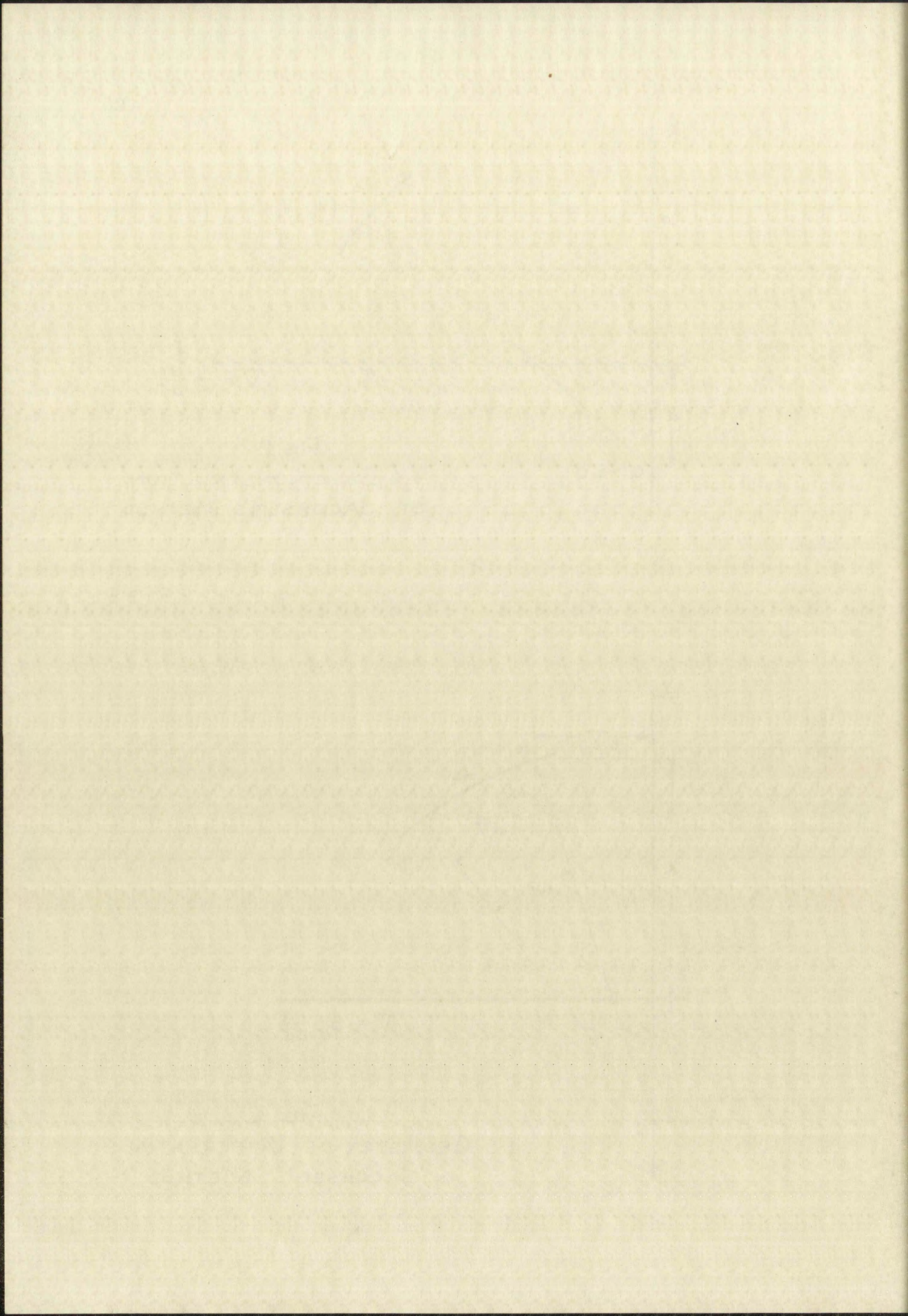
If the $X + Y$ plane is taken as shown in Figure 1, with the Z - axis vertical and the Y - axis horizontal, the coordinates of (15) can be readily interpreted. If a point

elsewhere are in known through the value Y, Z , the coordinates of the ellipse are $Z = 2, Y = 2$. The slope of the

ellipse is $\frac{1}{2}$ at $X = 2 + 2 = 4$. Hence, the slope of the ellipse at $X = 2$ is $\frac{1}{2}$. Thus, the elliptical equation

of the normal to the ellipse is $X = 2, Y = 2$ and the ellipse is $X = Y$ curve or the ellipse defined as that which passes through $X = Y$ is also normal to $X = Y$ since the ellipse is $X = Y$.





requires all parameters to be held constant for a finite step, δ must be held constant for a step of the integration. The approximation method hence consists of construction of a series of circular arcs, each with center at an appropriate point $Q(-\delta, 0)$.

A relation between X and τ may be obtained from the definition of \bar{V} given in equation (13), which may be transformed into

$$(16) \quad d\tau = \frac{1}{p} \frac{dX}{\bar{V}}.$$

For a differential element of a step of the integration, the following relations hold, and are apparent from the geometry shown in Figure 2, which also serves to explain the meaning of the symbols employed.

$$ds = r d\theta = \sqrt{(dX)^2 + (d\bar{V})^2}$$

$$r = \sqrt{\bar{V}^2 + (X + \delta)^2}$$

From these equations, it may be determined that

$$d\theta = \frac{ds}{r} = \frac{\sqrt{(dX)^2 + (d\bar{V})^2}}{\sqrt{\bar{V}^2 + (X + \delta)^2}} = \frac{dX}{\bar{V}} \sqrt{\frac{1 + \left(\frac{d\bar{V}}{dX}\right)^2}{1 + \left(\frac{X + \delta}{\bar{V}}\right)^2}}$$

the following relations are obtained for a fixed value of λ , μ and ν , α and β will be fixed, and the only variable is γ . The relations between γ and α and β are given by the following equations:

A relation between γ and α may be obtained from the definition of α given in equation (13), which may be written as

$$\alpha = \frac{1}{\gamma} \quad (14)$$

For a differential element of a step of the lattice, the following relations hold, and are constant from the geometry shown in Figure 2, which also serves to define the notation of the symbols employed.

$$\alpha = \frac{1}{\gamma} = \frac{1}{\sqrt{1 + \frac{1}{\gamma^2}}} = \frac{1}{\sqrt{1 + \frac{1}{\gamma^2}}}$$

From these equations, it may be determined that

$$\alpha = \frac{1}{\gamma} = \frac{1}{\sqrt{1 + \frac{1}{\gamma^2}}} = \frac{1}{\sqrt{1 + \frac{1}{\gamma^2}}}$$

But $\left(\frac{d\bar{v}}{dX}\right)^2 = \left(\frac{X + \delta}{\bar{v}}\right)^2$ from equation (14), so that the above may be reduced to

$$d\Theta = \frac{dX}{\bar{v}} .$$

When this result is substituted into (16), this becomes

$$d\tau = \frac{1}{p} d\Theta ,$$

which may be integrated with the result

$$(17) \quad \tau - \tau_0 = \frac{1}{p} (\Theta - \Theta_0), \text{ or}$$

$$\Delta\tau = \frac{1}{p} \Delta\Theta .$$

This last equation may be used readily for calculating values of τ corresponding to given values of X .

Appendix C illustrates the application of this graphic solution method to an undamped linear spring and the air spring with $\phi_0 = 0$.

Evaluation and comparison of methods of solution.

It was indicated that no analytic solution of equation (1) is known in the general case. Hence, it becomes necessary to resort to approximation methods. Of these, analytic approximation methods are not practical here because of

But $\left(\frac{dV}{dx}\right) = \left(\frac{3}{V}\right) \left(\frac{dx}{dx}\right)$ from equation (14), so that the

above may be reduced to

$$d\theta = \frac{dx}{V}$$

When this result is substituted into (15), this becomes

$$dT = \frac{1}{\theta} d\theta$$

which may be integrated with the result

$$T - T_0 = \frac{1}{\theta} (\theta - \theta_0) \quad (17)$$

$$\Delta T = \frac{1}{\theta} \Delta \theta$$

This last equation may be used readily for calculating values

of T corresponding to given values of θ .

Appendix A illustrates the application of this

graphic relation applied to an unheated linear spring and the

air spring with $\phi = 0$.

Estimation and comparison of results of analysis

It was indicated that no analytic solution of equation (1)

is known in the general case. Hence, if beyond necessary

to know to approximate methods. Of these, analytic

approximation methods are the most practical in the present of

integration difficulties, so that numerical or graphical methods were necessary for these integrations.

Table II gives a comparison between values found by numerical integration and an exact solution for an undamped linear spring. It is evident that the numerical solution is in this case sufficiently accurate for engineering. As pointed out in Appendix G, solution of this problem by the graphic method of Jacobsen yields values identical to those obtained from an exact solution. However, because of the extreme simplification that is obtained in the graphical solution method when it is applied to the linear spring equation, direct comparison of the numerical and graphical methods for solution of this particular differential equation is not significant.

In Graph 1 is plotted the V-X relation for a frictionless air spring. Values obtained from the exact solution are shown, and points calculated by the numerical (Appendix B) and graphical (Appendix G) methods are indicated. In the top half plane both the numerical and graphical methods are seen to give results very close to those obtained by the exact procedure. In the bottom half plane the numerical method is seen to deviate somewhat from the exact solution. This is due to an accumulation of errors that occurs in the numerical method. Since the integration in Graph 1 begins

indication of the fact that the numerical method is not

reliable for these large values.

Table II gives a comparison between various forms of

numerical integration and an exact solution for an unbounded

linear system. It is evident that the numerical solution

is in this case sufficiently accurate for engineering use.

Table III shows the results of the numerical method

applied to the method of Laplace which values are added to those

obtained from an exact solution. However, because of the

extreme simplification that is obtained in the numerical

solution method when it is applied to the linear system

equation, direct comparison of the numerical and graphical

methods for solution of this particular differential equation

is not significant.

In Table I is given the $Y-X$ relation for a system

less air spring. Values obtained from the exact solution

are shown, and values calculated by the numerical method (Appendix B)

and graphical (Appendix C) methods are indicated. In the

top half of the table both the numerical and graphical methods are

seen to give results very close to those obtained by the

exact procedure. In the bottom half of the table the numerical

method is seen to deviate somewhat from the exact solution.

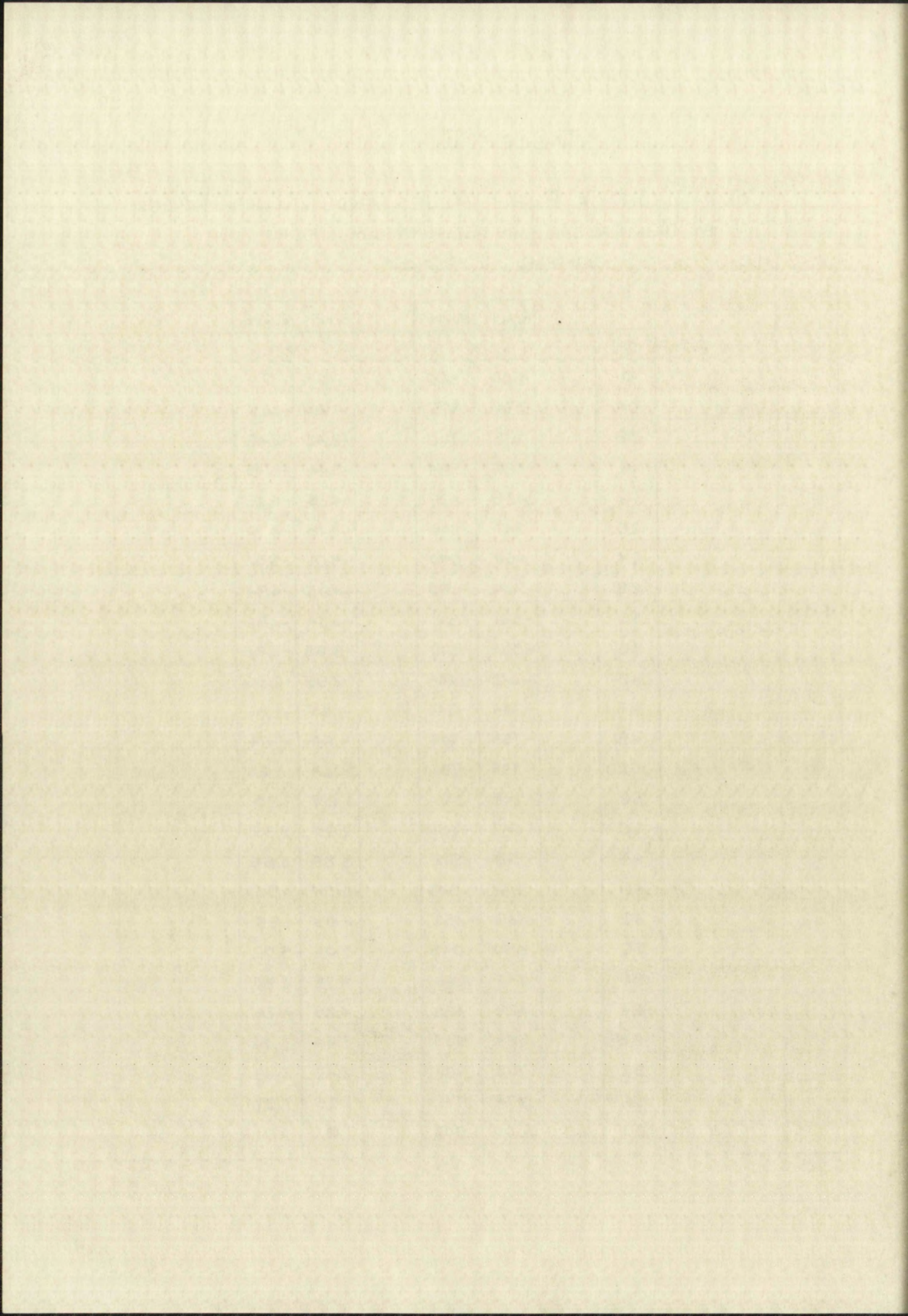
This is due to an accumulation of errors that become large

numerical method. Thus the integration is not a simple

TABLE II.

COMPARISON OF EXACT VALUES AND VALUES FOUND
BY NUMERICAL INTEGRATION FOR
LINEAR SPRING

	EXACT	NUMERIC	EXACT	NUMERIC
T	X		Y	
0	.800	.800	0	0
.04	.774	.775	-1.25	-1.25
.08	.702	.702	-2.42	-2.42
.12	.584	.584	-3.44	-3.45
.16	.428	.429	-4.25	-4.25
.20	.247	.248	-4.78	-4.79
.24	.050	.050	-5.01	-5.02
.28	-.149	-.150	-4.95	-4.94
.32	-.341	-.341	-4.54	-4.56
.36	-.510	-.510	-3.88	-3.88
.40	-.647	-.648	-2.95	-2.96
.44	-.744	-.744	-1.85	-1.86
.48	-.793	-.795	-.64	-.64
.52	-.793	-.796	.64	.63
.56	-.744	-.746	1.85	1.85
.60	-.647	-.650	2.95	2.95
.64	-.510	-.512	3.88	3.88
.68	-.341	-.343	4.54	4.55
.72	-.149	-.152	4.95	4.95
.76	.050	.048	5.01	5.02
.80	.247	.246	4.78	4.80
.84	.428	.428	4.25	4.26
.88	.584	.583	3.44	3.46
.92	.702	.702	2.42	2.43
.96	.774	.776	1.25	1.27
1.00	.800	.802	0	.01



on the negative X-axis and proceeds in a clockwise direction, the accumulation of errors is greatest in the bottom half plane near the negative X-axis. A similar discussion would apply also to the graphical solution method. However, only the points shown in the upper half plane of Graph 1 for the graphical method were actually found by that method; the points in the lower half plane were plotted by consideration of symmetry. Thus, only the upper half plane of Graph 1 can be used for comparison and evaluation of the two methods. For study of the air spring applied as a shock testing device the portion of the X-V plane for positive V is of greater importance, and for that half of Graph 1 neither the numerical nor the graphical method gives results that deviate much from the exact values.

A further comparison of the numerical and graphical solutions is given in Graph 2, which shows the X- γ relations obtained by these two methods corresponding to the X-V curves of Graph 1. Little difference between these two methods is evident in the portion for increasing X, but considerable disagreement in the portions of the curves where X decreases is apparent. Fortunately, only the portions for increasing X are of interest in the air spring analysis. The maximum error in X_m (the largest value of X) can be calculated by means of the error formulas given with equations (11). This

on the active X-axis and process in a clockwise direction. The accumulation of error is greatest in the lower half of the active X-axis. A similar distribution of error is also seen in the graphical solution method. However, the points shown in the lower half plane of Graph I for the graphical method were actually found by that method. The points in the lower half plane were plotted by graphical means. Thus, only the upper half plane of Graph I can be used for comparison and evaluation of the two methods. For study of the error, Graph I is used as a check against the position of the X-Y plane for positive Y is as greater importance, and for that half of Graph I neither the numerical nor the graphical method gives results that deviate too far from the exact values.

A further comparison of the numerical and graphical solutions is given in Graph II, which shows the X-Y coordinates obtained by these two methods corresponding to the X-Y curve of Graph I. Little difference between the two methods is evident in the position for intermediate X, but considerable displacement is the position of the curve where X is near its maximum. Fortunately, only the portion for intermediate X is of interest in the air motion analysis. The largest error in X (the largest value of X) can be obtained by means of the curve formula given with equation (17). This

error turns out to be extremely small (less than .005), so that for all practical purposes, the numerical solution may be regarded as exact.

The numerical method of integration discussed above is capable of good accuracy, but is tedious and requires much time. The previously discussed graphical method is much more rapid and less tedious. However, it shares a disadvantage common to all graphical methods: the error involved in use of this method can be known only empirically.

For purposes of the analysis of the air spring as presented in the next chapter, a great deal of accuracy is not required. The large number of calculations that are necessary make a rapid method very desirable. Hence, the graphic method of integration was used for calculations pertaining to the experimental air spring and is recommended for design purposes.

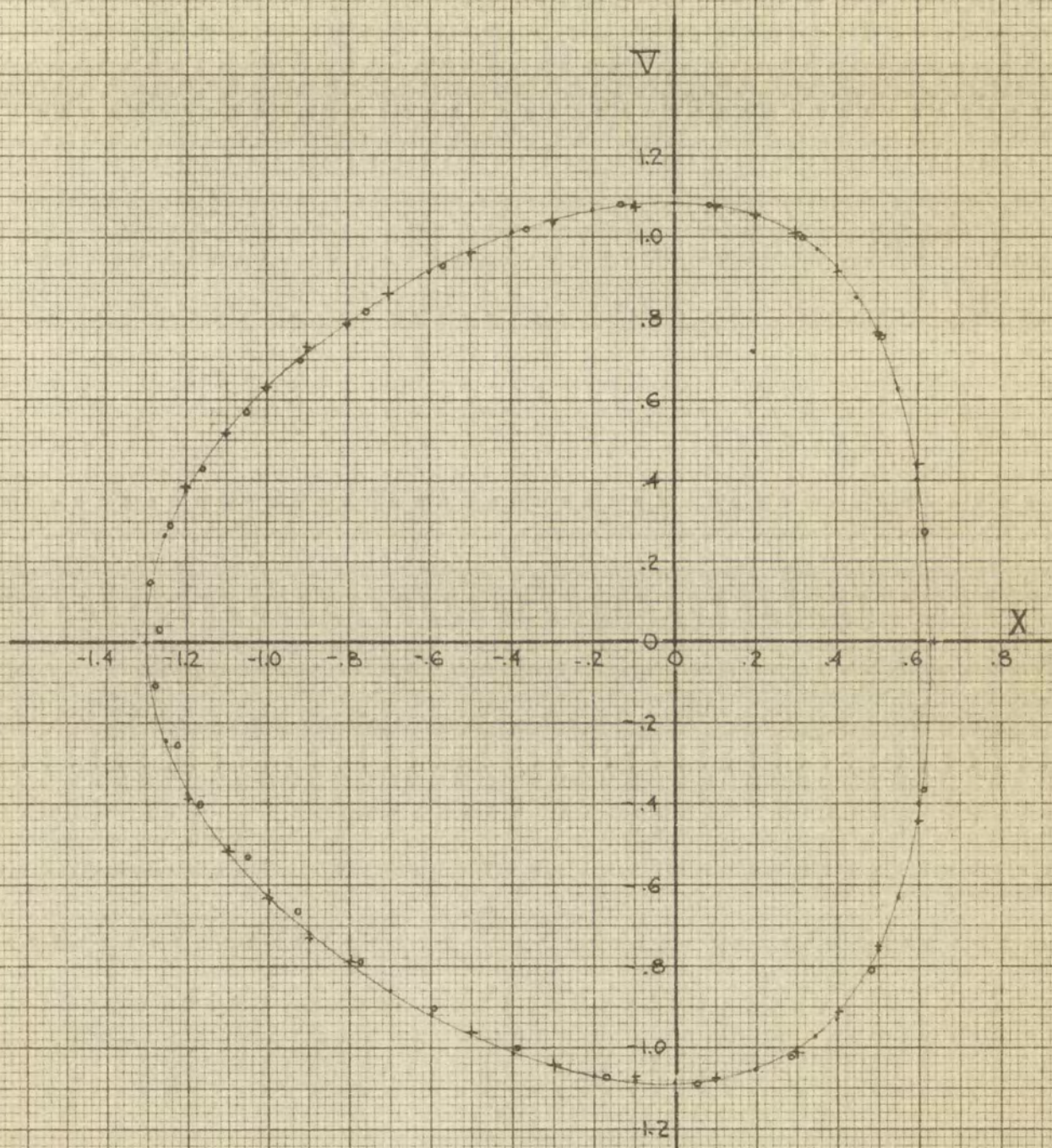
error curve out to be extremely small (less than .001) so that for all practical purposes, the numerical solution may be regarded as exact.

The numerical method of integration discussed above is capable of good accuracy, but is tedious and requires much time. The previously discussed graphic method is much more rapid and less tedious. However, it shares a disadvantage common to all graphical methods: the error involved in use of this method can be known only approximately.

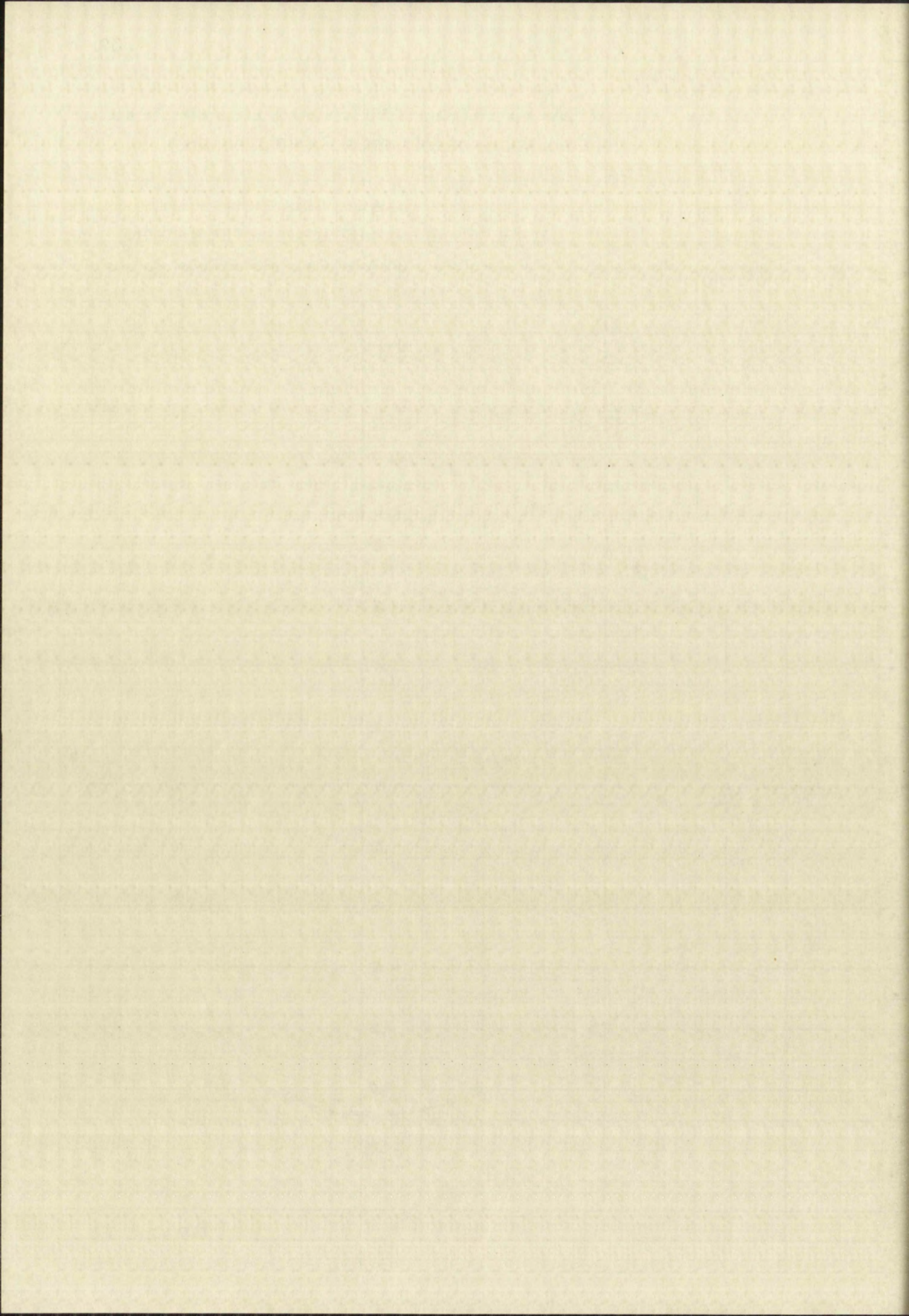
For purposes of the analysis of the air spring as presented in the next chapter, a great deal of accuracy is not required. The large number of calculations that are necessary make a rapid method very desirable. Hence, the graphic method of integration was used for calculations pertaining to the experimental air spring and its performance for design purposes.

$V-X$ RELATION FOR UNDAMPED AIR SPRING (EVALUATION OF METHODS OF COMPUTATION)

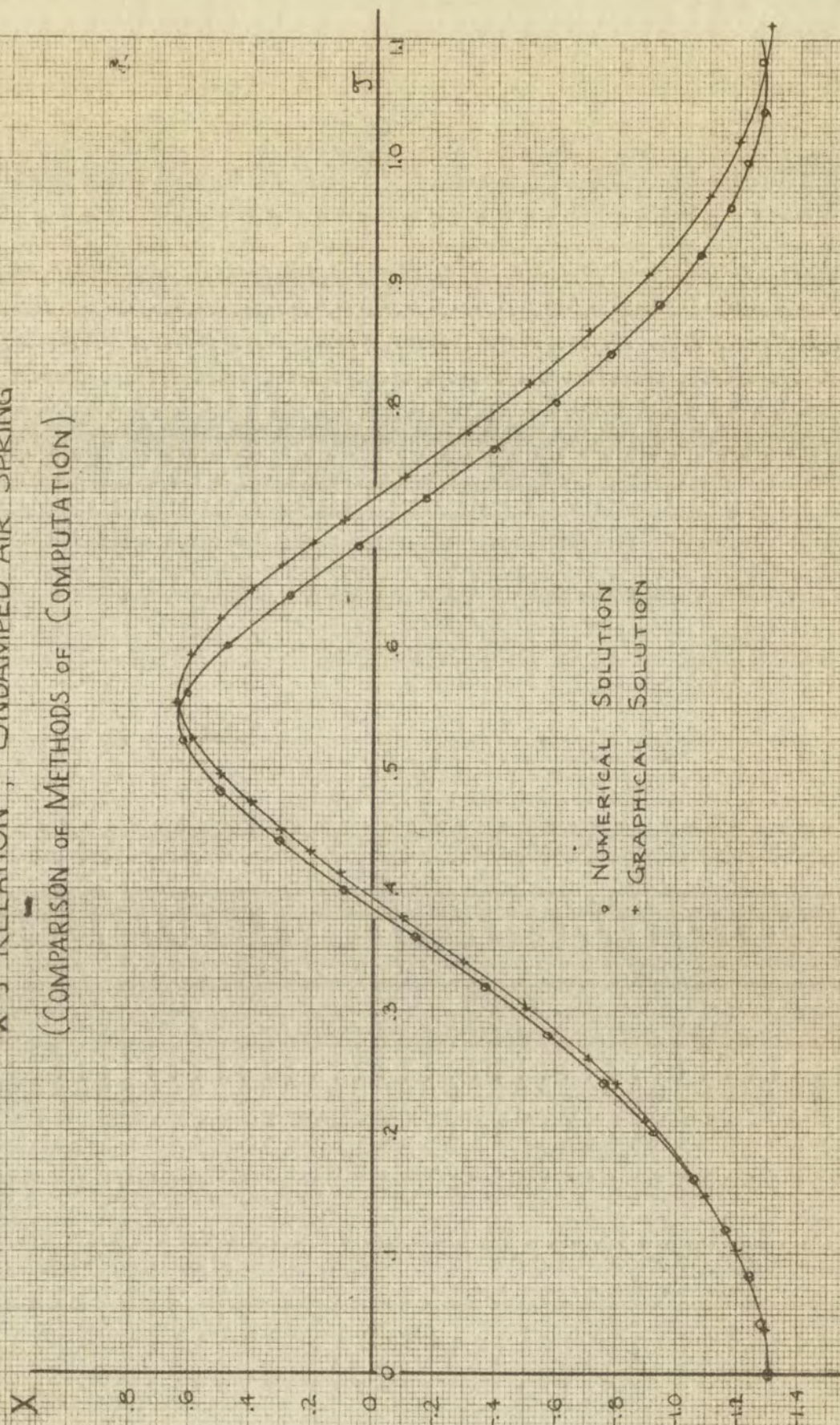
- EXACT SOLUTION
- NUMERICAL INTEGRATION
- + GRAPHICAL SOLUTION

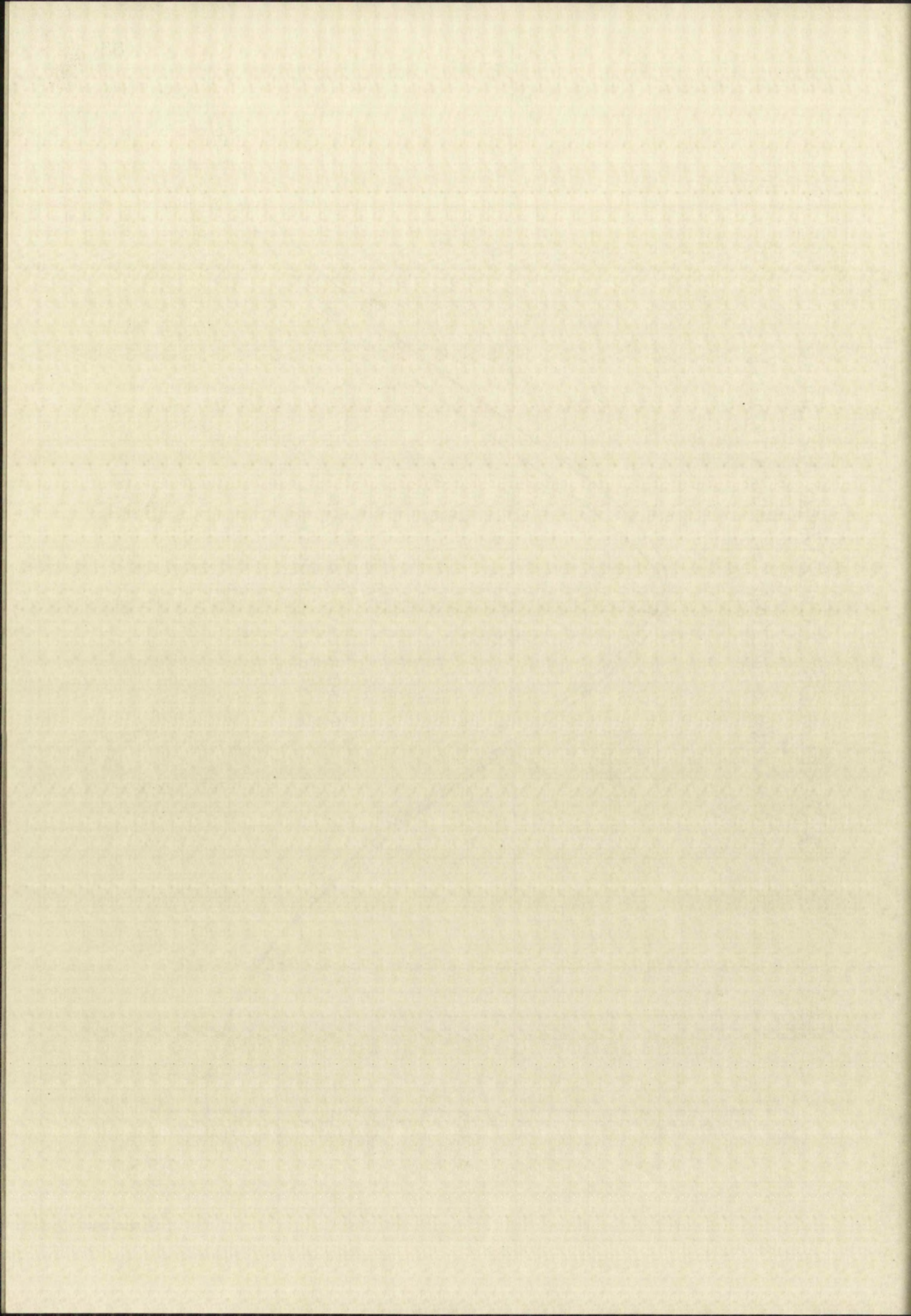


GRAPH I



$X-T$ RELATION, UNDAMPED AIR SPRING (COMPARISON OF METHODS OF COMPUTATION)





CHAPTER III

THEORETICAL INVESTIGATION OF AN AIR SPRING

In order to determine the feasibility of the use of an air spring in a device for shock testing in which both maximum acceleration and rise time can be adjusted, a theoretical analysis of the action of an air spring is desirable. Such a theoretical analysis is needed also in order to justify proceeding with testing of a real air spring, and in order to design the test apparatus.

I. THE DIFFERENTIAL EQUATION OF THE AIR SPRING

Definitions of symbols and assumptions. A schematic sketch of an air spring with axis horizontal is shown in Figure 3, and one with axis vertical is shown in Figure 4. As shown, the spring consists of a cylinder, closed at one end, and of a movable piston by which a column of air is confined in the cylinder.

The symbols used in the following discussion are as follows:

- P pressure within the confined air column
- P_0 ambient pressure
- L length of air column when the piston is in equilibrium under the action of the pressure forces and piston weight

- x displacement of piston from equilibrium, positive toward closed end of cylinder
 A cross sectional area of air column
 γ ratio of specific heats of air
 W weight of piston
 g acceleration of gravity

For purposes of the present analysis, the following assumptions are made:

1. At any instant, the pressure within the confined air column is uniform.
2. The thermodynamic process of the air within the air column is that of isentropic compression, $PV^\gamma = \text{constant}$, where V is the volume of the air column.
3. The pressure on the outside of the piston is constant.
4. Leakage, heat loss, and other dissipative effects, with the exception of friction between the piston and cylinder wall, are negligible.

The Restoring Force. For the horizontal air spring of Figure 3, application of the adiabatic compression law yields

$$P \left[A (L - x) \right]^\gamma = P_0 \left[AL \right]^\gamma$$

from which

$$(18) \quad P = P_0 \left[1 - \frac{x}{L} \right]^{-\gamma}$$

1. The first part of the paper is devoted to a general discussion of the problem.
2. The second part is devoted to a detailed analysis of the results of the experiments.
3. The third part is devoted to a discussion of the theoretical aspects of the problem.
4. The fourth part is devoted to a discussion of the practical aspects of the problem.
5. The fifth part is devoted to a discussion of the conclusions of the paper.

For purposes of comparison, the results of the experiments are compared with the results of the theoretical calculations. The results of the experiments are shown in Figure 1, and the results of the theoretical calculations are shown in Figure 2. The results of the experiments are in good agreement with the results of the theoretical calculations.

The results of the experiments are shown in Figure 1, and the results of the theoretical calculations are shown in Figure 2. The results of the experiments are in good agreement with the results of the theoretical calculations. The results of the experiments are shown in Figure 1, and the results of the theoretical calculations are shown in Figure 2.

The results of the experiments are shown in Figure 1, and the results of the theoretical calculations are shown in Figure 2. The results of the experiments are in good agreement with the results of the theoretical calculations. The results of the experiments are shown in Figure 1, and the results of the theoretical calculations are shown in Figure 2.

The results of the experiments are shown in Figure 1, and the results of the theoretical calculations are shown in Figure 2. The results of the experiments are in good agreement with the results of the theoretical calculations. The results of the experiments are shown in Figure 1, and the results of the theoretical calculations are shown in Figure 2.

The results of the experiments are shown in Figure 1, and the results of the theoretical calculations are shown in Figure 2. The results of the experiments are in good agreement with the results of the theoretical calculations. The results of the experiments are shown in Figure 1, and the results of the theoretical calculations are shown in Figure 2.

The results of the experiments are shown in Figure 1, and the results of the theoretical calculations are shown in Figure 2. The results of the experiments are in good agreement with the results of the theoretical calculations. The results of the experiments are shown in Figure 1, and the results of the theoretical calculations are shown in Figure 2.

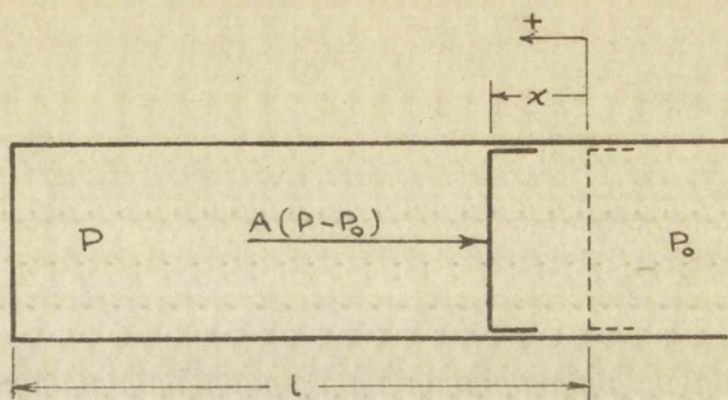


FIG 3
SCHEMATIC SKETCH OF HORIZONTAL
AIR SPRING

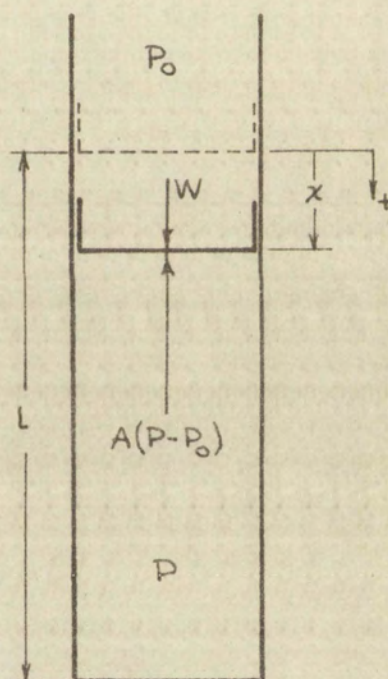
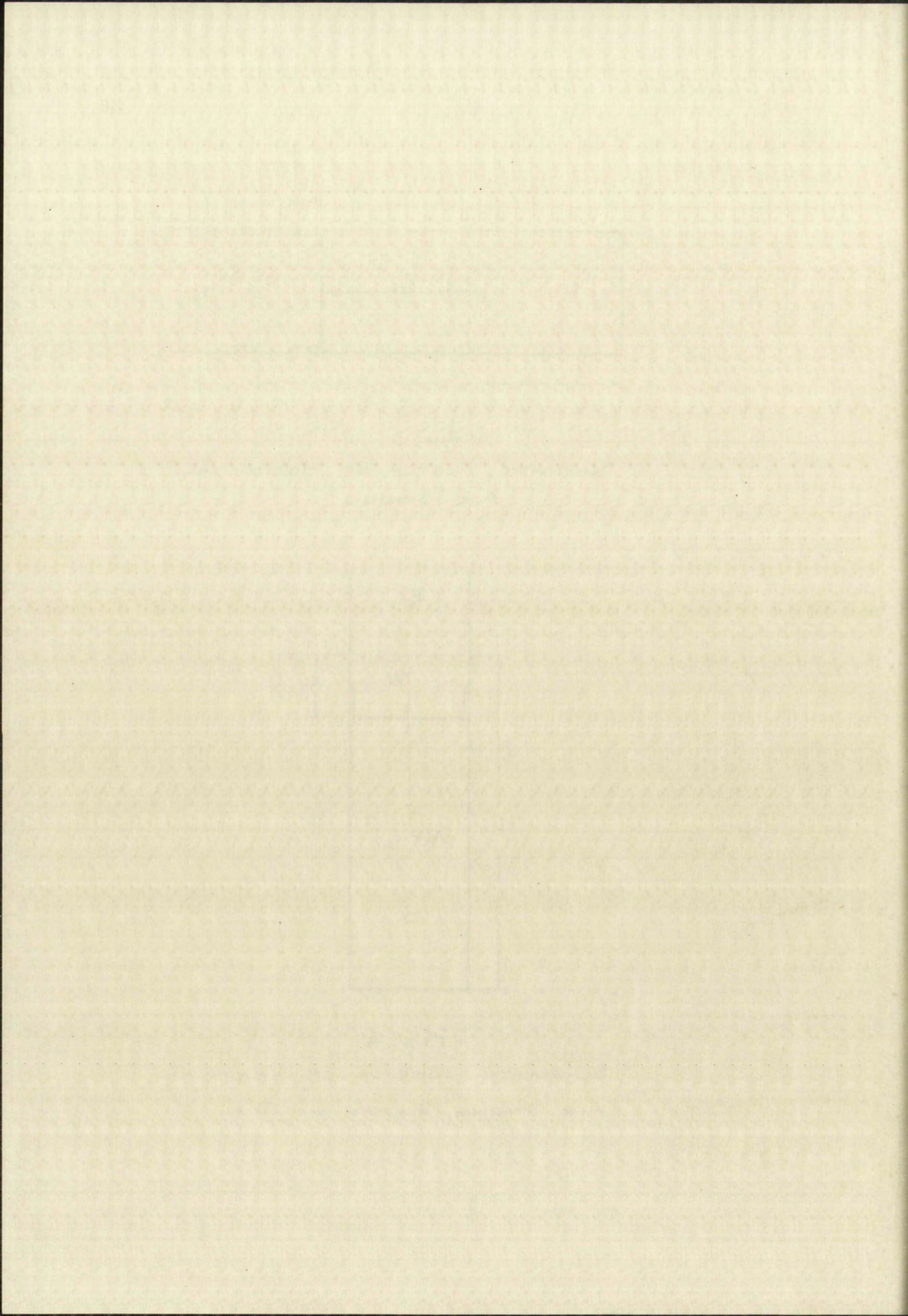


FIG 4
SCHEMATIC SKETCH OF VERTICAL
AIR SPRING, PISTON ON TOP.



The force exerted on the piston in the direction of positive x due to the difference between the external and the internal pressure is represented by $E_h(x)$ for the sake of convenience, so that

$$E_h(x) = A(P_o - P)$$

By substitution of (18) into this expression,

$$(19) \quad E_h(x) = AP_o \left[1 - \left(1 - \frac{x}{L} \right)^{-\gamma} \right].$$

For the vertical air spring of Figure 4, application of the aforementioned law of adiabatic compression gives the result

$$P \left[A(L - x) \right]^{\gamma} = \left(P_o + \frac{W}{A} \right) \left[AL \right]^{\gamma}$$

This may be transformed to

$$(20) \quad P = \left(P_o + \frac{W}{A} \right) \left(1 - \frac{x}{L} \right)^{-\gamma}$$

Here $E_v(x)$ is defined as

$$E_v(x) = A(P_o - P) + W$$

so that $E_v(x)$ accounts for both the action of the differential pressure forces and the weight. By substitution of (20) into the above,

The forces exerted in the direction of the axis of symmetry are due to the difference between the pressure and the tension. The pressure is represented by p and the tension by T .

$$F_A(x) = \int_0^x A(\xi) d\xi$$

By definition of $F_A(x)$ we have

$$F_A(x) = A(x) \cdot x \quad (18)$$

For the vertical force balance of the element we have

$$p \left[A(x) - A(x+dx) \right] + \left[F_A(x) - F_A(x+dx) \right] = 0$$

This may be rearranged as

$$p = \left(\frac{F_A}{A} + \frac{1}{2} \frac{dF_A}{dx} \right) \quad (19)$$

Now $F_A(x)$ is defined as

$$F_A(x) = A(x) \cdot x + \dots$$

so that $F_A(x)$ represents the force exerted by the pressure forces and the tension forces. Hence the above

$$(21) \quad E_v(x) = (AP_0 + W) \left[1 - \left(1 - \frac{x}{L} \right)^{-\gamma} \right] .$$

For an air spring similar to that of Figure 4, but with the piston on bottom instead, i.e. for an air spring upside-down from that in Figure 4, a procedure similar to that used above yields the following expression for $E_u(x)$

$$(22) \quad E_u(x) = (AP_0 - W) \left[1 - \left(1 - \frac{x}{L} \right)^{-\gamma} \right] .$$

To simplify the notation, define B as

$$\begin{aligned} B &= AP_0 && \text{for the horizontal air spring,} \\ B &= AP_0 + W && \text{for the vertical air spring, piston} \\ &&& \text{on top,} \\ B &= AP_0 - W && \text{for the vertical air spring, piston} \\ &&& \text{on bottom.} \end{aligned}$$

Then equations (19), (21) and (22) may be written as the single equation

$$(23) \quad E(x) = B \left[1 - \left(1 - \frac{x}{L} \right)^{-\gamma} \right] .$$

Note that $E(x)$ can be properly called a restoring force. Its algebraic sign is always opposite to that of x (since L and B are only positive by definition and since

$$(21) \quad \mathbf{y}(x) = \begin{bmatrix} y_1(x) \\ y_2(x) \end{bmatrix} = \begin{bmatrix} 1 \\ 0 \end{bmatrix} e^{x/2}$$

For an arbitrary vector \mathbf{y} , the system of equations $\mathbf{y}' = \mathbf{A}\mathbf{y}$ can be written in the form $\mathbf{y}' = \mathbf{A}\mathbf{y}$ where \mathbf{A} is a constant matrix. The system of equations $\mathbf{y}' = \mathbf{A}\mathbf{y}$ can be written in the form $\mathbf{y}' = \mathbf{A}\mathbf{y}$ where \mathbf{A} is a constant matrix.

$$(22) \quad \mathbf{y}(x) = \begin{bmatrix} y_1(x) \\ y_2(x) \end{bmatrix} = \begin{bmatrix} 1 \\ 0 \end{bmatrix} e^{x/2}$$

To simplify the notation, let $\mathbf{y} = \begin{bmatrix} y_1 \\ y_2 \end{bmatrix}$ and $\mathbf{A} = \begin{bmatrix} a_{11} & a_{12} \\ a_{21} & a_{22} \end{bmatrix}$. Then the system of equations $\mathbf{y}' = \mathbf{A}\mathbf{y}$ can be written in the form $\mathbf{y}' = \mathbf{A}\mathbf{y}$ where \mathbf{A} is a constant matrix.

Then the system of equations $\mathbf{y}' = \mathbf{A}\mathbf{y}$ can be written in the form $\mathbf{y}' = \mathbf{A}\mathbf{y}$ where \mathbf{A} is a constant matrix.

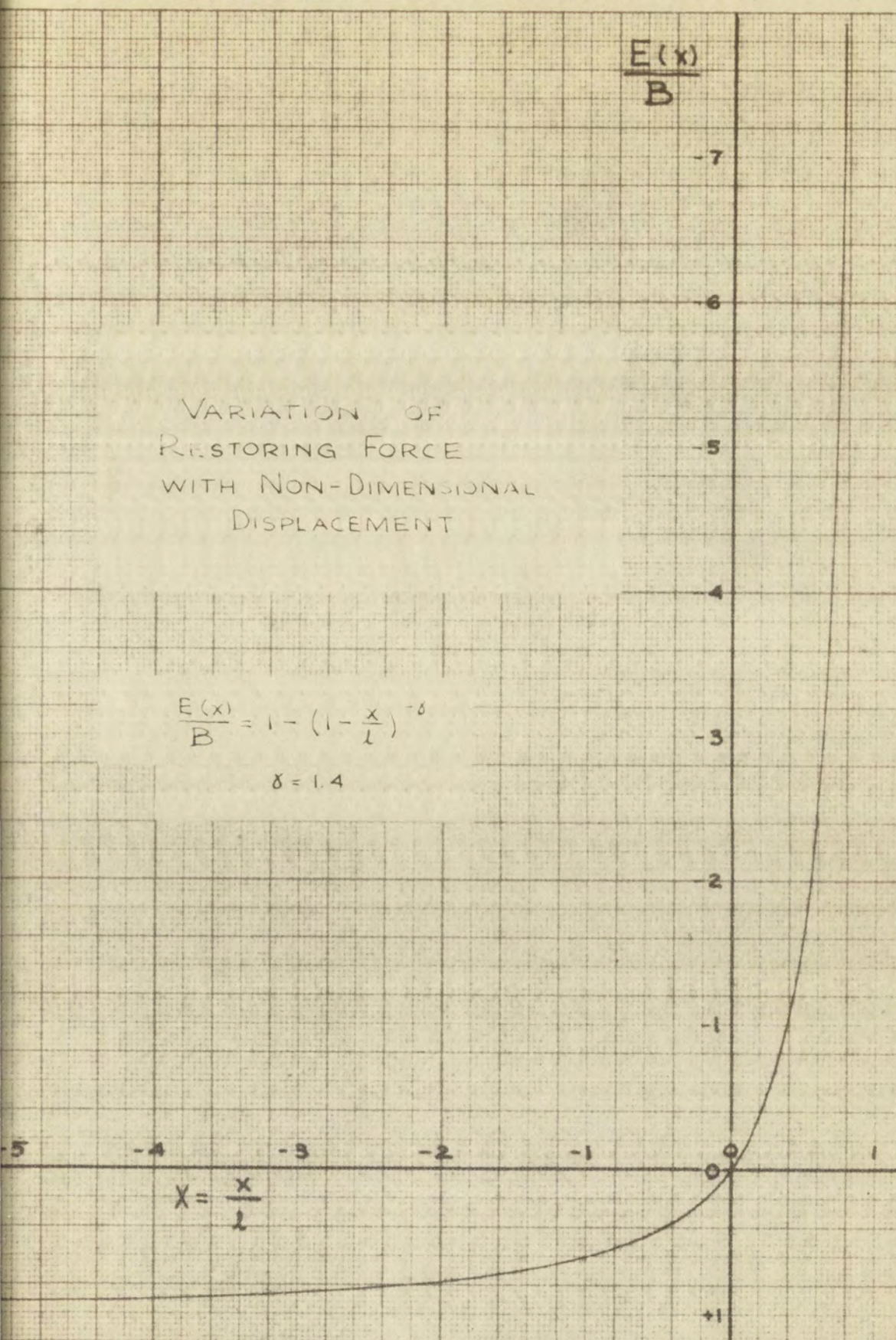
$$(23) \quad \mathbf{y}(x) = \begin{bmatrix} y_1(x) \\ y_2(x) \end{bmatrix} = \begin{bmatrix} 1 \\ 0 \end{bmatrix} e^{x/2}$$

Note that $\mathbf{y}(x)$ can be written in the form $\mathbf{y}(x) = \begin{bmatrix} 1 \\ 0 \end{bmatrix} e^{x/2}$ where $\mathbf{y}(x)$ is a vector and \mathbf{A} is a constant matrix.

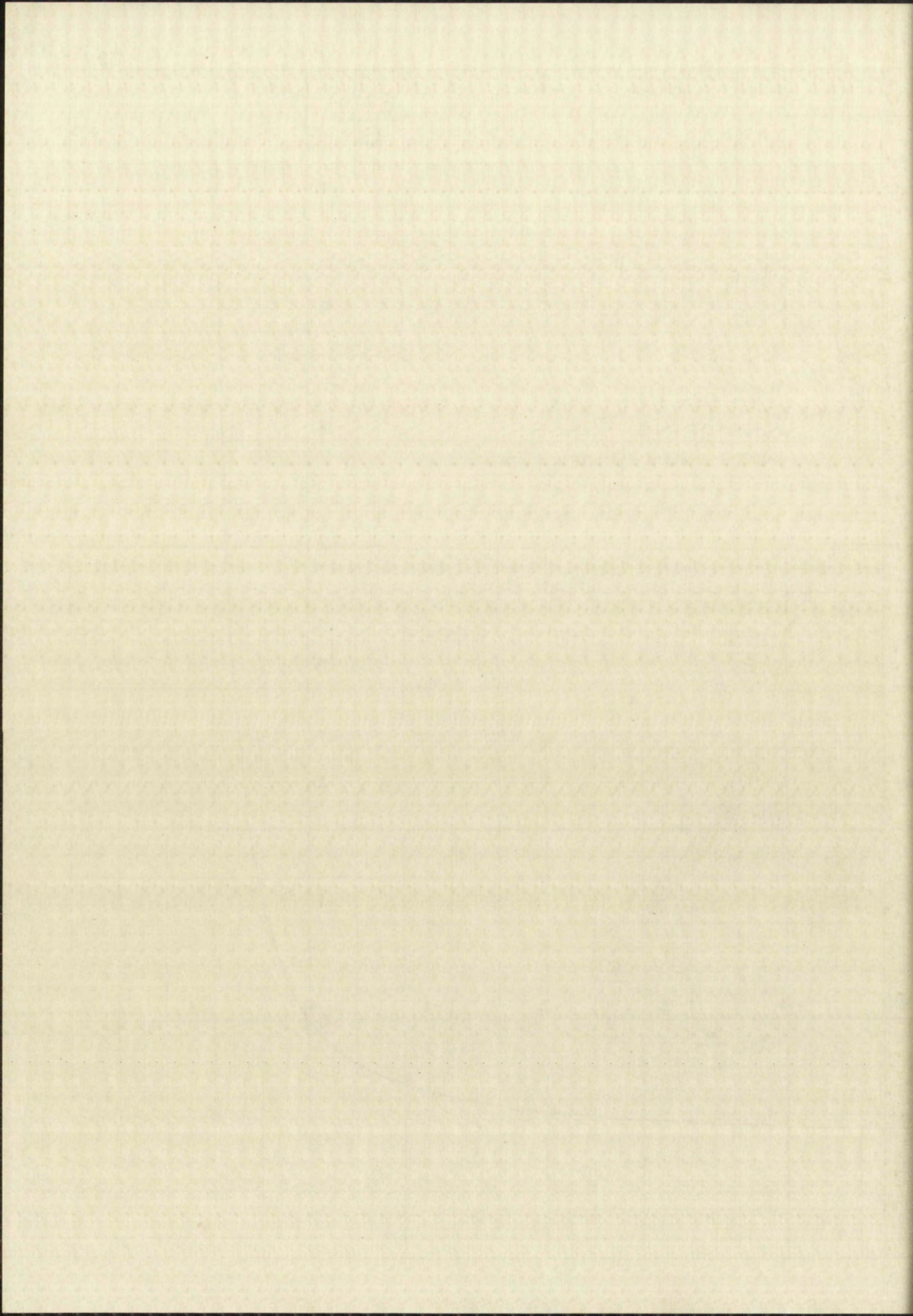
VARIATION OF
RESTORING FORCE
WITH NON-DIMENSIONAL
DISPLACEMENT

$$\frac{E(x)}{B} = 1 - \left(1 - \frac{x}{l}\right)^{-\delta}$$

$$\delta = 1.4$$



GRAPH 3



$$\frac{E(x)}{B}$$

$$\frac{E(x)}{B} \rightarrow -\infty \text{ as } x \rightarrow 1$$

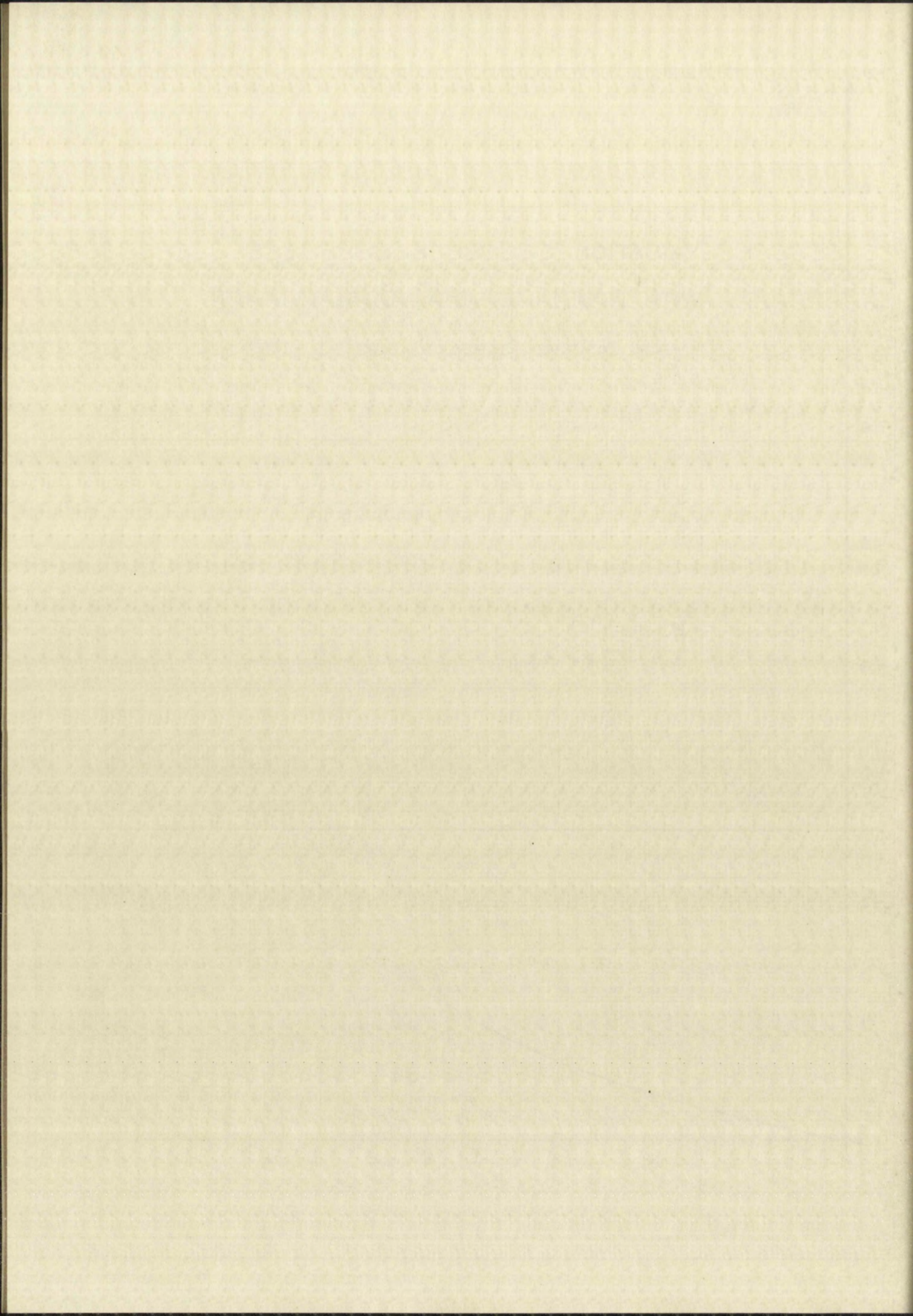
VARIATION OF RESTORING FORCE
WITH NON-DIMENSIONAL DISPLACEMENT
FOR POSITIVE DISPLACEMENT

$$\frac{E(x)}{B} = 1 - \left(1 - \frac{x}{l}\right)^{-\gamma}$$

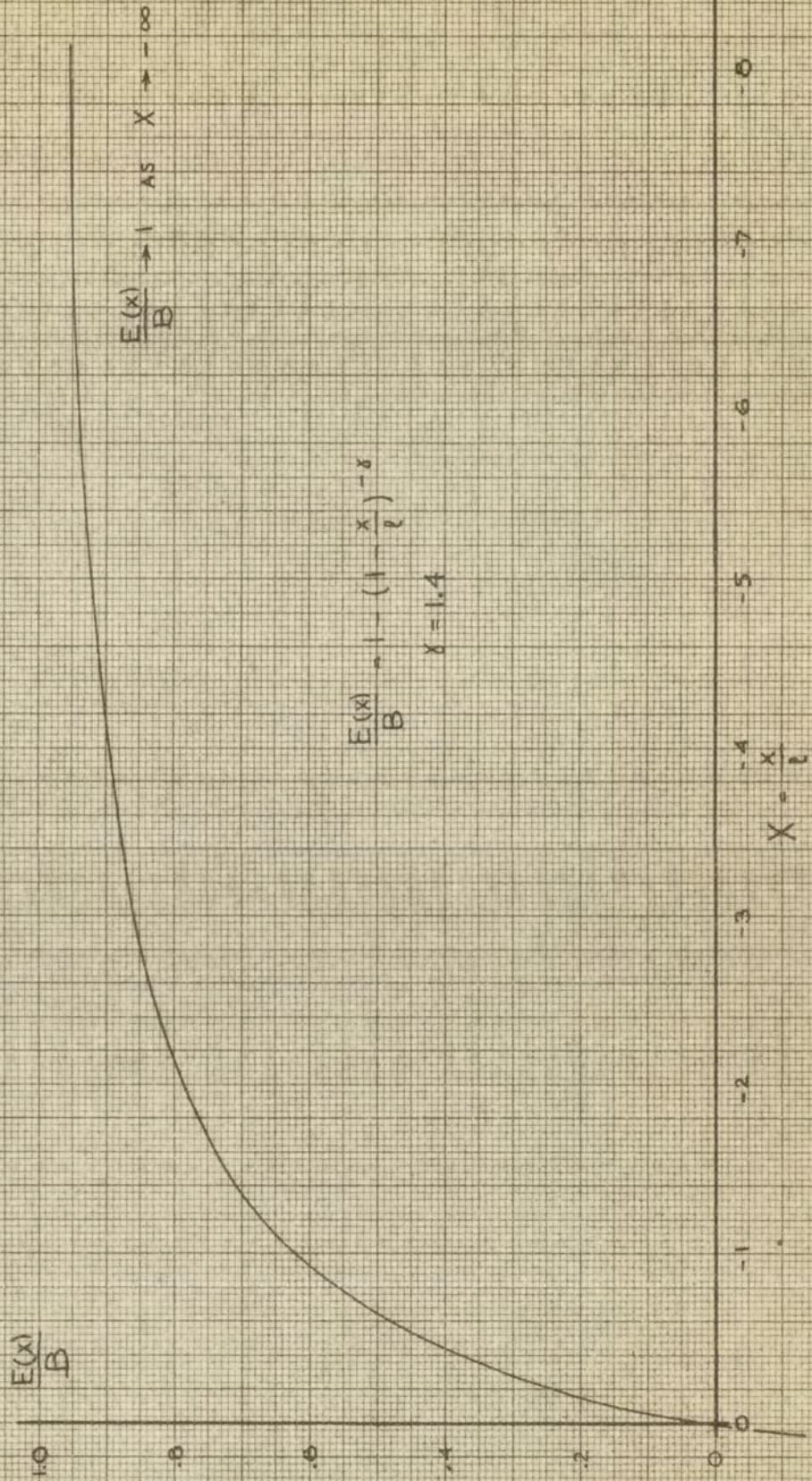
$\gamma = 1.4$

$$X = \frac{x}{l}$$

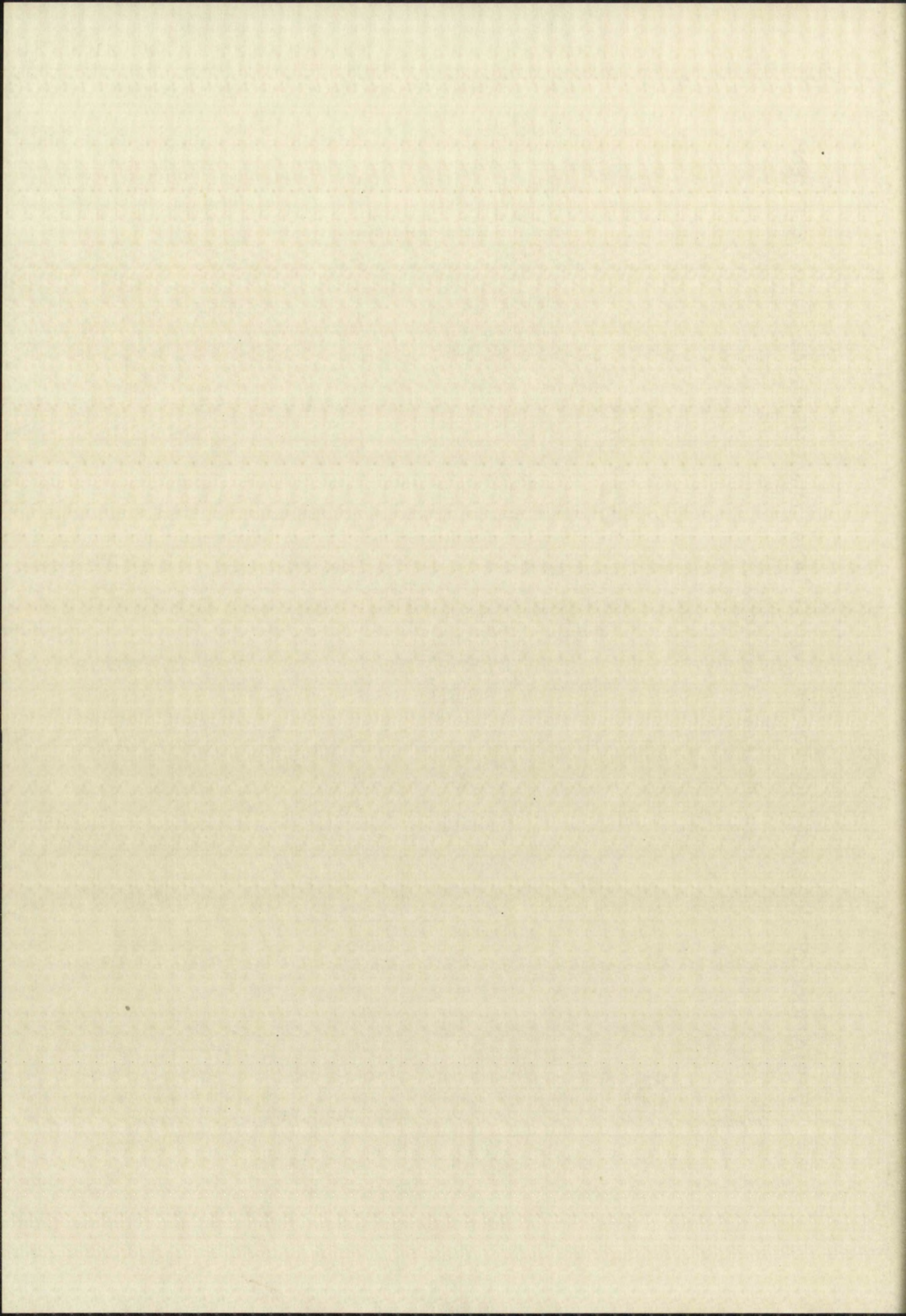
GRAPH 4



VARIATION OF RESTORING FORCE WITH NON-DIMENSIONAL DISPLACEMENT FOR NEGATIVE DISPLACEMENT



GRAPH 5



$x < L$), and $E(0) = 0$. Hence the action of $E(x)$ is always such that it tends to return the piston to the equilibrium position of $x = 0$.

The variation of $\frac{E(x)}{B}$ with $\frac{x}{L}$, for $\gamma = 1.4$ is shown in Graph 3. Graphs 4 and 5 are enlargements of Graph 3, showing respectively those portions of Graph 3 corresponding to positive and negative values of $\frac{x}{L}$.

The differential equation in nondimensional form.

Under the assumptions previously outlined only the restoring force $E(x)$ discussed above and the force of friction between piston and cylinder are considered as acting on the piston. The equation of motion of the piston is

$$(24) \quad \frac{W}{g} \frac{d^2 x}{dt^2} = E(x) + \phi$$

where t denotes time and ϕ denotes the force of friction, which may be a function of x and $\frac{dx}{dt}$. Substitution of (23) into (24) and division by W reduces (24) to the nondimensional form

$$(25) \quad \frac{1}{g} \frac{d^2 x}{dt^2} = \frac{B}{W} \left[1 - \left(1 - \frac{x}{L} \right)^{-\gamma} \right] + \frac{\phi}{W}.$$

Although each term in this equation is dimensionless, it will be of advantage to deal only with dimensionless

variables. Define dimensionless displacement X as $X = \frac{x}{L}$. In order to obtain a convenient non-dimensional time variable, as was done by Sussholz²⁴, one considers the air spring as a linear spring for an infinitely small displacement of the piston from its equilibrium position. The stiffness for this condition is given by

$$K = \left[\frac{d}{dx} E(x) \right]_{x=0} = \frac{B\gamma}{L}$$

The period of very small oscillations of the piston, if damping is neglected is

$$T_0 = 2\pi \sqrt{\frac{W}{\frac{B\gamma}{L}}} = 2\pi \sqrt{\frac{WL}{B\gamma}}$$

A dimensionless time variable may now be defined as

$$\tau = \frac{t}{T_0}.$$

The relations between the dimensional and non-dimensional velocities and accelerations are

$$\frac{dx}{dt} = \frac{dx}{dX} \frac{dX}{d\tau} \frac{d\tau}{dt} = \frac{L}{T_0} \frac{dX}{d\tau}, \text{ and}$$

²⁴ B. Sussholz op. cit., pp. A-102.

variables. In the dimensional analysis, x is $\frac{1}{L}$.
 In order to obtain a non-dimensional time variable,
 as was done by equation (2), we consider the air velocity as
 a linear velocity for an infinitely small displacement of the
 piston from the equilibrium position. The distance from
 zero position is given by

$$x = \left[\frac{2}{\pi} E(x) \right]_{x=0}^{\frac{\pi}{2}}$$

The period of very small oscillations of the piston is
 damping is neglected is

$$T_0 = 2\pi \sqrt{\frac{m}{k}}$$

A dimensionless time variable may now be defined as

$$\tau = \frac{t}{T_0}$$

The relations between the dimensional and non-dimensional
 velocities and accelerations are

$$\frac{dx}{dt} = \frac{dx}{d\tau} \frac{d\tau}{dt} = \frac{1}{T_0} \frac{dx}{d\tau}, \text{ and}$$

$$\frac{d^2 x}{dt^2} = \frac{d\gamma}{dt} \cdot \frac{d}{d\gamma} \left(\frac{L}{T_0} \frac{dx}{d\gamma} \right) = \frac{L}{T_0^2} \frac{d^2 x}{d\gamma^2} .$$

With these relations equation (25) becomes

$$(26) \quad \frac{d^2 x}{d\gamma^2} + g \frac{B}{W} \frac{T_0^2}{L} \left[(1-x)^{-\gamma} - 1 \right] + g \frac{\phi}{W} \frac{T_0^2}{L} = 0$$

However, from the definition of T_0 ,

$$\frac{g T_0^2}{WL} = \frac{4\pi^2}{B\gamma}$$

so that (26) may be simplified further to

$$(27) \quad \frac{d^2 x}{d\gamma^2} + \frac{4\pi^2}{\gamma} \left[(1-x)^{-\gamma} - 1 \right] + \frac{4\pi^2}{\gamma} \phi_0 = 0$$

where $\phi_0 = -\frac{\phi}{B}$. This equation then, is the non-dimensional differential equation of motion of the air spring in terms of non-dimensional variables. It has the advantage of reducing the number of variables to a minimum.

II. CHARACTERISTICS OF A FRICTIONLESS AIR SPRING

Regardless of whether friction in a real air spring can be reduced to a negligibly small value or not, a good deal may be learned about air springs in general by studying

$$\frac{d^2 x}{dt^2} = \frac{d^2}{dt^2} \left(\frac{1}{\sqrt{1 - \frac{v^2}{c^2}}} \right) = \frac{1}{\sqrt{1 - \frac{v^2}{c^2}}} \frac{d^2}{dt^2} \left(\frac{1}{\sqrt{1 - \frac{v^2}{c^2}}} \right)$$

With these relations equation (25) becomes

$$(26) \quad \frac{d^2 x}{dt^2} + \frac{d^2}{dt^2} \left(\frac{1}{\sqrt{1 - \frac{v^2}{c^2}}} \right) = \frac{1}{\sqrt{1 - \frac{v^2}{c^2}}} \frac{d^2}{dt^2} \left(\frac{1}{\sqrt{1 - \frac{v^2}{c^2}}} \right)$$

However, from the relation of

$$\frac{d^2 x}{dt^2} = \frac{d^2}{dt^2} \left(\frac{1}{\sqrt{1 - \frac{v^2}{c^2}}} \right)$$

so that (26) may be simplified to

$$(27) \quad \frac{d^2 x}{dt^2} + \frac{d^2}{dt^2} \left(\frac{1}{\sqrt{1 - \frac{v^2}{c^2}}} \right) = \frac{1}{\sqrt{1 - \frac{v^2}{c^2}}} \frac{d^2}{dt^2} \left(\frac{1}{\sqrt{1 - \frac{v^2}{c^2}}} \right)$$

where $\phi = \frac{1}{\sqrt{1 - \frac{v^2}{c^2}}}$. This equation may be written as

dimensional differential equation of order of 2.

Putting in terms of non-dimensional variables

advantage of reducing the number of variables is gained.

II. CHARACTERISTICS OF A SYSTEM

Regardless of whether the system is a mechanical system

can be reduced to a single differential equation.

It may be further shown that the system is a mechanical system

the characteristics of an ideal air spring in which there is no friction. A study of this type is prompted further by the relative ease with which it may be carried out; it is facilitated by the fact that it can be performed completely in dimensionless variables and also because one analytic integration of the differential equation of motion is possible.

Some properties of a frictionless air spring. The general differential equation in non-dimensional form was derived in the first section of this chapter. In the case of a frictionless spring, the friction function vanishes identically so that the basic differential equation here is

$$(28) \quad \frac{d^2 X}{d\gamma^2} + \frac{4\pi^2}{\gamma} \left[(1-X)^{-\gamma} - 1 \right] = 0$$

As indicated in section II of Chapter II, this equation may be integrated once, by letting $V = \frac{dX}{d\gamma}$, with the result

$$(29) \quad V^2 = \frac{8\pi^2}{\gamma} \left[X + \frac{1}{1-\gamma} (1-X)^{1-\gamma} - \left\{ X_0 + \frac{1}{1-\gamma} (1-X_0)^{1-\gamma} \right\} \right] + V_0^2.$$

X_0 and V_0 represent the values of X and V at $\gamma = \gamma_0$. For purposes of computation it is convenient to define a new function $q(X)$ as

$$q(X) = X + \frac{1}{1-\gamma} (1-X)^{1-\gamma}$$

the characteristic of an ideal air spring in which there is no friction. A study of this type is presented further by the relative mass with which it may be carried out. It is facilitated by the fact that it can be performed completely in dimensionless variables and also because one analytical integration of the differential equation of motion is possible.

Some properties of a frictionless air spring. The general differential equation in non-dimensional form was derived in the first section of this chapter. In the case of a frictionless spring, the friction function f vanishes identically so that the basic differential equation here is

$$(22) \quad \frac{d^2 x}{dt^2} + \frac{2x}{V} = 0 \quad \left[(1-x) - x \right]$$

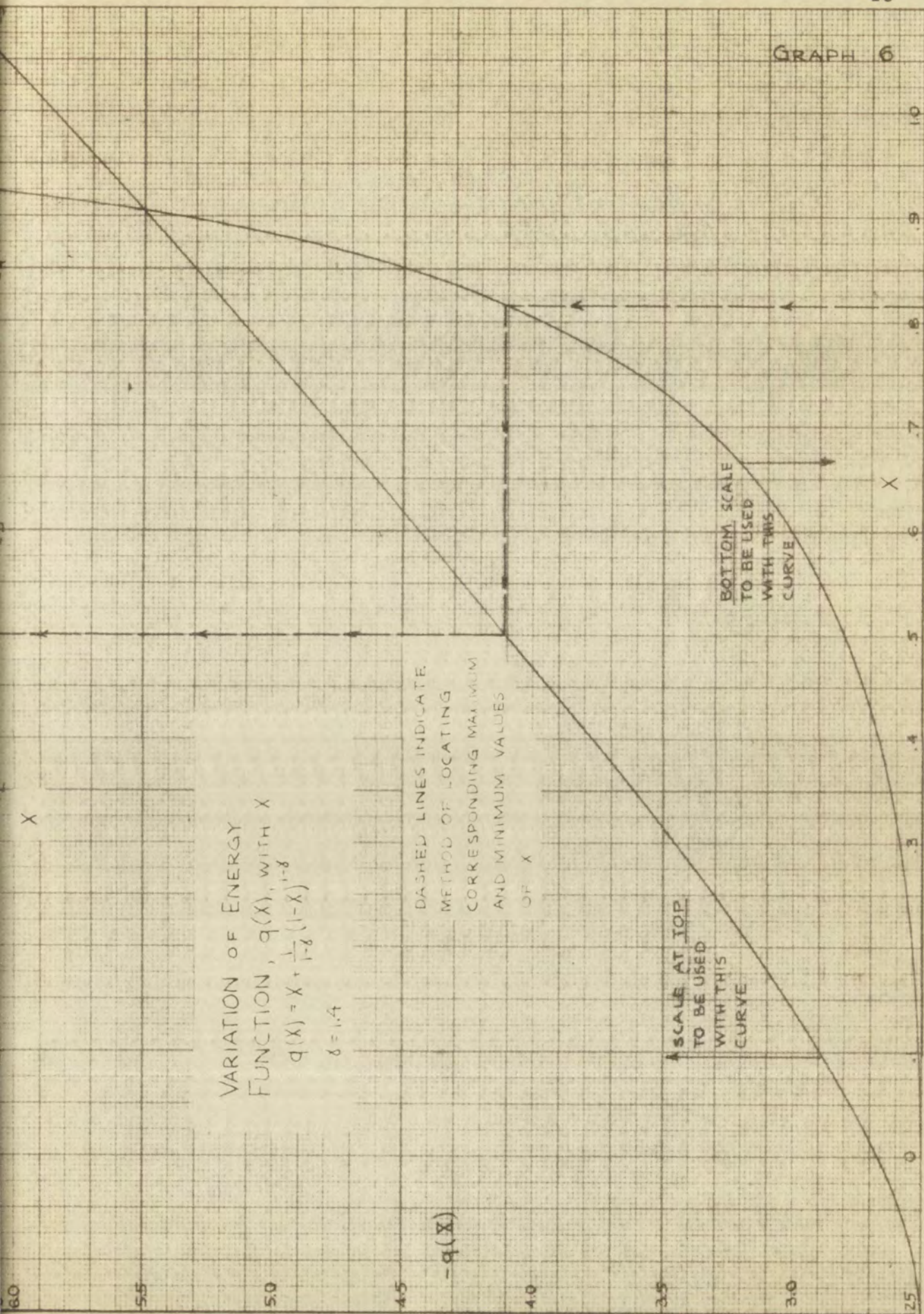
As indicated in section II of Chapter II, this equation may be integrated once, by letting $V = \frac{dx}{dt}$, with the result

$$(23) \quad V = \frac{dx}{dt} = \left[x + \frac{1}{1-x} \right]^{1/2} - \left[x_0 + \frac{1}{1-x_0} \right]^{1/2} \quad \left[(1-x_0) - x_0 \right]$$

x_0 and V_0 represent the values of x and V at $t=0$. For purposes of comparison it is convenient to define a new function $\phi(x)$ as

$$\phi(x) = x + \frac{1}{1-x} \quad (1-x_0) - x_0$$

GRAPH 6



by means of which (29) may be written as

$$(30) \quad v^2 = v_0^2 + \frac{8\pi^2}{\gamma} \left[q(X) - q(X_0) \right]$$

The function $q(X)$ is plotted in Graph 6. This graph greatly simplifies the calculation of the variation of V corresponding to a given set of initial conditions (X_0 and V_0). Since $q(X)$ is the integral of the restoring force with respect to displacement, it represents the potential energy stored in the system. This function is hence a valuable aid to understanding the action of the air spring.

Graph 7 shows several phase trajectories (i.e. X - V curves) for the frictionless air spring. It was found more convenient to plot $\bar{V} = \frac{V}{P}$, where $P^2 = \frac{4\pi^2}{\gamma}$, against X , instead of the more common V . The reason for this choice was to facilitate comparison with solutions obtained by the graphical method. The symmetry about the X -axis, as required by equations (29) and (30) is evident in Graph 7.

From the definition of V , $d\mathcal{T} = \frac{dX}{V}$. One would expect to be able to integrate this expression numerically with ease in order to find a relation between \mathcal{T} and X or V for a given set of initial conditions. Such an integration is easily performed where $V \neq 0$. However, all phase trajectories pass through $V = 0$, so that ordinary numerical

by means of which (23) can be written in the form

$$(23a) \quad V^2 = V_0^2 + \frac{2E}{m} \quad \text{or} \quad \frac{dV}{dt} = \frac{2E}{mV}$$

The function $p(x)$ is assumed to be a constant, and the function $V(x)$ is assumed to be a function of x only. The function $V(x)$ is assumed to be a function of x only, and the function $p(x)$ is assumed to be a constant.

With respect to the function $V(x)$, it is assumed that it is a function of x only, and the function $p(x)$ is assumed to be a constant. The function $V(x)$ is assumed to be a function of x only, and the function $p(x)$ is assumed to be a constant.

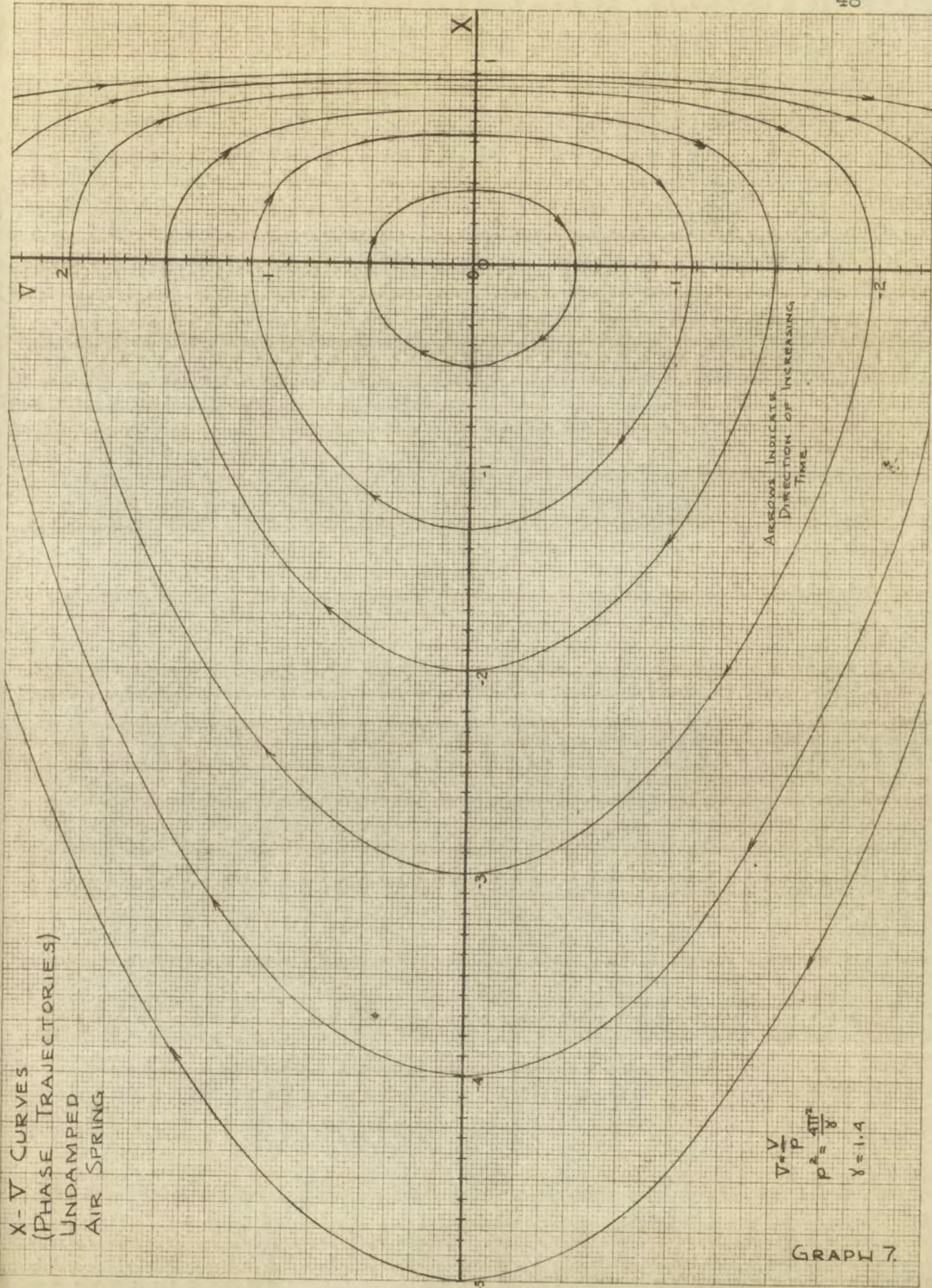
From (23) it follows that the function $V(x)$ is a function of x only, and the function $p(x)$ is assumed to be a constant.

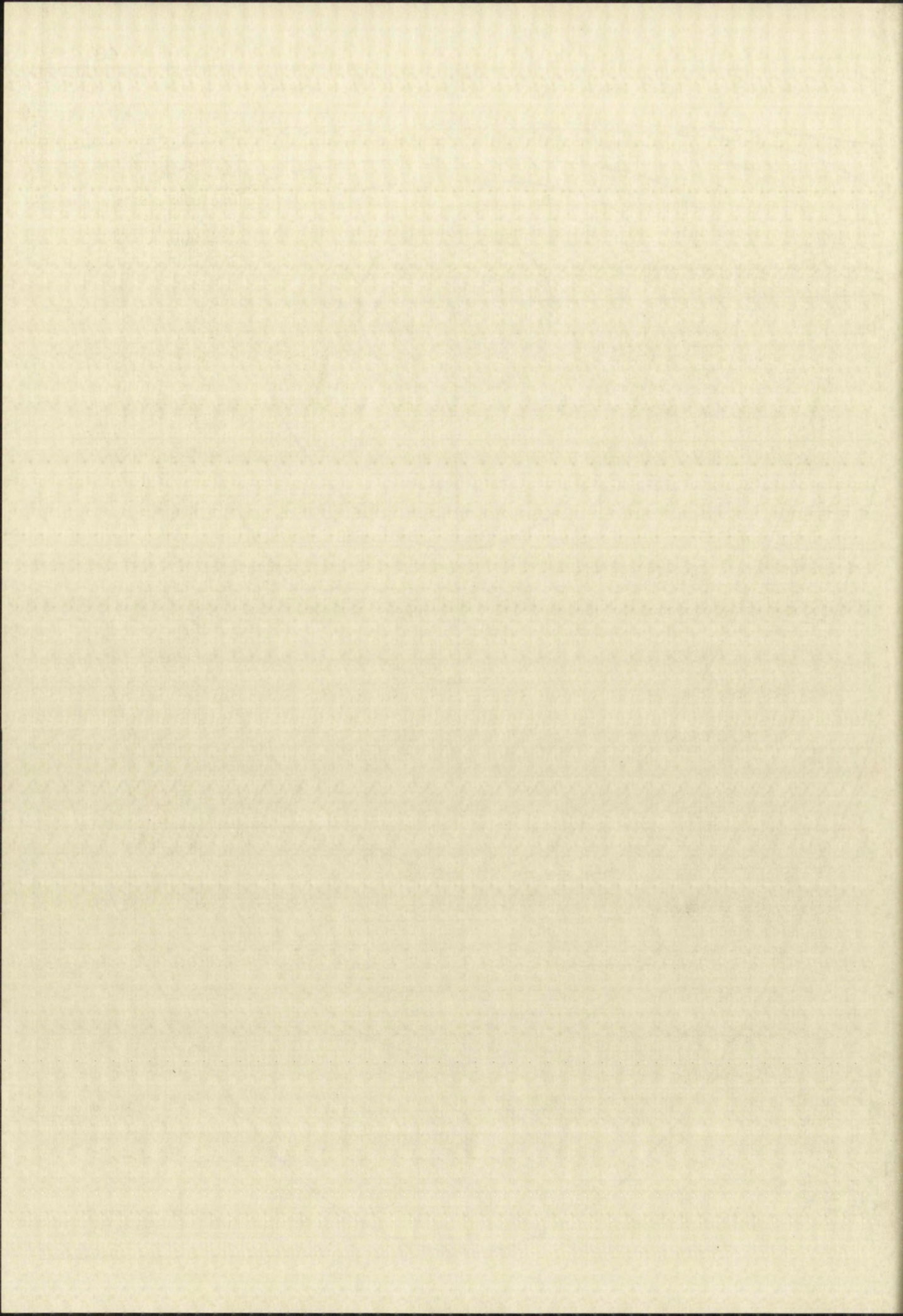
For the function $V(x)$ it is assumed that it is a function of x only, and the function $p(x)$ is assumed to be a constant. The function $V(x)$ is assumed to be a function of x only, and the function $p(x)$ is assumed to be a constant.

From the definition of $V(x)$ it follows that the function $V(x)$ is a function of x only, and the function $p(x)$ is assumed to be a constant.

It is assumed that the function $V(x)$ is a function of x only, and the function $p(x)$ is assumed to be a constant. The function $V(x)$ is assumed to be a function of x only, and the function $p(x)$ is assumed to be a constant.

X-V CURVES
(PHASE TRAJECTORIES)
UNDAMPED
AIR SPRING





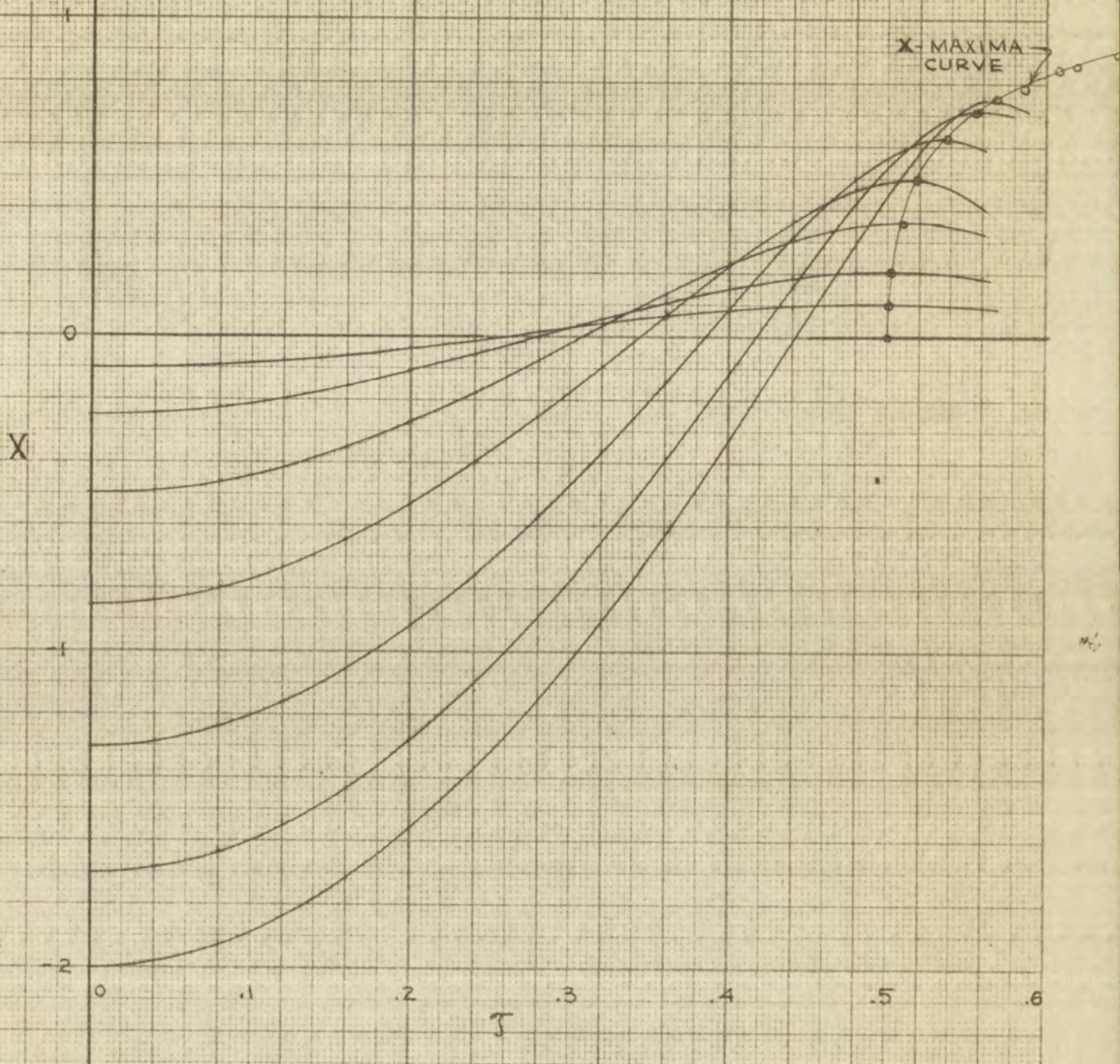
integration is impossible. Other methods that overcome this difficulty are too cumbersome, and are no better than integrating (28) numerically in the first place.

However, as was indicated previously, the relation between X and τ may be obtained without difficulty when the graphical method of solution is used. Graphs 8 and 9 are plots of the variation of X with τ for various initial values of X . From $d\tau = \frac{dX}{V}$ and from the symmetry of the phase trajectories, it is evident that any X - τ curve is symmetric about a line $X = X_m$, where X_m represents the maximum value of X on the X - τ curve considered. Hence it was not necessary to show X - τ curves with positive initial values of X also. The locus of these maximum values of X is also indicated in Graphs 8 and 9.

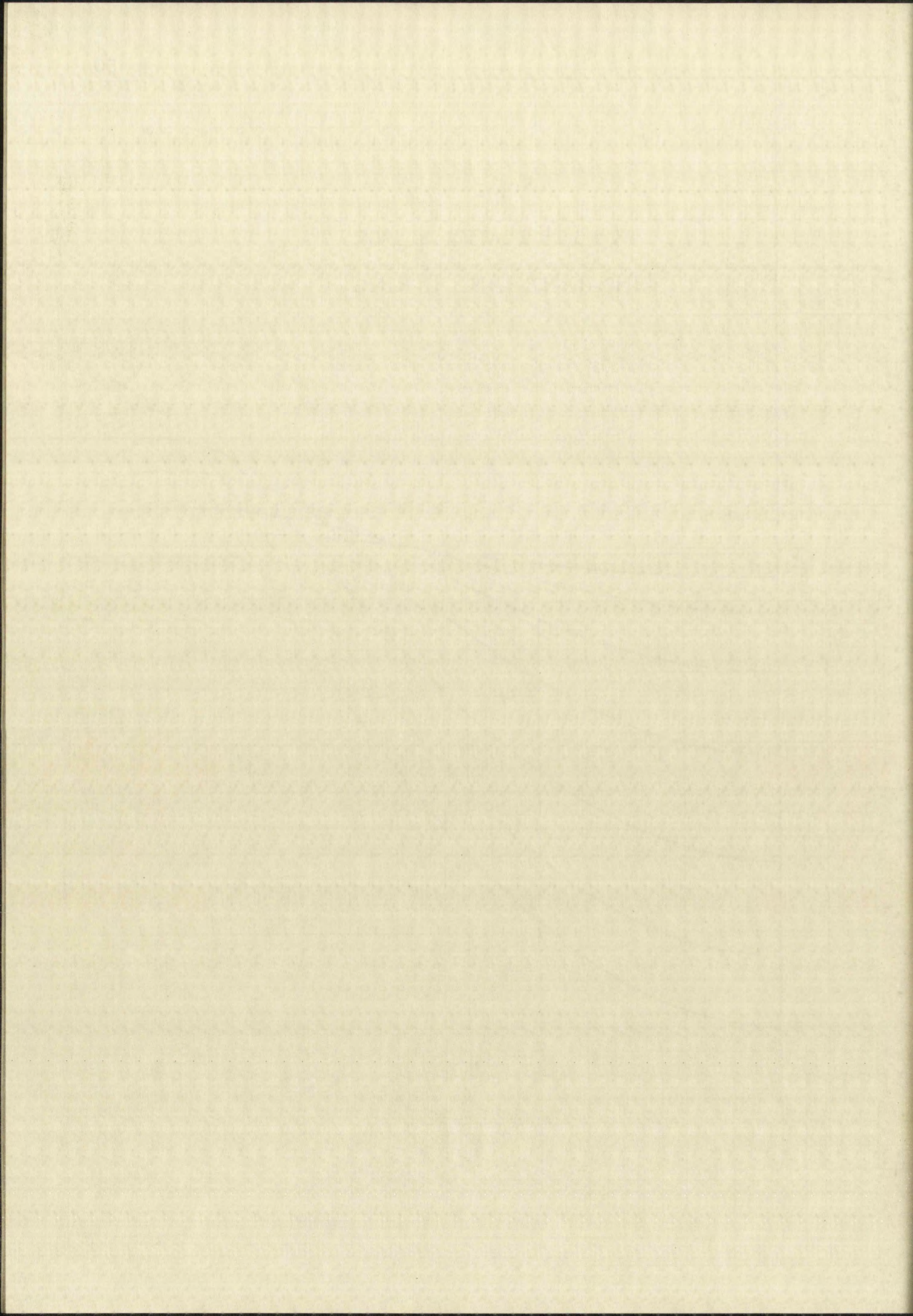
The variation of X_m with X_n , where X_n denotes the minimum value of X on the X - τ curve on which the maximum value of X is X_m , may be determined from Graphs 8 and 9 directly. These graphs were obtained by approximate methods, but more accurate determination of the variation of X_m with X_n is possible. By inspection of Graph 7 it is evident that X_m and X_n occur for $V = 0$. This is easily verified analytically when equation (30) is rewritten as

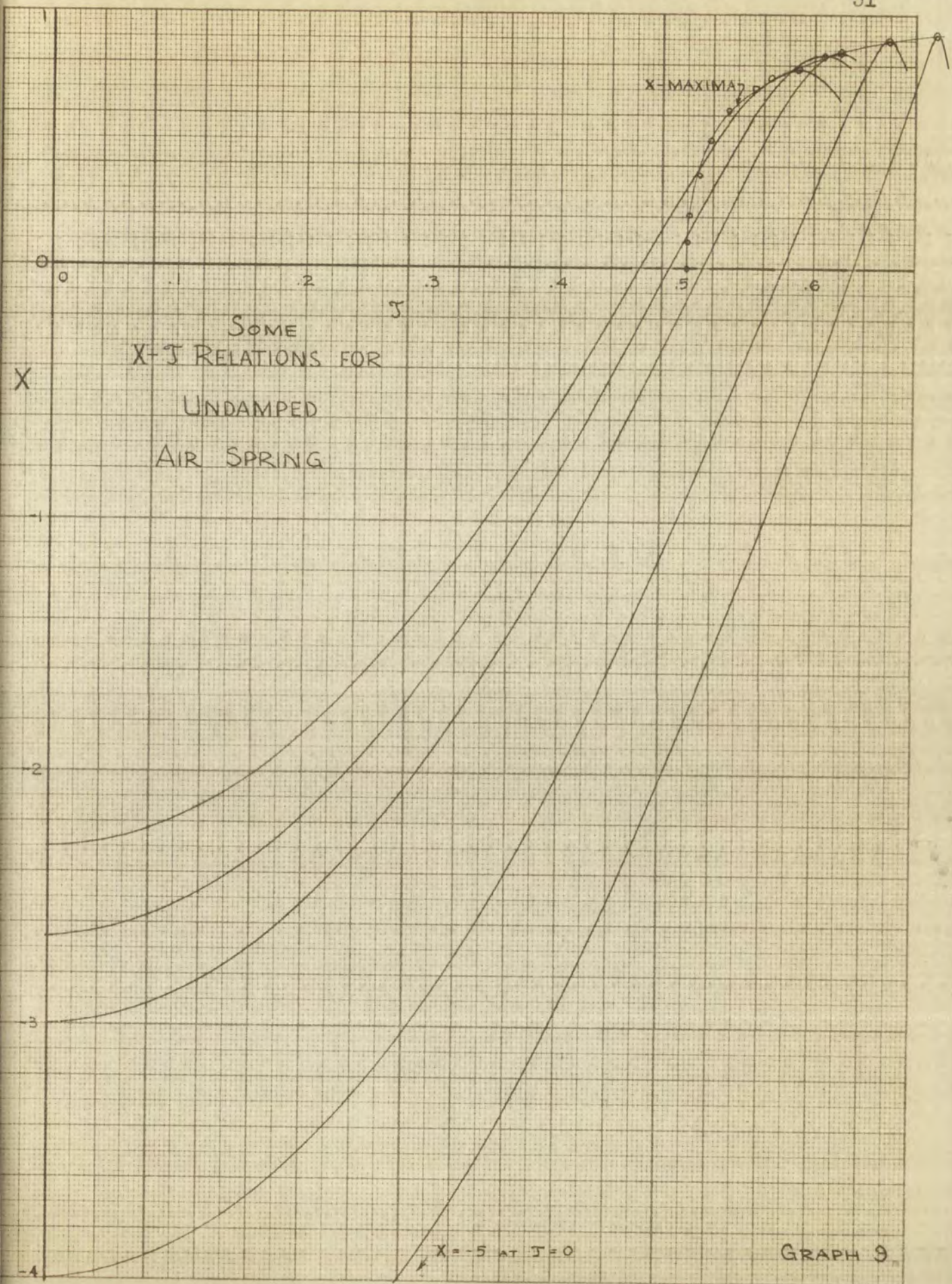
$$(31) \quad V^2 - \frac{8\pi^2}{\gamma} q(X) = V_0^2 - \frac{8\pi^2}{\gamma} q(X_0)$$

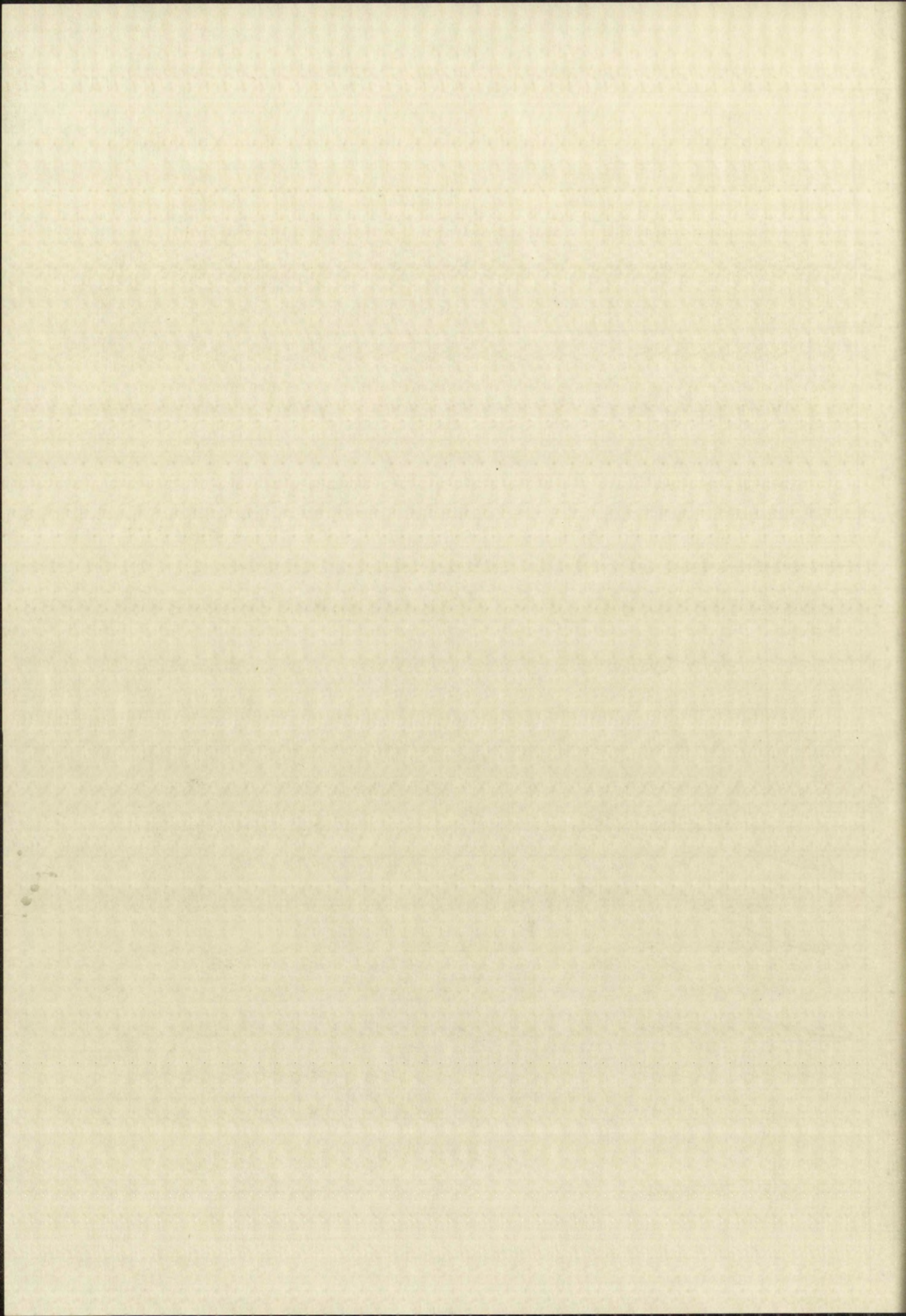
SOME
X- τ RELATIONS FOR
UNDAMPED AIR SPRING



GRAPH 8.



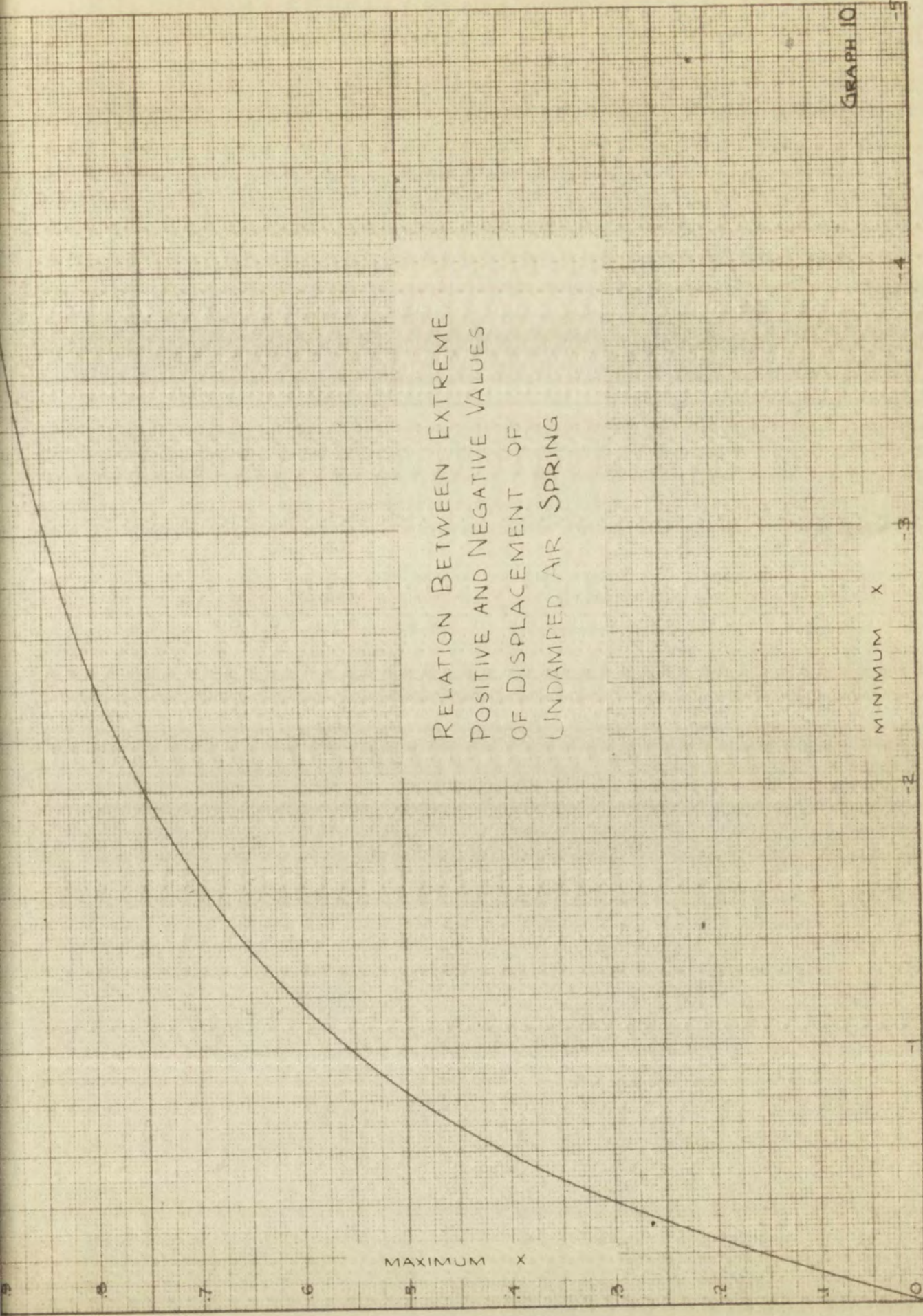


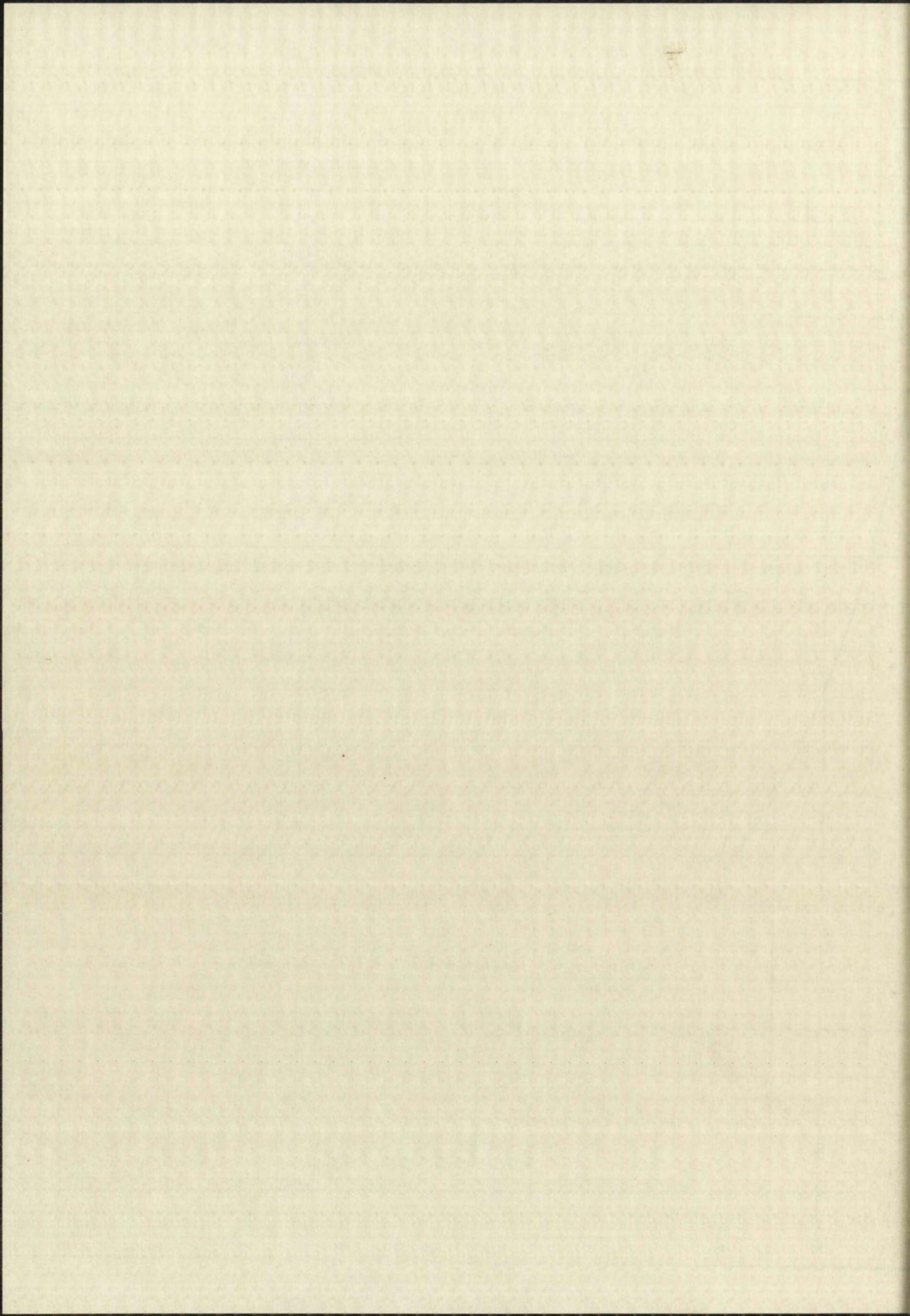


and when one notices that $q(X)$ is always negative and increases in absolute value as the absolute value of X increases. For given initial conditions, the right hand side of (31) is constant. If this constant is denoted by C , then one needs to find only the two solutions, X_m and X_n of $q(X) = -\frac{\gamma C}{8\pi^2}$. An easy method of finding corresponding values of X_m and X_n is to pick positive and negative values of X from Graph 6 which correspond to the same value of $q(X)$, as indicated by the dashed line in the aforementioned graph. The variation of X_m with X_n , as computed by the method just outlined, is shown in Graph 10.

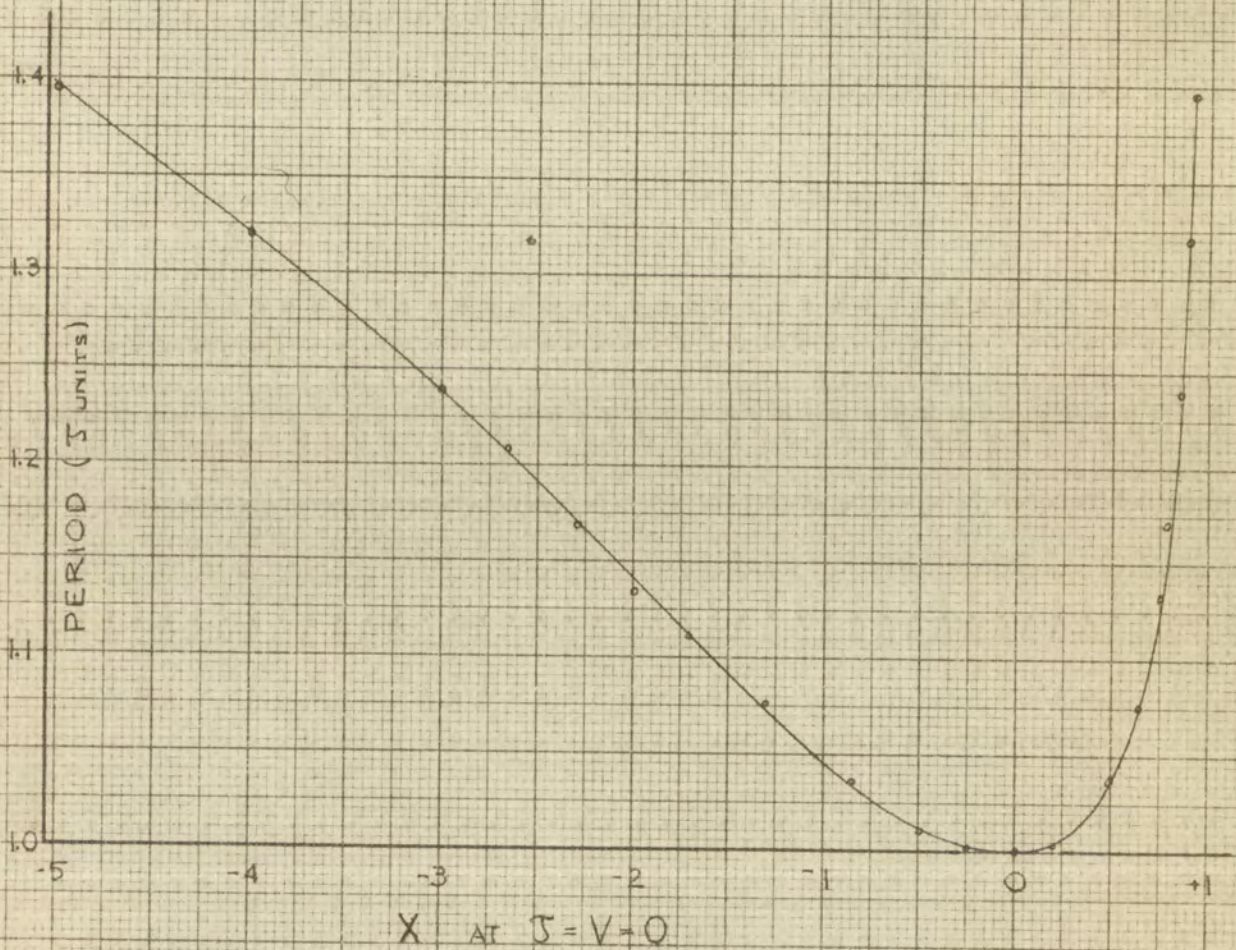
From Graphs 8 and 9, it is evident that the period of vibration of a frictionless air spring is dependent on the initial conditions. This dependence is shown in Graph 11, which was plotted directly from Graphs 8 and 9. Graph 11 shows the variation of period with initial displacement if $V_0 = 0$. However, equation (31) implies that any motion for which $V_0^2 - \frac{8\pi^2}{\gamma} q(X_0)$ has a given value C , will be represented by the same curve in the X - V plane, regardless of the values of X_0 and V_0 . Hence, Graph 11 may be considered to show indirectly the variation of period with C , for various values of X_0 and V_0 , within the range of the graph. The plot against X_0 rather than against C was chosen because it is more directly applicable to an air spring in a testing machine.

RELATION BETWEEN EXTREME
POSITIVE AND NEGATIVE VALUES
OF DISPLACEMENT OF
UNDAMPED AIR SPRING

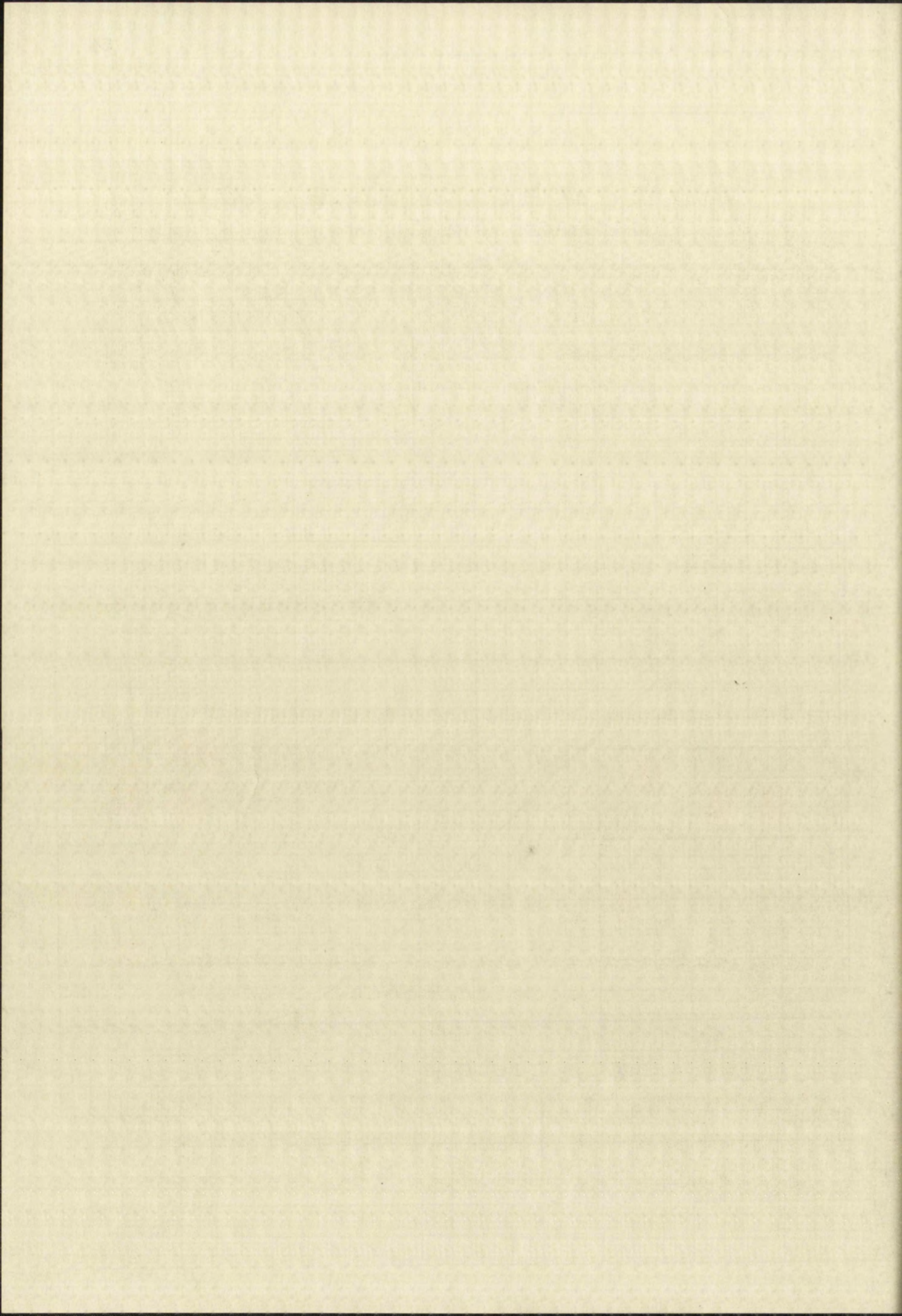




VARIATION OF PERIOD OF VIBRATION OF
UNDAMPED AIR SPRING
WITH
INITIAL POSITION, STARTING FROM REST



GRAPH II.



Acceleration and acceleration build-up time of a frictionless air spring. In a shock testing apparatus, acceleration obtained is of prime importance. From equation (12), the variation of acceleration (in non-dimensional form) with X is easily found:

$$(32) \quad \frac{\gamma}{4\pi^2} \frac{d^2 X}{d\tau^2} = 1 - (1 - X)^{-\gamma}.$$

Since this expression for $\frac{\gamma}{4\pi^2} \frac{d^2 X}{d\tau^2}$ is identical to that for $-\frac{E(X)}{B}$ as previously discussed, Graphs 3, 4, and 5, showing the variation $\frac{E(X)}{B}$ with X , also indicate the relation of $\frac{\gamma}{4\pi^2} \frac{d^2 X}{d\tau^2}$ and X . From these graphs it is also evident that maximum acceleration corresponds to maximum displacement and that zero acceleration occurs at zero displacement. Hence, the X - τ curves of Graphs 8 and 9 may be used in conjunction with the restoring force plots of Graphs 3, 4, and 5 for determination of the variation of maximum acceleration and of acceleration build-up time with initial displacement, assuming zero initial velocity. These relations are shown respectively in Graphs 12 and 13.

Utilization of characteristics of frictionless air springs in shock testing. It is convenient in the actual application of an air spring in a shock testing machine, always to release the piston from rest ($V_0 = 0$). Graph 12

(12) The variation of α with X is easily shown to be

$$(12) \quad \alpha = \frac{1}{2} \left(\frac{1}{1 + \frac{1}{2} \frac{dX}{d\alpha}} \right)$$

Since $\frac{dX}{d\alpha}$ is always positive, α is always positive, and α is always less than $\frac{1}{2}$.

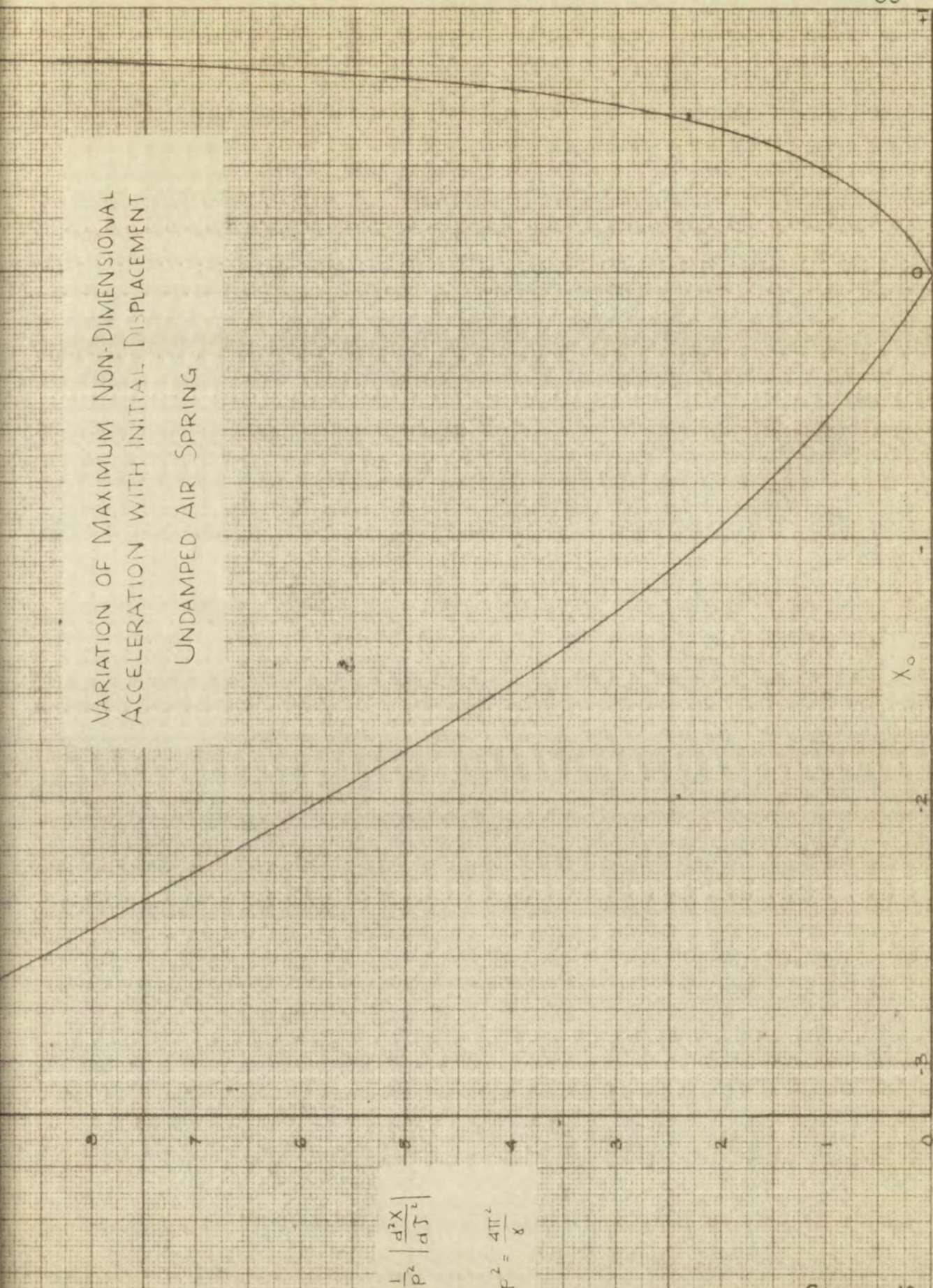
$$\text{Also of } \frac{1}{2} \frac{dX}{d\alpha} \text{ and } \frac{1}{2} \frac{d^2X}{d\alpha^2} \text{ are both positive, so that } \alpha \text{ is always positive.}$$

evident that maximum acceleration is not reached at $\alpha = \frac{1}{2}$.
 displacement and time are also positive, and α is always positive.
 displacement, time, and α are all positive, and α is always positive.
 be used in conjunction with the preceding results to show that
 graphs 2, 4, and 5 are consistent with the preceding results.
 maximum acceleration is not reached at $\alpha = \frac{1}{2}$, and α is always positive.
 initial displacement, velocity, and time are all positive, and α is always positive.
 relations are shown in graphs 2, 4, and 5.

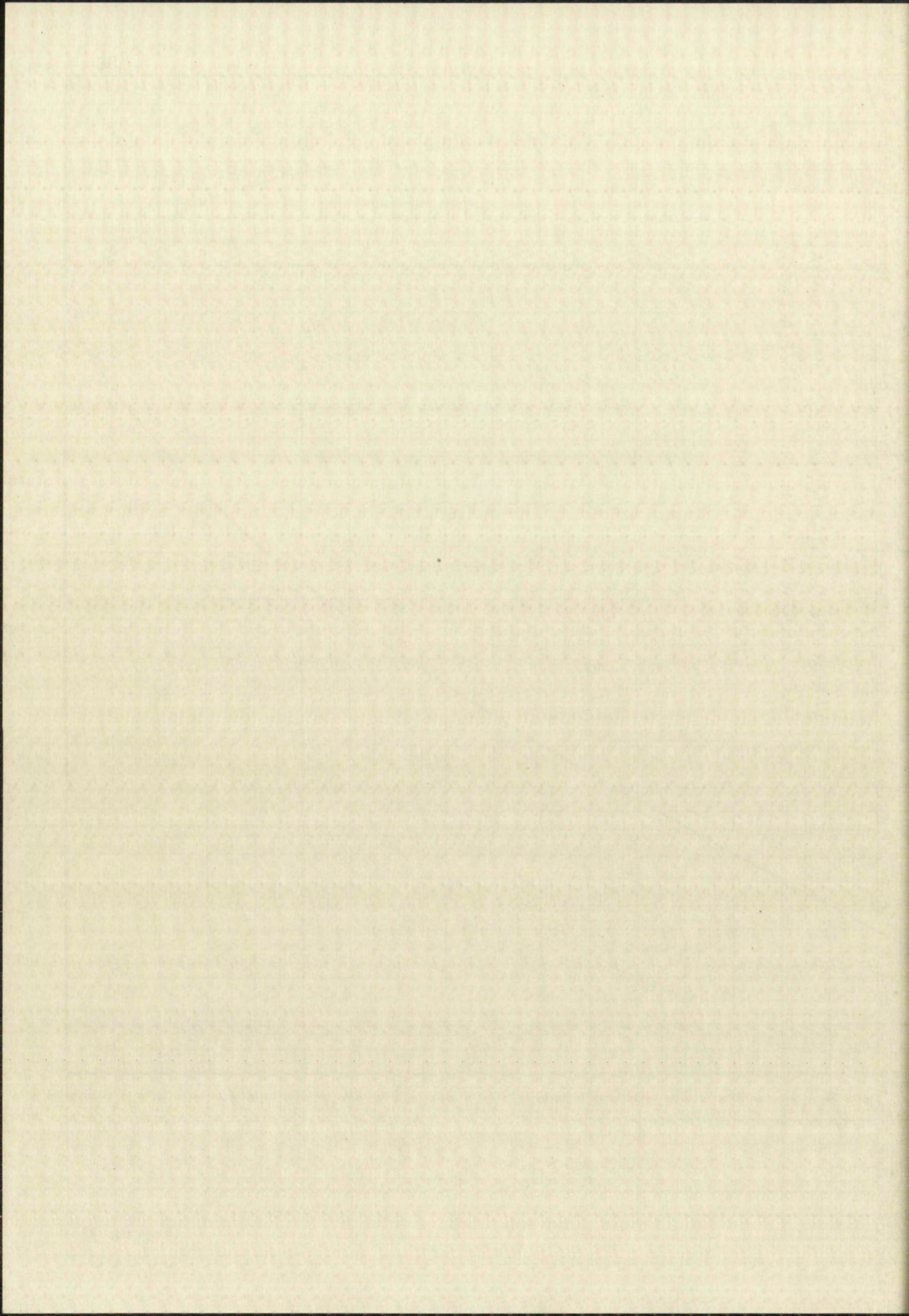
Verification of these results is given in the following table:
 applied in these results. The following table shows the results of
 application of the preceding results to the various cases.

VARIATION OF MAXIMUM NON-DIMENSIONAL
ACCELERATION WITH INITIAL DISPLACEMENT

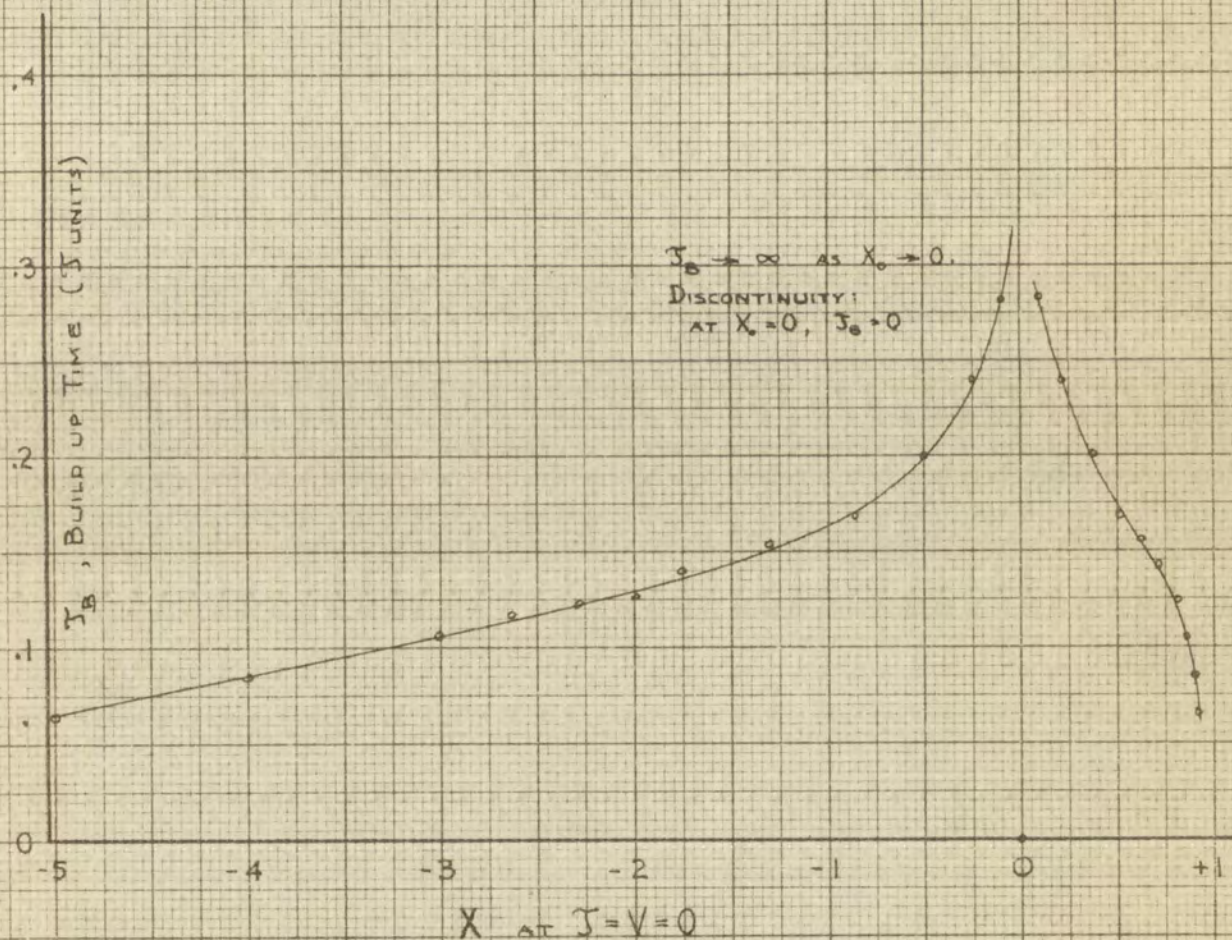
UNDAMPED AIR SPRING



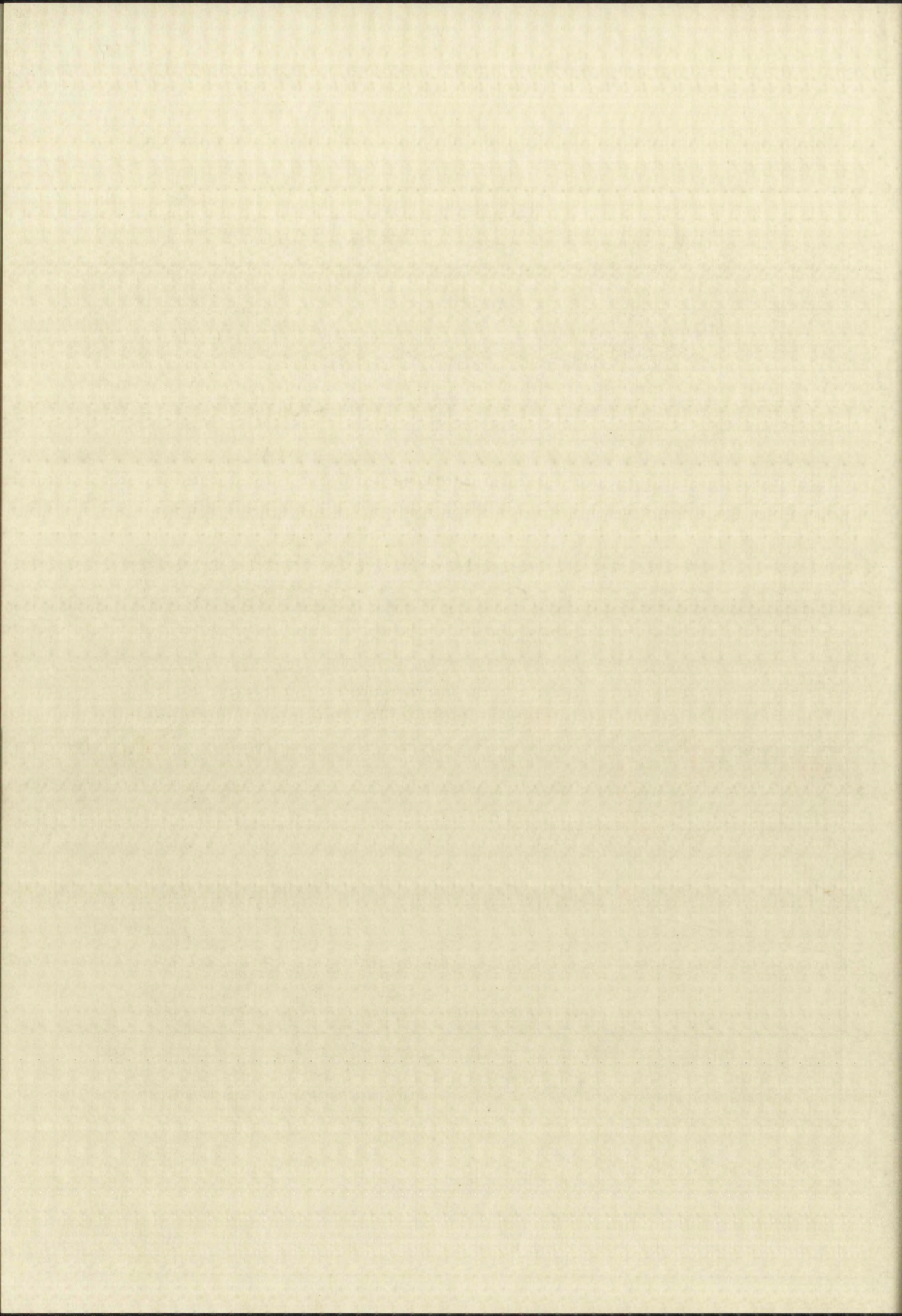
GRAPH 12.



VARIATION OF
TIME TAKEN FOR BUILD UP FROM ZERO TO
MAXIMUM ACCELERATION
WITH
INITIAL POSITION, STARTING FROM REST
(UNDAMPED AIR SPRING)



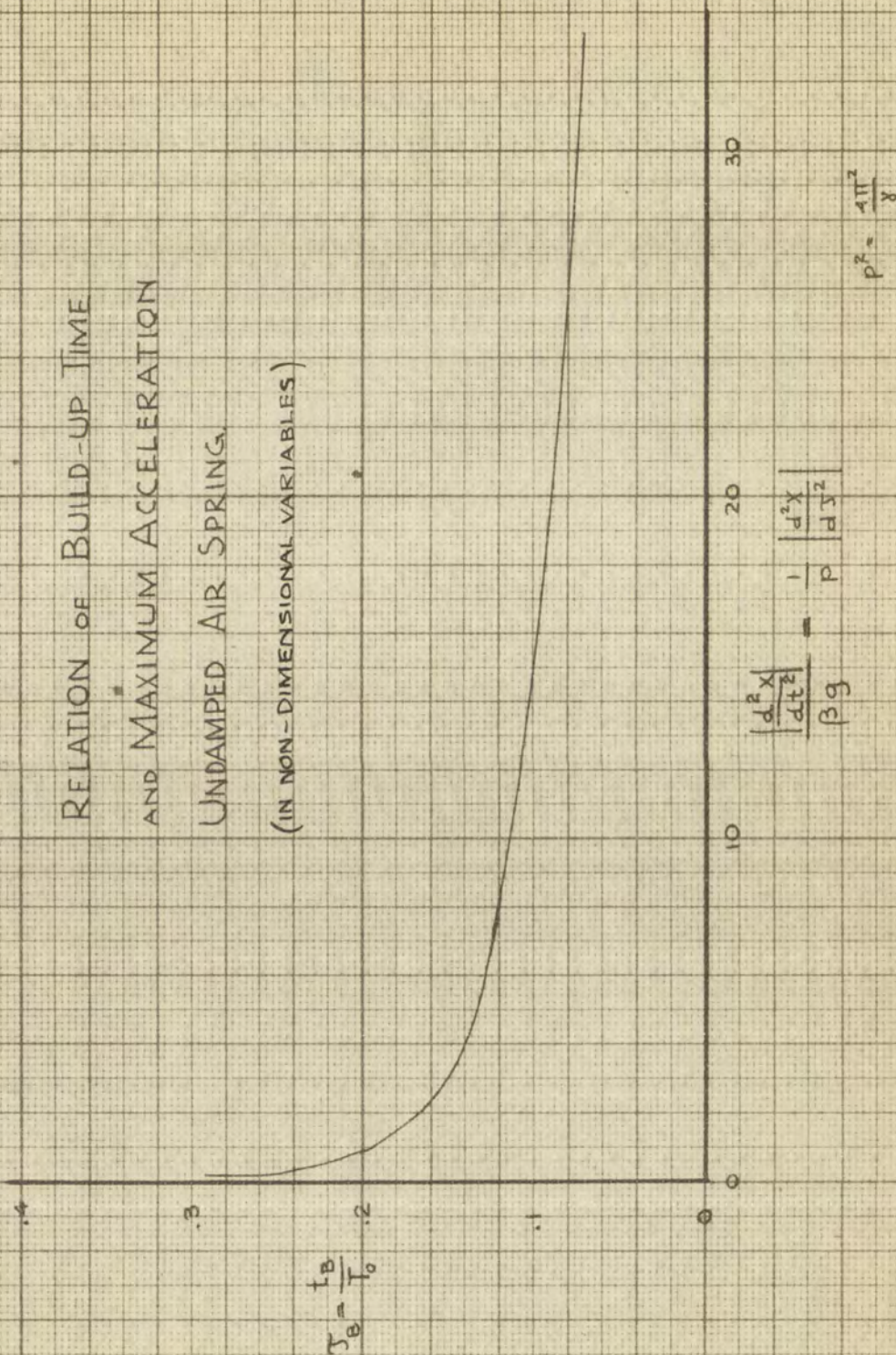
GRAPH 13.



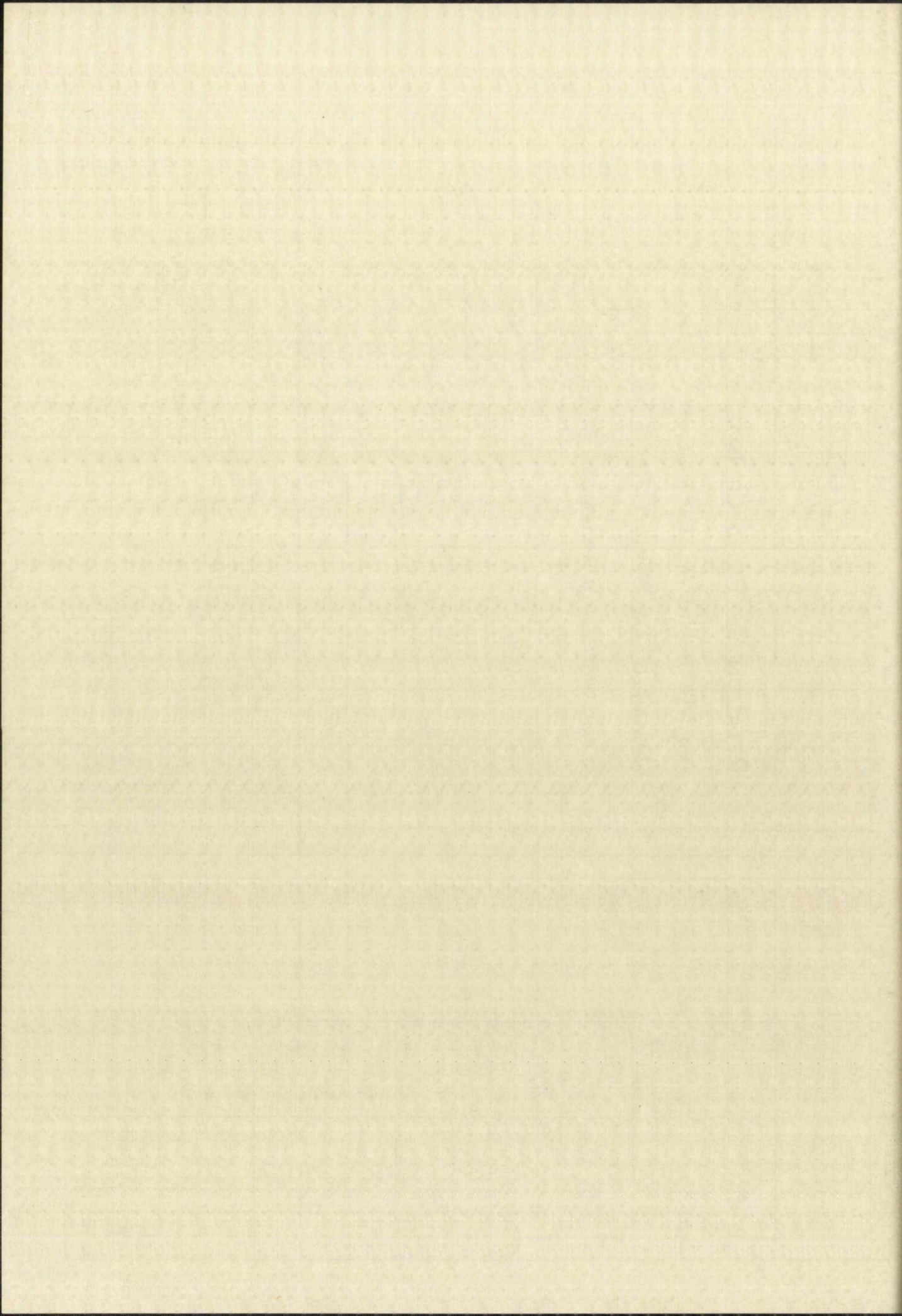
indicates that the same maximum acceleration can be obtained by starting from rest at either a positive or a corresponding negative initial position. It also shows that for a given value of acceleration, a certain error in the corresponding negative X_0 will cause a much smaller error in the acceleration than will the same error in the corresponding positive X_0 . X_0 can in practice be adjusted only within a certain accuracy; hence, the use of a negative X_0 is desirable. However, the maximum acceleration that can be obtained with a negative X_0 is limited by the length of the cylinder, whereas with positive X_0 any maximum acceleration can theoretically be obtained. From Graph 13, by reasoning similar to that applied to maximum accelerations, it may be deduced that acceleration build-up time may also be adjusted more accurately when negative initial displacements are used. Hence, the use of negative initial displacements seems generally most advantageous.

Assuming that the piston is always released from rest at a position of negative X_0 , then the foregoing work indicates that both maximum non-dimensional acceleration and non-dimensional acceleration build-up time depend only on X_0 . Thus, one and only one value of maximum dimensionless acceleration corresponds to one value of dimensionless acceleration build-up time. The relation between these two variables is shown in Graph 14.

RELATION OF BUILD-UP TIME
AND MAXIMUM ACCELERATION
UNDAMPED AIR SPRING
(IN NON-DIMENSIONAL VARIABLES)



GRAPH 14.



However, as will be demonstrated, this one-to-one correspondence does not apply to real maximum acceleration and acceleration build-up time since there is a difference in the number of variables involved in relating the real to the non-dimensional quantities.

From the definition of the dimensionless time variable, the relation between dimensionless acceleration build-up time τ_B , and real acceleration build-up time t_B is

$$t_B = 2\pi \tau_B \sqrt{\frac{WL}{gB\gamma}}$$

τ_B is a function of X_0 only, and W , B , g , and γ are constant for a given air spring, so that t_B is a function of both X_0 and L .

The relation between non-dimensional and real acceleration has been shown to be

$$\frac{d^2x}{dt^2} = \frac{L}{T_0^2} \frac{d^2X}{d\tau^2} = \frac{gB}{4\pi^2W} \frac{d^2X}{d\tau^2} .$$

For a given air spring, the non-dimensional maximum acceleration is a function of only X_0 , and W , B , g , and γ are constant, so that real maximum acceleration is dependent only on X_0 . Hence, control of both maximum acceleration and rise time is possible by control of the variables X_0 and L .

The foregoing results may be summarized conveniently with the help of the definitions $\beta = \frac{B}{W}$ and $P^2 = \frac{4\pi^2}{\gamma}$. The above equations then become

$$(33a) \quad t_B = \sqrt{\left(\frac{P^2}{\beta}\right) \frac{L}{g}} \quad \tau_B$$

$$(33b) \quad \frac{1}{g} \left| \frac{d^2 x}{dt^2} \right|_{\max} = \frac{\beta}{P^2} \left| \frac{d^2 x}{d\tau^2} \right|_{\max}$$

For example, for a vertical air spring with piston on top, $A = 5 \text{ in}^2$, $W = 10 \text{ lb}$, and $P_0 = 14.5 \text{ psi}$, B is found to be 8.25. If a maximum acceleration of $30g$ is desired the corresponding value of $\frac{1}{P^2} \left| \frac{d^2 x}{d\tau^2} \right|$ is found from (33b) to be $\frac{30}{8.25} = 3.64$.

From Graph 12, the necessary X_0 is determined as -1.44. The corresponding value of τ_B is found to be 0.142 from Graph 14. Hence, from (33a), $t_B = 0.0134 \sqrt{L}$. Thus, it is possible in theory to adjust the acceleration build-up time, t_B , to any desired value by selecting the proper L .

In reality, however, the available range of t_B is determined by the physical construction of the air spring. The maximum value of L (which gives the greatest t_B) is

The iterative procedure may be summarized as follows:

With the help of the definitions $\bar{Q} = \frac{1}{2}$ and $\bar{P} = \frac{1}{2}$

The above iterative procedure is:

$$(22a) \quad \bar{P} = \left[\frac{\frac{1}{2}}{\bar{Q}} \right] \left[\frac{\frac{1}{2}}{\bar{Q}} \right] \quad \bar{Q} = \frac{1}{2}$$

$$(22b) \quad \frac{1}{\bar{Q}} = \left[\frac{\frac{1}{2}}{\bar{Q}} \right] \left[\frac{\frac{1}{2}}{\bar{Q}} \right] \quad \bar{Q} = \frac{1}{2}$$

For example, for a vertical air column with radius

of 10 cm, $\bar{P} = 0.1$, $\bar{Q} = 0.1$, and $\bar{R} = 0.1$, it is

found to be 0.1. If a uniform distribution of 10 is given

the corresponding value of $\frac{1}{\bar{Q}}$ is found to be

$$(22c) \quad \frac{1}{\bar{Q}} = 0.1 \quad \bar{Q} = 0.1$$

From (22a) and (22b), the necessary \bar{Q} is determined as

0.1. The corresponding value of $\frac{1}{\bar{Q}}$ is found to be 0.1.

From (22c) and (22d), the necessary \bar{Q} is determined as

0.1. It is possible in theory to adjust the procedure

until the value of \bar{Q} is found by adjusting the

proper \bar{Q} .

In reality, however, the available value of \bar{Q} is

determined by the physical properties of the system.

The maximum value of \bar{Q} (which gives the maximum \bar{Q}) is

limited by the length of the air spring cylinder. The minimum value of L is dictated by the flatness of the piston face and of the cylinder bottom and by the construction of the seal on the cylinder. For instance, if the cylinder is 27 in. long, then for the above illustration it is required that $27 > (1 + 1.44) L$. This means that L can not be made larger than 11.05 in., and that the maximum acceleration build-up time that can be obtained for this example is 0.0445 sec. An increase in piston weight decreases β , thus increasing the value of $\frac{d^2x}{dt^2}$ necessary for a given physical acceleration, according to (33b). But, τ_B decreases when $\frac{d^2x}{dt^2}$ increases, as in Graph 16. Thus, an increase in piston weight serves to decrease τ_B , reducing the maximum t_B that can be obtained corresponding to a given maximum acceleration with a given cylinder. This is evident from (33a). Hence, low piston weights are necessary for large rise times.

CHAPTER IV

INVESTIGATION OF AN EXPERIMENTAL AIR SPRING

An experimental air spring was investigated with the purpose of determining to what extent the action of an actual air spring may be predicted by theoretical calculations.

I. APPARATUS

The air spring. The essential parts of the experimental air spring are shown in Fig. 5. Fig. 6 is a view of the entire experimental setup.

The cylinder of the spring was made from a 2 ft. length of commercial seamless steel pipe with an inside diameter of 2.500 ± 0.005 in. quoted by the manufacturer and a $\frac{1}{4}$ in. wall thickness. It was attempted to decrease the variation of the inside diameter by honing, but the results of this operation could not be evaluated precisely. The cylinder was closed off on bottom by means of a pipe cap which was provided with a rubber gasket and filled with heavy motor oil to prevent air leakage. A cast iron flange was threaded onto the top of the cylinder. This flange served to support the piston guide rods in relation to the cylinder and also aided in holding the entire assembly in the tripod mount.

EXPERIMENTAL
AIR SPRING.

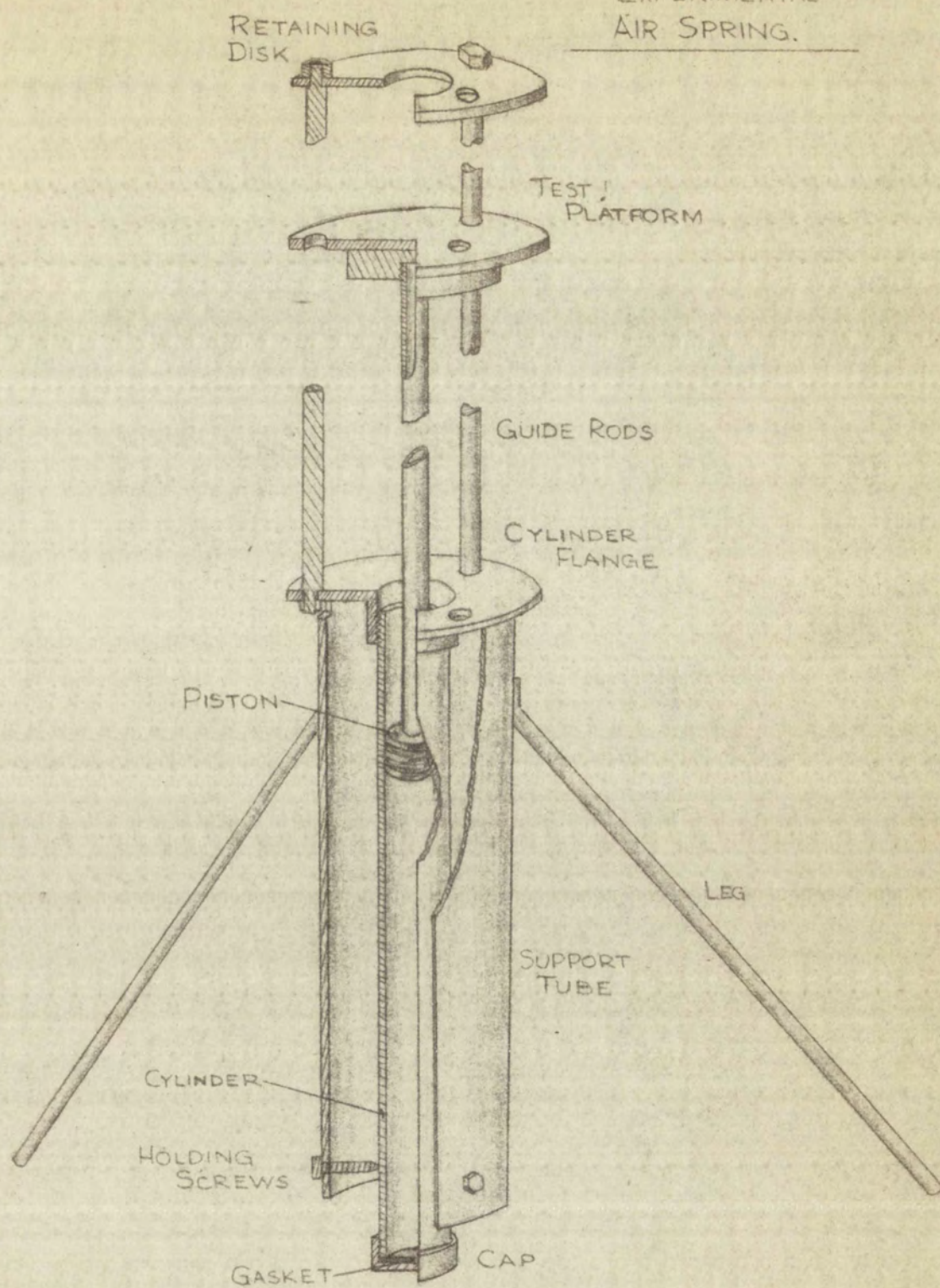


FIG 5

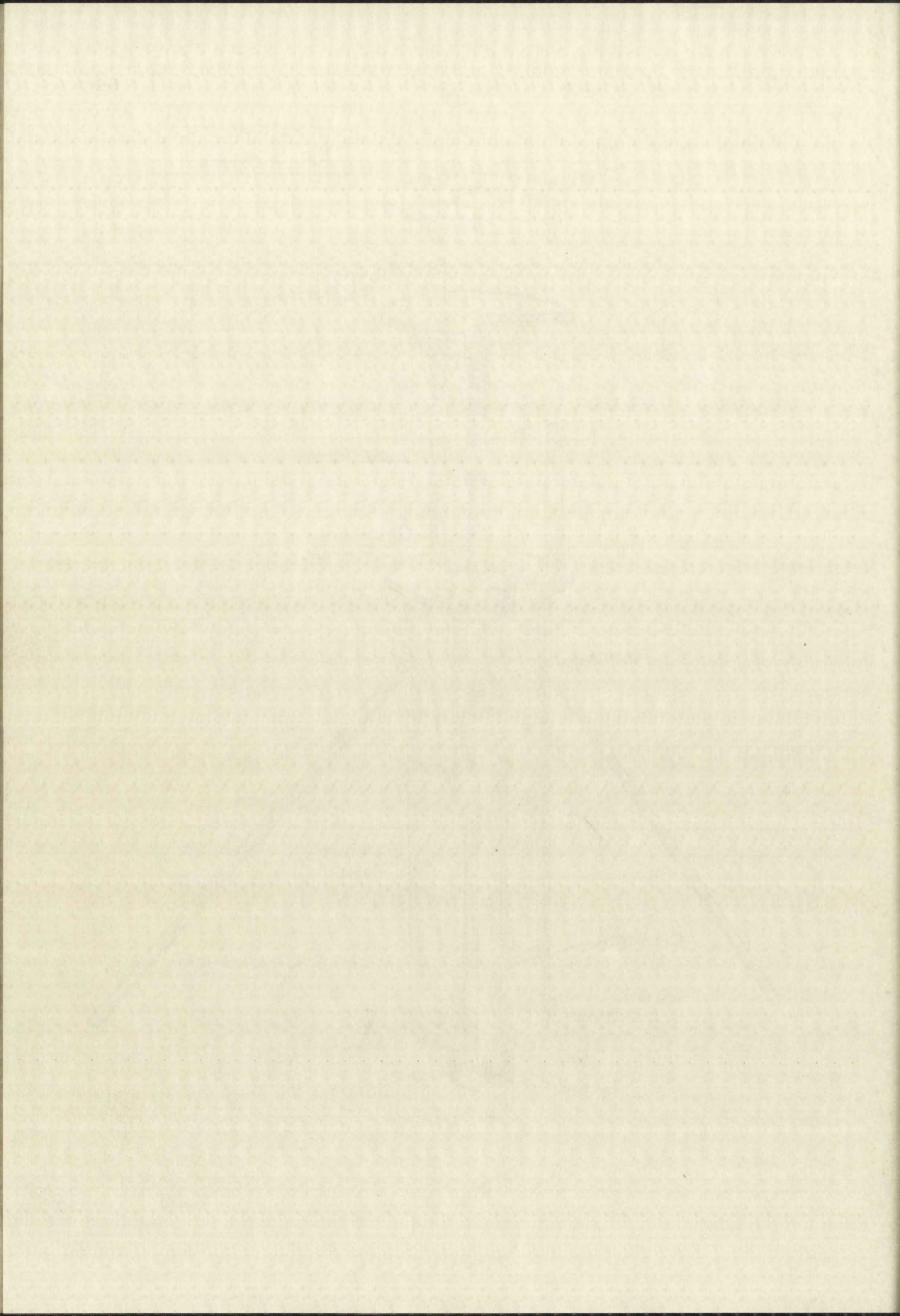




FIG. 6

OVERALL VIEW OF EXPERIMENTAL SETUP

- A Accelerometer
- F Fuse
- S Yard-stick with nichrome wire, Wiper
- W Weights
- O Oscillograph
- N Amplifier
- P Variable resistor and switch for displacement measuring potentiometer circuit.



FIG. 2

OVERALL VIEW OF EXPERIMENTAL SETUP

- | | |
|---|--|
| A | Accelerometer |
| B | Force |
| C | Light-stick with infrared diode, light |
| D | Relay |
| E | Sealograph |
| F | Amplifier |
| G | Variable resistor and switch for |
| H | Displacement measuring potentiometer |
| I | Output |

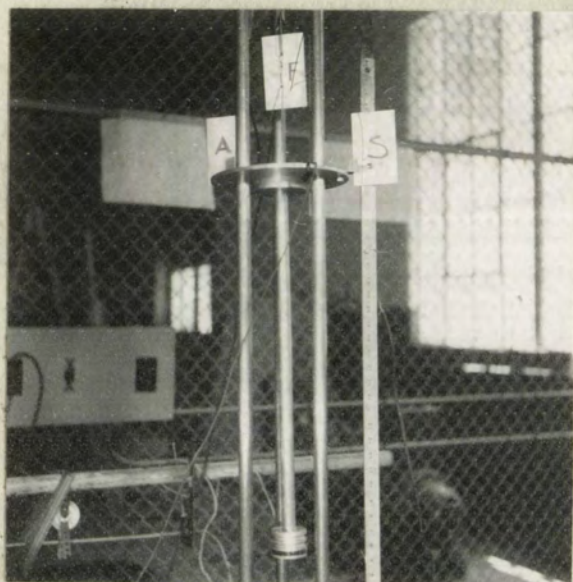


FIG. 7

PISTON ASSEMBLY ON GUIDE RODS

- | | |
|---|--|
| A | Accelerometer |
| F | Fuse |
| S | Wiper for displacement
measuring potentiometer
circuit |



PICTURE SHOWING THE RESULTS OF THE TEST

- | | |
|---|-------------------------------|
| A | 100% of the original strength |
| B | 75% of the original strength |
| C | 50% of the original strength |
| D | 25% of the original strength |
| E | 10% of the original strength |

The piston assembly is shown in Fig. 7. The piston itself was made from an aluminum cylinder turned so as to fit fairly snugly into the air cylinder. Three grooves were provided on the piston to retain rubber "O"-rings. However, it was found during the course of the experiments that one "O"-ring provided as much protection against leakage as three, and that more than one "O"-ring caused too much friction. A 10 inch diameter aluminum disk was connected to the piston by means of a 20 inch length of 1 inch O.D. aluminum pipe. This disk served as a test-platform. It was provided with holes for bolts for fastening weights and instrumentation, and also with holes for the guide rods.

The guide rods consisted of 48 inch lengths of 1 inch diameter cold rolled steel, fastened to the cylinder flange by large nuts. In order to hold these rods in proper alignment, a retaining disk was added at the top end of these rods.

The entire assembly was supported in a tripod made from an 18 inch long section of 8 inch pipe to which were fastened legs of $1\frac{1}{2}$ inch pipe. Three radial screws near the bottom of the support pipe served to fasten the cylinder to the support and to provide an adjustment for vertical positioning of the cylinder.

The first of these is the fact that the
 island was not an extension of the main land
 but a separate entity. It was a small island
 situated in the middle of the bay. It was
 not connected to the main land by any
 isthmus or causeway. It was a small
 island, about 100 feet in diameter, and
 it was situated in the middle of the bay.
 It was not connected to the main land by
 any isthmus or causeway. It was a small
 island, about 100 feet in diameter, and
 it was situated in the middle of the bay.

The second of these is the fact that the
 island was not a part of the main land
 but a separate entity. It was a small
 island, about 100 feet in diameter, and
 it was situated in the middle of the bay.
 It was not connected to the main land by
 any isthmus or causeway. It was a small
 island, about 100 feet in diameter, and
 it was situated in the middle of the bay.

The third of these is the fact that the
 island was not a part of the main land
 but a separate entity. It was a small
 island, about 100 feet in diameter, and
 it was situated in the middle of the bay.
 It was not connected to the main land by
 any isthmus or causeway. It was a small
 island, about 100 feet in diameter, and
 it was situated in the middle of the bay.

A steel wire hook was attached at the center of the test platform to aid in holding the piston assembly in a retracted position. One loop of a "fuse", consisting of a short piece of soft iron wire with loops on both ends, was placed over this hook. The other loop of the fuse was placed over another hook, which in turn was attached to the end of a perforated steel tape. This tape could be fastened to the top retaining disk through any one of its holes, so that the position in which the piston assembly was to be held before release, could be adjusted. Quick release of the piston was then obtained by cutting the "fuse" with a pair of wire cutters. The "fuse" and hooks appear near the letter F in Figures 6 and 7.

Instrumentation. Displacement of the piston was measured by means of a potentiometer arrangement. The potential of a 6-volt automobile battery was applied across a thin Nichrome wire which was stretched along a yard stick mounted parallel to one of the guide rods. A 500 ohm resistor was connected in series with this wire in order to provide more latitude of adjustment of sensitivity. A wiper, made from parts of a relay was mounted near the edge of the test platform disk so as to touch the nichrome wire. The voltage between the wiper and one end of the nichrome wire was led to a D. C. amplifier, the output of which was then fed to one channel of a double channel recorder.

A steel wire hook was attached to the center of the
 end of the wire in holding the piston assembly in a
 restricted position. One inch of a "line", consisting of
 a short piece of soft iron wire with loops on both ends,
 was placed over this hook. The other loop of the wire was
 placed over another hook, which in turn was attached to the
 end of a compressed steel tube. This tube could be loosened
 in the holding disk through one of its holes, so
 that the position in which the piston assembly was to be
 held before release, could be adjusted. When release of
 the piston was then obtained by cutting the "line" with a
 pair of wire cutters. The "line" and hook were held near the
 latter in Figure 6 and 7.

Investigation of the piston
 measured by means of a potentiometer arrangement. The
 potential of a 6-volt automobile battery was applied across
 a thin Nichrome wire which was stretched about a third of an
 inch parallel to one of the guide rods. A 500-ohm re-
 sistor was connected in series with this wire in order to
 provide some limiting of adjustment of sensitivity. A
 very fine transparency of a voltmeter was mounted near the edge
 of the test plate disk so as to touch the nichrome wire.
 The voltage between the wire and one end of the disk was
 wire was led to a D. C. amplifier, the output of which was
 then fed to one channel of a double channel recorder.

Piston acceleration was measured by means of a commercial accelerometer of the strain gage bridge type. The accelerometer output was amplified by means of an A.C. amplifier and recorded on the second channel of the recorder.

The following instruments were used:

D.C. Amplifier, Brush Development Co., Model BL-932, Serial #1216.

Strain Gage Amplifier, Brush Development Co., Model BL-310, Serial #99.

Dual Channel Magnetic Oscillograph, Brush Development Co., Model BL-202, Serial #1253.

Accelerometer, Statham Instruments Co., Model A5A-50-240, Serial #277, Range $\pm 50g$.

II. PROCEDURE

Calibration. The displacement measuring arrangement was calibrated against the yard stick mounted parallel to one of the guide rods. The deflection of the oscillograph needle was recorded for each of several piston positions, as read on the yard stick. In all cases, a linear relation between needle deflection and piston position was observed.

The apparatus for measuring accelerations was calibrated in a range of 2g only and the results were extrapolated to higher accelerations based on previous determinations

of the linearity of the accelerometer, amplifier, and oscillograph. The calibration in the 2g range was obtained simply by inverting the accelerometer and noting the deflection of the oscillograph needle caused by this 2g change on the accelerometer.

Preliminary adjustments and readings. Before each series of test runs the apparatus was thoroughly inspected. A thin coat of oil was applied to the rubber "O"-rings in order to reduce friction and air leakage. Where runs with the pipe cap in place were made, the cap was inspected for leakage by immersing the bottom of the cylinder in water and watching for bubbles when the pressure in the cylinder was increased by pushing on the piston.

The amplifiers were permitted to warm up for at least two hours before calibration prior to each series of test runs. The gain controls on the amplifiers were so adjusted as to give an easily read scale on the oscillograph records. The barometer was read before and after each series of runs.

Measurement of friction. In order to determine the magnitudes of the friction forces and their variation with piston velocity and position, the pipe cap was removed from the bottom of the cylinder so as to leave the air cylinder

open. Then acceleration and displacement of the piston were recorded on the same time base for motion of the piston under the action of gravity and friction only. To accomplish this, the piston assembly was released from various positions and with various weights mounted on it.

Piston weights of 4.25, 6.33, 14.26, 16.50 and 19.34 lbs were used. With each weight the piston was dropped first from a 3 inch height above its lowest possible position; then the drop heights were increased in approximate 3 inch increments until a total height of 21 inches was reached. A typical record obtained appears in graph 15, together with calibration curves.

Measurements of air spring action. The procedure employed here consisted of adjusting the free length of the air column by positioning the piston with the pipe cap removed from the bottom of the air cylinder. Next, after replacing the pipe cap, the piston was fastened in the initial position by means of the fuse arrangement. Then the oscillograph was turned on and the fuse was cut in order to permit the piston to move under the action of the differential air pressure.

The procedure was repeated for several free air column lengths, piston weights, and initial positions. The

values of these variables which were used appear in Table III. A typical record and calibration curves are shown in Graph 16.

III. DATA REDUCTION

Friction. When the piston falls under the action of gravity and the friction forces only, the net accelerating force on the piston is $W - \phi$, where W denotes the gravitational force on the piston assembly (which is equal in magnitude to the piston weight) and ϕ denotes the friction force. The negative sign accounts for the fact that the friction force here opposes the gravitational force. If g denotes the standard acceleration of gravity, then the mass of the piston may be written as W/g . Then, from Newton's second law, letting a denote the acceleration of the system,

$$\frac{W}{g} a = W - \phi$$

and
$$\phi = W \left(1 - \frac{a}{g} \right)$$

The ratio a/g may be read directly from the oscillograph record which was calibrated in g units. W was determined by direct weighing, so that ϕ may be evaluated from the above equation.

values of these quantities which were used in Table II. A typical plot of ϕ versus ω is shown in Figure 10.

III. DATA REDUCTION

Friction. When the plate falls under the action of gravity and the friction forces only, the net acceleration of the plate is $g - \phi$, where g denotes the gravitational force on the plate assembly (which is equal in magnitude to the plate weight) and ϕ denotes the friction force. The negative sign accounts for the fact that the friction force here opposes the gravitational force. If a denotes the standard acceleration of gravity, then the mass of the plate may be written as W/g . Then, from Newton's second law, for a force F the acceleration of the system

$$\frac{W}{g} a = W - \phi$$

$$\text{and } \phi = W \left(1 - \frac{a}{g} \right)$$

The ratio a/g may be read directly from the oscillograph record when the calibration is 2 units. It was determined by direct timing, at that ϕ may be evaluated from the above equation.

Acceleration and displacement were recorded simultaneously as functions of time, so that friction and displacement could be correlated for any instant. Velocity was not measured directly, but mean velocities for short time intervals were computed by dividing the change in displacement as read from the displacement record, by the time interval. For each displacement record a velocity-time curve was plotted, by means of which friction force and velocity could be correlated for any instant.

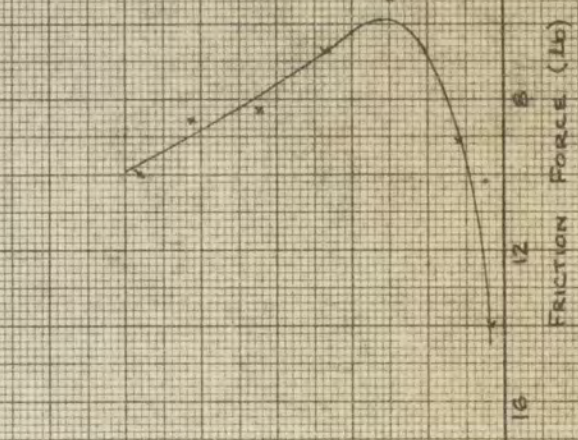
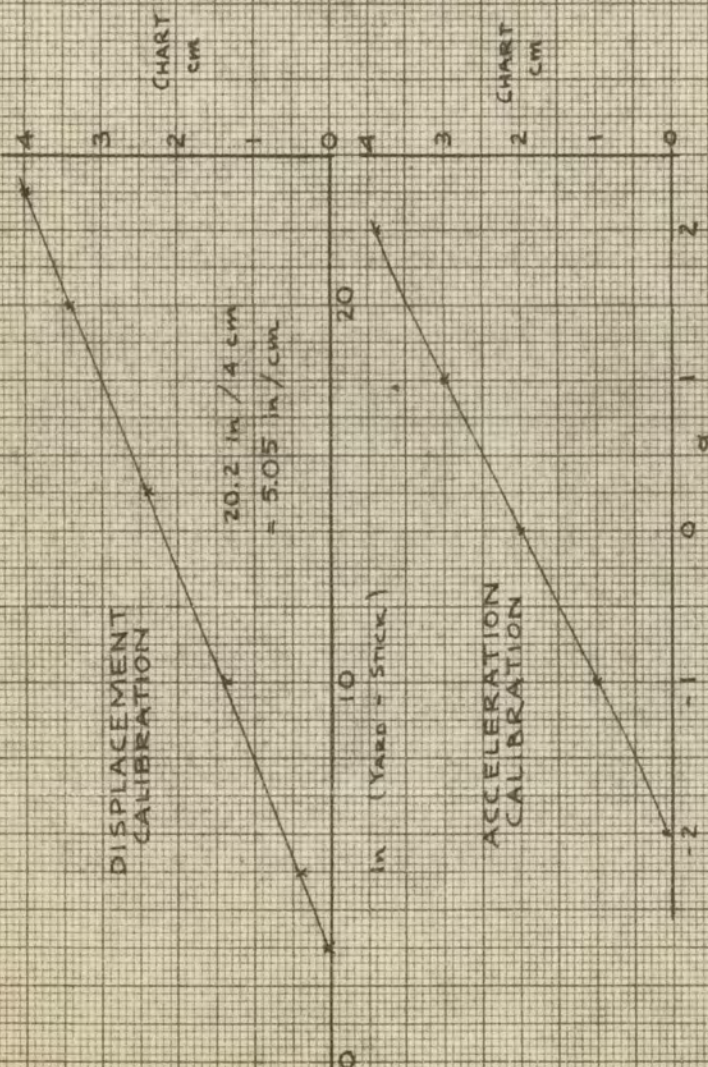
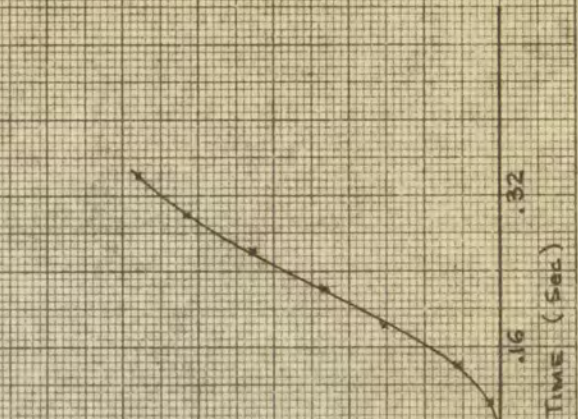
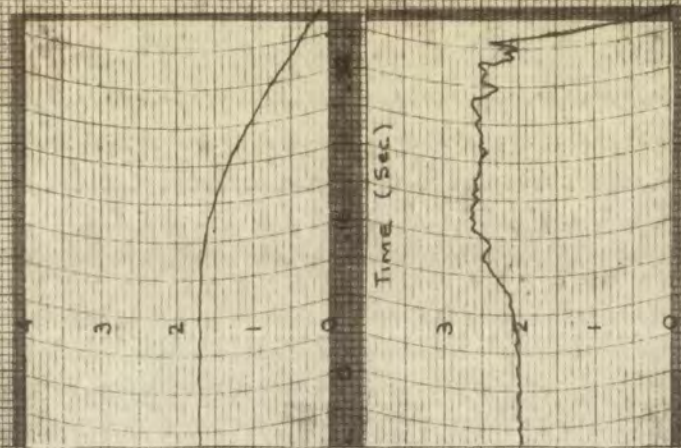
Graph 15 shows a typical oscillograph record for a friction test, together with calibration curves and the velocity-time curve constructed from the record and the friction force vs. velocity curve obtained from these data.

Air spring action. The initial displacement, maximum acceleration, and build-up time, could be read directly from the oscillograph record with the aid of the calibration curves. Graph 16 shows a sample record with corresponding calibration curves, and indicates how measurement of these quantities was performed. Table III lists data and experimental results and also shows calculations for reduction of these results into the terms of the nondimensional variables previously defined.

acceleration and displacement were recorded simultaneously as functions of time, so that friction and displacement could be correlated for any instant. Friction was not measured directly, but mass velocities for short time intervals were obtained by dividing the change in displacement as read from the displacement record, by the time interval. For each displacement record a velocity-time curve was plotted, by means of which friction force and velocity could be correlated for any instant.

Graph 15 shows a typical oscillation record for a friction test, together with calibration curves and the velocity-time curve constructed from the record and the friction force vs. velocity curve obtained from these data.

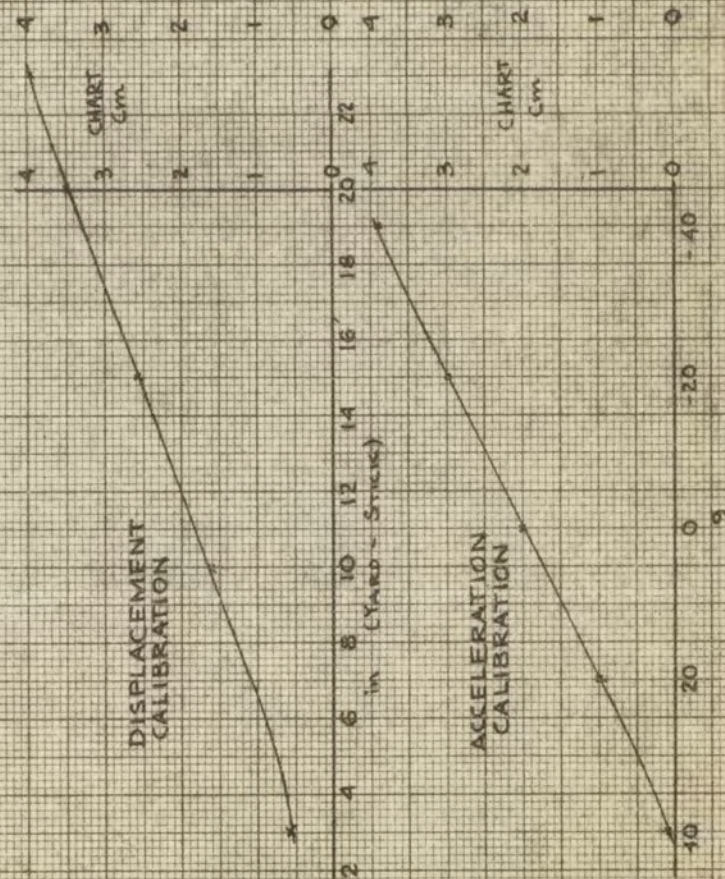
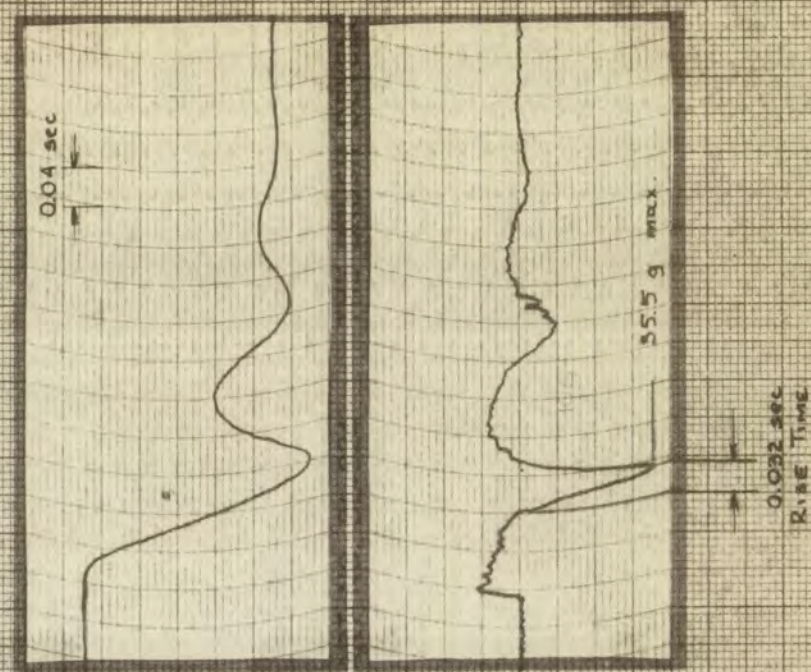
All testing results. The initial displacement, maximum acceleration, and falling time, could be read directly from the oscillation record with the aid of the calibration curves. Graph 16 shows a sample record with corresponding calibration curves, and indicates the measurement of these quantities was performed. Table III lists test and experimental results and also shows values for reduction of these results into the form of the nondimensional variables previously defined.



SAMPLE CALCULATION OF
VARIATION OF FRICTION WITH
VELOCITY, FROM
OSCILLOGRAPH RECORD
(16.5 lb PISTON)

SAMPLE REDUCTION OF OSKILLOGRAPH DATA, AIR SPRING VIBRATION

$L = 4.0 \text{ in.}$, $W = 4.26 \text{ lb.}$, $P_0 = 12.1 \text{ Psi}$



GRAPH 16

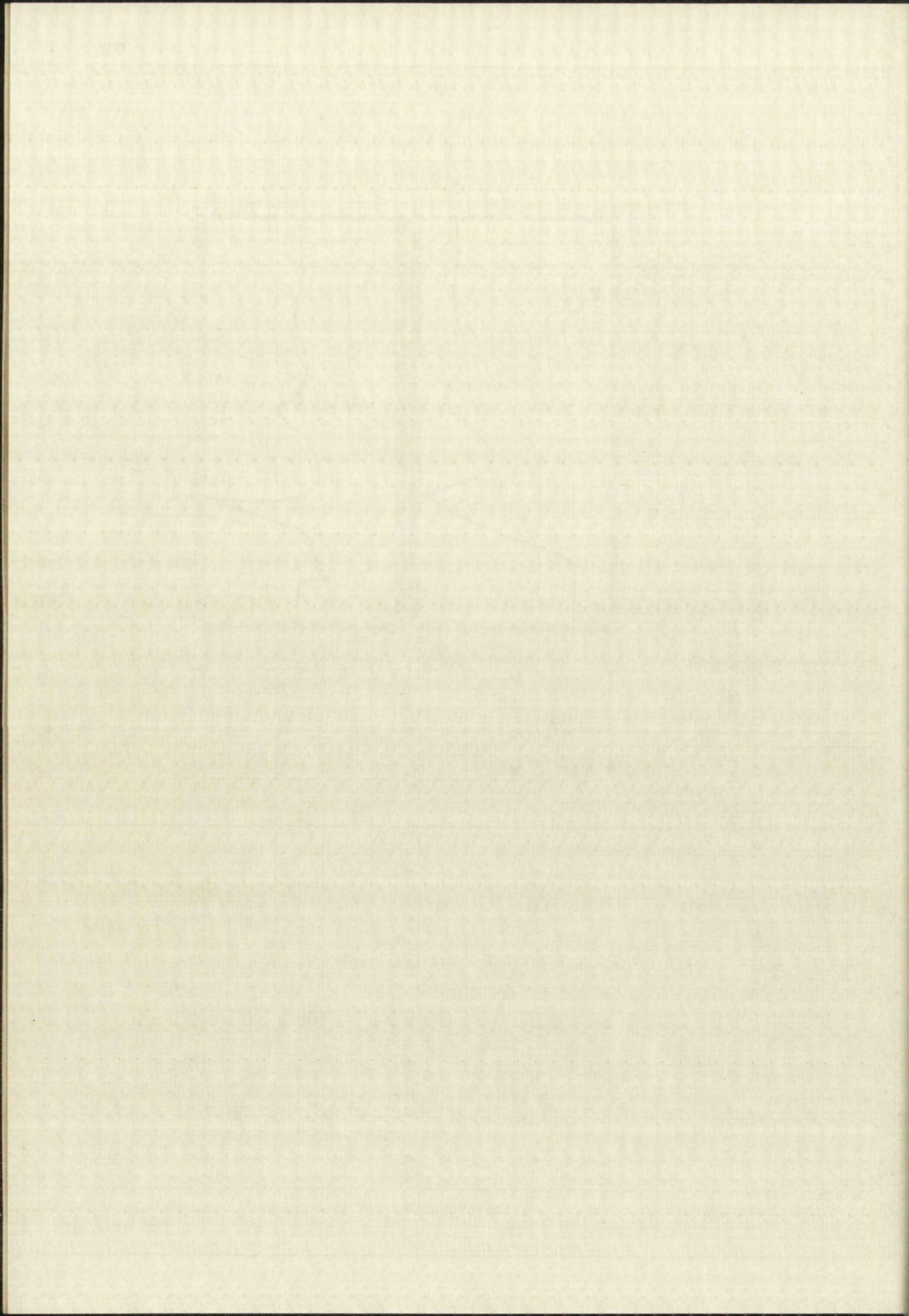


TABLE III

DATA AND RESULTS FOR TEST OF EXPERIMENTAL AIR SPRING

Symbols:	x_0	Initial displacement of piston from equilibrium position (in)
	L	Length of air column at equilibrium (in)
	β	$1 + \frac{AP_0}{W}$
	t_B	Acceleration build-up time (sec)
	$\left(\ddot{\frac{x}{g}}\right)_{\max}$	Maximum piston acceleration in terms of acceleration of gravity
	x	$\frac{x}{L}$
	\ddot{x}_{\max}	$\frac{1}{\beta} \left(\frac{\ddot{x}}{g} \right)_{\max}$
	T_0	$2\pi \sqrt{\frac{L}{g\gamma\beta}}$
	B	t_B/T_0
	A	Piston area (in ²) = 4.91 in ²
	P_0	Ambient pressure (psi) = 12.10 psi
	W	Piston weight (lb)

1. The first part of the experiment was to determine the effect of the concentration of the solution on the rate of reaction. The results are shown in Table I.

2. The second part of the experiment was to determine the effect of the temperature on the rate of reaction. The results are shown in Table II.

3. The third part of the experiment was to determine the effect of the catalyst on the rate of reaction. The results are shown in Table III.

4. The fourth part of the experiment was to determine the effect of the solvent on the rate of reaction. The results are shown in Table IV.

5. The fifth part of the experiment was to determine the effect of the pressure on the rate of reaction. The results are shown in Table V.

6. The sixth part of the experiment was to determine the effect of the time on the rate of reaction. The results are shown in Table VI.

7. The seventh part of the experiment was to determine the effect of the concentration of the solution on the rate of reaction. The results are shown in Table I.

8. The eighth part of the experiment was to determine the effect of the temperature on the rate of reaction. The results are shown in Table II.

9. The ninth part of the experiment was to determine the effect of the catalyst on the rate of reaction. The results are shown in Table III.

10. The tenth part of the experiment was to determine the effect of the solvent on the rate of reaction. The results are shown in Table IV.

11. The eleventh part of the experiment was to determine the effect of the pressure on the rate of reaction. The results are shown in Table V.

12. The twelfth part of the experiment was to determine the effect of the time on the rate of reaction. The results are shown in Table VI.

DATA AND RESULTS FOR EACH OF THE EXPERIMENTS ARE GIVEN

RUN NO.	W	L	x_0	β	t_B	$\ddot{\left(\frac{x}{g}\right)}_{\max}$	x_0	$\frac{x}{4\pi^2}$	\ddot{x}_{\max}	T_0	τ_B
1	4.26	4.0	4.5	14.98	.033	11.5	1.12	.77		0.14	.23
2	4.26	4.0	8.0	14.98	.038	15.7	2.00	1.05		0.14	.27
3	4.26	4.0	11.3	14.98	.036	22.0	2.83	1.47		0.14	.26
4	4.26	4.0	10.8	14.98	.033	25.0	2.70	1.60		0.14	.23
5	4.26	4.0	16.2	14.98	.032	35.5	4.05	2.37		0.14	.22
6	4.26	4.0	19.0	14.98	.033	41.3	4.70	2.76		0.14	.23
7	7.40	4.0	8.5	9.04	.042	5.0	2.13	.55		0.18	.24
8	7.40	4.0	7.0	9.04	.050	11.0	1.75	1.12		0.18	.28
9	7.40	4.0	10.5	9.04	.043	16.0	2.63	1.77		0.18	.24
10	7.40	4.0	12.7	9.04	.042	20	3.18	2.21		0.18	.23
11	7.40	4.0	15.1	9.04	.039	28	3.76	3.10		0.18	.22
12	7.40	4.0	16.3	9.04	.038	31	4.08	3.43		0.18	.21
13	10.40	3.75	4.9	6.72	.048	5.7	1.32	.85		0.20	.24
14	10.40	3.75	8.8	6.72	.049	10.3	2.36	1.53		0.20	.24
15	10.40	3.75	10.4	6.72	.047	12.2	2.79	1.81		0.20	.23
16	10.40	3.75	14.3	6.72	.048	17	3.82	2.53		0.20	.24

RUN NO.	W	L	X ₀	β	t _B	$\left(\frac{\ddot{x}}{g}\right)_{\max}$	X ₀	$\frac{\gamma}{4\pi^2}$	\ddot{x}_{\max}	T ₀	T _B
17	10.40	3.75	17.2	6.72		Illegible	Record			0.20	
18	14.42	3.5	6.7	5.12	.055	6	1.93	1.17		0.22	.25
19	14.42	3.5	10.6	5.12	.052	10	3.03	1.95		0.22	.23
20	14.42	3.5	14.0	5.12	.048	16	4.00	3.13		0.22	.21
21	19.44	3.4	4.7	4.06	.050	8	1.41	1.97		.22	.23
22	19.44	3.25	8.8	4.06	.054	13	2.72	3.21		.22	.25
23	19.44	3.25	11.2	4.06	.047	Stage	Hit	Bottom			
24	4.26	6.75	2.7	14.98	.020	6.5	.41	.43		.182	.14
25	4.26	6.75	6.0	14.98	.033	8.5	.90	.57		.182	.18
26	4.26	6.7	9.3	14.98	.047	10.0	1.39	.67		.181	.26
27	4.26	6.9	11.1	14.98	.042	12.0	1.62	.80		.183	.23
28	4.26	7.00	14.8	14.98	.047	17.0	2.11	1.13		.185	.26
29	7.40	6.4	3.7	9.04	.043	5.0	.57	.55		.229	.19
30	7.40	6.5	6.8	9.04	.046	7.0	1.05	.77		.230	.20
31	7.40	6.5	9.5	9.04	.046	8.0	1.46	.88		.230	.20
32	7.40	6.5	14.1	9.04	.045	11.4	2.17	1.26		.230	.19

RUN NO.	W	L	x_0	β	t_B	$\left(\frac{\bar{x}}{g}\right)_{\max}$	x_0	$\frac{\gamma}{4\pi^2}$	\bar{x}_{\max}	T_0	T_B
33	10.40	6.4	4.7	6.72	.040	2.2	.74	.33	.264	.15	
34	10.40	6.25	8.05	6.72	.046	6.0	1.29	.88	.261	.17	
35	10.40	6.2	10.0	6.72	.045	7.0	1.62	1.04	.260	.17	
36	10.40	6.25	12.0	6.72	.053	8.7	1.93	1.29	.261	.21	
37	10.40	6.25	14.4	6.72	.050	11.0	2.31	1.63	.261	.19	
38	10.40	5.8	3.7	6.72	.054	2.0	.63	.30	.253	.21	
39	10.40	5.9	7.2	6.72	.069	4.0	1.23	.60	.253	.27	
40	10.40	5.9	10.1	6.72	.058	6.0	1.73	.89	.253	.23	
41	10.40	5.8	12.4	6.72	.062	7.7	2.12	1.14	.25	.24	
42	10.40	5.9	15.9	6.72	.063	10.2	2.72	1.52	.25	.25	
43	14.42	5.5	4.9	5.12	.050	2.2	.89	.43	.28	.18	
44	14.42	5.5	8.4	5.12	.066	4.0	1.53	.78	.28	.23	
45	14.42	5.5	10.6	5.12	.066	5.5	1.93	1.07	.28	.23	
46	14.42	5.5	12.8	5.12	.065	7.0	2.32	1.37	.28	.23	
47	14.42	5.5	15.2	5.12	.062	8.4	2.76	1.64	.28	.22	
48	4.26	6.9	13.9	14.98	.046	16.4	2.03	1.09	.18	.25	

ST	Q ²	ROM	$\frac{X}{S.M.}$	Q ²	ROM	$\left(\frac{X}{S}\right)$	Q ²	Q	Q ²	L	V	NUM
31.	103.	22.		27.	2.5		040.	27.3	5.2	4.3	04.01	73
31.	104.	23.		28.1	0.0		240.	27.3	20.3	33.3	04.01	22
31.	023.	40.1		29.1	0.7		240.	27.3	0.01	3.0	04.01	32
32.	123.	40.1		29.1	0.3		240.	27.3	0.01	33.3	04.01	33
32.	120.	33.4		29.3	0.17		220.	27.3	2.41	22.3	04.01	76
32.	107.	07.		29.	0.3		140.	27.3	5.3	3.0	04.01	26
32.	0.0	02.		29.1	0.3		230.	27.3	0.7	3.3	04.01	27
32.	225.	25.		29.1	0.3		240.	27.3	1.01	2.3	04.01	28
32.	22.	41.1		29.3	5.7		220.	27.3	4.81	3.3	04.01	72
31.	22.	35.1		29.3	10.01		230.	27.3	9.21	3.3	04.01	25
31.	22.	14.		29.	2.1		020.	27.3	2.4	3.0	04.01	24
30.	22.	45.		29.1	0.3		230.	27.3	2.3	3.3	04.01	44
30.	08.	10.1		29.1	4.5		230.	27.3	0.01	3.0	04.01	35
30.	04.	14.1		29.3	0.7		240.	27.3	0.81	3.3	04.01	23
30.	27.	14.1		29.1	2.3		230.	27.3	1.61	3.0	04.01	74
30.	01.	14.1		29.3	4.37		240.	27.3	0.31	3.3	04.01	21

RUN NO.	W	L	x_0	β	t_B	$\left(\frac{x}{g}\right)_{\max}$	x_0	$\frac{\gamma}{4\pi^2}$	\ddot{x}_{\max}	T_0	T_B
49	19.44	5.5	13.9	4.06	.062	8.0	2.53	1.97		.31	.20
50	4.26	10.0	4.3	14.98	.026	2.5	.43	.17		.22	.12
51	4.26	10.1	7.1	14.98	.034	5.3	.70	.35		.22	.15
52	4.26	10.25	9.6	14.98	.042	6.4	.94	.43		.22	.19
53	4.26	10.25	11.0	14.98	.048	8.0	1.08	.53		.22	.21
54	7.40	9.6	4.7	9.04	.050	2.8	.50	.32		.28	.18
55	7.40	9.6	7.5	9.04	.055	4.3	.78	.48		.280	.20
56	7.40	9.6	9.7	9.04	.072	5.0	1.04	.55		.280	.26
57	7.40	9.6	13.1	9.04	.065	7.0	1.36	.77		.280	.23
58	10.40	9.1	6.1	6.72	.057	4.4	.67	.65		.32	.18
59	10.40	9.2	11.3	6.72	.056	5.0	1.23	.74		.32	.18
60	10.40	9.25	9.7	6.72	.063	6.9	1.05	1.03		.32	.20
61	10.40	9.25	12.1	6.72	.058	8.0	1.31	1.19		.32	.18
62	10.40	9.4	11.6	6.72	.066	12.1	1.24	1.80		.32	.21
63	10.40	9.25	13.1	6.72	.072	13.6	1.42	2.02		.32	.23
64	7.40	8.7	4.3	9.04	.086	5.4	.50	.60		.26	.33

NO.	A	B	C	D	E	F	G	H	I	J	K	L	M	N	O	P	Q	R	S	T	U	V	W	X	Y	Z	aa	ab	ac	ad	ae	af	ag	ah	ai	aj	ak	al	am	an	ao																																																																																																																																																																																																																																																																																																																																																																																																																																																																																																																																																																																																																																																																																																																																																																																																																																																																																																																																																																																	
01.	00.	00.	00.	00.	00.	00.	00.	00.	00.	00.	00.	00.	00.	00.	00.	00.	00.	00.	00.	00.	00.	00.	00.	00.	00.	00.	00.	00.	00.	00.	00.	00.	00.	00.	00.	00.	00.	00.	00.	00.	00.	00.	00.	00.	00.	00.	00.	00.	00.	00.	00.	00.	00.	00.	00.	00.	00.	00.	00.	00.	00.	00.	00.	00.	00.	00.	00.	00.	00.	00.	00.	00.	00.	00.	00.	00.	00.	00.	00.	00.	00.	00.	00.	00.	00.	00.	00.	00.	00.	00.	00.	00.	00.	00.	00.	00.	00.	00.	00.	00.	00.	00.	00.	00.	00.	00.	00.	00.	00.	00.	00.	00.	00.	00.	00.	00.	00.	00.	00.	00.	00.	00.	00.	00.	00.	00.	00.	00.	00.	00.	00.	00.	00.	00.	00.	00.	00.	00.	00.	00.	00.	00.	00.	00.	00.	00.	00.	00.	00.	00.	00.	00.	00.	00.	00.	00.	00.	00.	00.	00.	00.	00.	00.	00.	00.	00.	00.	00.	00.	00.	00.	00.	00.	00.	00.	00.	00.	00.	00.	00.	00.	00.	00.	00.	00.	00.	00.	00.	00.	00.	00.	00.	00.	00.	00.	00.	00.	00.	00.	00.	00.	00.	00.	00.	00.	00.	00.	00.	00.	00.	00.	00.	00.	00.	00.	00.	00.	00.	00.	00.	00.	00.	00.	00.	00.	00.	00.	00.	00.	00.	00.	00.	00.	00.	00.	00.	00.	00.	00.	00.	00.	00.	00.	00.	00.	00.	00.	00.	00.	00.	00.	00.	00.	00.	00.	00.	00.	00.	00.	00.	00.	00.	00.	00.	00.	00.	00.	00.	00.	00.	00.	00.	00.	00.	00.	00.	00.	00.	00.	00.	00.	00.	00.	00.	00.	00.	00.	00.	00.	00.	00.	00.	00.	00.	00.	00.	00.	00.	00.	00.	00.	00.	00.	00.	00.	00.	00.	00.	00.	00.	00.	00.	00.	00.	00.	00.	00.	00.	00.	00.	00.	00.	00.	00.	00.	00.	00.	00.	00.	00.	00.	00.	00.	00.	00.	00.	00.	00.	00.	00.	00.	00.	00.	00.	00.	00.	00.	00.	00.	00.	00.	00.	00.	00.	00.	00.	00.	00.	00.	00.	00.	00.	00.	00.	00.	00.	00.	00.	00.	00.	00.	00.	00.	00.	00.	00.	00.	00.	00.	00.	00.	00.	00.	00.	00.	00.	00.	00.	00.	00.	00.	00.	00.	00.	00.	00.	00.	00.	00.	00.	00.	00.	00.	00.	00.	00.	00.	00.	00.	00.	00.	00.	00.	00.	00.	00.	00.	00.	00.	00.	00.	00.	00.	00.	00.	00.	00.	00.	00.	00.	00.	00.	00.	00.	00.	00.	00.	00.	00.	00.	00.	00.	00.	00.	00.	00.	00.	00.	00.	00.	00.	00.	00.	00.	00.	00.	00.	00.	00.	00.	00.	00.	00.	00.	00.	00.	00.	00.	00.	00.	00.	00.	00.	00.	00.	00.	00.	00.	00.	00.	00.	00.	00.	00.	00.	00.	00.	00.	00.	00.	00.	00.	00.	00.	00.	00.	00.	00.	00.	00.	00.	00.	00.	00.	00.	00.	00.	00.	00.	00.	00.	00.	00.	00.	00.	00.	00.	00.	00.	00.	00.	00.	00.	00.	00.	00.	00.	00.	00.	00.	00.	00.	00.	00.	00.	00.	00.	00.	00.	00.	00.	00.	00.	00.	00.	00.	00.	00.	00.	00.	00.	00.	00.	00.	00.	00.	00.	00.	00.	00.	00.	00.	00.	00.	00.	00.	00.	00.	00.	00.	00.	00.	00.	00.	00.	00.	00.	00.	00.	00.	00.	00.	00.	00.	00.	00.	00.	00.	00.	00.	00.	00.	00.	00.	00.	00.	00.	00.	00.	00.	00.	00.	00.	00.	00.	00.	00.	00.	00.	00.	00.	00.	00.	00.	00.	00.	00.	00.	00.	00.	00.	00.	00.	00.	00.	00.	00.	00.	00.	00.	00.	00.	00.	00.	00.	00.	00.	00.	00.	00.	00.	00.	00.	00.	00.	00.	00.	00.	00.	00.	00.	00.	00.	00.	00.	00.	00.	00.	00.	00.	00.	00.	00.	00.	00.	00.	00.	00.	00.	00.	00.	00.	00.	00.	00.	00.	00.	00.	00.	00.	00.	00.	00.	00.	00.	00.	00.	00.	00.	00.	00.	00.	00.	00.	00.	00.	00.	00.	00.	00.	00.	00.	00.	00.	00.	00.	00.	00.	00.	00.	00.	00.	00.	00.	00.	00.	00.	00.	00.	00.	00.	00.	00.	00.	00.	00.	00.	00.	00.	00.	00.	00.	00.	00.	00.	00.	00.	00.	00.	00.	00.	00.	00.	00.	00.	00.	00.	00.	00.	00.	00.	00.	00.	00.	00.	00.	00.	00.	00.	00.	00.	00.	00.	00.	00.	00.	00.	00.	00.	00.	00.	00.	00.	00.	00.	00.	00.	00.	00.	00.	00.	00.	00.	00.	00.	00.	00.	00.	00.	00.	00.	00.	00.	00.	00.	00.	00.	00.	00.	00.	00.	00.	00.	00.	00.	00.	00.	00.	00.	00.	00.	00.	00.	00.	00.	00.	00.	00.	00.	00.	00.	00.	00.	00.	00.	00.	00.	00.	00.	00.	00.	00.	00.	00.	00.	00.	00.	00.	00.	00.	00.	00.	00.	00.	00.	00.	00.	00.	00.	00.	00.	00.	00.	00.	00.	00.	00.	00.	00.	00.	00.	00.	00.	00.	00.	00.	00.	00.	00.	00.	00.	00.	00.	00.	00.	00.	00.	00.	00.	00.	00.	00.	00.	00.	00.	00.	00.	00.	00.	00.	00.	00.	00.	00.	00.	00.	00.	00.	00.	00.	00.	00.	00.	00.	00.	00.	00.	00.	00.	00.	00.	00.	00.	00.	00.	00.	00.	00.	00.	00.	00.	00.	00.	00.	00.	00.	00.	00.	00.	00.	00.	00.	00.	00.	00.	00.	00.	00.	00.	00.	00.	00.	00.	00.	00.	00.	00.	00.	00.	00.	00.	00.	00.	00.	00.	00.	00.	00.	00.	00.	00.	00.	00.	00.	00.	00.	00.	00.	00.	00.	00.	00.	00.	00.	00.	00.	00.	00.	00.	00.	00.	00.	00.	00.	00.	00.</

RUN NO.	W	L	x_0	β	t_B	$\left(\frac{x}{g}\right)_{\max}$	x_0	$\frac{x}{4\pi g}$	x_{\max}	t_0	T_B
65	7.40	8.75	7.7	9.04	.076	7.3	.89	.81	.27	.27	.29
66	7.40	8.75	11.1	9.04	.078	10.0	1.27	1.11	.27	.27	.29
67	7.40	8.6	12.7	9.04	.096	12.0	1.49	1.33	.27	.27	.36
68	7.40	8.7	14.5	9.04	.080	13.5	1.67	1.49	.27	.27	.30
69	19.44	8.1	5.4	4.06	.082	4.5	.66	1.11	.38	.38	.21
70	19.44	8.1	7.6	4.06	.094	6.1	.93	1.50	.38	.38	.25
71	19.44	8.1	9.4	4.06	.094	7.8	1.06	1.92	.38	.38	.25
72	19.44	8.1	11.8	4.06	.089	10.5	1.45	2.59	.38	.38	.23
73	19.44	8.2	13.7	4.06	.094	11.7	1.67	2.89	.38	.38	.24
74	4.26	12.5	4.6	14.98	.050	2.0	.37	.13	.25	.25	.20
75	4.26	12.5	6.8	14.98	.051	2.8	.54	.19	.25	.25	.21
76	4.26	12.5	9.3	14.98	.082	6.0	.74	.40	.25	.25	.33
77	7.40	12.0	3.7	9.04	.046	2.2	.31	.24	.31	.31	.15
78	7.40	12.0	5.8	9.04	.063	2.6	.48	.29	.31	.31	.20
79	7.40	12.0	7.7	9.04	.062	3.5	.64	.39	.31	.31	.20
80	7.40	12.0	9.9	9.04	.062	4.0	.82	.44	.31	.31	.20

RUN NO.	W	L	x_0	β	t_B	$\left(\frac{\ddot{x}}{g}\right)_{\max}$	x_0	$\frac{\gamma}{4\pi^2}$	\ddot{x}_{\max}	T_0	T_B
81	10.40	11.5	4.3	6.72	.070	1.3	.37	.19	.37	.37	.19
82	10.40	11.5	5.2	6.72	.066	2.0	.45	.30	.37	.37	.18
83	10.40	11.5	8.0	6.72	.070	3.2	.70	.48	.37	.37	.19
84	10.40	11.5	9.4	6.72	.081	2.9	.82	.43	.370	.370	.22
85	14.42	10.9	4.5	5.12	.060	1.4	.41	.27	.40	.40	.16
86	14.42	10.75	7.4	5.12	.069	2.0	.69	.39	.39	.39	.17
87	14.42	10.9	10.9	5.12	.072	2.3	.99	.45	.40	.40	.18
88	19.44	10.4	5.1	4.06	.088	1.2	.49	.30	.43	.43	.20
89	19.44	10.25	8.2	4.06	.086	2.0	.81	.49	.43	.43	.20
90	19.44	10.25	9.5	4.06	.058	2.2	.93	.54	.43	.43	.13
91	19.44	10.25	12.6	4.06	.089	3.2	1.23	.79	.43	.43	.20
92	4.26	16.3	4.8	14.98	.030	1.0	.29	.07	.29	.29	.10
93	4.26	16.4	5.9	14.98	.066	2.0	.36	.13	.29	.29	.23
94	7.40	15.75	3.8	9.04	.053	1.2	.24	.13	.36	.36	.15
95	7.40	15.7	7.3	9.04	.082	2.1	.47	.23	.36	.36	.23
96	10.40	15.0	5.1	6.72	.088	1.4	.34	.21	.40	.40	.22

RUN NO.	W	L	x_0	β	t_B	$\left(\frac{\ddot{x}}{g}\right)_{\max}$	x_0	$\frac{\gamma}{4\pi^2} \ddot{x}_{\max}$	T_0	τ_B
97	10.40	15.0	8.6	6.72	.096	2.1	.57	.31	.40	.24
98	14.42	14.1	4.2	5.12	.094	1.0	.30	.20	.45	.21
99	14.42	14.2	8.1	5.12	.105	1.5	.57	.29	.45	.23
100	19.44	13.4	4.9	4.06	.101	1.2	.37	.30	.49	.20
101	19.44	13.4	5.4	4.06	.097	.8	.41	.20	.49	.20
102	19.44	13.4	6.7	4.06	.110	1.2	.51	.30	.49	.22
103	19.44	13.4	8.9	4.06	.118	1.7	.67	.42	.49	.24
104	4.26	3.1	4.5	14.98	.026	Illegible	1.44	Illegible	.13	.21
105	4.26	3.1	6.9	14.98	.035	21	2.21	1.40	.13	.27
106	4.26	3.1	8.9	14.98	.032	25	2.84	1.69	.13	.25
107	4.26	3.1	11.9	14.98	Stage	Hit	Bottom		.13	
108	7.40	3.0	4.3	9.04	.039	6.8	1.43	.75	.16	.25
109	7.40	3.0	4.8	9.04	.036	10.0	1.60	1.11	.16	.23
110	7.40	3.0	7.5	9.04	.035	15.0	2.50	1.66	.16	.23
111	7.40	3.0	10.5	9.04	Stage	Hit	Bottom		.16	
112	10.40	2.75	3.5	6.72	.035	6.0	1.29	.88	.17	.20
113	10.40	2.75	5.8	6.72	Stage	Hit	Bottom		.17	

IV. EXPERIMENTAL RESULTS

Friction. The experimental results are plotted in Graph 17. From this graph there appears to be no correlation between friction force and piston position. A relation between friction force and velocity, however, is evident. It is of interest to note that the shape of the mean curve obtained is like that of the curve showing the variation of friction coefficient with speed for a journal bearing with constant lubricant viscosity and bearing pressure. Graph 18, taken from Design of Machine Elements by V. M. Faires²⁵, is a reproduction of such a curve. The similarity observed is not surprising, since the measurements on the air spring and those for the bearing show essentially the variation of friction with speed in the presence of an oil film.

Air spring action. Results of work with the experimental air spring are shown in Table III in terms of both the actual and the dimensionless variables. Graphs 19 through 23 show plots of dimensionless acceleration and dimensionless acceleration build-up time against dimensionless

²⁵ V. M. Faires, Design of Machine Elements (New York: The Macmillan Company, 1941) p. 347. Taken from S.A. McKee and T.R. McKee, "Friction of Journal Bearings Influenced by Clearance and Length" A.S.M.E. Transactions, Vol. 51.

EXPERIMENTAL RESULTS

Experiment I. The experimental results are plotted in

Graph IV. From this graph there appears to be no correlation

between friction torque and piston position. A relation

between friction torque and velocity, however, is evident.

It is of interest to note that the shape of the curve in

Graph IV is like that of the curve showing the variation of

friction coefficient with speed for a journal bearing with

constant lubricant viscosity and bearing pressure. Graph

IV, taken from Journal of Applied Mechanics by V. M. Faires

is a reproduction of such a curve. The similarity observed

is not surprising, since the measurements on the air engine

and those for the bearing are essentially the variation of

friction with speed in the presence of an oil film.

Experiment II. Results of work with the

experimental air engine are shown in Table III in terms of

both air speed and the dimensionless variable, G/\sqrt{P} .

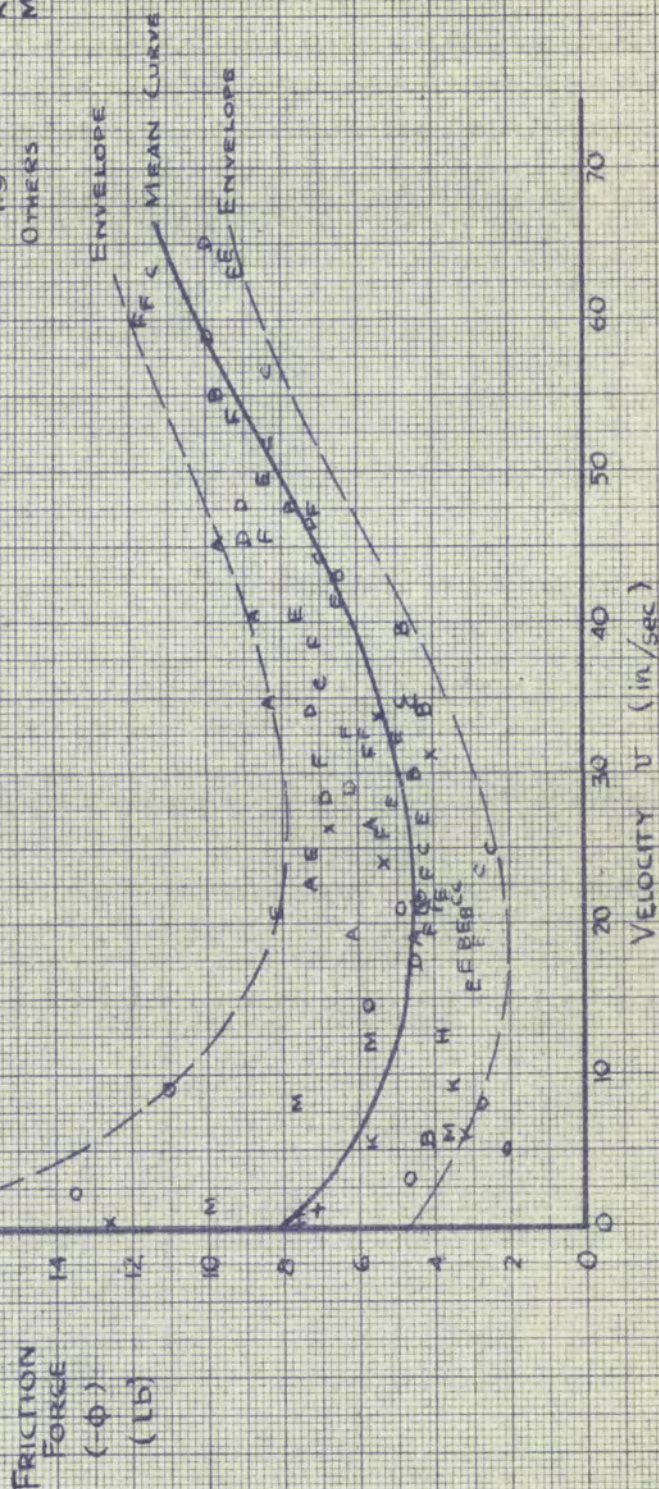
It should be noted that the dimensionless coefficient and

dimensionless acceleration being the same dimensionless

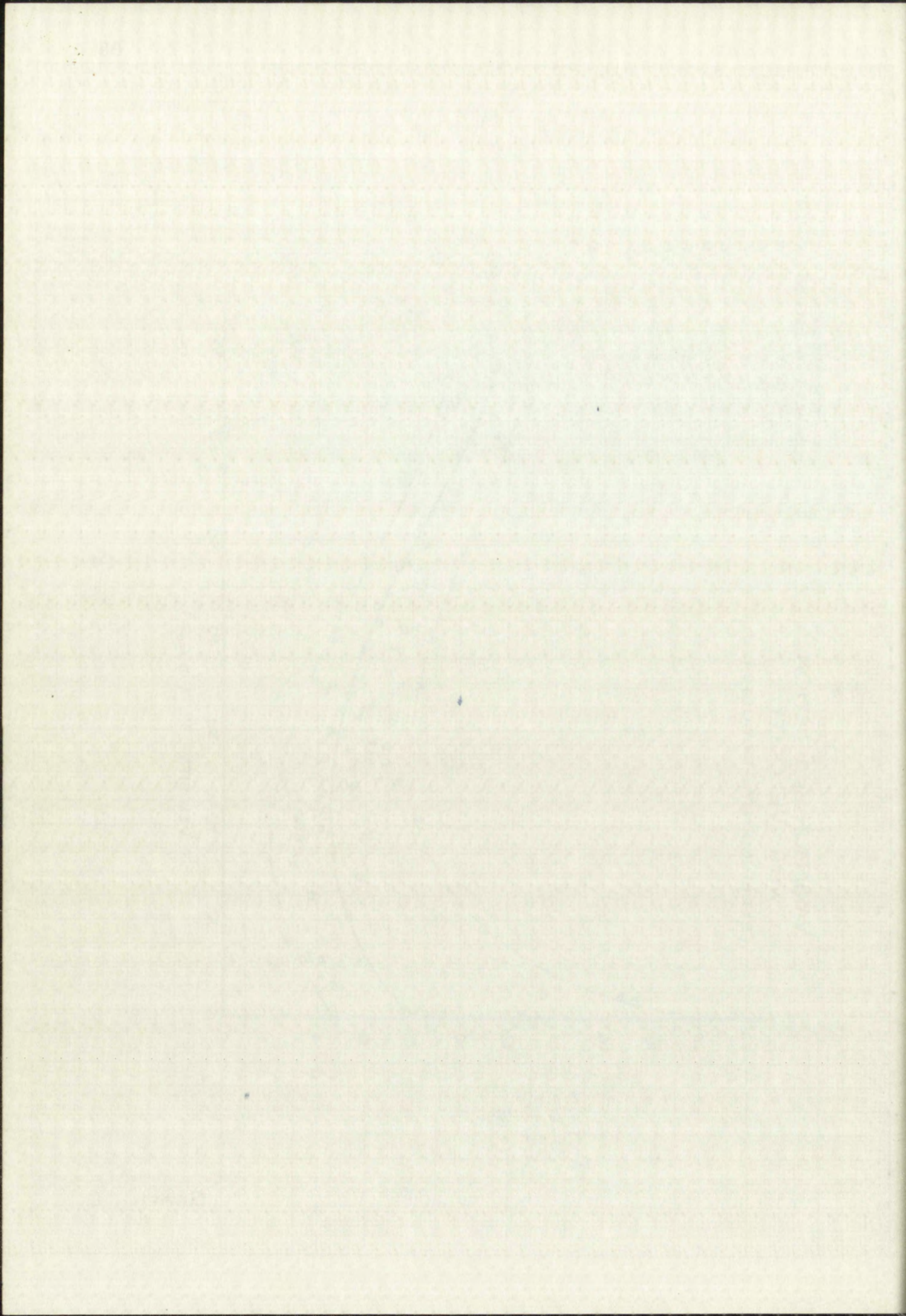
as T. E. Faires, Journal of Applied Mechanics (1925)
 Vol. 3, No. 2, p. 151. The author is indebted to
 E. A. Faires and R. E. Keese, "Friction of Journal Bearings",
Transactions of the American Society of Mechanical Engineers,
 Vol. 51, 1929.

VARIATION OF FRICTION WITH VELOCITY (EXPERIMENTAL RESULTS)

PISTON POSITION (INCHES FROM BOTTOM)	SYMBOL
16.8	X
14.4	A
12.0	B
9.6	C
7.2	D
4.8	E
2.4	F
18.7	O
11.5	H
6.7	J
1.9	K
OTHERS	M

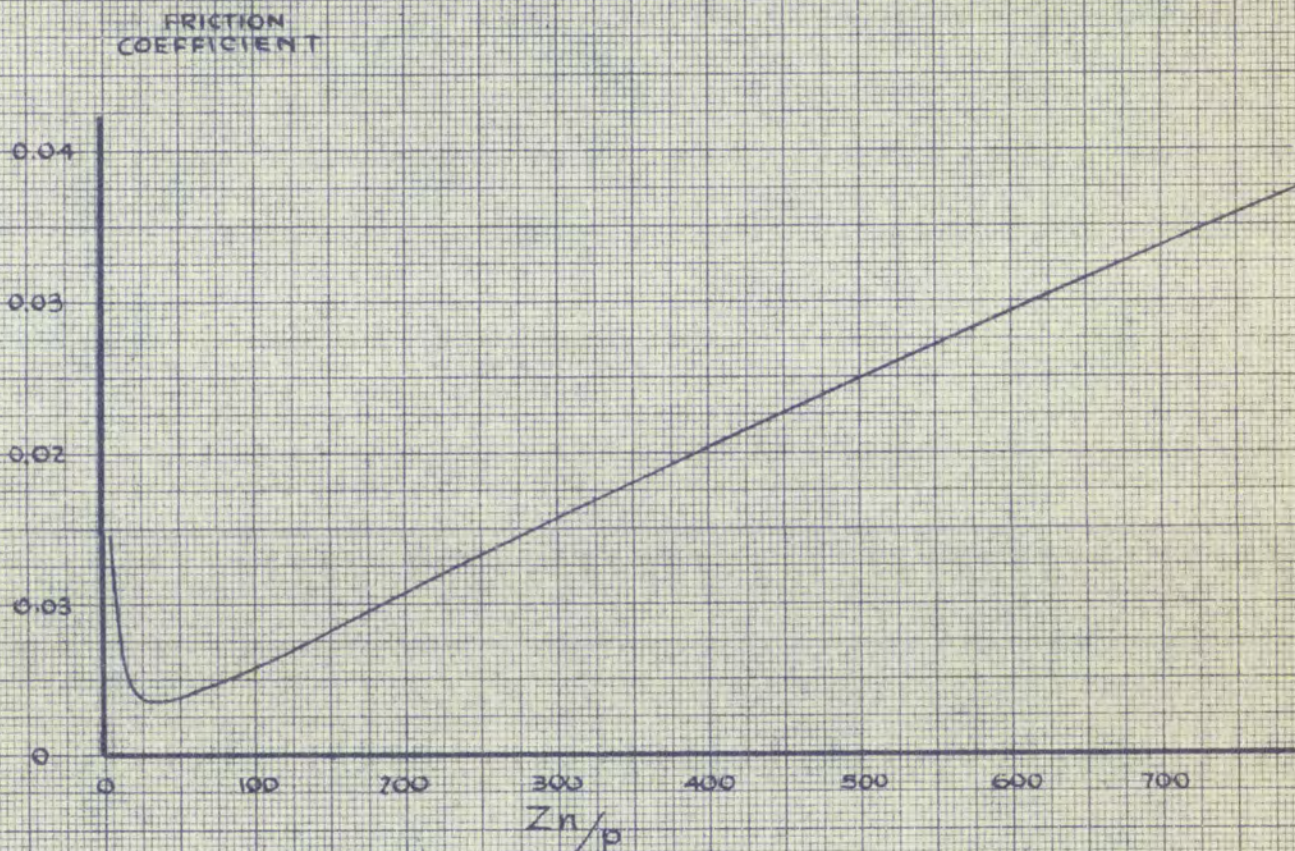


GRAPH 17

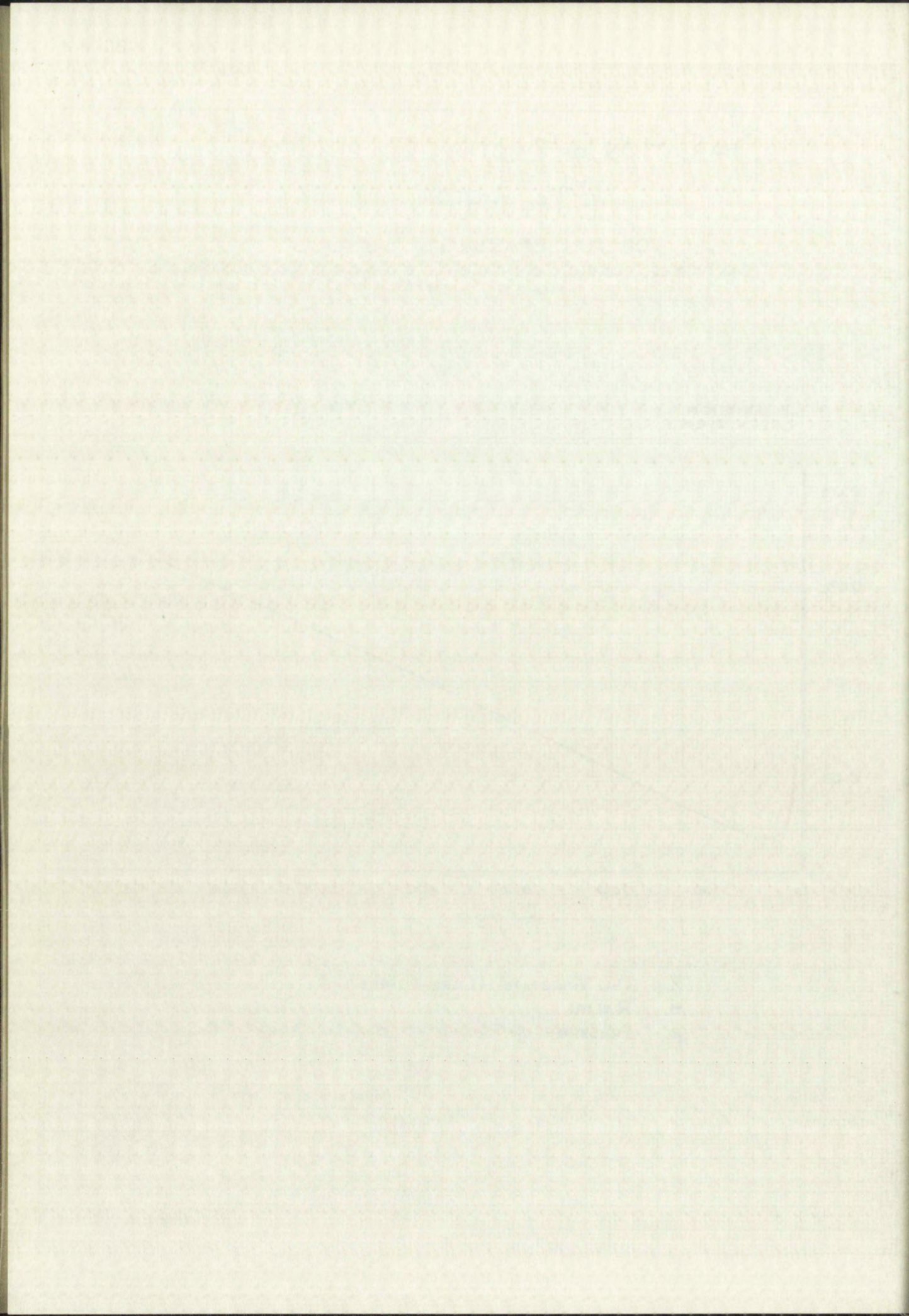


VARIATION OF FRICTION COEFFICIENT WITH Zn/p FACTOR

FOR FULL BEARINGS, (AFTER
V.M. FAIRES, "DESIGN OF MACHINE ELEMENTS", REVISED EDITION
FIG 277, p. 347)

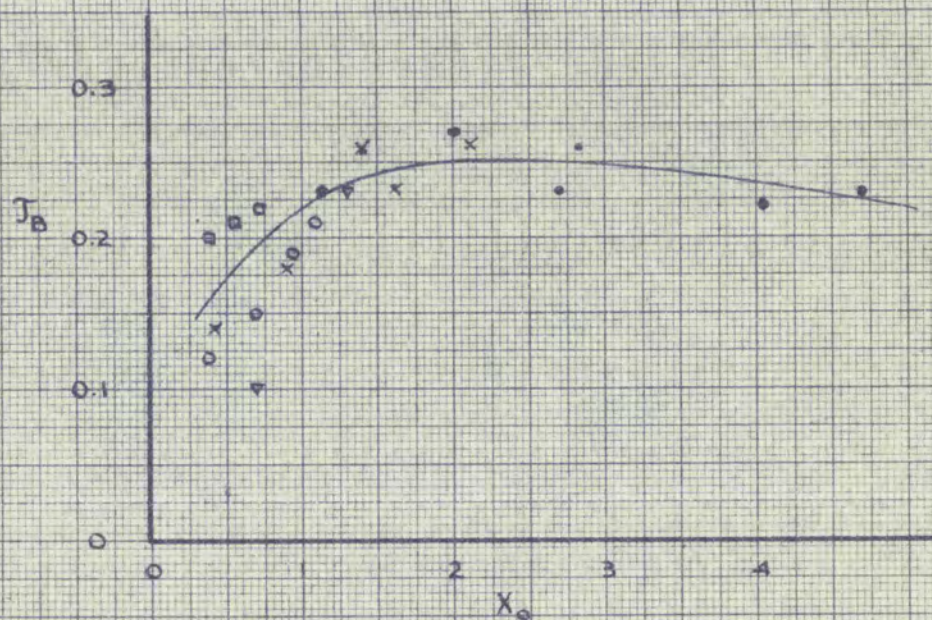
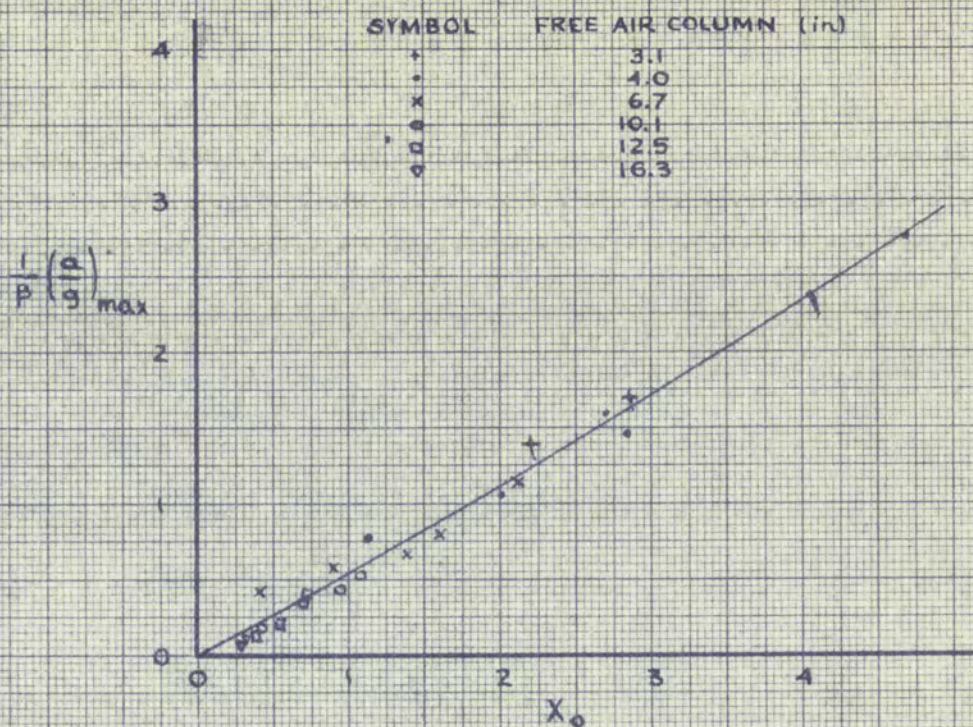


Z OIL VISCOSITY (CENTIPOISES)
 n R.p.m.
 p PRESSURE ON PROJECTED BEARING AREA (P.s.i.)

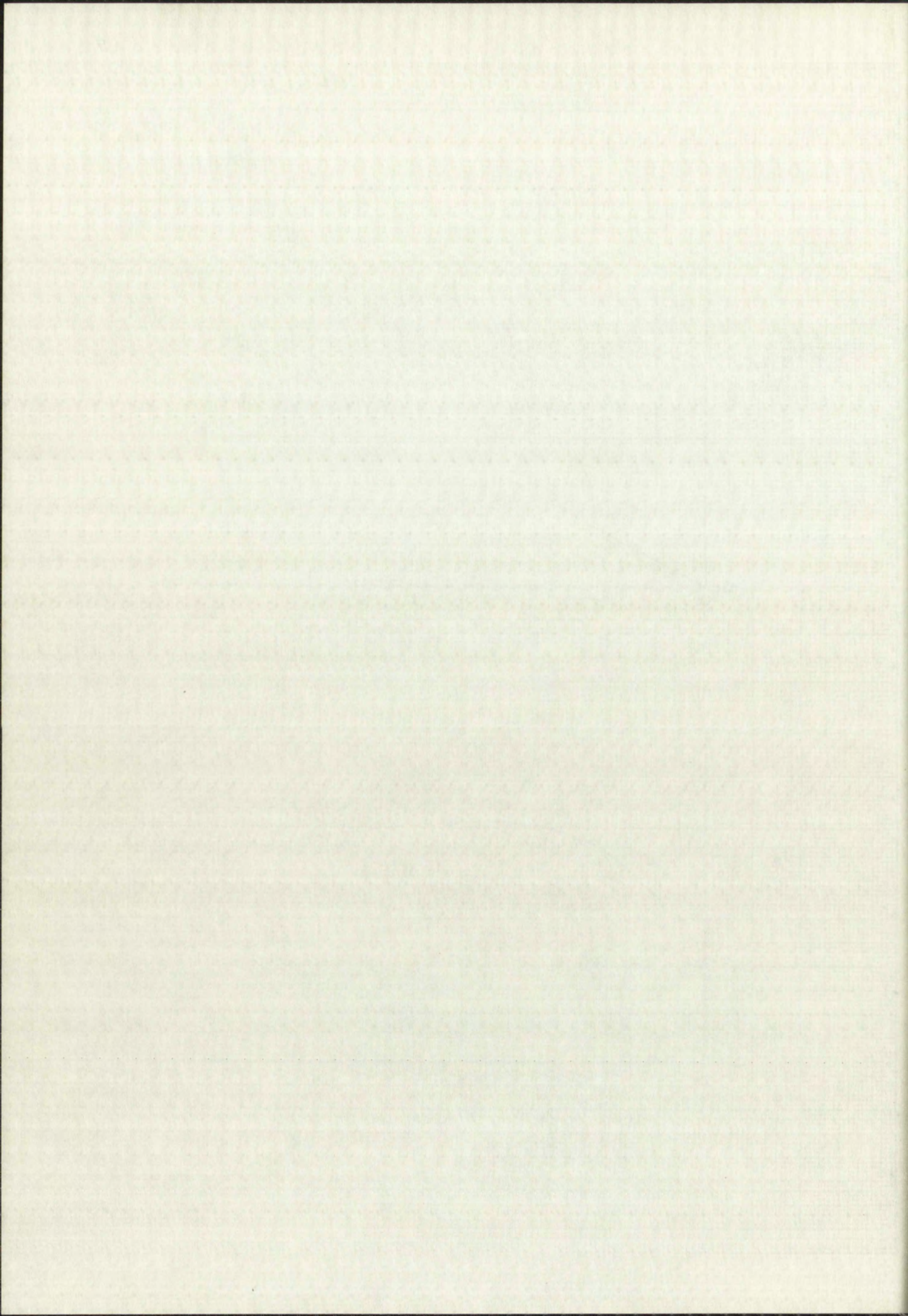


EXPERIMENTAL RESULTS

$$\beta = 14.98$$

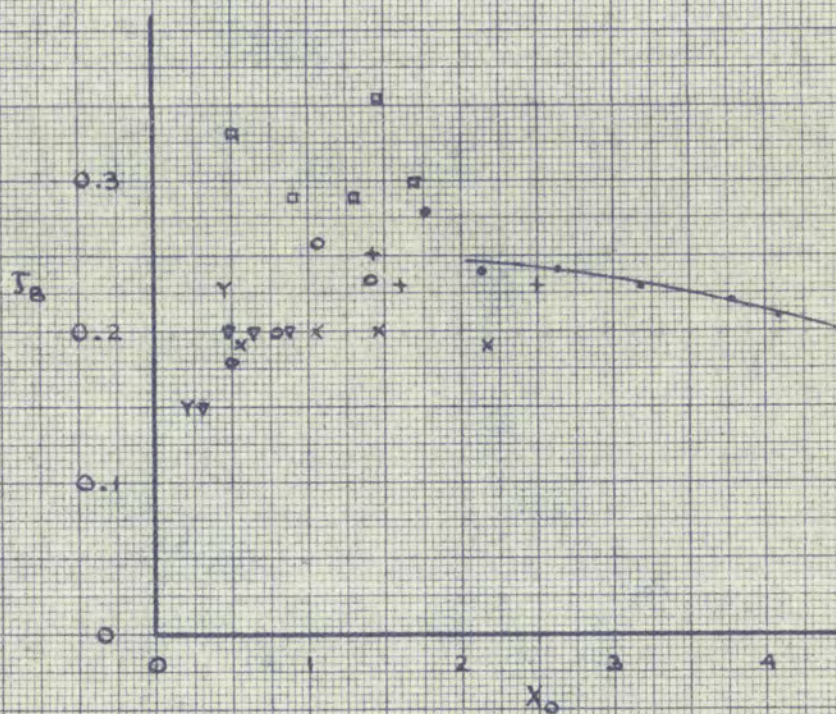
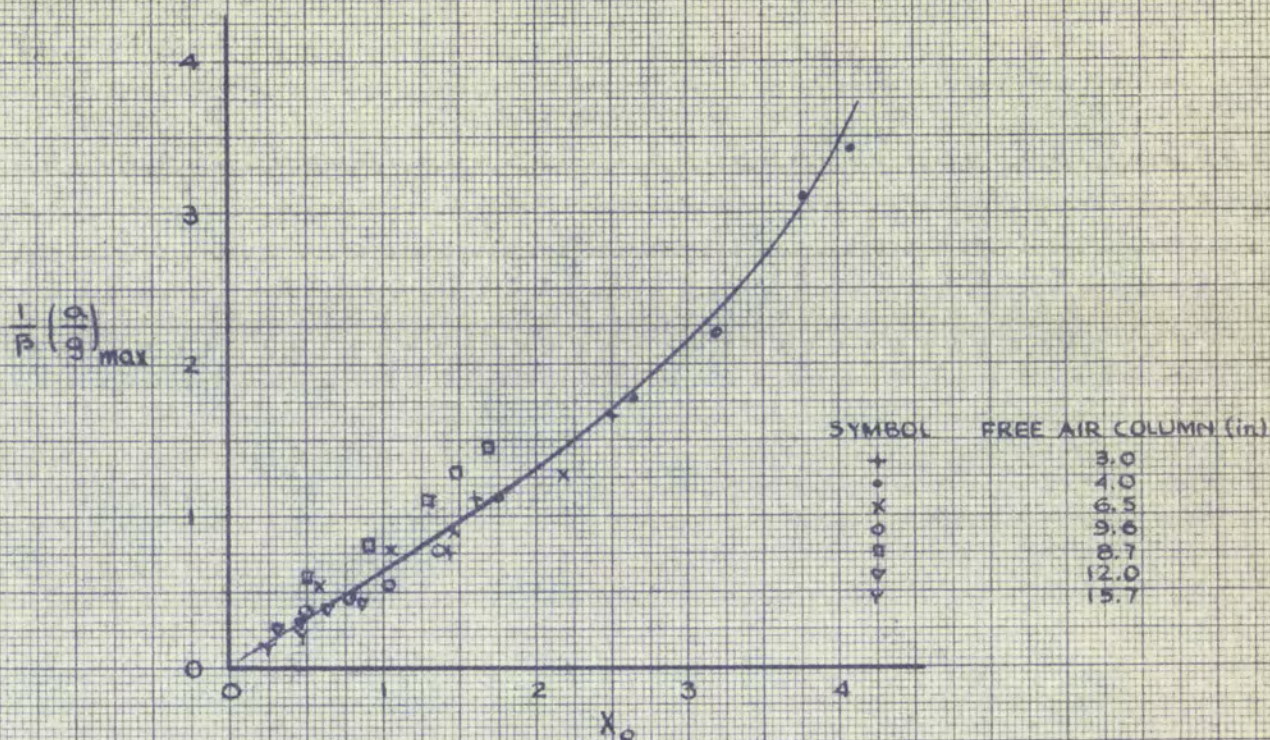


GRAPH 19

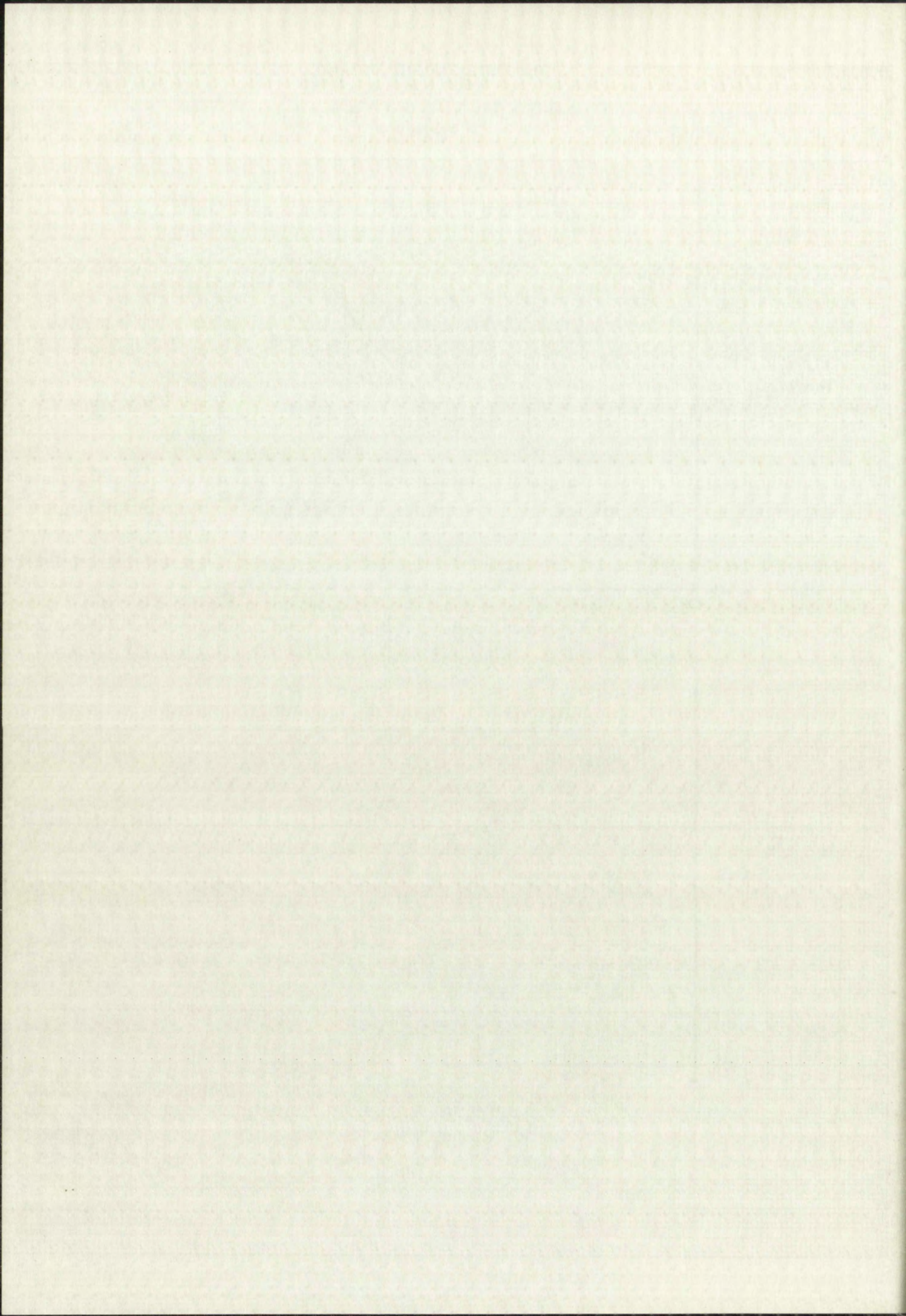


EXPERIMENTAL RESULTS

$$\beta = 9.04$$

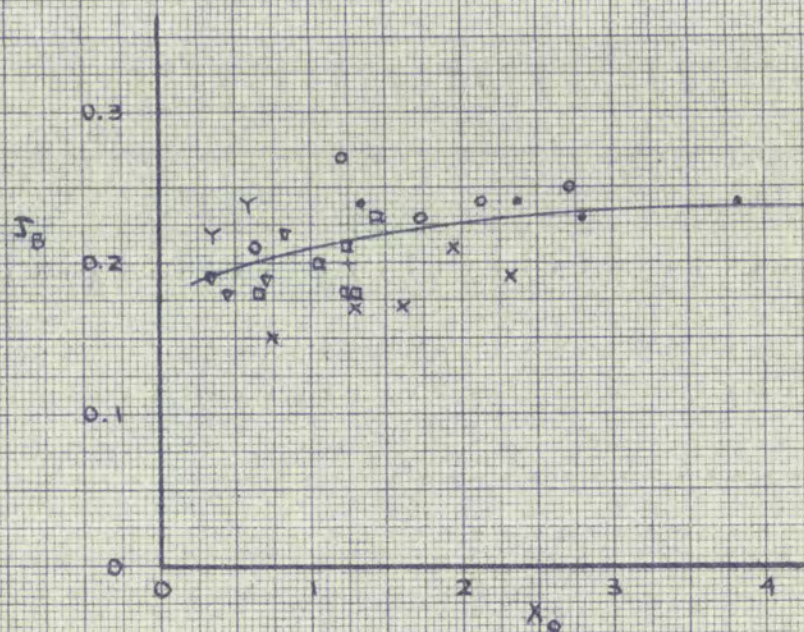
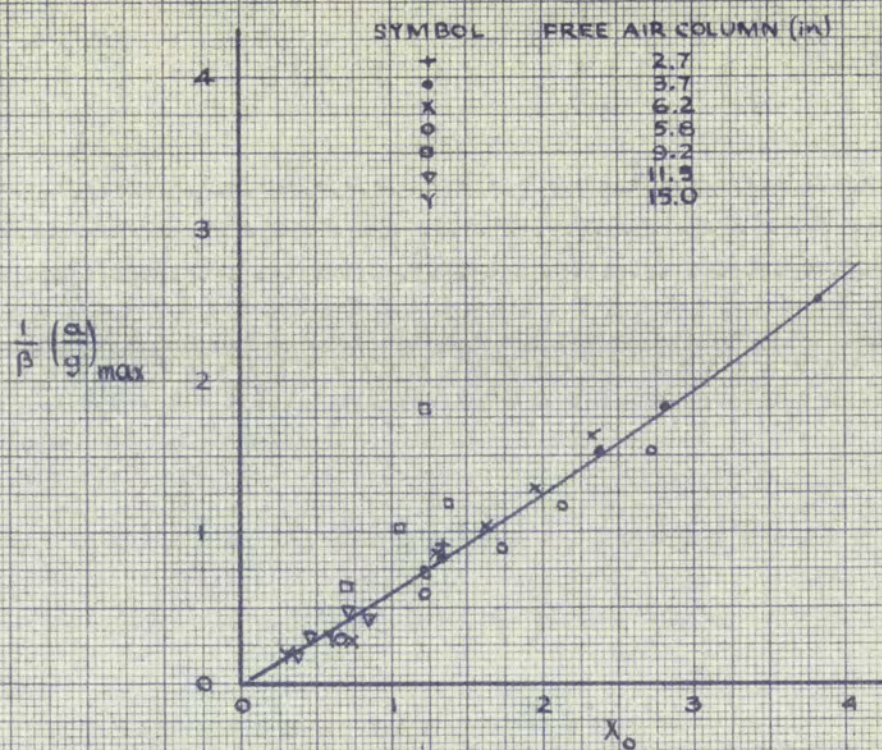


GRAPH 20

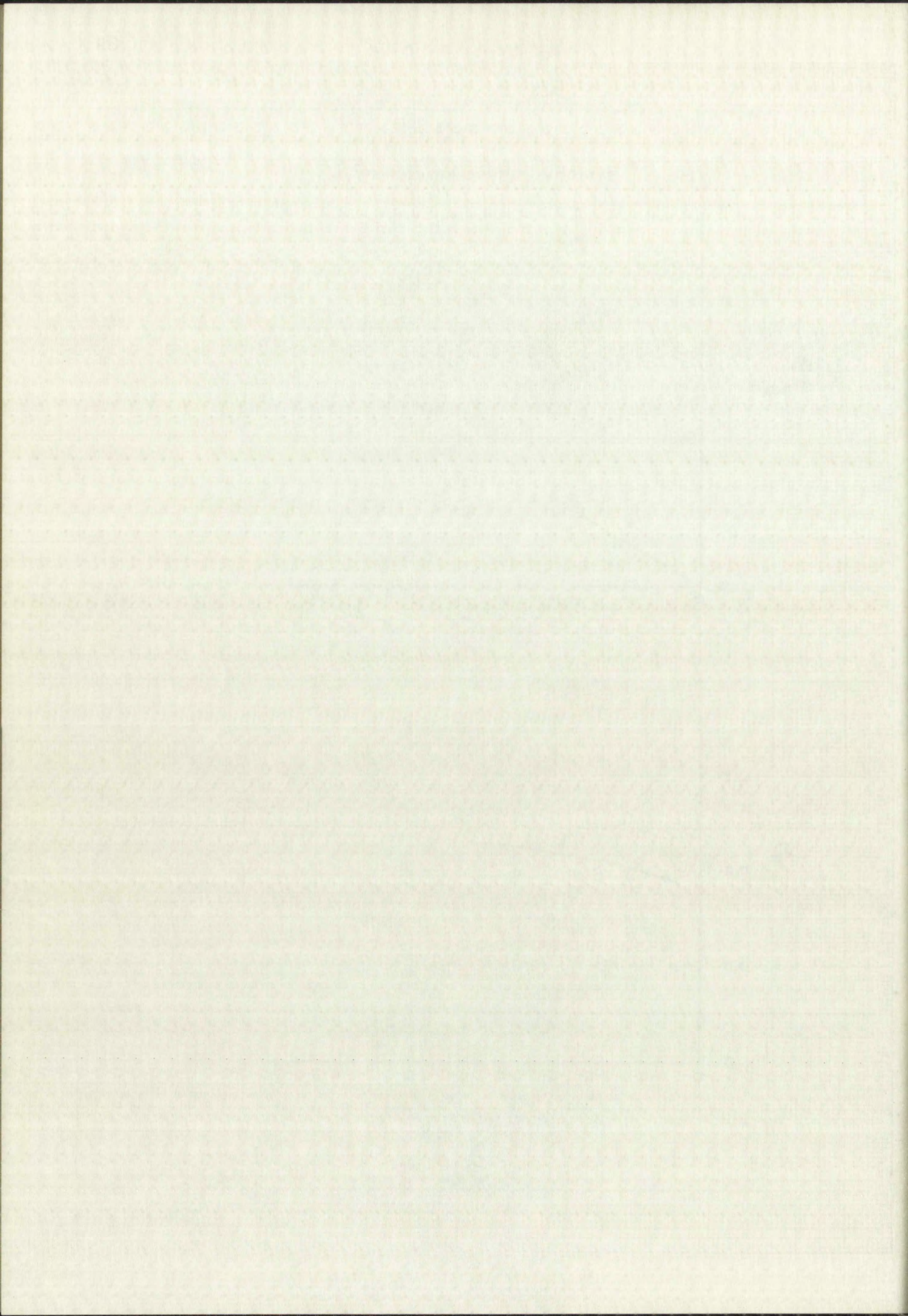


EXPERIMENTAL RESULTS

$$\beta \approx 0.72$$

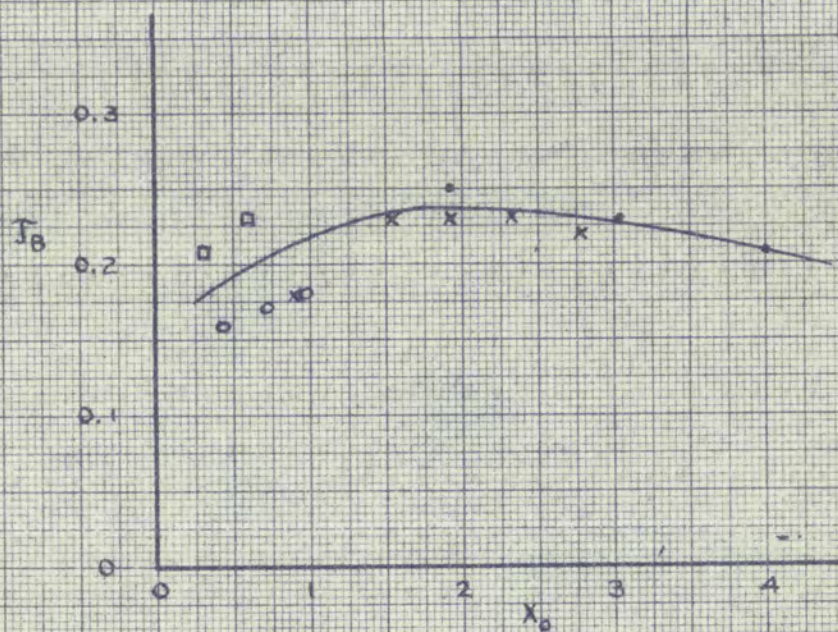
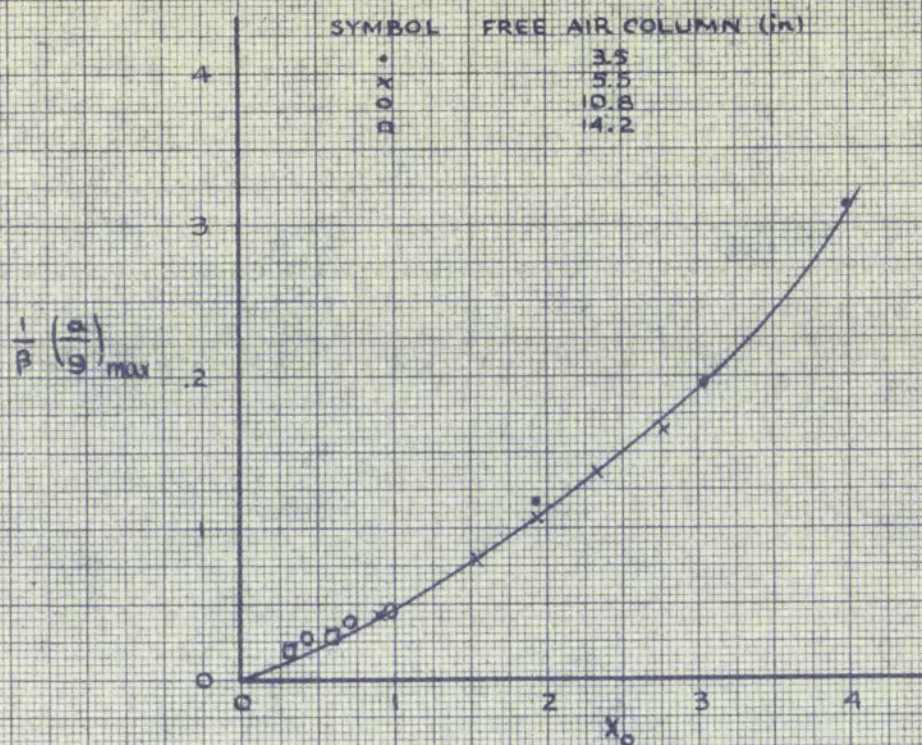


GRAPH 21

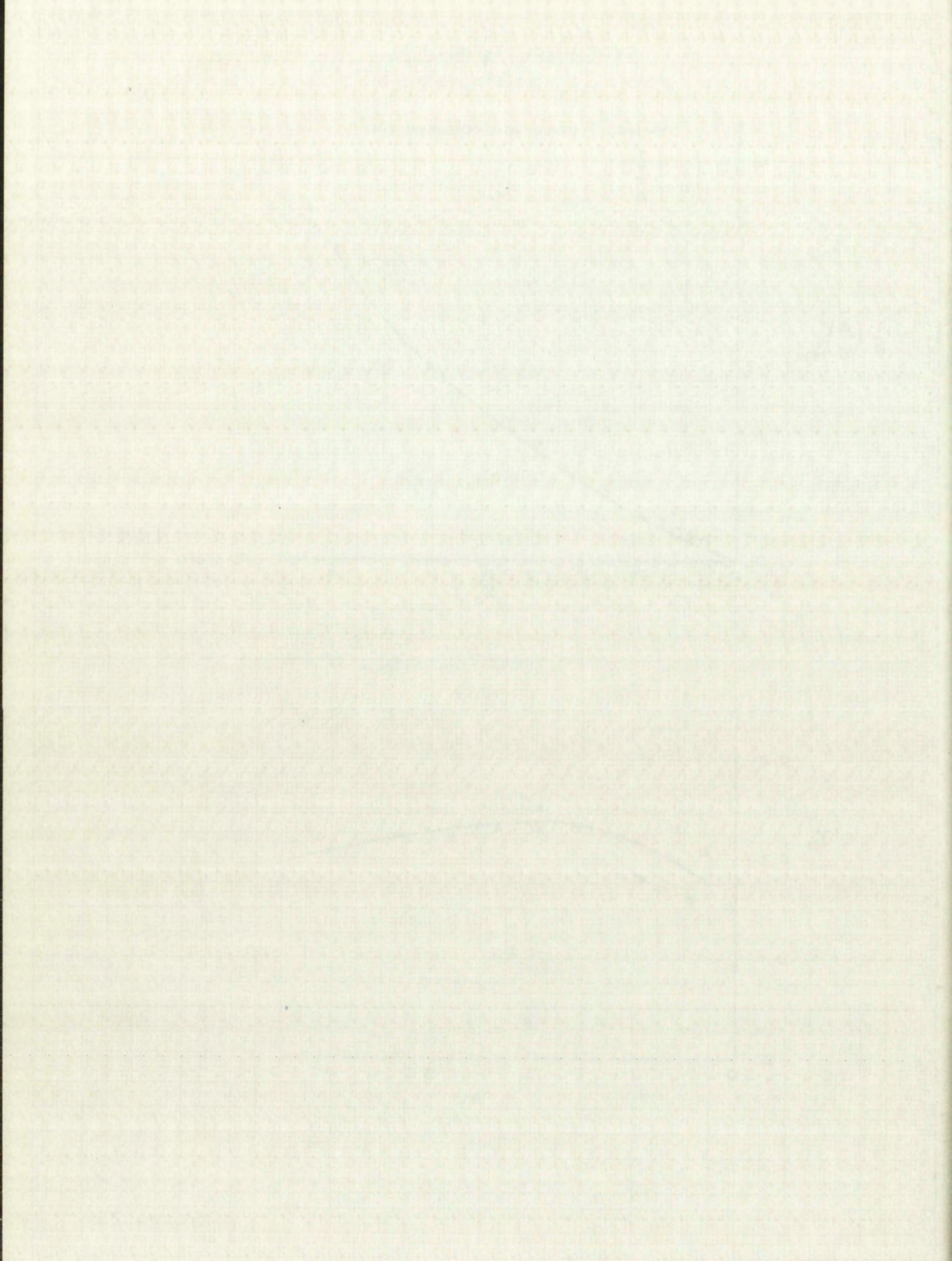


EXPERIMENTAL RESULTS

$$\beta = 5.12$$

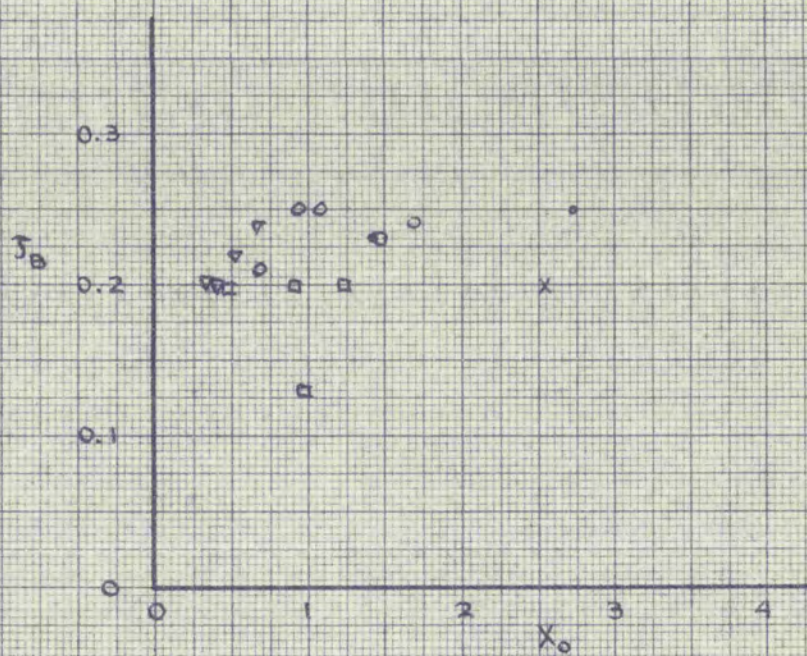
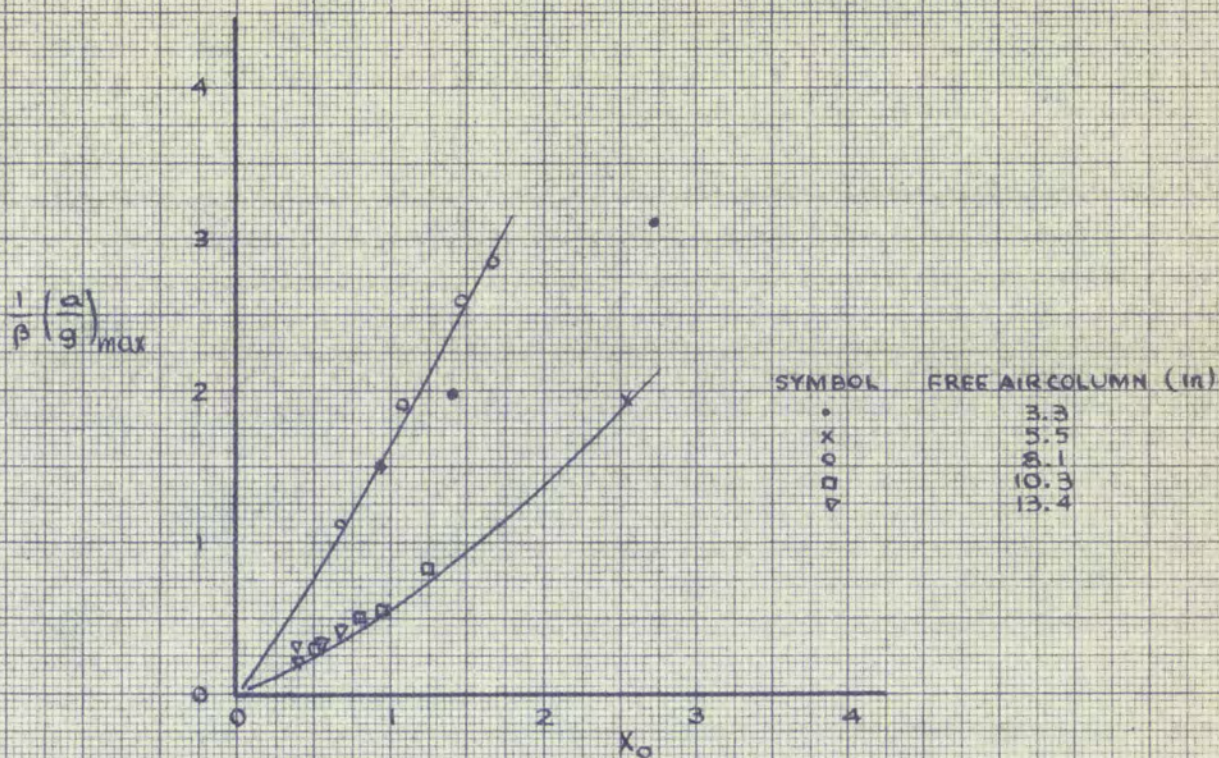


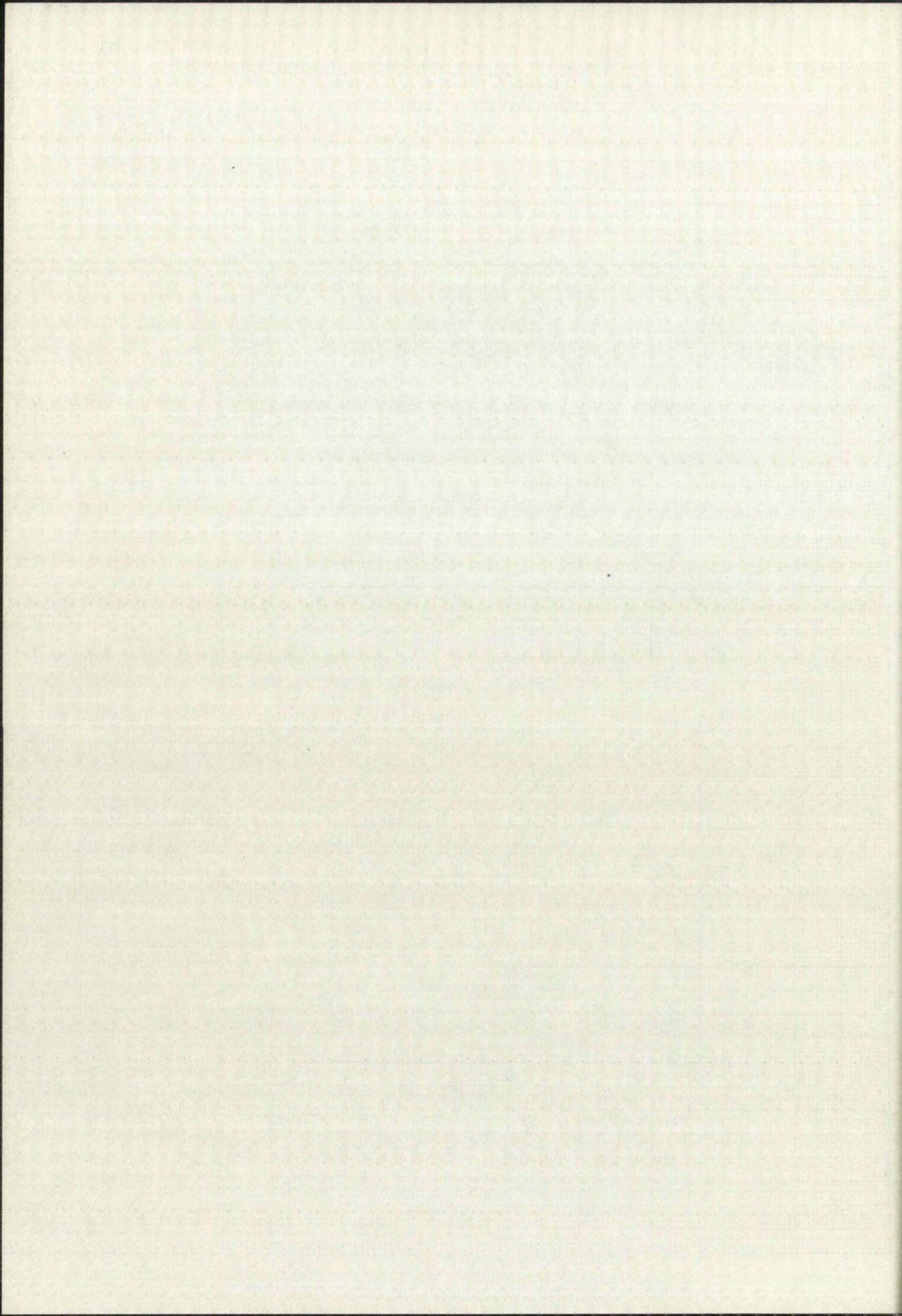
GRAPH 22



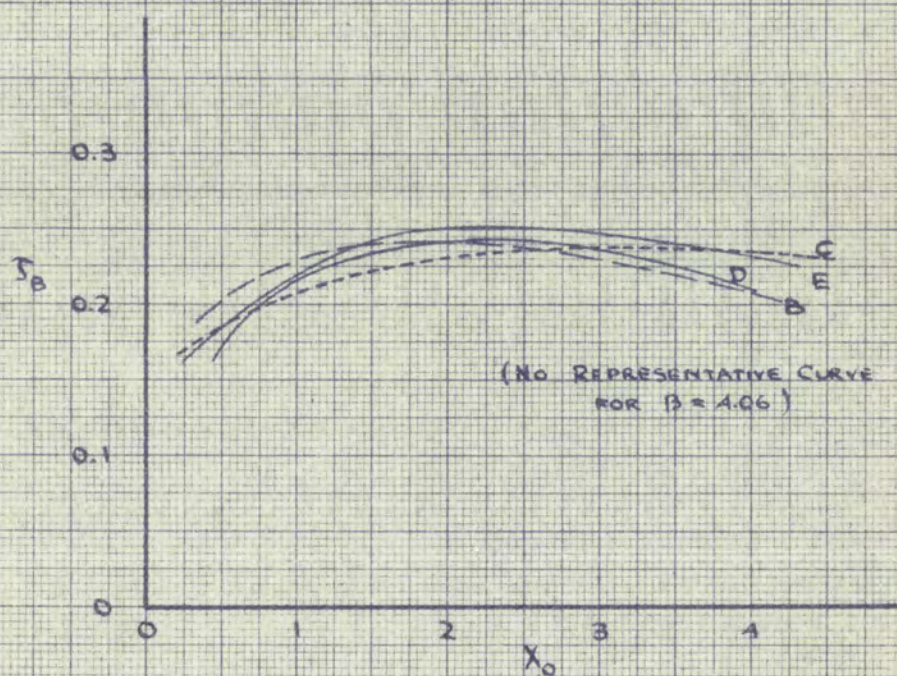
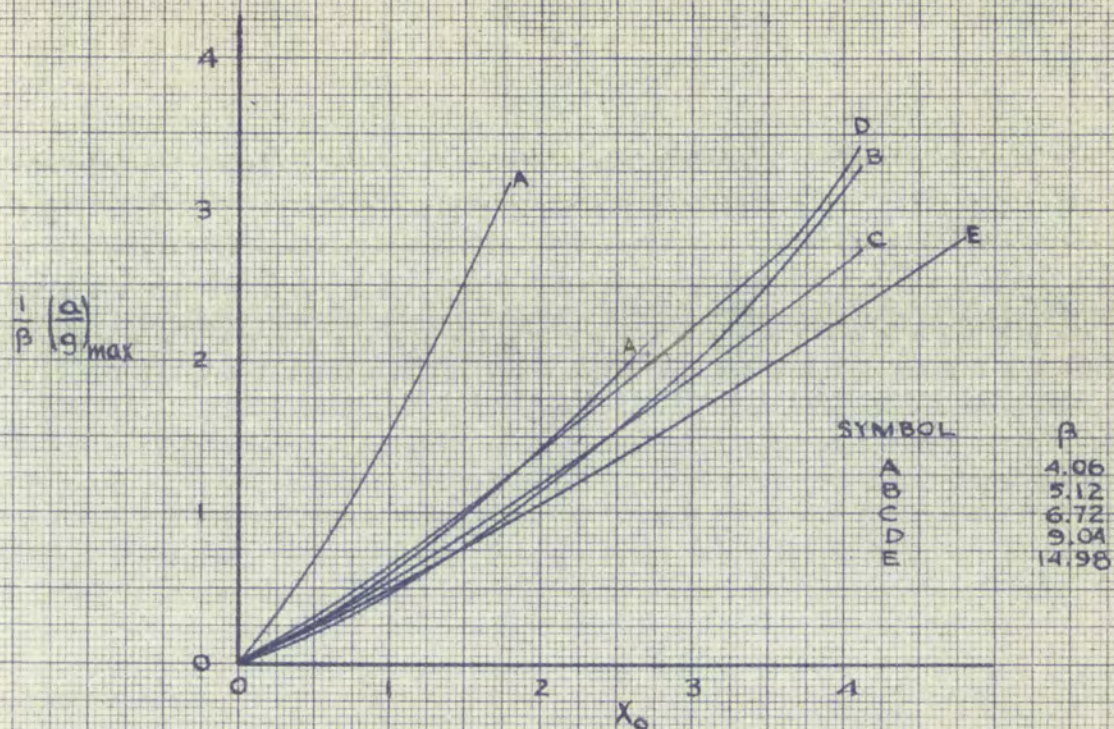
EXPERIMENTAL RESULTS

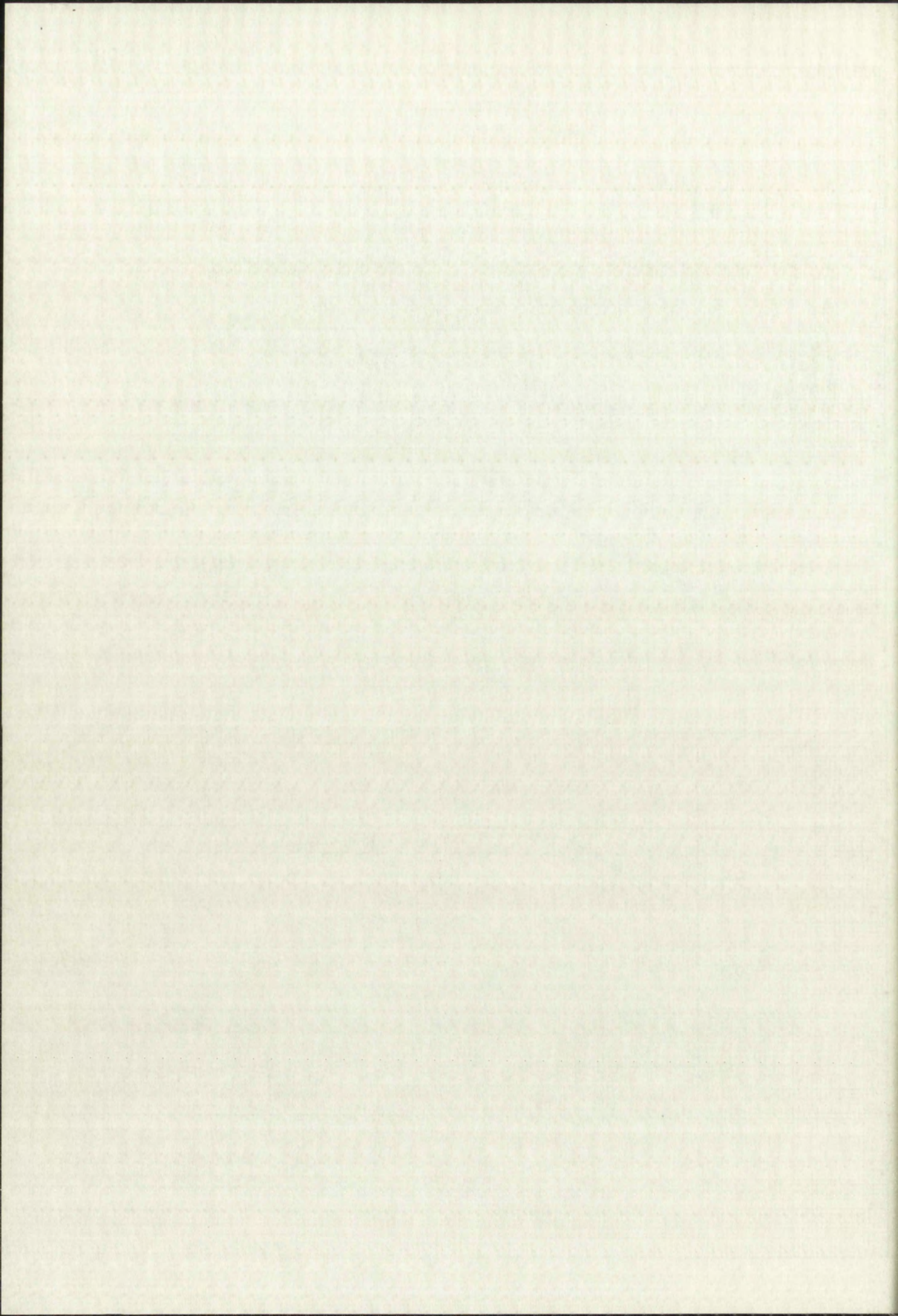
$$\beta = 4.06$$





EXPERIMENTAL RESULTS SUMMARY OF MEAN CURVES





initial displacement. Each of these graphs pertains to a different value of piston weight, as indicated by the dimensionless weight parameter β . Curves which seem to fit the experimental points best are also shown. In Graph 24 all of the curves plotted in Graphs 19 through 23 are shown superimposed on one another to facilitate comparison.

Graphs in terms of dimensionless variables were preferred because this treatment reduces the number of variables and lends itself to more uniform analysis and easier comparison with calculated results. A detailed discussion of these results is given under the subsequent heading "Evaluation of Results".

V. MATHEMATICAL TREATMENT OF THE EXPERIMENTAL AIR SPRING

In Chapter III it was shown that the differential equation for an air spring may be written as

$$(25) \quad \frac{1}{g} \frac{d^2 x}{dt^2} = \frac{B}{W} \left[1 - \left(1 - \frac{x}{L} \right)^{-\gamma} \right] + \frac{\phi}{W}$$

or, in terms of dimensionless variables, as

$$(27) \quad \frac{d^2 x}{d\gamma^2} + \frac{4\pi^2}{\gamma} \left[(1-x)^{-\gamma} - 1 \right] + \frac{4\pi^2}{\gamma} \phi_0 = 0$$

and the other two curves, which are shown in the same figure, are also of the same type. The curves are all of the same type, and the same value of the parameter α is used for all of them. The curves are all of the same type, and the same value of the parameter α is used for all of them. The curves are all of the same type, and the same value of the parameter α is used for all of them.

Graphs in Figure 2 show the results of the calculations for the same values of the parameter α as in Figure 1. The curves are all of the same type, and the same value of the parameter α is used for all of them. The curves are all of the same type, and the same value of the parameter α is used for all of them. The curves are all of the same type, and the same value of the parameter α is used for all of them.

V. REFERENCES

In connection with the study of the properties of the function $\Gamma(x)$ it is necessary to know the values of the function $\Gamma(x)$ for various values of x .

$$(55) \quad \frac{1}{x} = \frac{1}{x} + \frac{1}{x} + \frac{1}{x} + \dots$$

or, in terms of the function $\Gamma(x)$, we have

$$(56) \quad \frac{1}{x} = \frac{1}{x} + \frac{1}{x} + \frac{1}{x} + \dots$$

The following relations are repeated here for ease of reference.

$$\tau = \frac{t}{T_0}$$

$$x = \frac{\bar{x}}{L}$$

$$\phi_0 = - \frac{\phi}{B}$$

$$B = AP_0 + W$$

$$\beta = \frac{B}{W} = \frac{AP_0}{W} + 1$$

$$T_0 = 2\pi \sqrt{\frac{WL}{gB\gamma}} = 2\pi \sqrt{\frac{L}{g\gamma\beta}}$$

From these relations, the following equations relating velocities and accelerations in actual and dimensionless variables may be deduced.

$$v = \frac{dx}{dt} = \frac{L}{T_0} \cdot \frac{dX}{d\tau} = \frac{1}{2\pi} \sqrt{g\gamma\beta L} \quad v$$

$$a = \frac{d^2x}{dt^2} = \frac{L}{T_0^2} \cdot \frac{d^2X}{d\tau^2} = \frac{g\gamma\beta}{4\pi^2} \cdot \frac{d^2X}{d\tau^2}$$

The relations are repeated here for ease of reference.

$$\frac{f}{f_0} = \gamma$$

$$\frac{x}{x_0} = \chi$$

$$\frac{\phi}{\phi_0} = \Phi$$

$$B = B_0 + \epsilon$$

$$\rho = \frac{H}{v} = \frac{H_0}{v_0} + 1$$

$$\tau_0 = \tau \sqrt{\frac{H_0}{H}} = \tau \sqrt{\frac{v}{v_0}}$$

From these relations, the following equations relating velocities and accelerations in actual and dimensionless variables may be deduced.

$$v = \frac{dx}{dt} = \frac{dx}{\tau_0} \cdot \frac{\tau_0}{\tau} = \frac{dx}{\tau_0} \cdot \frac{1}{\gamma} = \frac{1}{\gamma} \frac{dx}{\tau_0}$$

$$a = \frac{dv}{dt} = \frac{dv}{\tau_0} \cdot \frac{\tau_0}{\tau} = \frac{dv}{\tau_0} \cdot \frac{1}{\gamma} = \frac{1}{\gamma} \frac{dv}{\tau_0}$$

The latter of these yields an alternate representation of the dimensionless acceleration:

$$\frac{1}{\beta} \left(\frac{a}{g} \right) = \frac{\gamma}{4\pi^2} \frac{d^2x}{d\gamma^2}$$

It is to be noted that for a given run β is constant, so that actual acceleration and dimensionless acceleration are directly proportional.

The friction tests showed that the friction force in the air spring was a function of piston velocity only. That is, $\phi = \phi \left(\frac{dx}{dt} \right)$. But, since the relation between $\frac{dx}{dt}$ and $\frac{dX}{d\gamma}$ involves also the variables β and L , ϕ in terms of non-dimensional velocity must be written as

$$\phi = \phi \left(\frac{dX}{d\gamma}, \beta L \right).$$

Mathematical treatment of the experimental air spring hence requires finding of solutions of the equation

$$\frac{d^2X}{d\gamma^2} + \frac{4\pi^2}{\gamma} \left[(1-X)^{-\gamma} - 1 \right] - \frac{4\pi^2}{\gamma} \frac{\phi}{B} = 0$$

where ϕ is an empirically known function of

$$\frac{dx}{dt} = \frac{1}{2\pi} \cdot \sqrt{g \gamma \beta L} \frac{dX}{d\gamma}. \quad \text{These solutions depend on}$$

$$\phi = \phi \left(\frac{dX}{d\gamma}, \beta L \right) \quad \text{and on } B = W\beta = AP_0 + W. \quad \text{The}$$

The latter of these yields an algebraic representation of

the dimensional relationship:

$$\frac{\partial^2 X}{\partial t^2} = \left(\frac{\partial}{\partial t} \right) \left(\frac{\partial X}{\partial t} \right)$$

It is to be noted that for a given run ϕ is constant, so

that actual acceleration and dimensional acceleration

are directly proportional.

The friction tests showed that the friction force

in the air spring was a function of piston velocity only.

That is, $\phi = \phi \left(\frac{\partial X}{\partial t} \right)$. But, since the relation between

$\frac{\partial X}{\partial t}$ and $\frac{\partial^2 X}{\partial t^2}$ involves also the variables ϕ and λ , ϕ in

terms of non-dimensional velocity must be written as

$$\phi = \phi \left(\frac{\partial X}{\partial t}, \lambda \right)$$

Mathematical treatment of the experimental air spring

shows relative timing of evolution of the equation

$$0 = \frac{\phi}{\lambda} + \frac{\partial^2 X}{\partial t^2} - \left[1 - X \right] \frac{\partial^2 X}{\partial t^2}$$

where ϕ is an empirically known function of

$\frac{\partial X}{\partial t}$ and λ . These relations depend on

$$\phi = \phi \left(\frac{\partial X}{\partial t}, \lambda \right) \quad \text{and on } \lambda = \frac{\partial^2 X}{\partial t^2} = \lambda_0 + \lambda_1$$

observed variations in P_0 were so small that B , and hence β , could be considered as functions of W only. Then, by eliminating W , B may be expressed as a function of β :

$$B = AP_0 \left(\frac{\beta}{\beta - 1} \right)$$

Hence, it may be expected that non-dimensional maximum acceleration and acceleration build-up time depend on L as well as on the initial position of the piston and on the constants for the experimental air spring, since all of these parameters influence the solution of the differential equation. Complete mathematical analysis of the experimental air spring thus requires the calculation of solutions of the above differential equation for various values of the parameters X_0 , β , and L .

Jacobsen's graphical method was used for this purpose. The application of this method to analysis of the experimental air spring is shown in Appendix D, as well as an illustration of a complete solution.

During the course of these calculations it was found that the experimental friction measurements did not extend to high enough velocities. Hence, the friction curve shown in Graph 17 had to be extrapolated. The extrapolation used was performed in accordance with the curves of Graph

observed variations in V_0 were so small that V_0 and hence

\dot{V} could be considered as functions of V only. Then

the differential V may be expressed as a function of V

$$V = V_0 \left(\frac{a}{a-1} \right)$$

where a is a constant. It may be expected that a is a function of V_0

and V_0 is well known the initial position of the piston and

on the contrary for the experimental air engine, since all

of these parameters influence the solution of the differential

equation. Complete mathematical analysis of the exact

mathematical solution thus requires the calculation of solutions

of the above differential equation for various values of

parameters V_0 , a , and V .

For this purpose Jacobson's graphical method was used for this purpose.

The application of this method to analysis of the exact

mathematical solution is shown in Appendix B, as well as an

illustration of a complete solution.

During the course of these calculations it was

found that the experimental piston measurements did not

extend to high enough velocities. Hence, the piston curve

shown in Graph 17 had to be extrapolated. The extrapolation

used was based on the agreement with the curve of Graph

18 for bearing friction measurements. The extrapolated friction graph which was used for the calculations appears in Graph 25.

The results of these calculations are plotted in Graphs 26 to 30, inclusive. Each of these graphs pertains to one value of the weight parameter β and shows the variation of maximum dimensionless acceleration and acceleration build-up time with initial displacement for several values of free air column length.

VI. EVALUATION OF RESULTS OBTAINED FOR EXPERIMENTAL AIR SPRING

Accuracies of experimental measurements. The weight parameter β could be calculated with good accuracy, since it depends only on piston area A , atmospheric pressure P_0 , and piston weight W . The piston area was calculated from micrometer measurements of piston diameter. The atmospheric pressure was determined with sufficient accuracy by a barometer, and the weight of the piston assembly was weighed accurately. The error in the calculated value of β did not exceed 2%.

The accelerometer, amplifiers, and oscillographs were calibrated by the staff of Sandia Corporation's testing laboratory who found the combined inaccuracies introduced

In the case of the first experiment, the average of
the results was used for the calculation of the
in Group 1.

The results of these calculations are listed in
Group 2 to 10, inclusive. Each of these groups contains
the value of the relative parameter β and the
variation of maximum atmospheric concentration as a function
of the initial displacement for several
values of the initial length.

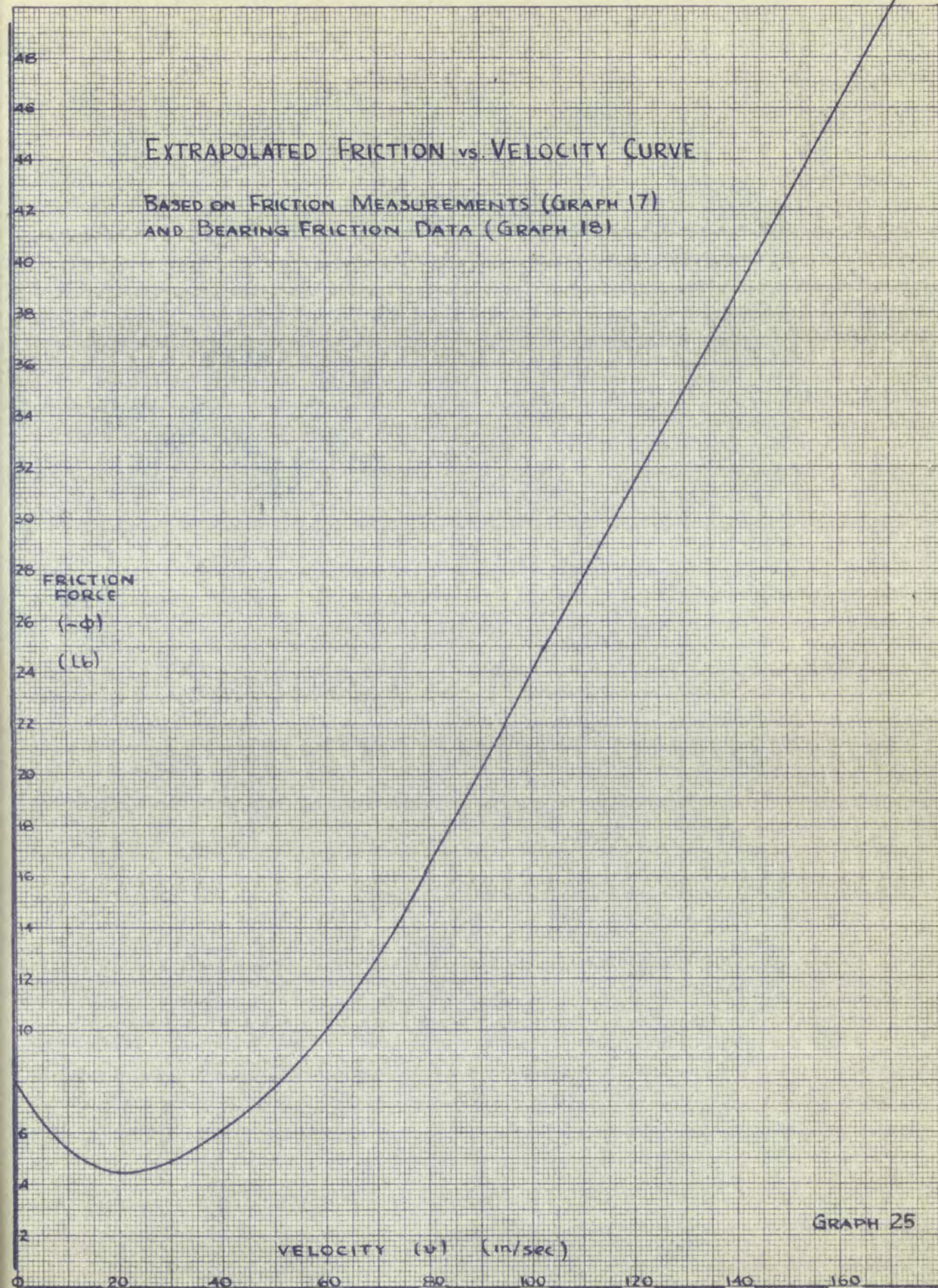
VI. EVALUATION OF RESULTS OBTAINED FROM REPRESENTATIVE AIR TESTS

As pointed out previously, the results of the
parameter β could be calculated with good accuracy, since
it depends only on the initial mass A , atmospheric pressure P_0 ,
and initial weight w . The piston area was calculated from
the cross-sectional area of the piston diameter. The atmospheric
pressure was determined with sufficient accuracy by a
barometer, and the weight of the piston assembly was weighed
accurately. The error in the calculated value of β did
not exceed 1%.

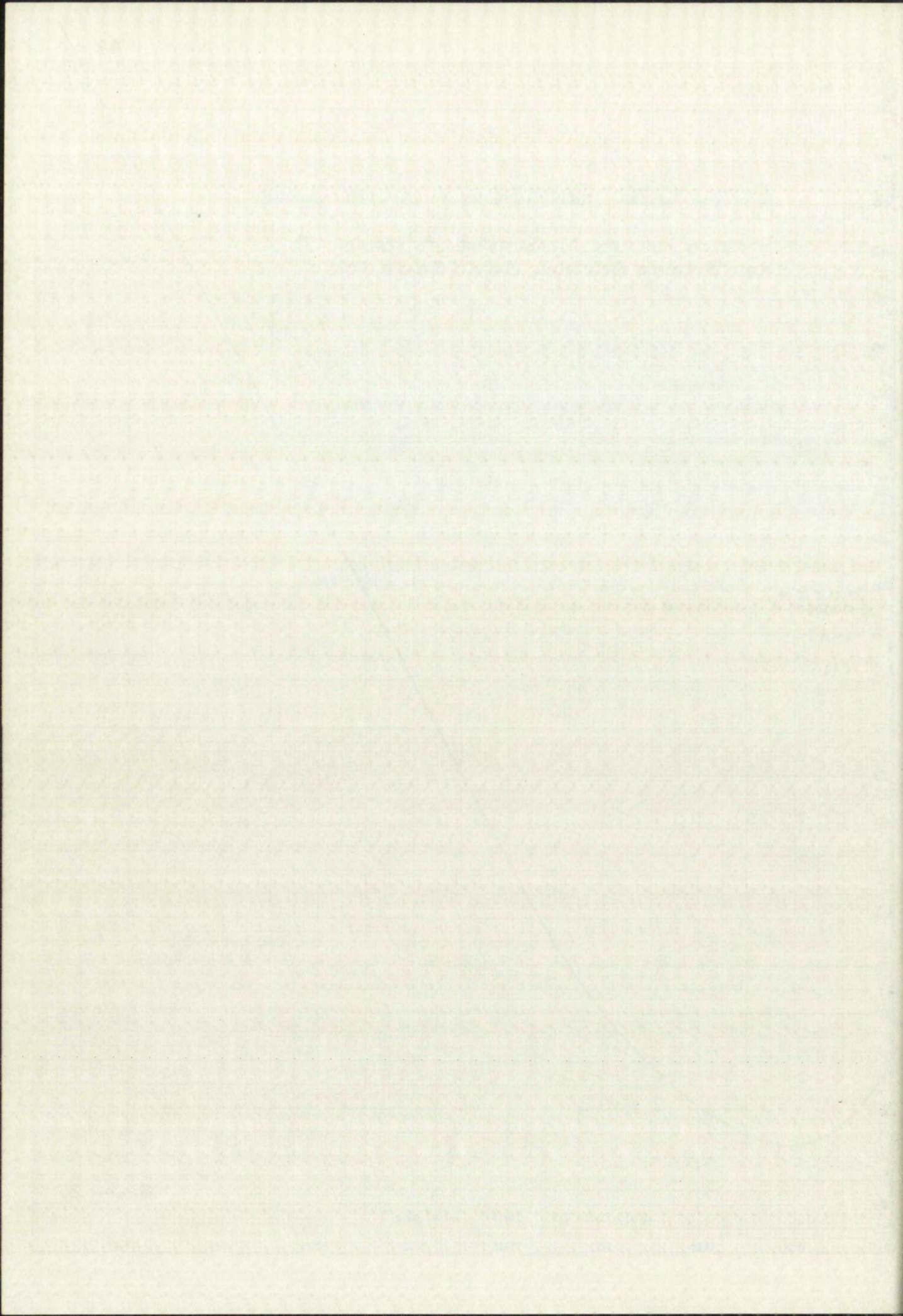
The acceleration, initial velocity, and initial
position were obtained by the staff of the British Commonwealth
Laboratory who found the combined instrument in use.

EXTRAPOLATED FRICTION vs. VELOCITY CURVE

BASED ON FRICTION MEASUREMENTS (GRAPH 17)
AND BEARING FRICTION DATA (GRAPH 18)

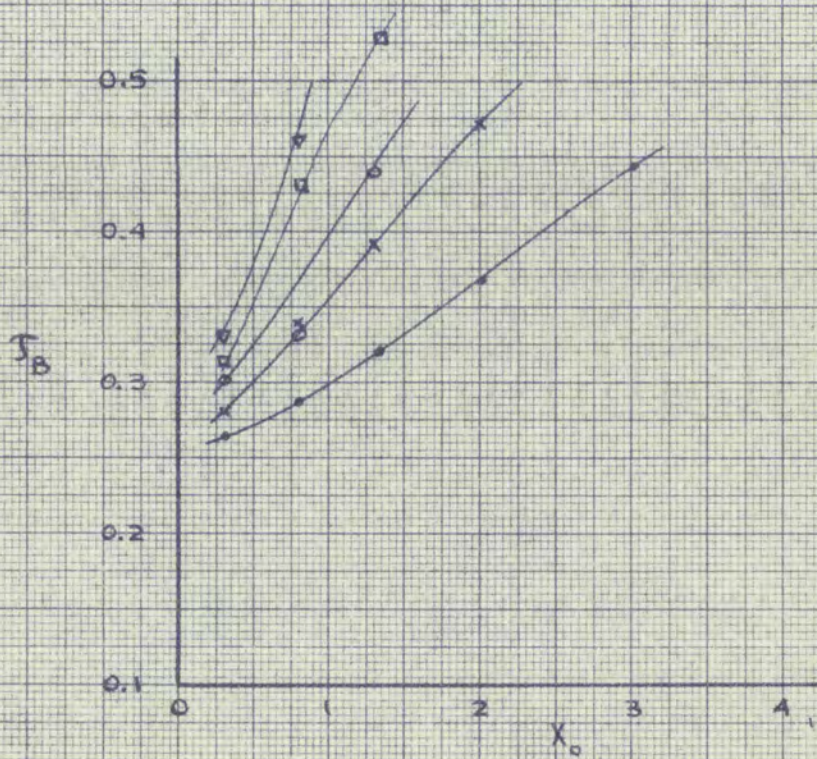
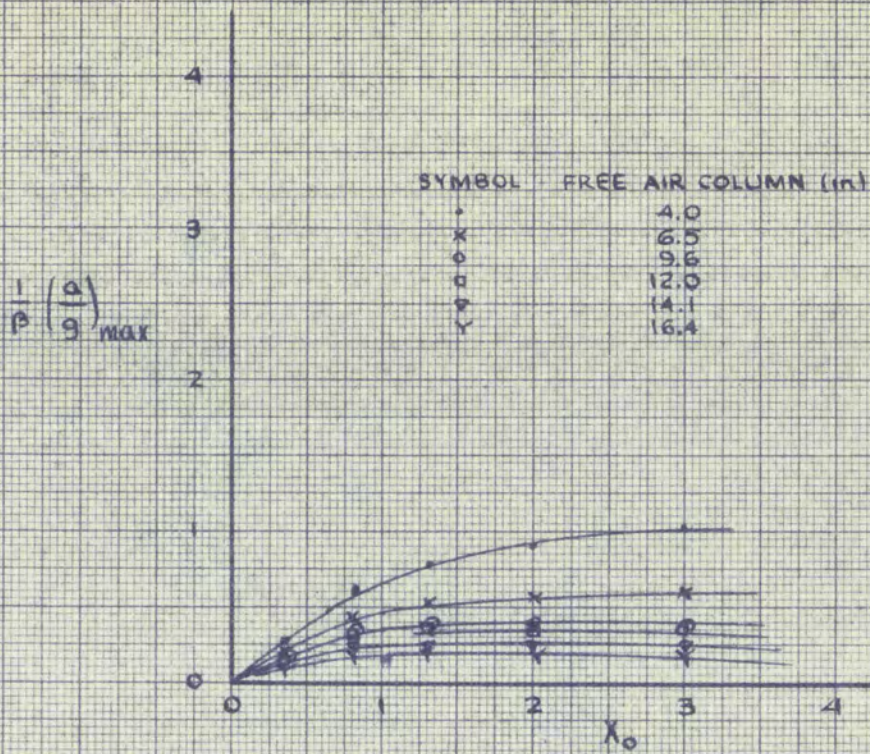


GRAPH 25

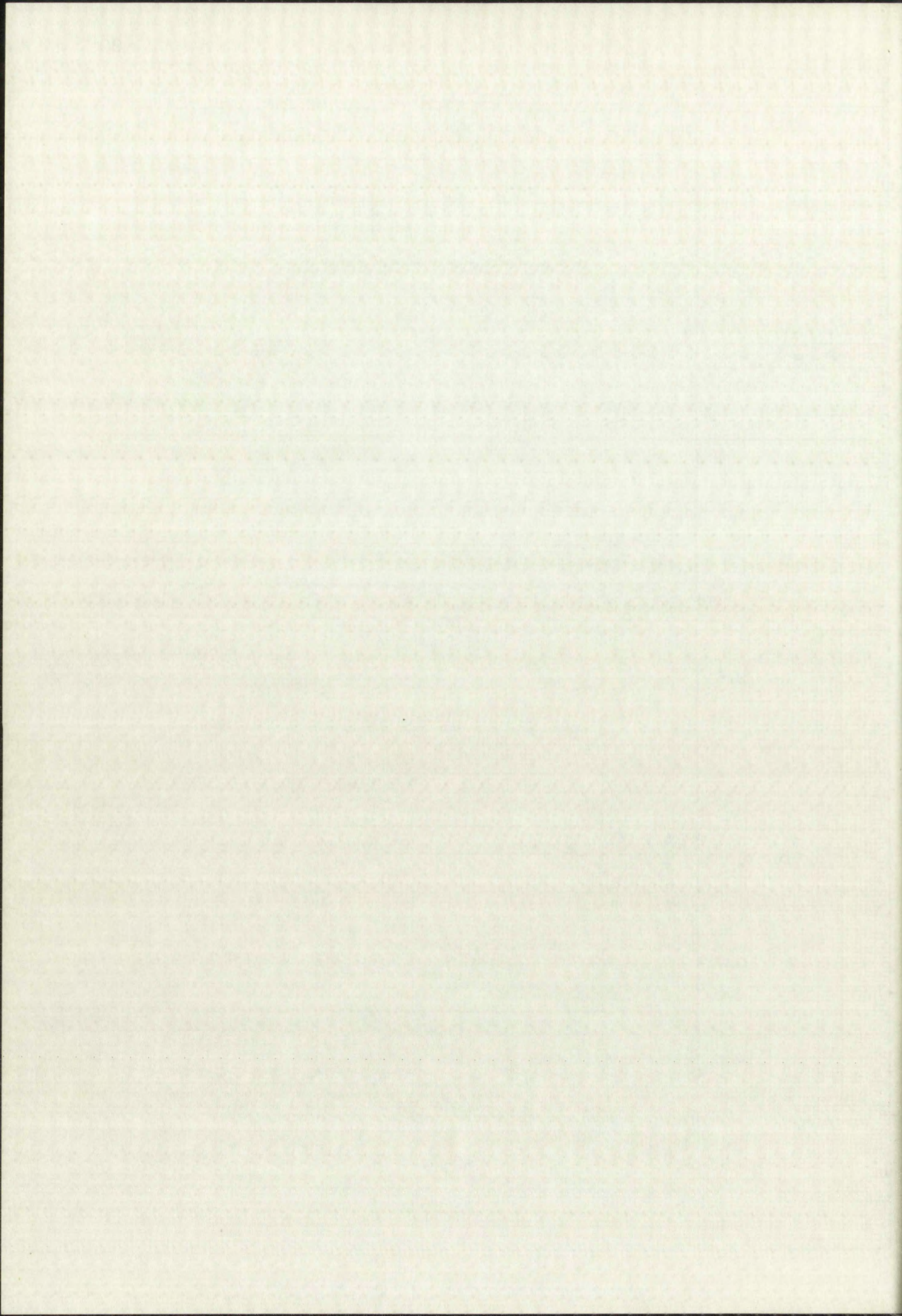


CALCULATED RESULTS

$$\beta = 14.98$$

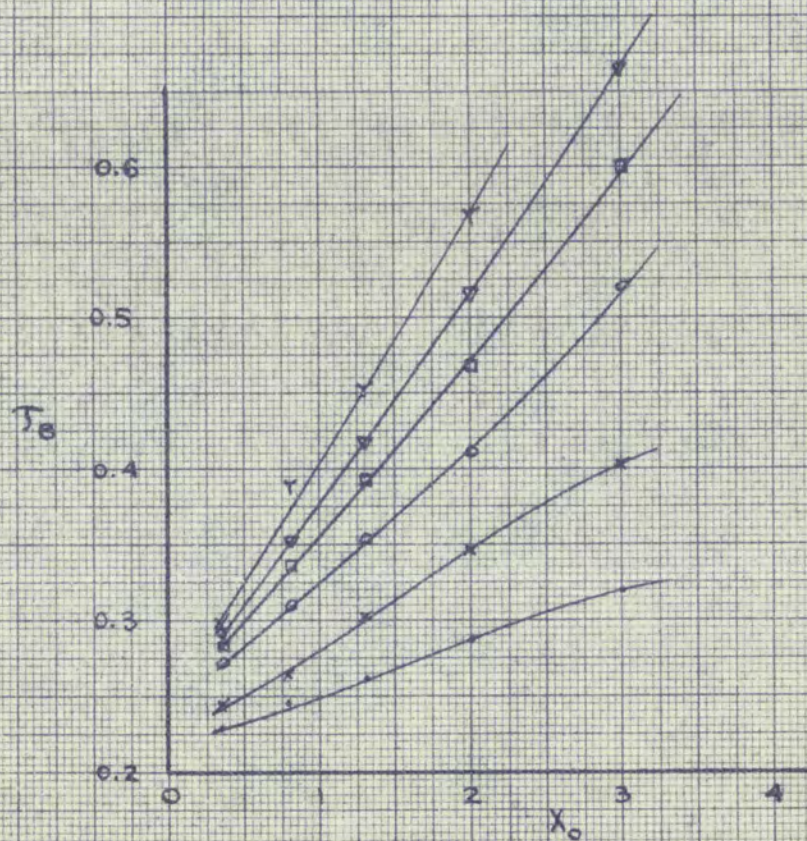
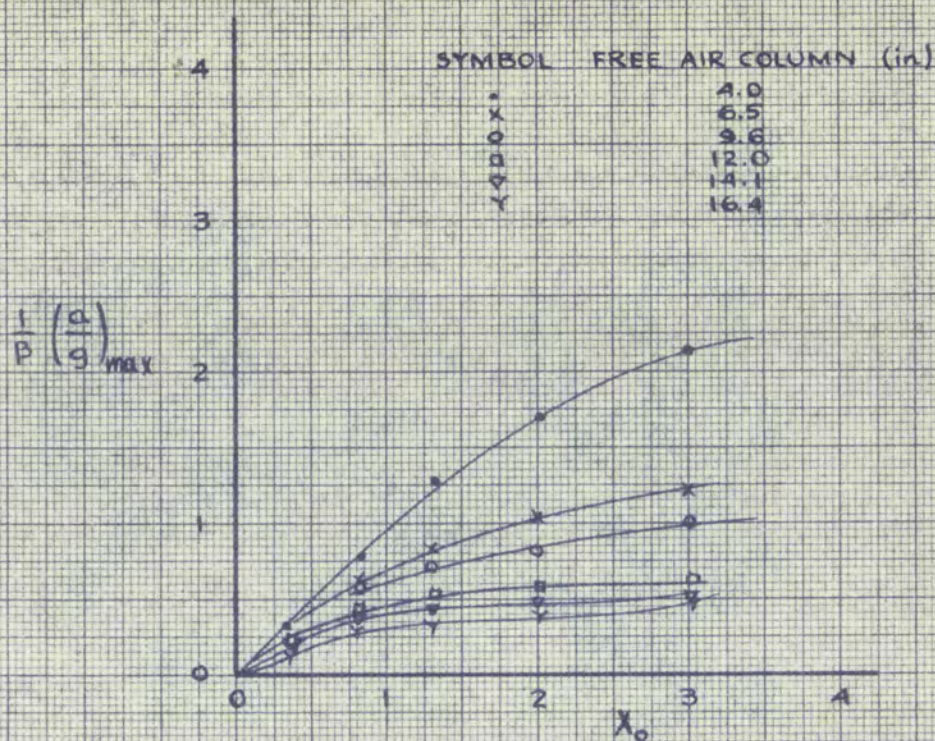


GRAPH 26

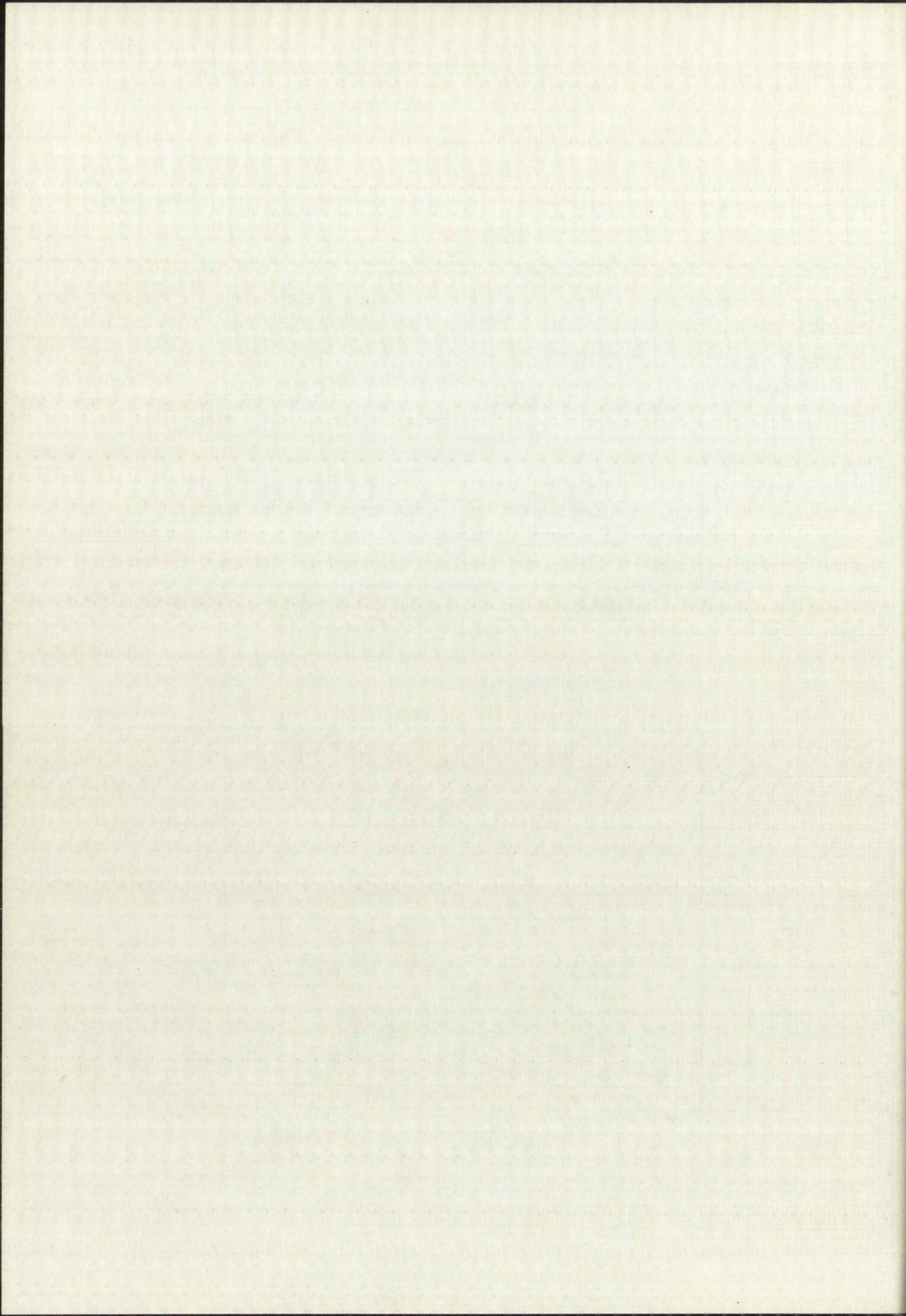


CALCULATED RESULTS

$$\beta = 9.04$$



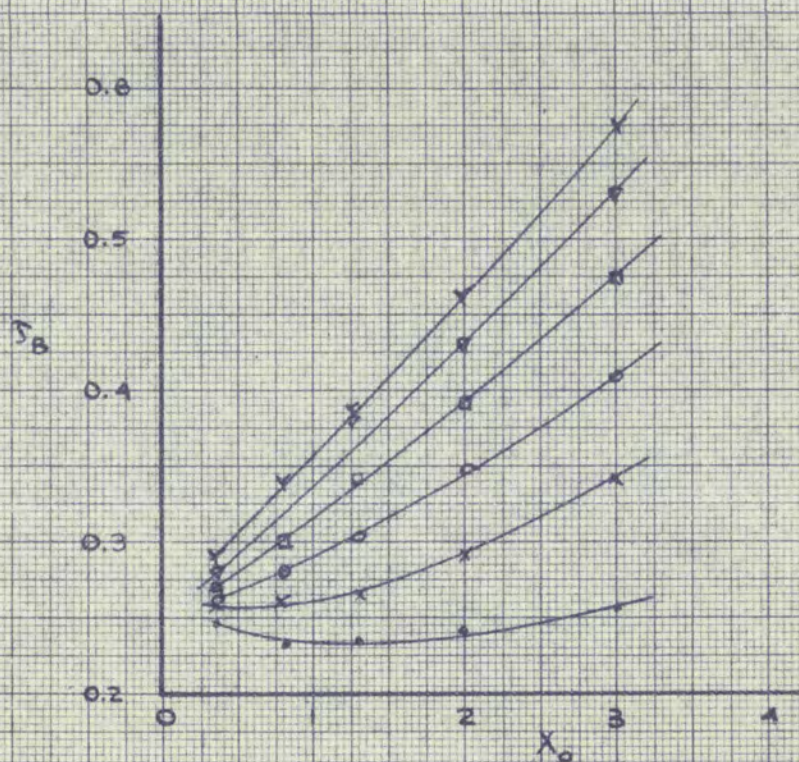
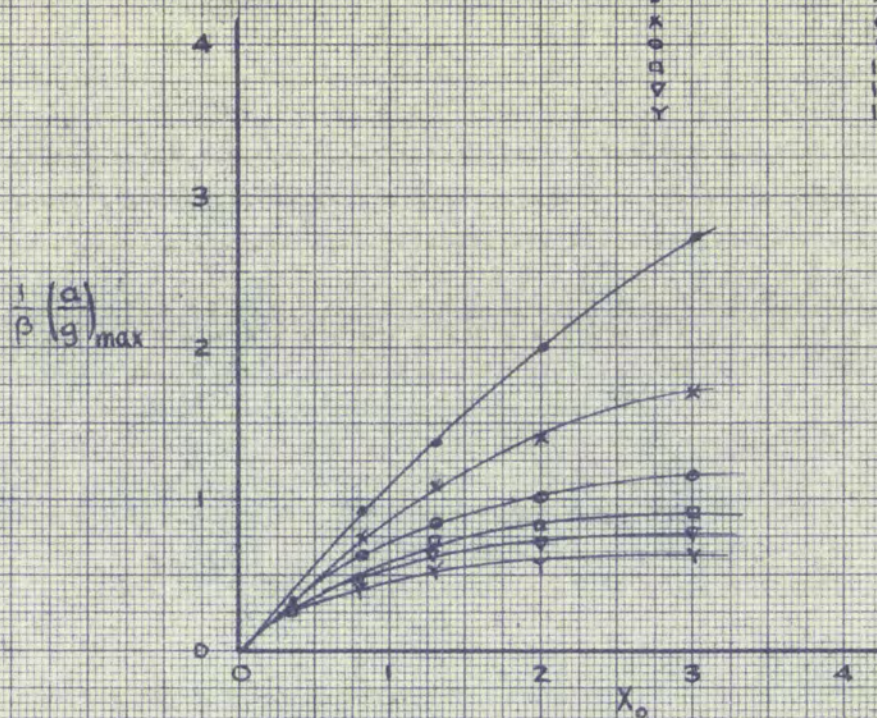
GRAPH 27



CALCULATED RESULTS

$$\beta = 6.72$$

SYMBOL	FREE AIR COLUMN (in)
•	4.0
x	6.5
o	9.6
□	12.0
▽	14.1
Y	16.4

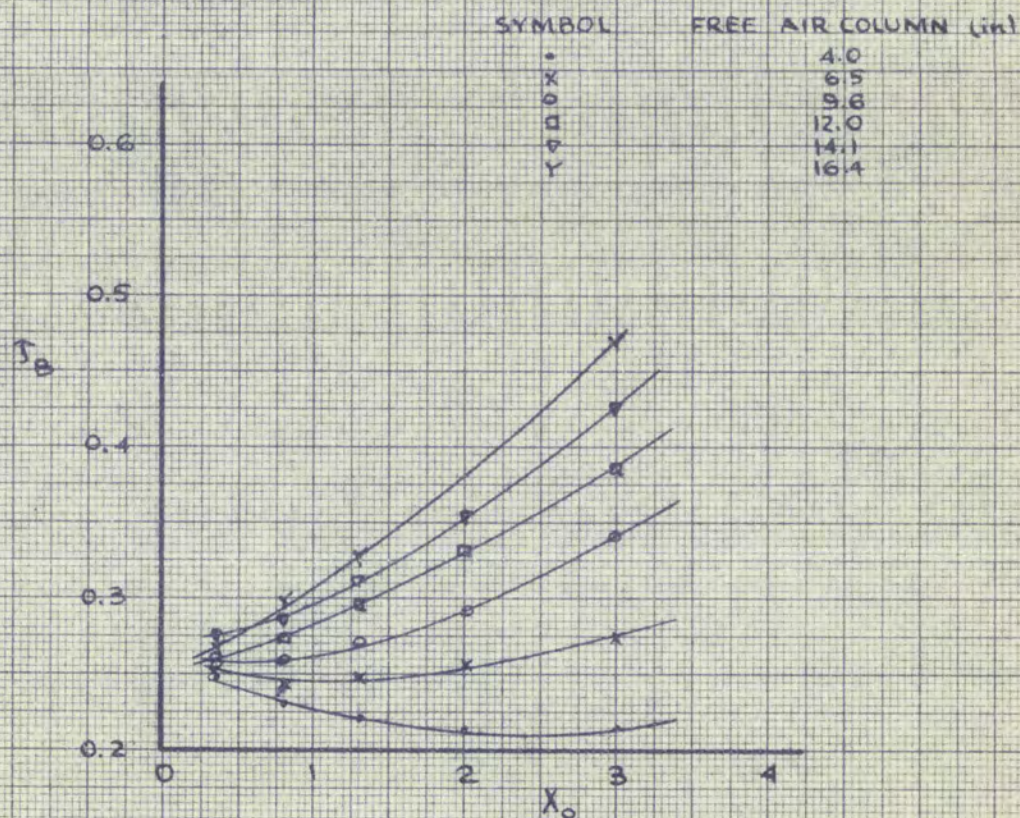
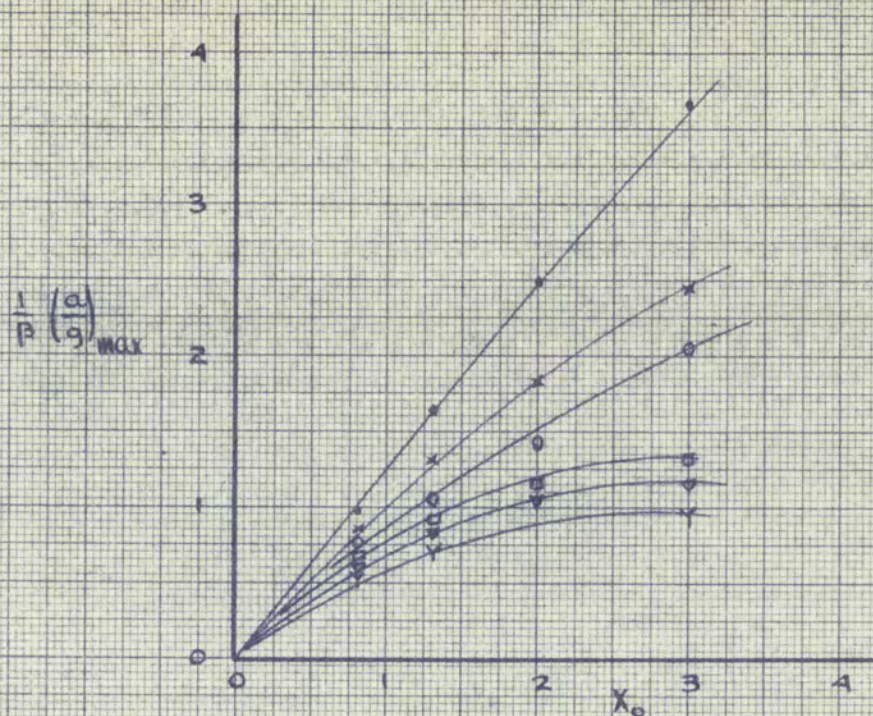


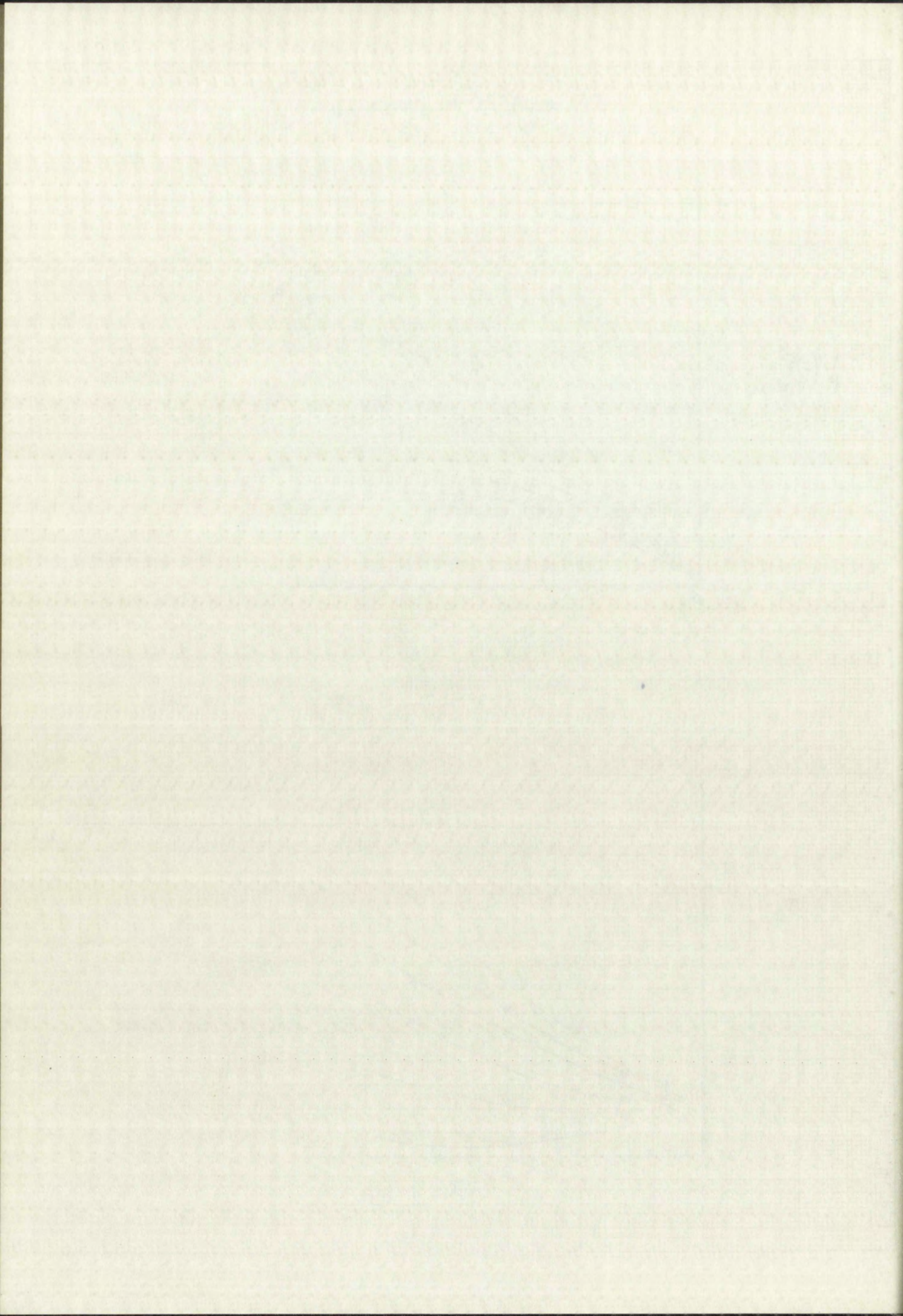
GRAPH 28



CALCULATED RESULTS

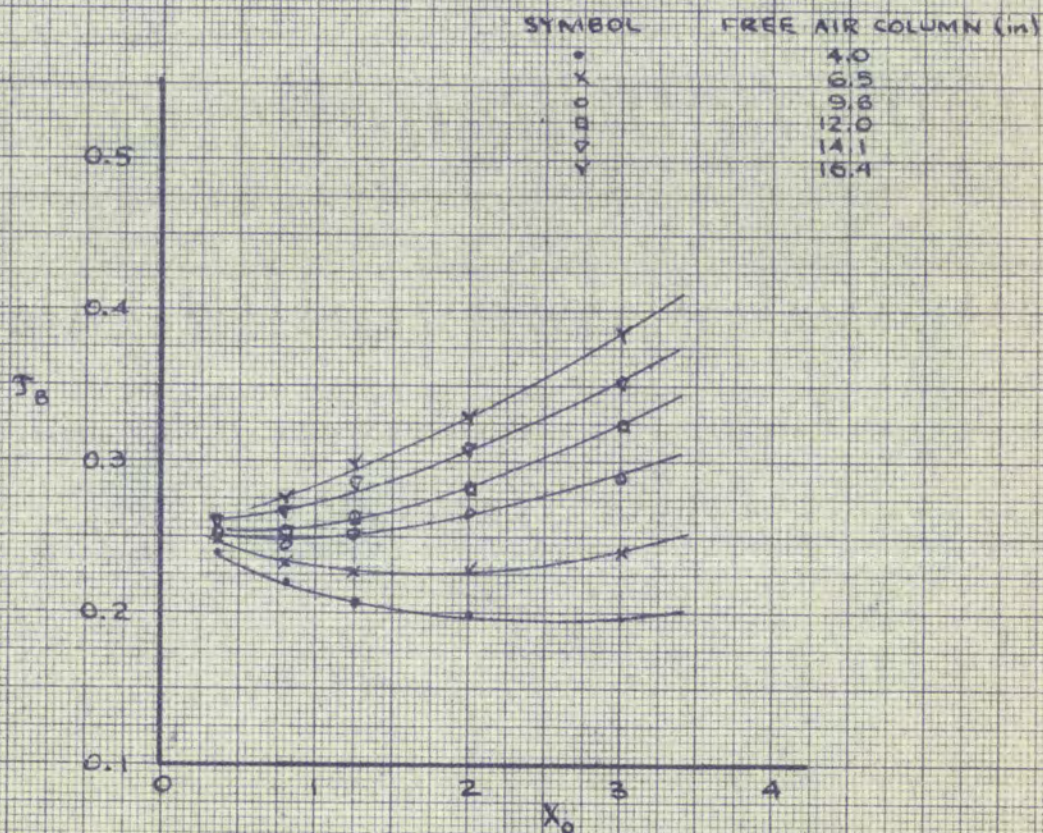
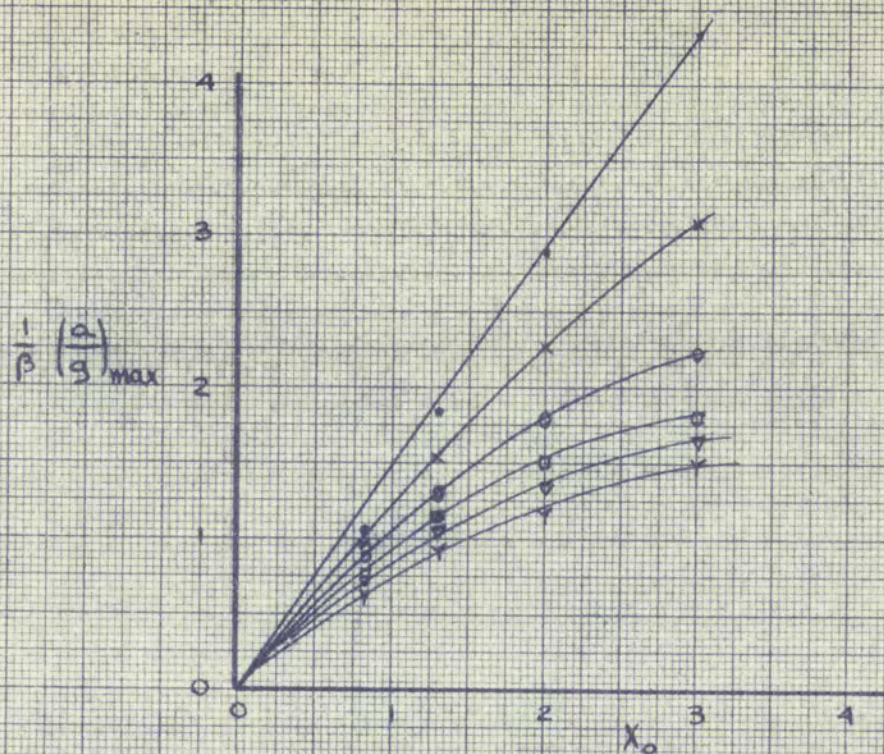
$$\beta = 5.12$$



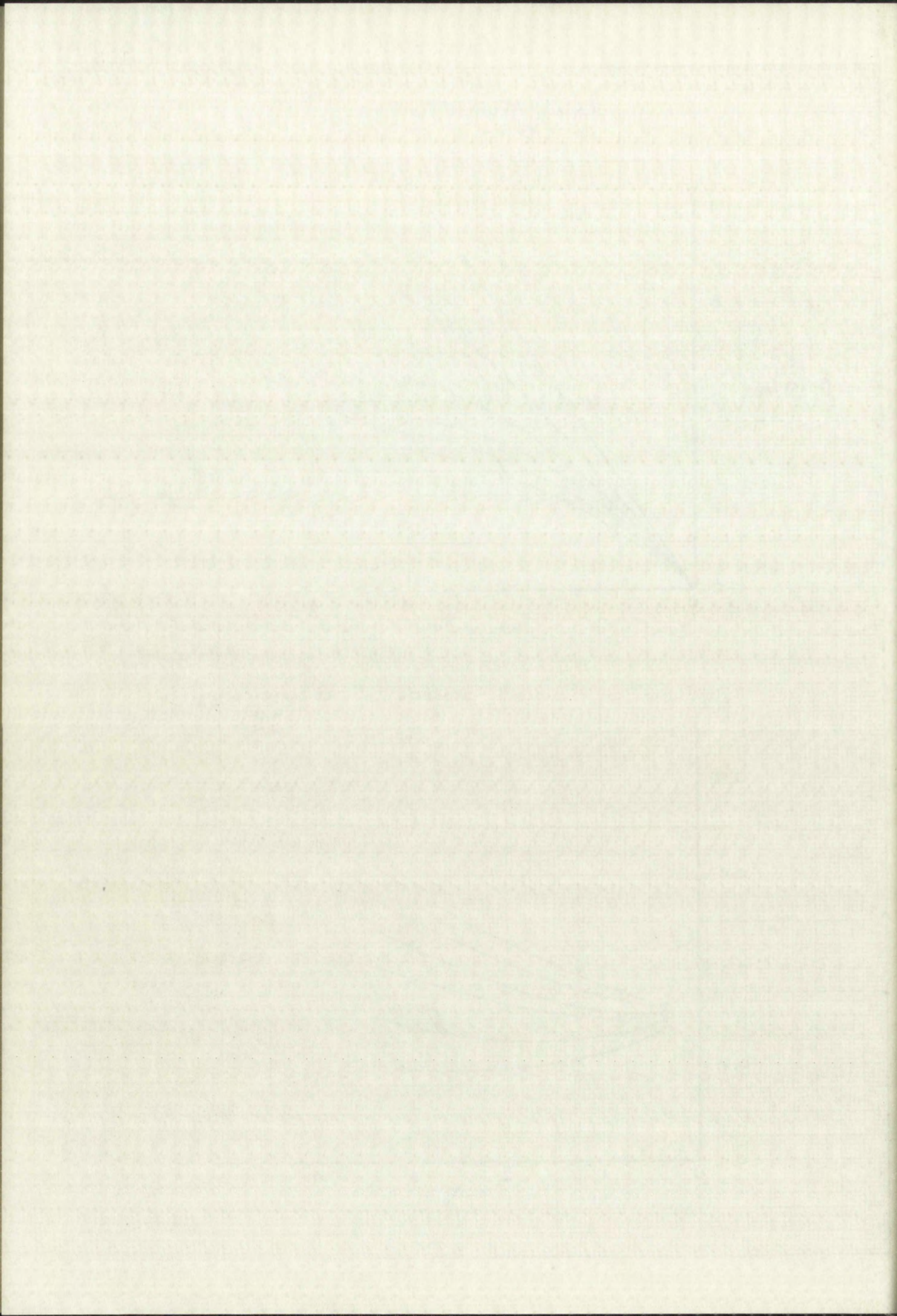


CALCULATED RESULTS

$$\beta = 4.06$$



GRAPH 30



by these devices not to exceed 5% of the full range deflection of the oscillograph needle. Drift, i.e. variation of the amplification constant with time, which occurs in most amplifier circuits, was held to a minimum during the tests by frequent checking and calibration, and by allowing sufficient time for the instruments to warm up before each series of test runs.

Displacement records were found to be legible to the nearest half millimeter without difficulty. Since, according to the calibration 10 mm on the chart corresponded to approximately 5 inches for all the runs, this means that displacements could be read within about $\frac{1}{4}$ inch. Frequent checks disclosed no measurable drift in the displacement recording circuit.

Acceleration records were more difficult to read than those of displacement, due to the large number of tiny oscillations that were recorded. Some of these small oscillations were due to extraneous signals picked up by the amplifier, but others were undoubtedly due to the actual oscillations of the accelerometer. Separation of these two types was not possible. Acceleration records could be read to the nearest millimeter. For an average run a deflection of 10 mm corresponded to 20g, so that an error of 1mm in this case would amount to 2g.

by these devices not to exceed 2% of the full range of the
side of the oscilloscope screen. This, too, variation of
the amplification constant with time, which occurs in the
amplifier circuit, was held to a minimum during the tests
by frequent checking and calibration and by allowing
sufficient time for the instruments to settle before
series of test runs.

Displacement records were found to be false to the
nearest millimeter or about 0.1 mm. Since, according
to the definition of μ in the chart, this means that
approximately 5 inches for all the runs, this means that
displacement could be read within about 1 inch. Frequent
checks of record no measurable drift in the displacement
recording circuit.

Accelerating records were difficult to read
than those of displacement, due to the large number of
tiny oscillations that were superimposed. Some of these small
oscillations were due to extraneous signals picked up by
the amplifier, but others were undoubtedly due to the actual
oscillations of the accelerometer. Separation of these two
types was not possible. Acceleration records could be read
to the nearest millimeter. For an average run a displacement
of 10 mm corresponded to 20g, so that an error of 1 mm
case would amount to 2g.

Measurements of time were somewhat inaccurate, due to the low speed of the recording device. Since the record was driven by a synchronous motor in the recorder, its speed was most likely very little in error. However, the resolution was poor, since 5 mm on the record corresponded to 0.04 seconds, so that the accuracy of reading to about 1 mm corresponded to an error of 0.01 seconds in the times. This error was in most cases a considerable percentage of the times which were to be determined.

The dimensionless accelerations plotted in Graphs 19 through 24 were computed by dividing the values of acceleration as read from the oscillograph records by appropriate values of β . Since β in these experiments ranged from 4 to 15 approximately, and since β contains at most a 2% error, one may compute errors in the dimensionless acceleration values between 0.5 and 0.13, based on the errors in the actual accelerations. The largest errors correspond to the smallest β , and vice versa.

The plotted values of dimensionless acceleration build-up time were calculated by dividing the times read from the records by the appropriate values of T_0 , where T_0 was computed from $T_0 = 2\pi \sqrt{\frac{L}{g \gamma \beta}}$. The quantities on which T_0 is based were known with sufficient accuracy, so

Measurements of time were converted into seconds, but to the low speed of the recording device. Since the speed was given by a synchronous motor in the 100 r.p.m. line, speed was most likely very little in error. However, the resolution was poor, since 5 ms on the record corresponded to 0.04 seconds, so that the accuracy of reading the film corresponded to an error of 0.01 seconds in the time. This error was in most cases a considerable percentage of the time which was to be determined.

The dimensional associations plotted in figures 19 through 24 were computed by dividing the values of association as read from the oscillograph records by appropriate values of ϕ . Since ϕ in these experiments ranged from 4 to 15 approximately, and since ϕ contains a small 2% error, one may expect errors in the dimensional association values between 0.5 and 0.15, based on the errors in the actual associations. The largest errors correspond to the smallest ϕ , and vice versa.

The plotted values of dimensional association built-up also were calculated by dividing the times read from the records by the appropriate values of ϕ , where ϕ was computed from $T_0 = 2\pi \sqrt{\frac{L}{g}}$. The quantity on which T_0 is based were known with sufficient accuracy, and

that they introduced no appreciable error. Values of T_0 for the tests ranged from 0.14 to 0.49, so that an error of 0.01 sec in reading of the record amounted to errors between 0.0715 and 0.0205 in the dimensionless times, the larger errors corresponding to the smaller values of T_0 .

Reproducibility of experimental measurements. Each of the runs numbered 11 and 70 in Table III were repeated three times. The three records for each run were found to coincide within the accuracy to which they could be read. This means that in run 11 the maximum acceleration was reproduced at least within 2g, and in run 70, within 1g. In both cases, the observed acceleration build-up times for each run were reproduced within 0.01 seconds. Since these runs represented widely differing values of the parameters β , L , and X_0 , it may be expected that the reproducibility of the air spring results was good in general, and that accelerations could be reproduced within 2g and acceleration build-up times within 0.01 seconds at worst.

Accuracies of calculations. As pointed out in the discussion of the computational methods, the accuracy obtained by Jacobsen's graphical method can be known only empirically. Very fortunately, however, it was possible to check some of the results presented here by means of an electronic

analog computer. The differential equation for the experimental air spring (equation 27) with the friction function as given in Graph 25 was integrated with an estimated maximum error of 5%. Checks run for the frictionless air spring, where the exact solutions are known, showed accuracies which were very much better. More than half of the values plotted in Graphs 26 through 30 were checked by the analog computer. No value of the dimensionless acceleration so computed differed by more than 0.2 from the corresponding value computed by Jacobsen's method. The values of dimensionless acceleration build-up time differed by 0.01 from those computed by Jacobsen's method in the worst case. Hence, the points shown in Graphs 26 through 30 are most likely accurate within 0.2 for acceleration and 0.01 for build-up time.

Comparison of experimental and calculated results.

No relation between non-dimensional maximum acceleration and free air column length is apparent from Graphs 19 through 24, which show experimental results. It is possible that experimental inaccuracies obscure such a relation. Graphs 26 through 30, which are based on calculated results, show a definite increase in dimensionless acceleration as air column length decreases.

Non-dimensional maximum accelerations were found to increase with non-dimensional initial displacement, both from experiment and calculation. However, the calculated and measured values differ vastly. Also, the experiment indicated acceleration increasing at a constant or slightly increasing rate with initial displacement, whereas from the calculations the rate was found to decrease.

Calculated and experimental results also differ as to the influence of piston weight on maximum dimensionless acceleration obtained with a given dimensionless initial displacement. As may be seen from Graph 24 the variation of β over the entire range of experimental values seemed to affect the maximum dimensionless acceleration very little, in contrast to the calculations which predicted a uniform rise in this acceleration as β decreases (that is, as the piston weight increases).

Similar discrepancies were encountered between the calculated and measured values of dimensionless acceleration build-up time. Due to the limited accuracy of the experimental work no definite dependence of this time on free air column length could be noted. Also, variation of β seemed to have no definite influence on dimensionless acceleration build-up time, as evident from Graph 24. However, the

The first of the three conditions was found to agree with the theoretical initial displacement, from experiment and calculation. However, the initial displacement was found to be smaller. Also, the experimental initial displacement increasing at a rate and in a direction opposite to that of the theoretical displacement, whereas from the calculation the rate was found to decrease.

Calculated and experimental results also differ as to the influence of piston weight on maximum displacement. Acceleration obtained with a given displacement initial displacement. As was seen from graph 2 the variation of \dot{x} over the entire range of experimental values seemed to affect the maximum displacement acceleration very little. In contrast to the calculations which predicted a uniform rise in this acceleration as \dot{x} increases (that is, as the piston weight increases).

Further discrepancies were encountered between the calculated and measured values of displacement acceleration build-up time. Due to the limited accuracy of the experimental work no definite dependence of this time on free air column length could be noted. Also, variation of \dot{x} seemed to have no definite influence on displacement acceleration build-up time, as evident from graph 2. However, the

calculated acceleration build-up times were found to increase very markedly with air column length and β . Even the trends of the nondimensional build-up time vs. displacement curves obtained experimentally differ from those found by computation. The calculations show either a continuous increase or else a slight decrease followed by an increase in acceleration build-up time with initial displacement. The experimental values, on the other hand, show an increase followed by a slight decrease. It must be remembered, however, that the experimental measurements of the acceleration build-up times involved considerable error, especially for small T_0 (large β and small L), so that these errors probably obscured some results.

Discussion of results. The differences between the calculated and experimentally determined values are nearly everywhere obviously greater than can be explained by experimental inaccuracies alone. Since both the experimental data and calculated values were judged essentially reliable, the discrepancies between the two must be explained on other grounds.

The friction-velocity curve is probably the greatest source of these discrepancies. As seen from Graph 17, the data are widely spread and are especially ill defined for

velocities of less than 10 in/sec. A still greater source of difficulty, however, lies in the extrapolation of the friction curve for higher velocities. Although the general trend of the extrapolation is probably valid if hydrodynamic lubrication between the piston "O"-ring and cylinder wall is present, it is not known whether this condition exists. Further, although the trend may be correct, the actual values may be considerably in error.

Chatter of the "O"-ring, that is, alternate sliding and seizing of the ring against the cylinder wall, may have contributed a great deal to the deviation of the actual friction relation from the extrapolated curve. As may be observed from a close observation of the acceleration records, this chattering increased as velocity increased. Chattering may not only have served to alter the friction-velocity relation, but it may further have distorted the experimental results by promoting air leakage past the piston.

The effect of air leakage past the piston could not have been very large. Since the free air column lengths were recorded before and after each run, and since no readable change in air column length was found in any case, the net volume of air that leaked past the piston was very

velocity of flow than is indicated. It will, however, be noted that the velocity of flow is in the direction of the friction curve is higher velocity. Although the general trend of the extrapolation is probably valid it hydrodynamic interaction between the piston and cylinder wall is present, it is not known whether this condition exists. However, although the trend may be correct, the actual values may be considerably in error.

Character of the friction curve is also somewhat different and indicates the ring against the cylinder wall, say by a contact area a great deal to the deviation of the actual friction relation from the extrapolated curve. As may be observed from a close observation of the relationship between the two, this observation increased as velocity increased. Character may not only have varied to alter the friction velocity relation, but it may further have altered the experimental results by providing air leakage past the piston.

The effect of air leakage past the piston could not have been very large. Since the two air column lengths were recorded before and after each run, and since no appreciable change in air column length was found in any case, the net volume of air that leaked past the piston was very

small. The chance of as much air leaking out of the air column as into it is small since during any run the pressure in the air column was below ambient for a much longer time than it was above ambient.

It was possible to calculate the variation of friction with velocity from experimental data. This was done by substituting measured quantities into the equation

$$\phi = \frac{W}{g} \frac{d^2x}{dt^2} + B \left[\left(1 - \frac{x}{L} \right)^{-\gamma} - 1 \right]$$

$$= W \left[\frac{a}{g} + \beta \left\{ \left(1 - \frac{x}{L} \right)^{-\gamma} - 1 \right\} \right]$$

which was obtained from equation (25) by solution for ϕ . Such calculations are shown in Table IV, and the results are plotted in Graph 31, superimposed on the assumed friction curve. Only oscillograph records that were clearly and easily legible were used for these calculations, so that accelerations could be read with an accuracy of about $\frac{1}{2}$ g. However, most of the accelerations used for computation in Table IV are less than 3g, so that a $\frac{1}{2}$ g error amounts to more than 15%. Velocities were determined by dividing a measured displacement increment by a measured time increment. A constant displacement interval was conveniently used for

small. The change of an atom's position during the time
between two measurements is so small that during any one of the pressure
in the column and being subject for a small fraction of time
than is the above relation.

It was possible to calculate the variation of the
from the velocity from experimental data. This was done
by substituting measured quantities into the equation

$$\phi = \frac{1}{2} \frac{d^2 x}{dt^2} + \frac{1}{2} \left[\left(1 - \frac{x}{L} \right) \right]^{-1} \left[1 - \frac{x}{L} \right]^{-1}$$

$$= \frac{1}{2} \left[\frac{A}{B} + C \right] \left(1 - \frac{x}{L} \right) \left[1 - \frac{x}{L} \right]^{-1}$$

which was obtained from equation (23) by solution for ϕ .
Such calculations are shown in Table IV, and the results
are plotted in Graph 21, superimposed on the measured position
curve. Only acceleration records that were clearly and
readily legible were used for these calculations, so that
accelerations could be read with an accuracy of about ± 1 g.
However, most of the accelerations used for comparison in
Table IV are less than 2g, so that a ± 1 g error amounts to
more than 50%. Velocities were determined by dividing the
measured displacement interval by a measured time interval.
A constant displacement interval was conveniently used for

this series of measurements, hence the error in the calculated velocity due to a given small error in the time reading increased with velocity. These errors are clearly evident from the spread of the data in Graph 31.

Due to the spread of the above results, which was caused by the lack of accuracy of the oscillograph records, no conclusions can be drawn from these calculated results. However, since the upper envelope of the plotted points in Graph 31 deviates more from the originally assumed curve than the lower envelope, and from physical reasoning, it is probable that the friction force was larger than that which was originally assumed, especially at the higher velocities.

Increased friction at the higher velocities would tend to decrease the maximum accelerations observed and thus to decrease the difference between acceleration values measured for different free air column lengths, since shorter air columns theoretically tend to produce higher accelerations and higher velocities.

It is reasonable to expect that the forces produced by chatter at a given velocity do not depend on piston weight, so that at a given velocity a lighter piston would be retarded more by these forces than a heavier one. Since the velocities attained with lighter pistons were greater than

This series of experiments, hence the error in the calculated velocity due to a given small error in the measured increased with velocity. These errors are clearly evident from the spread of the data in Graph 21.

Due to the spread of the above results, which are caused by the lack of accuracy of the measurements, no conclusions can be drawn from these calculated results. However, since the upper envelope of the plotted data is much flatter than the lower envelope, it is probable that the friction force was larger than that which was originally assumed, especially at the higher velocities.

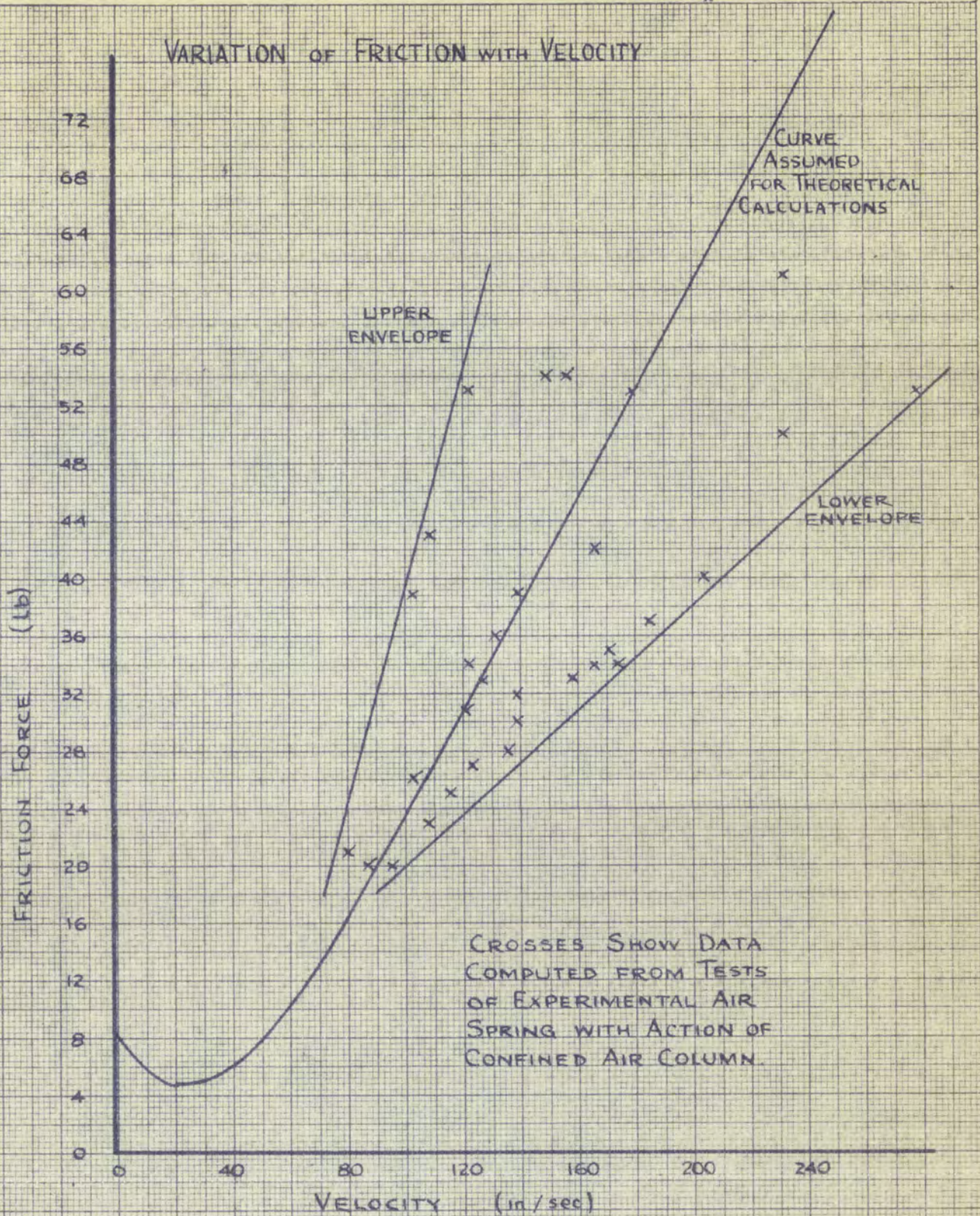
Increased friction at the higher velocities would tend to decrease the maximum acceleration observed and thus to decrease the difference between acceleration values measured for different knee air column lengths, which, however, air column theoretically tend to produce higher acceleration and higher velocities.

It is reasonable to expect that the forces produced by contact at a given velocity do not depend on knee height, so that at a given velocity a shorter knee would be subjected more by these forces than a heavier one. Since the velocities associated with higher knee were greater than

those with heavier pistons, and since the lighter piston theoretically produces greater maximum accelerations, such chatter forces would help also to bring the maximum acceleration values obtained with various piston weights closer together.

An increase of friction with velocity above that assumed for the calculations would also help to explain the discrepancies observed between the measured and computed values of acceleration build-up time. A more marked increase of friction with velocity would theoretically tend to increase the acceleration build-up times. Since light pistons and short free air columns tend to produce higher velocities and shorter acceleration build-up times, a large increase in friction with velocity hence would tend to make all of these times more nearly alike. Such a friction variation could also account very easily for the observed variations of acceleration build-up time with initial displacement, by similar reasoning.

It is unlikely that there were sources of appreciable discrepancy between the calculated and experimentally measured values, other than those due to the error in the friction-velocity variation. However, as has been demonstrated above, that single source of error alone is sufficient to account for all the discrepancies.



GRAPH 31

RUN	W	β	L	X	$1 - \left(1 - \frac{X}{L}\right)^{-\gamma}$	$\frac{a}{g}$	ϕ (lb)	v (in/sec)
13	7.40	9.04	4.0	8.3	.81	1.4	53	179
13	7.40	9.04	4.0	4.9	.67	-3.0	82	206
14	7.40	9.04	4.0	10.5	.83	3.2	39	139
14	7.40	9.04	4.0	7.4	.77	1.0	54	156
19	10.40	6.72	3.75	8.85	.82	2.0	36	387
21	14.42	5.12	3.5	6.4	.77	1.0	42	166
22	14.42	5.12	3.5	5.9	.75	0.7	53	122
31	4.26	14.98	7.0	7.5	.64	1.5	35	171
35	7.40	9.04	6.5	6.0	.60	1.0	33	158
40	10.40	6.72	6.25	9.75	.73	2.5	25	115
40	10.40	6.72	6.25	3.35	.46	0	32	139
45	10.40	6.72	5.81	5.93	.62	1.5	28	136
50	14.42	5.12	5.5	9.0	.74	2.0	26	103
52	19.44	4.06	5.5	7.0	.68	2.5	39	103
56	4.26	14.98	10.12	5.48	.46	-1.5	36	131

Run	π	ϕ	β	α	$\gamma - \left(\frac{\gamma}{\beta} - \beta \right) - \lambda$	$\frac{\alpha}{\beta}$	ϕ (JD)	$\log V_{\text{rot}} = \alpha$ (km/sec)
577	01.5	40.0	0.3	0.0	82	4.1	23	5.5
578	00.5	20.0	0.0	0.0	70	0.0	28	5.5
579	00.0	00.0	0.0	0.0	60	0.0	30	5.5
580	00.0	00.0	0.0	0.0	50	0.0	30	5.5
581	00.0	00.0	0.0	0.0	40	0.0	30	5.5
582	00.0	00.0	0.0	0.0	30	0.0	30	5.5
583	00.0	00.0	0.0	0.0	20	0.0	30	5.5
584	00.0	00.0	0.0	0.0	10	0.0	30	5.5
585	00.0	00.0	0.0	0.0	0	0.0	30	5.5
586	00.0	00.0	0.0	0.0	0	0.0	30	5.5
587	00.0	00.0	0.0	0.0	0	0.0	30	5.5
588	00.0	00.0	0.0	0.0	0	0.0	30	5.5
589	00.0	00.0	0.0	0.0	0	0.0	30	5.5
590	00.0	00.0	0.0	0.0	0	0.0	30	5.5
591	00.0	00.0	0.0	0.0	0	0.0	30	5.5
592	00.0	00.0	0.0	0.0	0	0.0	30	5.5
593	00.0	00.0	0.0	0.0	0	0.0	30	5.5
594	00.0	00.0	0.0	0.0	0	0.0	30	5.5
595	00.0	00.0	0.0	0.0	0	0.0	30	5.5
596	00.0	00.0	0.0	0.0	0	0.0	30	5.5
597	00.0	00.0	0.0	0.0	0	0.0	30	5.5
598	00.0	00.0	0.0	0.0	0	0.0	30	5.5
599	00.0	00.0	0.0	0.0	0	0.0	30	5.5
600	00.0	00.0	0.0	0.0	0	0.0	30	5.5

RUN	W	β	L	x	$1 - \left(1 - \frac{x}{L}\right)^{-\lambda}$	$\frac{a}{g}$	ϕ (lb)	v (in/sec)
64	10.40	6.72	9.25	4.95	.46	0.5	27	123
67	10.40	6.72	9.25	7.75	.58	1.7	23	108
70	14.42	5.12	8.75	4.25	.44	0.8	20	87
72	14.42	5.12	8.75	8.25	.61	1.7	20	95
72	14.42	5.12	8.75	3.15	.35	-1.2	43	109
81	4.26	14.98	12.5	3.0	.26	-1.0	21	80

CHAPTER V

CONCLUSIONS AND RECOMMENDATIONS

I. FEASIBILITY OF USING AIR SPRING AS TESTING MACHINE

The experimental air spring model, although rather crudely constructed, proved that the air spring may be employed successfully to produce a considerable range of maximum accelerations and times taken by these accelerations to build up from zero. As shown in Table III, maximum accelerations between 0.8 and 41.2 were measured, and acceleration build-up times between 0.026 and 0.118 seconds were obtained with different piston weights. With the same weight of the piston assembly, the ranges were narrowed slightly. With a 4.26 lb piston, maximum acceleration varied between 1.0 and 41.3 g and acceleration build-up time between 0.026 and 0.082 sec. Results obtained with the experimental spring further indicate that acceleration build-up time depended essentially only on the length of the free air column, whereas the maximum acceleration obtained depended both on the free air column length and the position from which the piston was released. Thus, the possibility of adjusting both the maximum acceleration and the time taken for the acceleration to increase from zero to its maximum value was demonstrated.

COMBUSTION AND ENGINE CHARACTERISTICS

1. CHARACTERISTICS OF THE AIR FLOW AS THE ENGINE RUNS

The experimental air engine model, the only model of its kind, proved that the air engine may be employed successfully to produce a considerable range of maximum accelerations and times taken by these accelerations to build up from zero. As shown in Table III, maximum accelerations between 0.2 and 0.5 were measured, and acceleration build-up times between 0.025 and 0.112 seconds were obtained with different piston weights. With the same weight of the piston assembly, the ranges were narrowed slightly. With a 0.25 lb piston, maximum acceleration varied between 0.2 and 0.5 g and acceleration build-up times between 0.025 and 0.088 sec. Results obtained with the experimental engine further indicate that acceleration build-up time depended essentially only on the weight of the free air column, whereas the maximum acceleration obtained depended both on the free air column length and the position from which the piston was released. Thus, the possibility of adjusting both the maximum acceleration and the time taken for the acceleration to increase from zero to its maximum value was demonstrated.

II. PREDICTION OF AIR SPRING ACTION BY MATHEMATICAL ANALYSIS

A graphical integration method was applied to the solution of the air spring equation for various initial conditions and various values of the important parameters. The method was found to give mathematically good results, as proven by comparing values obtained by it with corresponding values calculated by means of a commercial electronic analog computer.

However, there was some discrepancy between the computed and the experimentally determined maximum accelerations and acceleration build-up times. This discrepancy was ascribed mostly to a difference between the actual variation of friction with velocity and the variation assumed in the calculations. The calculations were based on an extrapolation of measured data for low velocities, based on comparison with similar published friction data. It was not discovered until too late that chattering of the rubber "O"-ring on the piston could distort the friction variation considerably. Thus, validation of the mathematical analysis can not be complete without further experimentation.

III. IMPROVEMENTS IN APPARATUS

The following suggested improvements should eliminate all of the major difficulties.

II. PREDICTION OF AIR FRICTION ACTION BY MATHEMATICAL ANALYSIS

A classical integrated method was applied to the

solution of the air friction equation for various initial conditions and various values of the important parameters. The method was found to give mathematically good results, as proven by comparing values obtained by it with corresponding values obtained by means of a commercial electronic analog computer.

However, there was some discrepancy between the computed and the experimentally determined maximum accelerations and acceleration build-up times. This discrepancy was ascribed mostly to a difference between the actual variation of friction with velocity and the variation assumed in the calculations. The calculations were based on an extrapolation of measured data for low velocities, based on comparison with similar published friction data. It was not discovered until too late that characterizing of the rubber ring on the piston could distort the friction variation considerably. Thus, validation of the mathematical analysis can not be complete without further experimentation.

III. IMPROVEMENTS IN APPARATUS

The following suggested improvements should eliminate

all of the major difficulties.

Micro-honing of the air cylinder and a tightly fitting accurately machined and polished piston made entirely of metal and using no soft sealing materials of any sort should eliminate chattering to a large extent. Further, chattering between the guide rods and guide holes in the test platform should be reduced by attaching sleeves to the platform so that the total contact area between it and the guide rods is increased. Also, the weights on the test platform should be balanced in order to decrease the chances for chattering further.

A recording apparatus which possesses better time resolution, i.e. is capable of higher recording speeds, would aid in obtaining better measurements of build-up time. Direct recording of velocity would be very useful in improving the accuracy of friction-velocity data. A mechanism by means of which quick release of the piston may be obtained more reliably and uniformly would further help to increase the precision of the experimental work.

Finally, it is very important that friction measurements are obtained at higher velocities than can be reached by permitting the piston to drop due to gravity alone. This may probably be accomplished most easily by using a mechanical spring whose spring constant has been measured

carefully. Use of the air spring itself for this purpose is possible also, but its force-displacement characteristics would have to be measured accurately. These arrangements would permit computation of the force due to the spring and hence would permit calculation of the friction forces from the observed accelerations.

IV. FURTHER DEVELOPMENTS

Some other variations of the air spring apparatus may be fruitful. One of these would consist of an arrangement somewhat like the one described herein, except that only one withdrawn position is provided for the piston assembly and that the air cylinder is connected to an air compressor and vacuum pump so that high or low pressure may be applied to it at will and controlled to desired values. This would be extremely desirable for large installations. The high pressure in the cylinder could be used to raise the piston until it reaches the withdrawn position, where a holding arrangement may take hold automatically. Then the air would be exhausted from the cylinder until a pressure is reached which from previous calibration is known to give a certain desired maximum acceleration. In this arrangement, the time taken for the acceleration to increase from zero to its maximum value would have to be adjusted by the addition or removal of weight on the piston.

Another possibility consists of using the air spring merely as a controlled shock absorber. When used in this way, the items to be tested are mounted on a test stage which is permitted to fall under the action of gravity alone until it strikes the air spring. The acceleration in this case is controlled by the height of the free fall and by the adjustment of the air spring. Such a device, in fact, is currently being made by the American Research Corporation of Hartford, Connecticut. The commercially available device consists of a test platform which drops onto a cylinder connected to an air chamber. The acceleration is controlled by presetting the air pressure in the chamber.²⁶ However, in the commercial apparatus no attempt is made to control the acceleration build-up time, so that more work could be done along this line.

²⁶ Industrial Laboratories, August, 1953, Volume 4, No. 8, p. 68.

CHAPTER VI

ACKNOWLEDGEMENTS

Without the use of the instrumentation lent to the writer by the Sandia Corporation the experimental work would have been greatly hampered. Mr. R.S. Wilson generously authorized the loan of the instruments, and Mr. W. Hollenbeck and his staff calibrated and serviced them.

A special debt of gratitude is owed to Mr. W. Lane of the analog computer section of Sandia Corporation for the use of his machines and for his help in setting up and running a difficult problem.

This list of acknowledgements would be incomplete without mentioning Dr. V.J. Skoglund of the University of New Mexico who gave of his time and efforts far beyond the usual requirements, and without whom this thesis could not have been accomplished.

BIBLIOGRAPHY

- Andronow, A. A., and C. E. Chaikin, Theory of Oscillations, Princeton University Press, 1949.
- Bieberbach, L., Theorie der Differentialgleichungen, 3. Aufl. New York: Dover Publications, Inc., 1944 (Berlin: Verlag Springer, 1930).
- Brown, R. W., "Air Springs - Tomorrow's Ride", Journal of the Society of Automotive Engineers, 38:126-32, April, 1936.
- Bruce, V. G., "A Graphical Method for Solving Vibration Problems of a Single Degree of Freedom", Bulletin of the Seismological Society of America, 41:101-109, April, 1951.
- Church, A. H., Elementary Mechanical Vibrations, New York: Pitman Publishing Corporation, 1948.
- "Compressed Air Cuts Bounce", Business Week, p. 78, October 18, 1952.
- Den Hartog, J. P., Mechanical Vibrations, New York: McGraw-Hill Book Company, Inc., 1947.
- Den Hartog, J. P., "Forced Vibrations with Combined Viscous and Coulomb Damping", Philosophical Magazine, 9:801-817, May, 1930. Supplement.
- Den Hartog, J. P., and R. M. Heiles, "Forced Vibrations in Nonlinear Systems with Various Combinations of Linear Springs", Journal of Applied Mechanics, 3:A127-30, December, 1936.
- "Discussion of Papers", Journal of Applied Mechanics, 12:A-179, September, 1945.
- Faires, V. M., Design of Machine Elements, New York: The Macmillan Company, 1941.
- Falkner, V. M., "Numerical Solution of Differential Equations", Philosophical Magazine, 21:624-40, March, 1936.
- Ford, L. R., Differential Equations, New York: McGraw-Hill Book Company, Inc., 1933.
- Fuchs, H. O., "Spiral Diagrams to Solve Vibration Problems", Product Engineering, 7:294-96, 1936.

"The Gruss Auxiliary Air Spring", Automobile Engineering, 20:276, August, 1930.

Hartree, D. R., "A Practical Method for the Numerical Solution of Differential Equations", Memoirs of the Manchester Philosophical Society, 77:91-107.

Industrial Laboratories, 4:68, August, 1953.

Jacobsen, L. S., On a General Method of Solving Second-Order Ordinary Differential Equations by Phase Plane Displacements, Paper No. 52--A-1. Presented at meeting of American Society of Mechanical Engineers, November 30-December 5, 1952.

Kamke, E., Differentialgleichungen; Lösungsmethoden und Lösungen, Vol. I, 2nd Ed., Leipzig, Germany: Becker & Erler Kom-Ges., 1943.

Kryloff, N., and N. Bogoliuboff, Introduction to Non-Linear Mechanics, S. Lefschetz, translator, Princeton: Princeton University Press, 1943.

Lefschetz, S., editor, Contributions to the Theory of Non-linear Oscillations, Princeton: Princeton University Press, 1950.

Levy, H. and E.A. Baggott, Numerical Solutions of Differential Equations, New York: Dover Publications, Inc., 1950.

Lotkin, M., "An Integration Procedure of High Accuracy", Journal of Mathematics and Physics, 31, 1952.

Lotkin, M., An Integration Procedure of High Accuracy, Ballistic Research Laboratories Report No. 838, Aberdeen, Maryland: Ballistic Research Laboratories, November, 1952.

Ludeke, C. A., "A Method of Equivalent Linearization for Nonlinear Oscillatory Systems with Large Nonlinearity", Journal of Applied Physics, 20:694-99, July, 1949.

McLachlan, N. W., Theory of Vibrations, New York: Dover Publications, Inc., 1951.

Manley, R. G., Fundamentals of Vibration Study, New York: John Wiley & Sons, Inc., 1942.

Meissner, E., Graphische Analysis Vermittelst des Linienbildes einer Funktion, Zürich: Verlag der Schweizerischen Bauzeitung, 1932.

- Meissner, E., "Über eine Nicht-Harmonische Schwingung", Schweizerische Bauzeitung, 109:35-36, July 28, 1934.
- Milne, W. E., Numerical Solution of Differential Equations, New York: John Wiley & Sons, Inc., 1953.
- Minorsky, N., "Modern Trends in Non-Linear Mechanics", Advances in Applied Mechanics, Vol. I, Academic Press, Inc., 1948.
- Minorsky, N., Introduction to Non-Linear Mechanics, Ann Arbor, Michigan: Edwards Brothers, Inc., 1947.
- Numerical Integration of Differential Equations, Bulletin No. 92 of the National Research Council, Washington, D. C.: United States Government Printing Office, November, 1953.
- Rauscher, M., "Steady Oscillations of Systems with Nonlinear and Unsymmetrical Elasticity", Journal of Applied Mechanics, 5:A169-A177, 1938.
- Sadowsky, M. A., "Non-linear Springs", Journal of the Franklin Institute, 240:467-76, December, 1945.
- Scarborough, J. B., Numerical Mathematical Analysis, Baltimore, Maryland: The Johns Hopkins Press, 1930.
- Stoker, J. J., Nonlinear Vibrations in Mechanical and Electrical Systems, New York: Interscience Publishers, Inc., 1950.
- Sussholz, B., "Forced and Free Motion of a Mass on an Air Spring", Journal of Applied Mechanics, 11:A-101 - A-107, June, 1944.
- Thomas, S., "Vibrations Damped by Solid Friction", Philosophical Magazine, 9:329-45, March, 1930.
- Thomson, W. T., Mechanical Vibration, 2nd Ed., New York: Prentice-Hall, Inc., 1953.
- Timoshenko, S., Vibration Problems in Engineering, 2nd Ed., New York: D. Van Nostrand Company, Inc., 1937.
- Tulpin, W. A., "Vibration in Springs with Nonlinear Characteristics", Engineering, 158:103, August 11, 1944 and 158:124-5, August 18, 1944.

Reichardt, E., "Über eine nicht-Newton'sche Schwerkraft", Zeitschrift für Physik, 193:33-35, July 23, 1933.

Wine, W. E., Experimental Analysis of Differential Equations, New York: John Wiley & Sons, Inc., 1933.

Wintner, S., "Wobbling Orbits in Non-linear Mechanics", Advances in Applied Mechanics, Vol. 1, Academic Press, Inc., 1945.

Wintner, S., Introduction to Non-linear Mechanics, New York: McGraw-Hill Book Co., Inc., 1947.

Wintner, S., Mathematical Foundations of Non-linear Mechanics, New York: McGraw-Hill Book Co., Inc., 1947.

Wintner, S., "Steady Oscillations of Systems with Nonlinear and Dissipative Elements", Journal of Applied Mechanics, 5:153-157, 1938.

Wintner, S., "Non-linear Oscillations", Journal of the Franklin Institute, 243:487-78, December, 1948.

Wintner, S., Mathematical Foundations of Non-linear Mechanics, New York: McGraw-Hill Book Co., Inc., 1947.

Wintner, S., Nonlinear Oscillations in Mechanical and Electrical Systems, New York: Interscience Publishers, Inc., 1950.

Wintner, S., "Forced and Free Motion of a Mass on an Air Spring", Journal of Applied Mechanics, 11:101-107, June, 1944.

Wintner, S., "Oscillations Forced by a Sinusoidal Force", Philosophical Magazine, 3:333-35, March, 1930.

Wintner, S., Mathematical Foundations of Non-linear Mechanics, New York: Prentice-Hall, Inc., 1947.

Wintner, S., Nonlinear Problems in Mechanics, New York: Van Nostrand Company, Inc., 1950.

Wintner, S., "Vibration in Systems with Nonlinear Damping", Engineering, 158:193, August 11, 1944, and 158:194-5, August 18, 1944.

APPENDIX A

SAMPLE SOLUTION OF DIFFERENTIAL EQUATION FOR
LINEAR SPRING BY NUMERICAL INTEGRATION

For a linear spring of stiffness K , with an attached weight W , the differential equation is:

$$(A1) \quad \frac{W}{g} \frac{d^2 x}{dt^2} + Kx = 0$$

In order to reduce this equation to non-dimensional form, the following definitions are made. A dimensionless displacement is defined by $X = \frac{x}{L}$ where L is the length of the undeflected spring. A stiffness per unit length of the spring is defined as $K_0 = KL$. From the solution of equation (A1) the period of the vibration is found as $T_0 = 2\pi \sqrt{\frac{W}{Kg}}$. Then a reduced time variable may be defined as $\tau = \frac{t}{T_0}$.

With these definitions, equation (A1) may be transformed into the non-dimensional form

$$(A2) \quad \frac{d^2 X}{d\tau^2} + 4\pi^2 X = 0.$$

As an illustration of the application of the numerical solution method, (A2) will be solved subject to the arbitrarily selected initial conditions $X = 0.8$, $\frac{dX}{d\tau} = 0$, at $\tau = 0$.

APPENDIX

EXAMPLE 2: THE CASE OF A LINEAR SYSTEM WITH A SINGLE INPUT AND A SINGLE OUTPUT

For a linear system of the form (1), the differential equation is:

$$\frac{d^2 x}{dt^2} + 2\zeta \omega_n \frac{dx}{dt} + \omega_n^2 x = \omega_n^2 u(t) \quad (A1)$$

In order to reduce this equation to a standard form, the following definitions are made. The natural frequency ω_n is defined by $\omega_n^2 = 1/m$, where m is the mass of the undamped spring. The damping ratio ζ is defined as $\zeta = c/(2\sqrt{km})$, where c is the coefficient of viscous friction.

(A1) the period of the vibration is $T = 2\pi/\omega_n$. Then a reduced time variable τ is defined by $\tau = t/T$. With these definitions, equation (A1) can be written into the non-dimensional form:

$$\frac{d^2 x}{d\tau^2} + 2\zeta \frac{dx}{d\tau} + x = u(\tau) \quad (A2)$$

As an illustration of the application of the Laplace transform method, (A2) will be solved for a unit step input. The initial conditions are $x(0) = 0$ and $\dot{x}(0) = 0$.

$\Delta T = 0.04$ is selected as a convenient time interval. The initial conditions may be expressed in the notation of Chapter II, as $X_0 = 0.8$, $V_0 = \left(\frac{dX}{dT}\right)_0 = 0$, $T_0 = 0$. Here $f(X) = -4\pi^2 X$, so that $f_0 = f(X_0) = -31.6$.

Formulas (7) and (8) are now applied, with $m = 0$. The results are indicated in the following tabulation. The subscript outside the parentheses denotes the number of the approximation, higher subscripts indicating better approximations.

n	$(\Delta V_1)_n$	$(V_1)_n$	$(\Delta X_1)_n$	$(X_1)_n$	$(f_1)_n$
1	-1.264	-1.264	0	0.8	-31.6
2	-1.264	-1.264	-0.025	0.775	-30.6
3	-1.244	-1.244	-0.025	0.775	-30.6

No further improvement in V_1 and X_1 to three decimal places was obtained after the third approximation. Hence these last values, $(V_1)_3$ and $(X_1)_3$, are now used to determine the values of X_2 and V_2 , again by use of formulas (7) and (8), but this time with $m = 1$. The following table lists the results.

n	$(\Delta V_2)_n$	$(V_2)_n$	$(\Delta X_2)_n$	$(X_2)_n$	$(f_2)_n$
1	-1.224	-2.468	-0.050	0.725	-28.6
2	-1.184	-2.428	-0.073	0.702	-27.7
3	-1.166	-2.410	-0.073	0.702	-27.7

$\Delta T = 0.04$ is selected as a convenient time interval.

val. The initial conditions may be expressed in the notation

$$\text{of Chapter II, as } X_0 = 0.6, Y_0 = \left(\frac{dX}{dt}\right)_0 = 0, T_0 = 0.$$

$$\text{Here } T(X) = -4\pi^2 X, \text{ so that } T_0 = T(X_0) = -31.6.$$

Formulas (7) and (8) are now applied, with $n = 0$.

The results are tabulated in the following tabulation. The

subscript denotes the parentheses denotes the number of the

approximation, higher subscripts indicating better approxi-

mations.

n	$(\Delta V)_n$	$(V)_n$	$(\Delta X)_n$	$(X)_n$	$(T)_n$
1	-1.384	-1.384	0	0.6	-31.6
2	-1.384	-1.384	-0.032	0.568	-30.8
3	-1.384	-1.384	-0.032	0.536	-30.6

No further improvement in V and X for three decimal places

was obtained after the third approximation. Hence these

last values, $(V)_3$ and $(X)_3$, are now used to determine

the values of X_0 and V_0 , again by use of formulas (7)

and (8), but this time with $n = 1$. The following table

lists the results.

n	$(\Delta V)_n$	$(V)_n$	$(\Delta X)_n$	$(X)_n$	$(T)_n$
1	-1.384	-1.384	-0.032	0.568	-30.8
2	-1.184	-1.184	-0.073	0.495	-29.7
3	-1.184	-1.184	-0.073	0.422	-27.9

Calculations by means of equations (7) and (8) are then performed with $m = 2$ and $m = 3$, with the results:

n	$(\Delta V_3)_n$	$(V_3)_n$	$(\Delta X_3)_n$	$(X_3)_n$	$(f_3)_n$
1	-1.108	-3.518	-0.096	0.606	-23.9
2	-1.032	-3.442	-0.117	0.585	-23.1
3	-1.016	-3.426	-0.117	0.585	-23.1

n	$(\Delta V_4)_n$	$(V_4)_n$	$(\Delta X_4)_n$	$(X_4)_n$	$(f_4)_n$
1	-0.924	-4.350	-0.137	0.448	-17.7
2	-0.816	-4.242	-0.153	0.432	-17.1
3	-0.804	-4.230	-0.153	0.432	-17.1

Before the values found above are checked and corrected by means of equations (10), it is convenient to summarize the results obtained so far, and to compute the " Δ -differences", as shown in the following table.

n	T	X_n	V_n	ΔV	$\Delta^2 V$	$\Delta^3 V$	$\Delta^4 V$	f_n	Δf	$\Delta^2 f$	$\Delta^3 f$	$\Delta^4 f$
0	0	.800	0					-31.6				
1	.04	.775	-1.244	-1.244	.078			-30.6	1.0			
2	.08	.702	-2.410	-1.166	.072			-27.7	2.9	1.9		
3	.12	.585	-3.426	-1.016	.150	.062	-.010	-23.1	4.6	1.7	-.2	
4	.16	.432	-4.230	-.804	.212			-17.1	6.0	1.4	-.3	-.1

The next step in the computation consists of checking and correcting the values found so far. This is done by

Calculations by means of equations (V) and (VI) are then performed with $n = 2$ and $n = 3$, with the results:

n	$(\Delta V)_{\frac{1}{2}n}$	$(V)_{\frac{1}{2}n}$	$(\Delta X)_{\frac{1}{2}n}$	$(X)_{\frac{1}{2}n}$	$(\Delta)_{\frac{1}{2}n}$
1	-1.108	-2.618	-0.098	0.208	-22.9
2	-1.032	-2.442	-0.117	0.205	-23.1
3	-1.016	-2.426	-0.117	0.205	-23.1

n	$(\Delta V)_{\frac{1}{2}n}$	$(V)_{\frac{1}{2}n}$	$(\Delta X)_{\frac{1}{2}n}$	$(X)_{\frac{1}{2}n}$	$(\Delta)_{\frac{1}{2}n}$
1	-0.364	-4.280	-0.137	0.448	-17.7
2	-0.368	-4.242	-0.115	0.452	-17.1
3	-0.364	-4.230	-0.133	0.452	-17.1

Before the values found above are checked and corrected

by means of equation (10), it is convenient to summarize

the results obtained so far, and to compare the Δ -differences, as shown in the following table.

n	ΔV	V	ΔV	V	ΔV	V	ΔV	V	ΔV	V
0	0.000	0.000								
1	1.04	1.04	1.04	1.04	1.04	1.04	1.04	1.04	1.04	1.04
2	2.08	2.08	2.08	2.08	2.08	2.08	2.08	2.08	2.08	2.08
3	3.12	3.12	3.12	3.12	3.12	3.12	3.12	3.12	3.12	3.12
4	4.16	4.16	4.16	4.16	4.16	4.16	4.16	4.16	4.16	4.16

The next step in the computation consists of checking

and correcting the values found so far. This is done by

use of equations (10). The results are given in the following table.

n	\overline{x}_n	\overline{v}_n	\overline{f}_n
1	0.775	-1.254	-30.6
2	0.702	-2.423	-27.7
3	0.584	-3.447	-23.0
4	0.429	-4.247	-16.9

The remainder of the integration consists of application of formulas (11), starting with $n = 5$ and making use of the values listed above. These computations may be carried out conveniently in tabular form and are shown in the subsequent pages.

Equation (A2) may be solved analytically. Its general solution is

$$(A3) \quad X = C_1 \sin(2\pi \tau) + C_2 \cos(2\pi \tau)$$

where C_1 and C_2 are constants that depend on the initial conditions. The initial conditions in this example require that $C_1 = 0$, $C_2 = 0.8$, so that the specific solution of (A2) is

$$(A4) \quad X = 0.8 \cos(2\pi \tau).$$

use of equation (11). The results are given in the

following table.

n	\bar{X}_n	\bar{V}_n	\bar{T}_n
1	0.776	-1.196	-30.3
2	0.702	-2.483	-37.7
3	0.686	-3.447	-38.0
4	0.679	-4.247	-38.3

The remainder of the investigation consists of application of formula (11), starting with $n = 5$ and using one of the values listed above. These computations may be carried out conveniently in tabular form and are shown in the subsequent pages.

Equation (11) may be solved analytically. The

general solution is

$$(A2) \quad X = C_1 \sin(2\pi T) + C_2 \cos(2\pi T)$$

where C_1 and C_2 are constants that depend on the initial conditions. The initial conditions in this example require that $C_1 = 0$, $C_2 = 0.8$, so that the specific solution of (A2) is

$$(A3) \quad X = 0.8 \cos(2\pi T)$$

Values computed by the numerical method and exact values found from equation (4) are compared in Table II. From this table it is evident that the numerical method is capable of good accuracy.

Values computed by the numerical method and exact values
 found from equation (4) are compared in Table II. From
 this table it is evident that the numerical method is
 capable of good agreement.

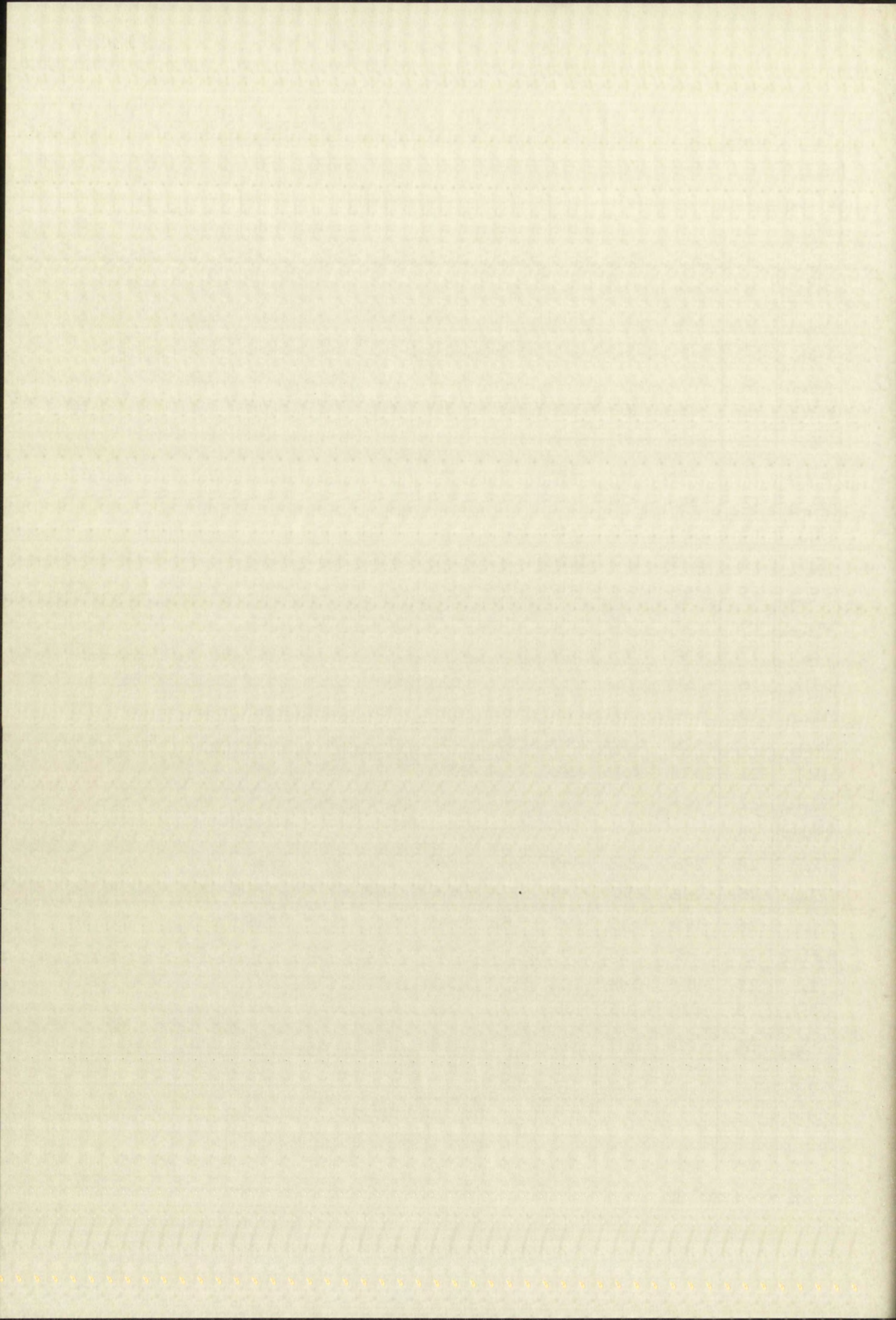
NUMERICAL INTEGRATION - LINEAR SPRING

	n	τ	X	ΔX	$\Delta^2 X$	V	ΔV	$\Delta^2 V$	f	Δf	$\Delta^2 f$	$\Delta^3 f$	
170	0	0	.800			0			-31.6				
160				-.025			-1.254			1.0			
150	1	.04	.775		-.048	-1.254		.085	-30.6		1.9		
140				-.073			-1.169			2.9		-.1	
130	2	.08	.702		-.045	-2.423		.145	-27.7		1.8		
120				-.118			-1.024			4.7		-.4	
110	3	.12	.584		-.037	-3.447		.224	-23.0		3.9		
100				-.155			-.800			6.1		-.4	
90	4	.16	.429		-.026	-4.247		.260 .286	-16.9		1.01		
80				-.181			-.540 -.544			7.11		-.3	
70	5	.20	.248		-.017	-4.787 -4.791		.304 .304	-9.79		.71		
60				-.198			-.236 -.236			7.82		-.68	
50	6	.24	.050		-.002	-5.023 -5.023		.315 .322	-1.97		.03		
40				-.200			.079 .086			7.85		-.31	
30	7	.28	-.150		+.009	-4.944 -4.937		.309 .299	+5.88		-.20		
20				-.191			.388 .378			7.57		-.62	
10	8	.32	-.341		.002	-4.956 -4.886		.288 .297	13.45		-.90		
0				-.169			.076 .685			6.67		-.32	
	9	.36	-.510		.031	-3.880 -3.871		.241 .235	20.12		-1.22		
				-.138			.917 .909			5.45		-.44	
	10	.40	-.648		.042	-2.963 -2.971		.190 .185	25.57		-1.66		
				-.096			1.107 1.112			3.70		-.08	
	11	.44	-.744		.045	-1.856 -1.851		.112 .105	29.36		-1.74		
				-.051			1.219 1.212			2.01		-.27	
	12	.48	-.795		.050	-.637 -.644		.045 .032	31.37		-2.01		
				-.001			1.284 1.271			0		+.07	
	13	.52	-.796		.051	.827 .634		-.044 -.051	31.37		-1.94		
				.050			1.220 1.215			-1.94		+.10	
	14	.56	-.746		.046	1.847 1.840		-.118 -.108	29.43		-1.84		
				.096			1.102 1.114			-3.78		.17	
	15	.60	-.650		.042	2.949 2.981		-.174 -.175	25.65		-1.67		
				.138			.928 .927			-5.45		.45	
	16	.64	-.521		.031	3.871 3.876		-.256 -.259	20.20		-1.22		
		JANUARY	FEBRUARY	MARCH	APRIL	MAY	JUNE	JULY	AUGUST	SEPTEMBER	OCTOBER	NOVEMBER	DECEMBER

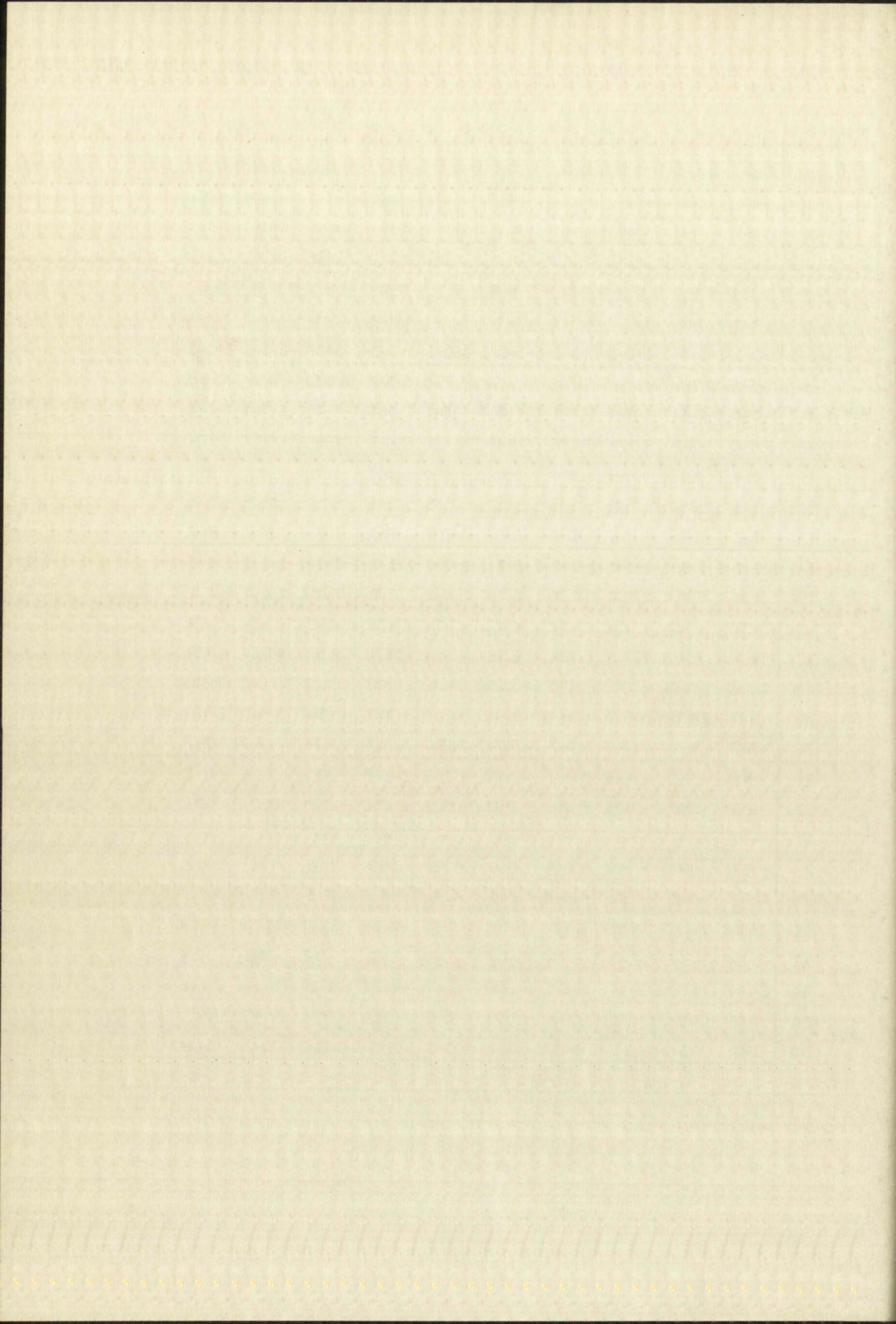
19

170	n	T	X	ΔX	$\Delta^2 X$	Y	ΔY	$\Delta^2 Y$	f	Δf	$\Delta^2 f$	$\Delta^3 f$
				.169			.627 .565			-6.67		.36
160	17	.68	-.343		.002	4.549 4.546		-.273 -.268	13.53		-8.6	
				.191			.399 .404			-7.53		.50
150	18	.72	-.152		.009	4.948 4.953		-.323 -.326	6.00		-1.36	
				.200			.076 .073			-7.89		.43
140	19	.76	+.048		-.002	5.024 5.021		-.502 -.500	-1.89		+.07	
				.198			-.226 -.224			-7.82		.57
130	20	.80	.246		-.016	4.798 4.800		-.316 -.318	-9.71		.64	
				.182			-.542 -.545			-7.18		.42
120	21	.84	.428		-.027	4.256 4.253		-.253 -.255	-16.89		1.06	
				.155			-.798 -.827			-6.12		.37
110	22	.88	.583		-.036	3.461 3.429		-.232 -.223	-23.01		1.43	
				.119			-1.027 -1.028			-4.69		.34
100	23	.92	.702		-.045	2.431 2.433		-.138 -.139	-27.70		1.77	
				.074			-1.163 -1.166			-2.92		.12
90	24	.96	.776		-.048	1.269 1.268		-.093 -.092	-30.62		1.89	
				.026			-1.298 -1.287			-1.03		
80	25	1.00	.802			.011 .012			-31.65			
70												
60												
50												
40												
30												
20												
10												
0												
	JANUARY	FEBRUARY	MARCH	APRIL	MAY	JUNE	JULY	AUGUST	SEPTEMBER	OCTOBER	NOVEMBER	DECEMBER

170	n	COLUMN	5	6	7	8	9	10	11	12	13	14	15
	$2f_{(n-1)}$	1	-33.8	-19.6	-3.94	11.76	26.90	40.24	51.14	58.72	62.74	62.74	58.86
160	$\frac{1}{3}\Delta^2 f_{(n-2)}$	2	.6	.6	.5	.34	.24	.01	-.09	-.30	-.41	-.55	-.58
	$\Delta^3 f_{(n-4)}$	3	-.4	-.4	-.30	-.68	-.31	-.62	-.32	-.44	-.08	-.27	+.07
150	Σ_1	4	-33.6	-19.4	-3.74	11.42	26.83	39.63	50.73	57.98	62.25	61.92	58.35
	$(\Delta^2)\Sigma_1$	5	-1.344	-.776	-.150	.457	1.073	1.585	2.029	2.319	2.490	2.477	2.334
140	$V_{(n-2)}$	6	-3.447	-4.247	-4.787	-5.023	-4.944	-4.556	-3.880	-2.963	-1.856	-.637	+.627
	$(V_n)_1$	7	-4.791	-5.023	-4.937	-4.566	-3.871	-2.971	-1.851	-.644	.634	1.840	2.961
130	$2V_{(n-1)}$	8	-8.494	-9.574	-10.046	-9.888	-9.112	-7.760	-5.926	-3.712	-1.328	+1.254	3.694
	$\frac{1}{3}\Delta^2 V_{(n-2)}$	9	.058	.101	.107	.100	.099	.078	.065	.028	.017	-.017	-.035
120	Σ_2	10	-8.409	-9.473	-9.939	-9.788	-9.031	-7.682	-5.861	-3.684	-1.311	-1.237	3.659
	$(\Delta^2)\Sigma_2$	11	-.336	-.379	-.397	-.391	-.360	-.307	-.234	-.147	-.052	+.049	.146
110	$X_{(n-2)}$	12	.584	.429	.248	.050	-.150	-.341	-.510	-.648	-.744	-.795	-.796
	$(X_n)_1$	13	.248	.050	-.149	-.341	-.510	-.648	-.744	-.795	-.796	-.746	-.650
100	f_n	14	-9.79	-1.97	+5.88	13.45	20.12	25.57	29.36	31.37	31.37	29.43	25.65
	$2f_{(n-1)}$	15	-33.8	-19.6	-3.94	+11.76	26.90	40.24	51.14	58.72	62.74	62.74	58.68
90	$\frac{1}{3}\Delta^2 f_{(n-2)}$	16	.3	.2	.01	-.09	-.30	-.41	-.55	-.58	-.67	-.65	-.61
	Σ_3	17	-33.5	-19.4	-3.93	11.67	26.60	39.83	50.59	58.14	62.07	62.09	58.07
80	$(\Delta^2)\Sigma_3$	18	-1.340	-.776	-.157	.467	1.064	1.593	2.024	2.326	2.483	2.484	2.322
	$V_{(n-2)}$	19	-3.447	-4.247	-4.787	-5.023	-4.944	-4.556	-3.880	-2.963	-1.856	-.637	+.627
70	$(V_n)_2$	20	-4.787	-5.023	-4.944	-4.556	-3.880	-2.963	-1.856	-.637	+.627	1.847	2.949
	$(V_n)_1$	21	-4.791	-5.023	-4.937	-4.566	-3.871	-2.971	-1.851	-.644	.634	1.840	2.961
60	$(V_n)_2 - (V_n)_1$	22	+.004	—	-.007	+.010	-.009	+.008	-.005	+.007	-.007	+.007	-.012
	$\frac{\Delta^2}{3}(V_n)_2 - (V_n)_1$	23	—	—	—	—	—	—	—	—	—	—	—
50	$(X_n)_1$	24	.248	.050	-.149	-.341	-.510	-.648	-.744	-.795	-.796	-.746	-.650
	$(X_n)_2$	25	.248	.050	-.149	-.341	-.510	-.648	-.744	-.795	-.796	-.746	-.650
40	$f_{(n-1)}$	26	-16.9	-9.79	-1.97	5.88	13.45	20.12	25.57	29.36	31.37	31.37	29.43
	$\frac{1}{2}\Delta^2 f_{(n-2)}$	27	+.5	.35	.01	-.14	-.45	-.61	-.83	-.87	-1.00	-.97	-.92
30	Σ_4	28	-16.4	-9.44	-1.96	+5.74	+13.00	19.51	24.74	28.49	30.37	30.40	28.51
	$(\Delta^2)\Sigma_4$	29	-.026	-.015	-.003	+.009	.021	.031	.039	.045	.048	.049	.044
20	$\Delta^3 X_{(n-2)}$	30	-.026	-.017	-.002	+.009	.022	.031	.042	.045	.050	.051	.046
			✓	✓	✓	✓	✓	✓	✓	✓	✓	✓	✓
10													
0													
	JANUARY	FEBRUARY	MARCH	APRIL	MAY	JUNE	JULY	AUGUST	SEPTEMBER	OCTOBER	NOVEMBER	DECEMBER	
	$f_n = -(2\pi)^2 X_n$												



170	COLUMN	16	17	18	19	20	21	22	23	24	25		
	1	51.30	40.40	27.06	12.00	-3.78	-19.42	-33.78	-46.02	-55.40	-61.24		
160	2	-.67	-.65	-.61	-.56	-.41	-.29	-.12	+.02	+.21	+.35		
	3	+.10	.17	.45	.36	.50	.43	.57	.42	.37	.34		
150	4	50.73	39.92	26.90	11.80	-3.69	-19.28	-34.23	-45.58	-54.82	-60.55		
	5	2.029	1.597	1.076	.472	-.148	-.771	-1.369	-1.823	-2.193	-2.422		
140	6	1.847	2.949	3.877	4.549	4.948	5.024	4.798	4.256	3.461	2.434		
	7	3.876	4.546	4.953	5.021	4.800	4.253	3.429	2.433	1.268	.012		
130	8	5.898	7.754	9.098	9.896	10.048	9.596	8.512	6.922	4.868	2.538		
	9	-.058	-.086	-.089	-.109	-.100	-.106	-.095	-.078	-.046	-.031		
120	10	5.840	7.668	9.009	9.787	9.948	9.490	8.417	6.844	4.822	2.507		
	11	.234	.307	.360	.391	.398	.380	.337	.274	.193	.100		
110	12	-.746	-.650	-.512	-.343	-.152	+.048	.246	.428	.583	.702		
	13	-.512	-.343	-.152	+.048	.246	.428	.583	.702	.776	.802		
100	14	20.20	13.53	6.00	-1.89	-9.71	-16.89	-23.01	-27.70	-30.62	-31.65		
	15	51.30	40.40	27.06	12.00	-3.78	-19.42	-33.78	-46.02	-55.40	-61.20		
90	16	-.56	-.41	-.29	-.12	+.02	.21	.35	.48	.59	.63		
	17	50.74	39.99	26.77	11.88	-3.76	-19.21	-33.43	-45.54	-54.81	-60.57		
80	18	2.030	1.600	1.071	.475	-.150	-.768	-1.337	-1.822	-2.192	-2.423		
	19	1.847	2.949	3.877	4.549	4.948	5.024	4.798	4.256	3.461	2.434		
70	20	3.877	4.549	4.948	5.024	4.798	4.256	3.461	2.434	1.269	.011		
	21	3.876	4.547	4.953	5.021	4.800	4.253	3.429	2.433	1.268	.012		
60	22	+.001	+.002	-.005	+.003	-.002	+.003	+.032	+.001	+.001	-.001		
	23	—	—	—	—	—	—	—	—	—	—		
50	24	-.512	-.343	-.152	+.048	.246	.428	.583	.702	.776	.802		
	25	-.512	-.343	-.152	+.048	.246	.428	.583	.702	.776	.802		
40	26	25.65	20.20	13.53	6.00	-1.89	-9.71	-16.89	-23.01	-27.70	-30.62		
	27	-.84	-.61	-.43	-.18	+.04	.31	.52	.72	.89	.95		
30	28	24.81	19.59	13.10	5.82	-1.85	-9.40	-16.37	-22.29	-26.81	-29.68		
	29	.040	.031	.021	.009	-.003	-.015	-.026	-.036	-.043	-.047		
20	30	.042	.031	.022	.009	-.002	-.016	-.027	-.036	-.045	-.048		
		✓	✓	✓	✓	✓	✓	✓	✓	✓	✓		
10													
0													
	JANUARY	FEBRUARY	MARCH	APRIL	MAY	JUNE	JULY	AUGUST	SEPTEMBER	OCTOBER	NOVEMBER	DECEMBER	



APPENDIX B

SAMPLE SOLUTION OF DIFFERENTIAL EQUATION
FOR FRICTIONLESS AIR SPRING BY NUMERICAL INTEGRATION

As previously shown, the differential equation for the frictionless air spring may be written in the non-dimensional form:

$$(28) \quad \frac{d^2 X}{d\tau^2} + \frac{4\pi^2}{\gamma} \left[(1-X)^{-\gamma} - 1 \right] = 0$$

With the definition $V = \frac{dX}{d\tau}$, this equation may be replaced by the two simultaneous equations:

$$(B1) \quad V = \frac{dX}{d\tau}$$

$$\frac{dV}{d\tau} = \varphi(X), \text{ where } \varphi(X) = \frac{4\pi^2}{\gamma} \left[1 - (1-X)^{-\gamma} \right]$$

With the arbitrarily chosen initial conditions $X_0 = -1.3$, $V_0 = 0$, $\tau_0 = 0$, and with a convenient time interval $\Delta\tau = 0.04$, the first stage of the numerical integration procedure may be undertaken. This stage consists of use of formulas (7) and (8), as discussed in Chapter II, first with $m = 0$, then with $m = 1, 2$, and 3 in turn. The results are tabulated below.

ANALYSIS OF THE DATA FOR THE FIRST TWO YEARS OF THE PROJECT

As previously shown, the differential equation for

the probability of survival may be written in the form

discrete form

$$(28) \quad \frac{dS}{dt} = -\lambda S \quad \text{or} \quad S = S_0 e^{-\lambda t}$$

With the definition $\lambda = \frac{1}{T}$, this equation may be written

by the two alternative forms

$$(29) \quad \frac{dS}{dt} = -\frac{S}{T} \quad \text{or} \quad S = S_0 e^{-t/T}$$

$$(30) \quad \frac{dS}{dt} = -\lambda S \quad \text{or} \quad S = S_0 e^{-\lambda t}$$

With the arbitrary constant initial condition $S = S_0$ at $t = 0$,

$S_0 = 0$, $T = 0$, and with a constant time interval

$\Delta t = 0.04$, the first three of the numerical calculations

procedure may be illustrated. The results are shown in Table I.

Formulas (7) and (8), as discussed in Chapter II, show that

$m = 0$, then with $n = 1, 2, 3, \dots$, and $t = 0, 0.04, 0.08, \dots$

tabulated below.

$$m = 0$$

n	$(\Delta V_1)_n$	$(V_1)_n$	$(\Delta X_1)_n$	$(X_1)_n$	$(\varphi_1)_n$
1	0.7764	0.7764	0	-1.3000	19.41
2	0.7764	0.7764	0.0155	-1.2845	19.33
3	0.7748	0.7748	0.0155	-1.2845	19.33

$$m = 1$$

n	$(\Delta V_2)_n$	$(V_2)_n$	$(\Delta X_2)_n$	$(X_2)_n$	$(\varphi_2)_n$
1	0.7732	1.5480	0.0310	-1.2535	19.16
2	0.7689	1.5446	0.0464	-1.2381	19.07
3	0.7680	1.5428	0.0464	-1.2381	19.07

$$m = 2$$

n	$(\Delta V_3)_n$	$(V_3)_n$	$(\Delta X_3)_n$	$(X_3)_n$	$(\varphi_3)_n$
1	0.7628	2.3056	0.0617	-1.1764	18.71
2	0.7556	2.2984	0.0768	-1.1613	18.61
3	0.7536	2.2946	0.0768	-1.1613	18.61

$$m = 3$$

n	$(\Delta V_4)_n$	$(V_4)_n$	$(\Delta X_4)_n$	$(X_4)_n$	$(\varphi_4)_n$
1	0.7444	3.0408	0.0918	-1.0695	18.01
2	0.7324	3.0288	0.1065	-1.0548	17.91
3	0.7304	3.0268	0.1065	-1.0548	17.91

$$n = 1$$

n	$(\Delta V)_1$	$(V)_1$	$(\Delta X)_1$	$(X)_1$	$(Y)_1$
1	0.7784	0.7784	0	-1.3000	19.41
2	0.7784	0.7784	0.0758	-1.3848	19.33
3	0.7748	0.7748	0.0735	-1.3848	19.33

$$n = 1$$

n	$(\Delta V)_2$	$(V)_2$	$(\Delta X)_2$	$(X)_2$	$(Y)_2$
1	0.7732	1.8490	0.0930	-1.8835	19.10
2	0.7832	1.8442	0.0464	-1.8831	19.07
3	0.7830	1.8428	0.0461	-1.8831	19.07

$$n = 2$$

n	$(\Delta V)_3$	$(V)_3$	$(\Delta X)_3$	$(X)_3$	$(Y)_3$
1	0.7832	2.3032	0.0877	-1.1784	18.71
2	0.7856	2.2894	0.0768	-1.1813	18.81
3	0.7836	2.2846	0.0768	-1.1813	18.81

$$n = 2$$

n	$(\Delta V)_4$	$(V)_4$	$(\Delta X)_4$	$(X)_4$	$(Y)_4$
1	0.7444	2.0402	0.0918	-1.4898	18.07
2	0.7304	2.0288	0.1088	-1.0848	17.91
3	0.7304	2.0268	0.1088	-1.0848	17.91

Before the values found above are corrected, it is convenient to arrange the results obtained so far in the following tabular form, and to compute " Δ -differences" of the various orders required in the correction formulas:

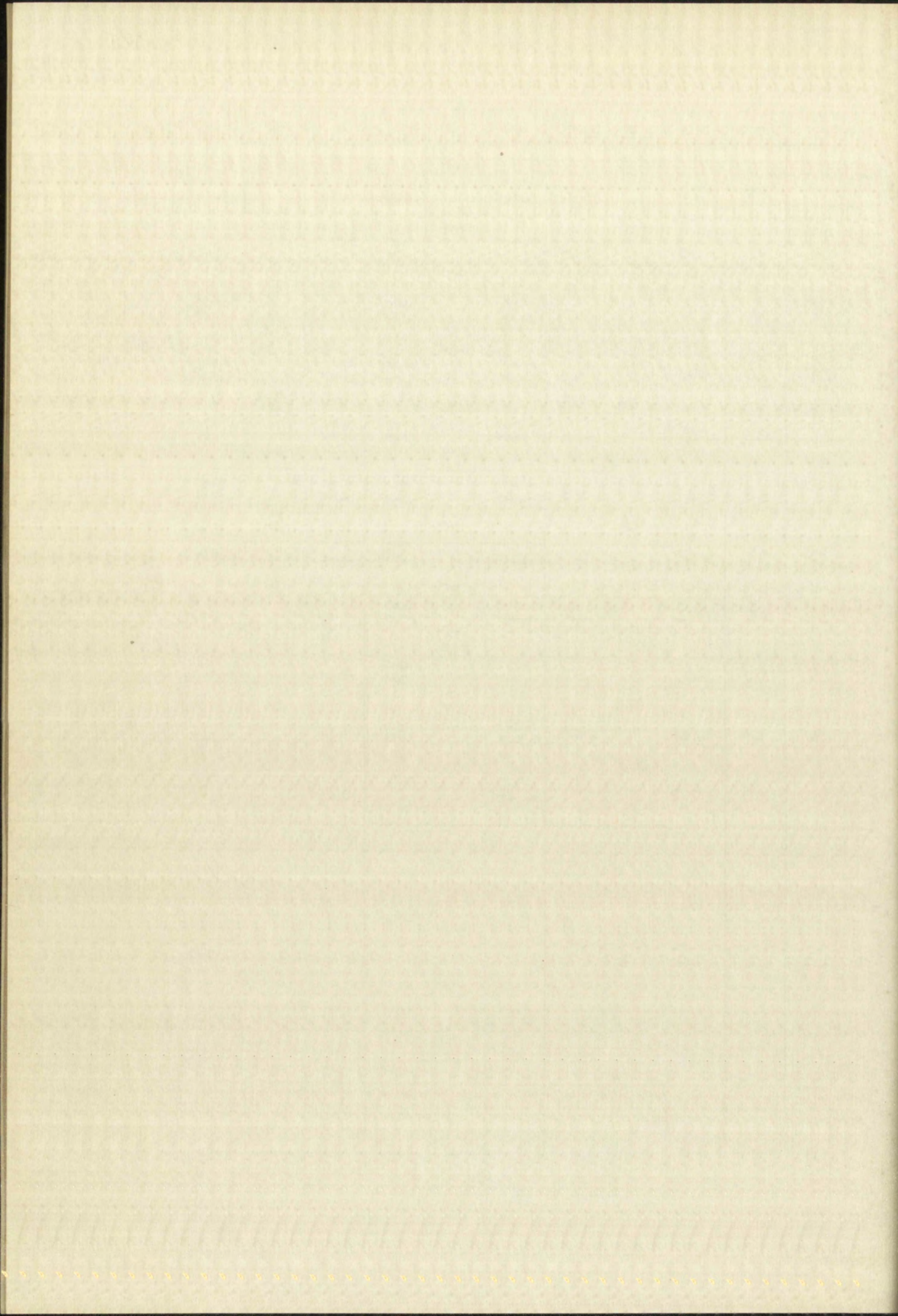
n	τ	X_n	V_n	ΔV	$\Delta^2 V$	$\Delta^3 V$	$\Delta^4 V$	φ_n	$\Delta \varphi$	$\Delta^2 \varphi$	$\Delta^3 \varphi$	$\Delta^4 \varphi$
0	0	-1.3000	0					19.41				
				.7748					-.08			
1	.04	-1.2845	.7748		-.0068			19.33		-.18		
				.7680		-.0076			-.26		-.02	
2	.08	-1.2381	.7680		-.0144	.0002		19.07		-.20		-.02
				.7536		-.0074			-.46		-.04	
3	.12	-1.1613	.7536		-.0218			18.61		-.24		
				.7318					-.70			
4	.16	-1.0548	.7318					17.91				

Now the above values of X_n and V_n may be checked and corrected by use of formulas (10). The corrected values are tabulated below.

n	$\overline{X_n}$	$\overline{V_n}$	$\overline{\varphi_n}$
1	-1.2845	0.7752	19.33
2	-1.2381	1.5440	19.07
3	-1.1612	2.2981	18.61
4	-1.0546	3.0296	17.91

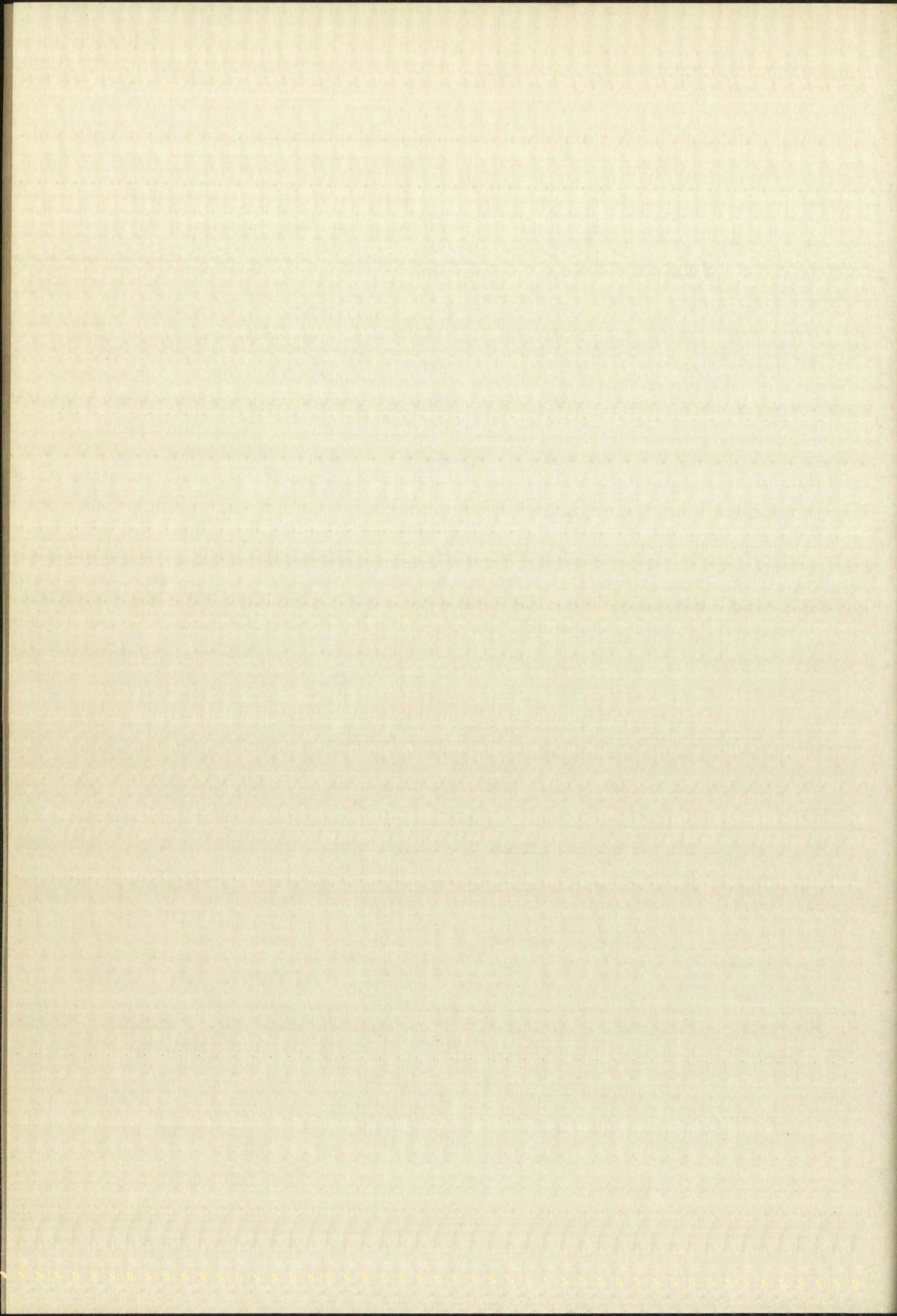
The remaining calculations consist of repeated application of formulas (11), starting with $n = 5$ and increasing n by one in each successive cycle. The computations were done in tabular form, as shown in the following pages.

The results of these calculations appear under the X and V headings in the following table, and are shown superimposed on an exact X-V curve in Graph 1. The integration starts on the negative X-axis and proceeds clockwise in the plane of Graph 1. The accumulation of errors in the numerical method is evident, since the calculated points deviate more nearer the end of the calculation, where the curve again meets the negative X-axis. No exact solutions are known from which $X-\tau$ or $V-\tau$ relations can be obtained.

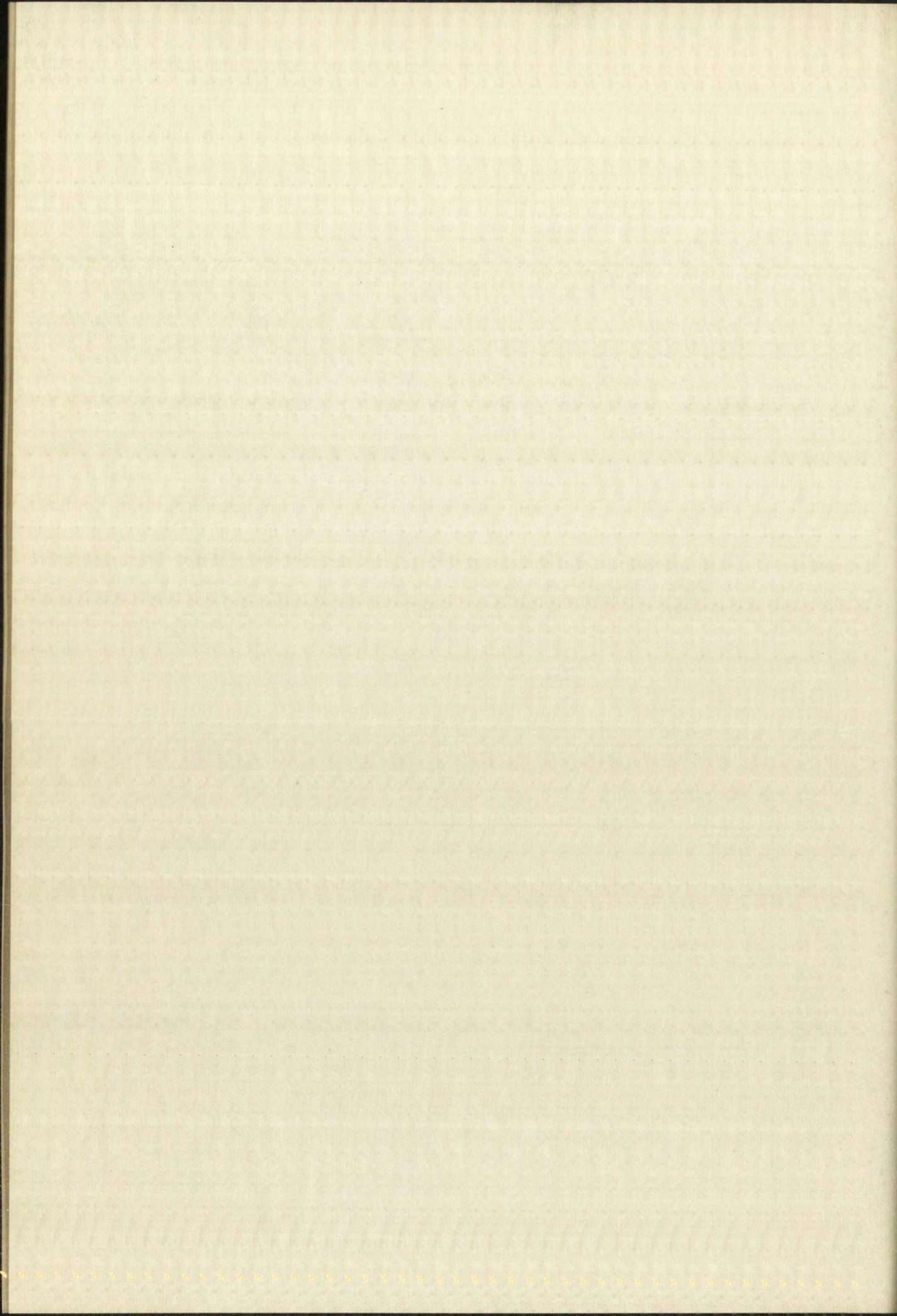


170		n	5	6	7	8	9	10	11	12	13	13a	14
160	1	$2\varphi_{(n-1)}$	35.82	33.76	30.80	26.40	19.88	9.40	-7.96	-39.20	-93.70		-161.36
	2	$\frac{1}{3}\Delta^2\varphi_{(n-2)}$	-.06	-.07	-.08	-.11	-.15	-.24	-.35	-.66	-1.15		-2.31
150	3	$\Delta^3\varphi_{(n-4)}$	-.04	-.09	-.12	-.27	-.34	-.92	-1.46	-3.50	-4.69		+5.05
	4	Σ	35.72	33.60	30.60	26.02	19.39	8.24	-9.77	-43.36	-99.54		-158.62
140	5	$(\Delta T)\Sigma$	1.429	1.344	1.224	1.041	.776	.330	-.391	-1.734	-3.982		-6.345
	6	$V_{(n-2)}$	2.300	3.030	3.728	4.374	4.950	5.416	5.719	5.746	5.308		4.023
130	7	$(V_n)_1$	3.729	4.374	4.952	5.415	5.726	5.746	5.328	4.012	1.326	1.483	-2.322
	8	$2V_{(n-1)}$	6.060	7.456	8.748	9.900	10.832	11.438	11.492	10.616	8.046		2.944
120	9	$\frac{1}{3}\Delta^2V_{(n-2)}$	-.010	-.017	-.023	-.037	-.052	-.092	-.138	-.286	-.471		-.414
	10	Σ	6.050	7.439	8.725	9.863	10.780	11.346	11.354	10.330	7.575		2.530
110	11	$(\Delta T)\Sigma$.242	.297	.349	.394	.431	.454	.453	.413	.303		.101
	12	$\Sigma_{(n-2)}$	-1.161	-1.055	-.919	-.758	-.570	-.364	-.139	.090	.314		.503
100	13	$(\Sigma_n)_1$	-.919	-.758	-.570	-.364	-.139	+.090	.314	.503	.617	.619	.604
	14	$\varphi[(\Sigma_n)]$	16.88	15.40	13.20	9.94	4.70	-3.98	-19.60	-46.85	-79.88	-80.68	-74.95
90	15	$2\varphi_{(n-1)}$	35.82	33.76	30.80	26.40	19.88	9.40	-7.96	-39.20	-93.70	-93.70	-161.36
	16	$\frac{1}{3}\Delta^2\varphi_{(n-2)}$	-.11	-.15	-.24	-.35	-.66	-1.55	-2.31	-3.88	-1.93	-2.19	+13.19
80	17	Σ	35.71	33.61	30.56	26.05	19.22	8.25	-10.27	-43.08	-95.63	-95.89	-146.17
	18	$(\Delta T)\Sigma$	1.428	1.344	1.222	1.042	.769	.330	-.411	-1.723	-3.825	-3.836	-5.927
70	19	$V_{(n-2)}$	2.300	3.030	3.728	4.374	4.950	5.416	5.719	5.746	5.308	5.308	4.023
	20	$(V_n)_2$	3.728	4.374	4.950	5.416	5.719	5.746	5.308	4.023	1.483	1.472	-1.904
60	21	$(V_n)_1$	3.729	4.374	4.952	5.415	5.726	5.746	5.328	4.012	1.326	1.483	-2.322
	22	$(V_n)_2 - (V_n)_1$	-.001	0	-.002	+.001	+.007	0	-.020	+.011	+.157	-.011	+.418
50	23	$\frac{\Delta T}{3}[\Sigma]$	—	—	—	—	—	—	—	—	+.002	—	+.006
	24	$(\Sigma_n)_1$	-.919	-.758	-.570	-.364	-.139	+.090	.314	.503	.617	.619	.604
40	25	$(\Sigma_n)_2$	-.919	-.758	-.570	-.364	-.139	+.090	.314	.503	.619	.619	.610
	26	$\varphi_{(n-1)}$	17.91	16.88	15.40	13.20	9.94	4.70	-3.98	-19.60		-46.85	
30	27	$\frac{1}{3}\Delta^2\varphi_{(n-2)}$	-.16	-.23	-.36	-.53	-.99	-1.72	-3.47	-5.81		-3.29	
	28	Σ	17.75	16.65	15.04	12.67	8.95	2.98	-7.45	-25.41		-50.14	
20	29	$(\Delta T)^2\Sigma$.028	.027	.024	.020	.014	.005	-.012	-.041		-.080	
	30	$\Delta^2\Sigma_{(n-2)}$.030	.025	.027	.018	.019	.004	-.005	-.035		-.073	
10													
0													
		JANUARY	FEBRUARY	MARCH	APRIL	MAY	JUNE	JULY	AUGUST	SEPTEMBER	OCTOBER	NOVEMBER	DECEMBER

	14a	15	15a	16	16a	17	17a	18	18a	19	20	20a
170												
160	1	-153.70		-84.10		-33.80		-4.74		+1.112	25.46	
	2	-3.88		-2.19		+12.55		+10.32		-3.22	-3.54	
150	3	+44.24		-6.69		-40.62		-.97		+4.02	+5.84	
	4	-113.34		-92.98		-61.87		+4.61		+11.92	27.76	
140	5	-453.4		-3.719		-2.475		+.184		.477	1.110	
	6	1.472		-1.929		-4.263		-5.422		-5.757	-5.667	
130	7	-1.904	-3.062	-4.305	-5.648	-5.418	-6.738	-5.749	-5.238	-5.701	-5.280	-4.557
	8		-3.858		-8.526		-10.844		-11.514		-11.334	-10.644
120	9		+.756		+.316		-.052		+.285		+.159	+.140
	10		-3.102		-8.210		-10.896		-11.229		-11.175	-10.504
110	11		-.124		-.328		-.436		-.449		-.447	-.420
	12		.619		.610		.479		.285		.056	-.170
100	13	.610	.495	.479	.282	.285	.043	.056	-.164	-.170	-.391	-.590
	14	-76.85	-45.19	-42.05	-16.64	-16.90	-1.79	-2.37	+5.45	5.56	12.73	13.47
90	15	-161.36	-153.70	-153.70	-84.10	-84.10	-33.80	-33.80	-4.74	-4.74	11.12	25.46
	16	12.55	9.28	10.32	-3.12	-3.22	-3.35	-3.54	-2.24	-2.20	-.25	-2.64
80	17	-148.81	-144.42	-143.38	-87.22	-87.32	-37.15	-37.34	-6.98	-6.94	+10.87	22.82
	18	-5952	-5.777	-5.735	-3.489	-3.493	-1.486	-1.494	-.279	-.278	+.435	.913
70	19	4.023	1.472	1.472	-1.929	-1.929	-4.263	-4.263	-5.422	-5.422	-5.757	-5.667
	20	-1.929	-4.305	-4.263	-5.418	-5.422	-5.749	-5.757	-5.701	-5.700	-5.322	-4.754
60	21	-1.904	-3.062	-4.305	-5.648	-5.418	-6.738	-5.749	-5.238	-5.701	-5.280	-4.557
	22	-.025	-1.243	+.038	.230	-.004	+.989	-.008	-.463	+.001	-.042	-.197
50	23	—	-.016	—	+.003	—	+.013	—	-.006	—	—	-.003
	24	.610	.495	.479	.282	.285	.043	.056	-.164	-.170	-.391	-.590
40	25	.610	.479	.479	.285	.285	.056	.056	-.170	-.170	-.391	-.593
	26	-80.68		-76.85		-42.05		-16.90		-2.37	+5.56	75.56 12.73
30	27	+18.83		+15.48		-4.82		-5.31		-2.07	-.38	-4.07
	28	-61.88		-61.37		-46.87		-22.21		-4.44	+5.18	8.66
20	29	-.099		-.098		-.075		-.035		-.007	+.008	.014
	30	-.125		-.135		-.063		-.035		+.003	+.005	.019
10												
0												
	JANUARY	FEBRUARY	MARCH	APRIL	MAY	JUNE	JULY	AUGUST	SEPTEMBER	OCTOBER	NOVEMBER	DECEMBER



	21	21a	22	22a	23	23a	24	25	26	27		
170												
160	1	21.42		31.08		33.88		35.80	36.78	37.94	38.62	
	2	-2.20		-.25		-2.72		-.94	-.14	-.15	-.17	
150	3	-7.39		10.96		-3.24		-.01	-.06	+.59	-.23	
	4	17.83		41.79		27.92		34.85	36.58	38.38	38.22	
140	5	.713		1.672		1.117		1.394	1.463	1.535	1.529	
	6	-5.322		-4.767		-4.188		-3.529	-2.839	-2.104	-1.367	
130	7	-4.609	-4.187	-3.095	-3.530	-3.071	-2.838	-2.135	-1.376	-.569	+.162	
	8	-9.534		-8.376		-7.058		-6.142	-4.208	-2.734	-1.170	
120	9	-.132		+.171		-.034		+.005	-.002	+.014	+.010	
	10	-9.666		-8.205		-7.092		-6.137	-4.210	-2.720	-1.186	
110	11	-.387		-.328		-.284		-.245	-.186	-.109	-.047	
	12	-.391		-.593		-.772		-.927	-1.053	-1.172	-1.221	
100	13	-.778	-.772	-.921	-.927	-1.056	-1.053	-1.172	-1.221	-1.281	-1.268	
	14	15.60	15.54	16.89	16.94	17.92	17.90	18.39	18.97	19.31	19.23	
90	15	21.42	21.42	31.08	31.08	33.88	33.88	35.80	36.78	37.94	38.62	
	16	+.96	.94	-.16	-.14	-.14	-.15	-.17	+.03	-.05	-.14	
80	17	28.38	28.36	30.92	30.94	33.74	33.73	35.63	36.81	37.89	38.48	
	18	1.135	1.134	1.237	1.238	1.350	1.349	1.425	1.472	1.516	1.539	
70	19	-5.322	-5.322	-4.767	-4.767	-4.188	-4.188	-3.529	-2.839	-2.104	-1.367	
	20	-4.187	-4.188	-3.530	-3.529	-2.838	-2.839	-2.104	-1.367	-.588	+.172	
60	21	-4.609	-4.187	-3.095	-3.530	-3.071	-2.838	-2.135	-1.376	-.596	+.162	
	22	+.422	-.001	-.435	+.001	+.233	-.001	+.031	+.009	+.008	+.010	
50	23	+.006	—	-.006	—	+.003	—	—	—	—	—	
	24	-.778	-.772	-.921	-.927	-1.056	-1.053	-1.172	-1.221	-1.281	-1.268	
40	25	-.772	-.772	-.927	-.927	-1.053	-1.053	-1.172	-1.221	-1.281	-1.268	
	26		13.71		15.54		16.94	17.90	18.39	18.97	19.31	
30	27		+.140		-.21		-.22	-.25	+.05	-.07	-.21	
	28		15.11		15.33		16.72	17.65	18.44	18.90	19.10	
20	29		.024		.024		.027	.028	.030	.028	.028	
	30		.023		.024		.029	.007	.070	-.011	+.073	
10												
0												
	JANUARY	FEBRUARY	MARCH	APRIL	MAY	JUNE	JULY	AUGUST	SEPTEMBER	OCTOBER	NOVEMBER	DECEMBER



APPENDIX C

SAMPLE APPLICATIONS OF JACOBSEN'S GRAPHICAL METHOD

I. SOLUTION OF THE DIFFERENTIAL EQUATION OF THE LINEAR SPRING

As demonstrated in Appendix A, the differential equation for a linear spring may be written in the non-dimensional form

$$\frac{d^2x}{d\tau^2} + 4\pi^2 x = 0.$$

Jacobsen's method, however, requires that the differential equation to be solved be expressed so as to appear as

$$\frac{d^2x}{d\tau^2} + p^2 (x + \delta) = 0.$$

The equation of the linear spring is most simply transformed into the required form by letting $p^2 = 4\pi^2$ and $\delta = 0$. Since $\delta = 0$, no matter what the values of x and v are, all of Jacobsen's circular arcs have their center at the origin of the phase plane. Hence, the phase trajectories for linear springs are circles in the x - \dot{v} plane, where

134

I. SUBSTITUTION OF THE LINEAR FORM

As shown in the preceding section, the linear form

can be substituted into the equation

to obtain

$$\frac{1}{2} \left(\frac{1}{2} + \frac{1}{2} \right) = \frac{1}{2}$$

Since the left-hand side of the equation is a constant, the equation

can be written in the form

$$\frac{1}{2} \left(\frac{1}{2} + \frac{1}{2} \right) = \frac{1}{2}$$

The equation of the line is therefore

into the required form by taking

Since $\frac{1}{2} = 0$, no further simplification is required.

All of the above steps are necessary to obtain the

equation of the line in the form

for linear factors and the answer is

$\bar{V} = \frac{1}{p} \frac{dX}{d\tau}$. If, for purposes of comparison with the numerical integration method, the same initial conditions as for the latter method are specified here also, then the phase plane construction will appear as in Graph 32.

The relation between X and τ is obtained from the expression

$$\Delta\tau = \frac{1}{p} \Delta\theta$$

which here becomes $\Delta\tau = \frac{\Delta\theta}{2\pi}$. The X - τ curve for this motion is also shown in Graph 32. It is of interest that the period of the oscillation in reduced units is $\tau_0 = \frac{2\pi}{2\pi} = 1$ (as is to be expected) since θ increases from 0 to 2π as the phase trajectory closes on itself.

From Graph 32 and the relation $\Delta\theta = 2\pi\Delta\tau$ it is apparent that the relation between X and τ may be expressed as

$$X = 0.8 \cos (2\pi \cdot \tau).$$

This, however, is identical to the exact solution of the differential equation derived in Appendix A. For the linear spring then, the graphical method gives exact results which are limited in accuracy only by the technicalities of drawing.

For the purpose of comparison with the theoretical expression, the same initial conditions as for the latter method are specified here also. Then the phase plane representation will appear as in Graph 22.

The relation between X and T is obtained from the

expression

$$\Delta T = \frac{1}{\Delta \theta}$$

which here becomes $\Delta T = \frac{1}{\Delta \theta}$ for the $X-T$ curve. This relation is also shown in Graph 22. It is of interest that the period of the oscillation is reduced with Δ as $\Delta \theta = \frac{\pi}{2\Delta}$ (as is to be expected) since Δ increases from 0 to ∞ as the phase trajectory closes on itself.

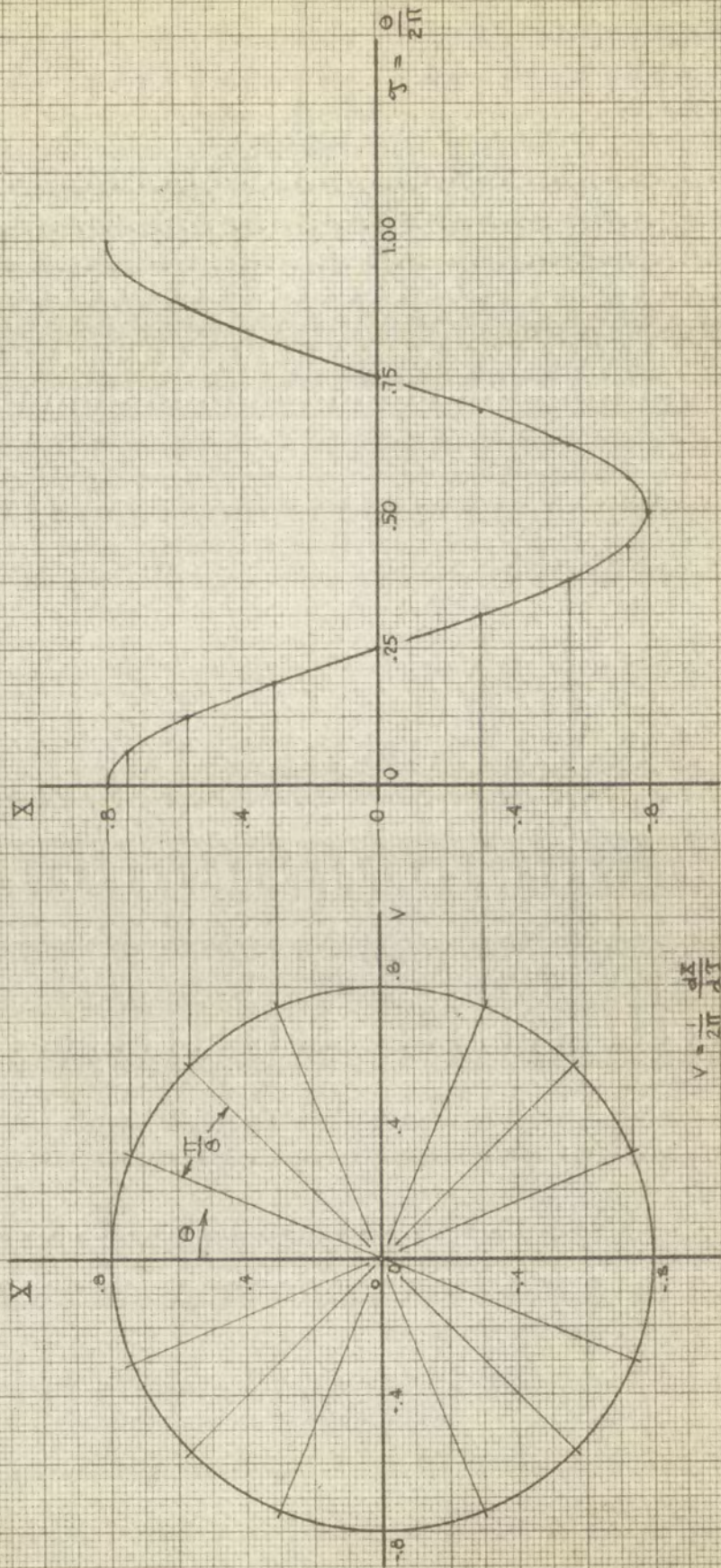
From Graph 22 and the relation $\Delta \theta = 2\pi \Delta T$ it

is apparent that the relation between X and T may be expressed as

$$X = 0.5 \cos (2\pi T)$$

This, however, is identical to the exact solution of the differential equation derived in Appendix A. For the linear spring limit, the graphical method gives exact results which are limited in accuracy only by the resolution of the line.

GRAPHIC SOLUTION - LINEAR SPRING



GRAPH 32

II. SOLUTION OF THE DIFFERENTIAL EQUATION OF A FRICTIONLESS AIR SPRING

The dimensionless differential equation applicable to a frictionless air spring was shown to be

$$(28) \quad \frac{d^2x}{d\delta^2} + \frac{4\pi^2}{\gamma} \left[(1-x)^{-\gamma} - 1 \right] = 0$$

In order to apply Jacobsen's graphical solution method it is necessary to change this equation into the form

$$\frac{d^2x}{d\delta^2} + p^2 (x + \delta) = 0$$

This transformation is most easily accomplished by letting

$$p^2 = \frac{4\pi^2}{\gamma} \quad \text{and defining } \delta \text{ as}$$

$$\delta = (1-x)^{-\gamma} - 1 - x$$

In order to carry out the graphic integration most conveniently, curves showing the variation of δ with x are desirable. Graphs 33 and 34 are such curves, applicable to positive and negative values of x , respectively.

In this illustration, the same initial conditions as for the numerical integration illustration are used.

That is, $x_0 = -1.3$, $v_0 = 0$, $\tau_0 = 0$. The construction by Jacobsen's method is then performed as

III. THEORETICAL ANALYSIS OF THE PROBLEM

The first step in the analysis is to consider the case of a constant velocity of the particle, i.e., $v = v_0$.

$$(38) \quad \frac{d^2 x}{dt^2} = -\frac{e^2}{4\pi\epsilon_0 m} \frac{1}{x^3} \quad (38)$$

In order to solve this equation, it is necessary to assume that the particle is moving in a straight line, i.e., $y = z = 0$.

$$(39) \quad \frac{d^2 x}{dt^2} = -\frac{e^2}{4\pi\epsilon_0 m} \frac{1}{x^3} \quad (39)$$

This equation is a special case of the more general equation (37) for $v = v_0$.

$$(40) \quad \frac{d^2 x}{dt^2} = -\frac{e^2}{4\pi\epsilon_0 m} \frac{1}{x^3} \quad (40)$$

In order to solve this equation, it is necessary to assume that the particle is moving in a straight line, i.e., $y = z = 0$.

$$(41) \quad \frac{d^2 x}{dt^2} = -\frac{e^2}{4\pi\epsilon_0 m} \frac{1}{x^3} \quad (41)$$

In this case, the equation is identical to the one for a constant velocity, i.e., $v = v_0$.

$$(42) \quad \frac{d^2 x}{dt^2} = -\frac{e^2}{4\pi\epsilon_0 m} \frac{1}{x^3} \quad (42)$$

For the case of a constant velocity, the equation is identical to the one for a constant velocity, i.e., $v = v_0$.

follows, as shown in Graph 35. At first the X and \bar{V} axes are laid out, and divided into equal convenient units. The X -axis is drawn vertically with the positive part on bottom, the \bar{V} -axis horizontal with the positive half on the right. The initial point $P_0 (X_0, \bar{V}_0)$ is then located and marked. For the first step, a convenient X interval is chosen, say 0.1. The mean value of X within that interval starting from $X_0 = -1.3$, is -1.25 . From Graph 34, the value of δ corresponding to $X = -1.25$ is found to be 0.57. This value is laid off along the negative X -axis to locate $Q_1 (0, -0.57)$. This point is the center of the first circular arc. This arc is drawn, starting from P_0 and ending where it intersects the line $X = -1.2$. The end of the arc is marked P_1 , and the angle $P_0 Q_1 P_1$ is measured. It is found to be 30.3° or 0.545 radians. From the formula

$$\Delta \tau = \frac{1}{p} \Delta \theta, \quad \Delta \tau \text{ is found to be } 0.103 \text{ for this}$$

first interval.

A new point, P_2 may now be determined in a similar manner. If an interval of 0.1 for X is chosen once more, the average value of X in this interval will now be -1.15 , for which the corresponding δ is 0.49. The center of the second circular arc, $Q_2 (0, -0.49)$ may now be located, and the arc drawn from P_1 until it intersects the line

$X = -1.1$. The angle $P_1 Q_2 P_2$ where P_2 is on the second arc, may be measured. It is found to be 13.0 degrees, corresponding to a $\Delta \mathcal{T}$ of 0.044.

The procedures outlined above are now repeated until the entire desired portion of the phase trajectory has been described. In this particular case it was only necessary to perform the integration in the half plane for positive \bar{V} , since it was known that the phase trajectory is symmetric about the X-axis.

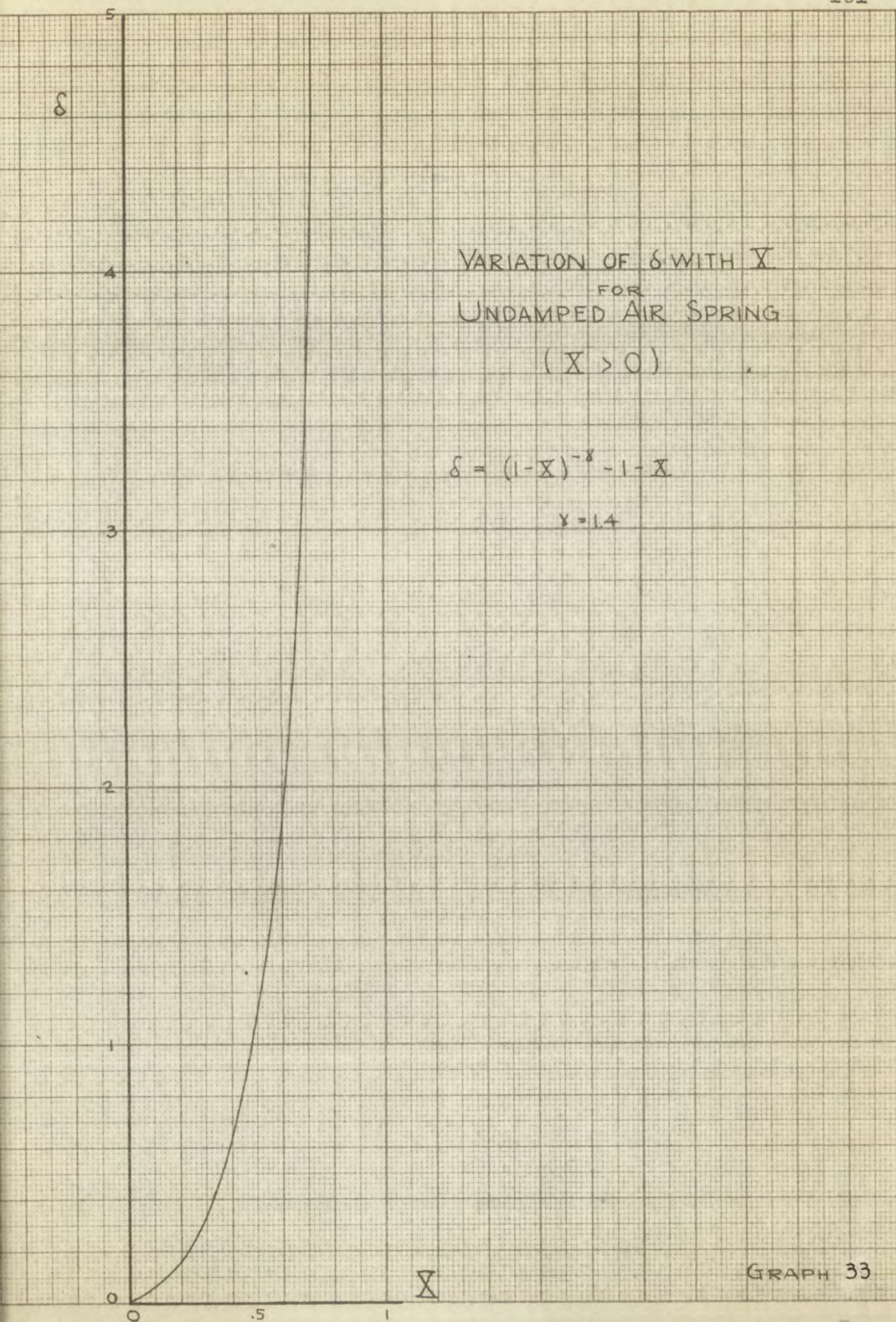
The relation between X and \mathcal{T} obtained by this method is shown in Table V, which shows also a convenient arrangement for computing this relation from Graph 35.

Points calculated from the analytic solution of the differential equation are shown in Graph 35 in order to demonstrate the good accuracy obtainable with the graphical method. Analytic X- \mathcal{T} and V- \mathcal{T} relations are not known; hence no comparison of graphically obtained with exact values is possible. A comparison of the X- \mathcal{T} relation obtained graphically with that obtained numerically appears in Graph 2. The numerical method is the more accurate, so that some error is evident in the graphical solution.

VARIATION OF δ WITH X
 FOR
 UNDAMPED AIR SPRING
 ($X > 0$)

$$\delta = (1-X)^{-\gamma} - 1 - X$$

$$\gamma = 1.4$$



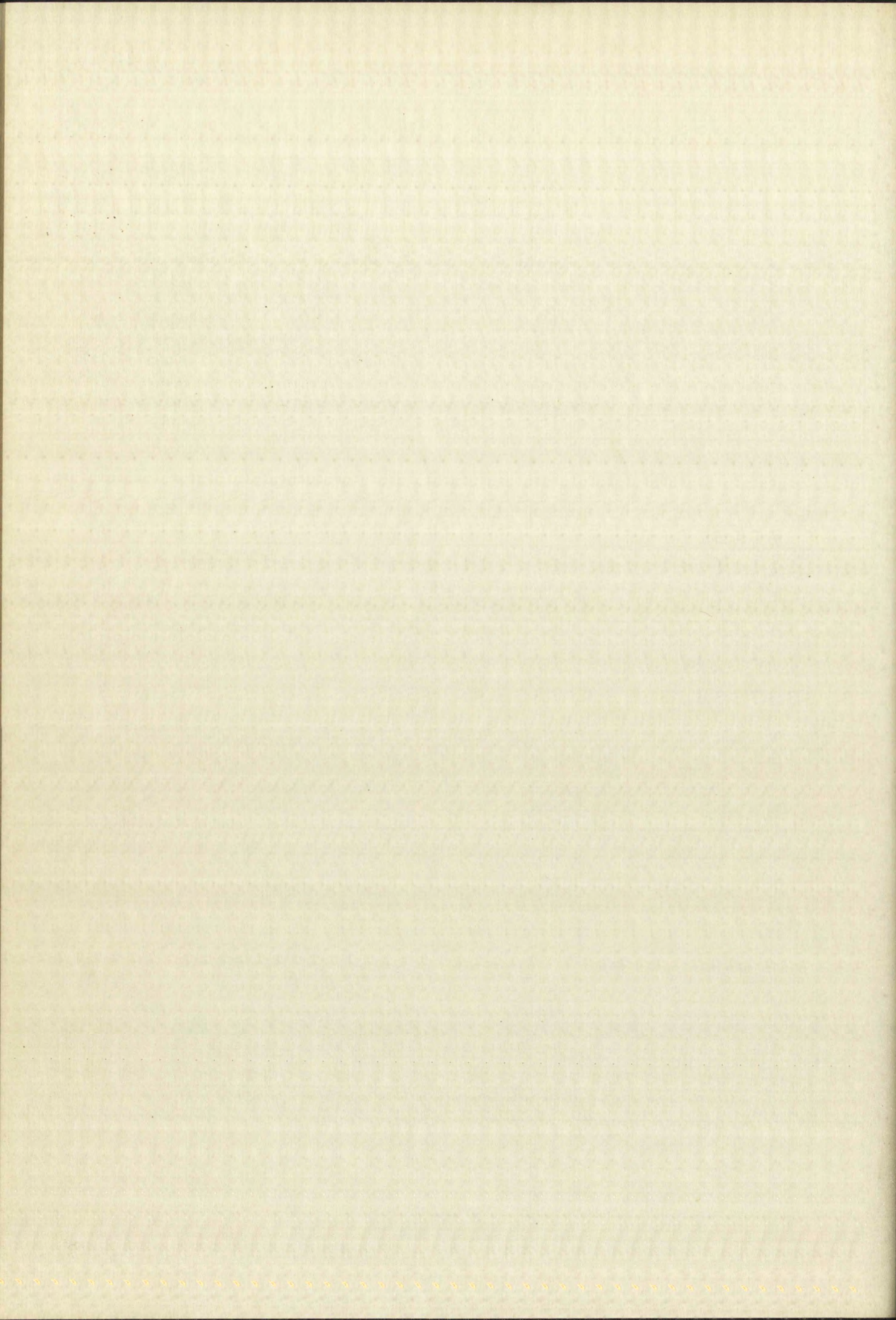
GRAPH 33

VARIATION OF δ WITH X
 FOR
 UNDAMPED AIR SPRING
 ($X < 0$)

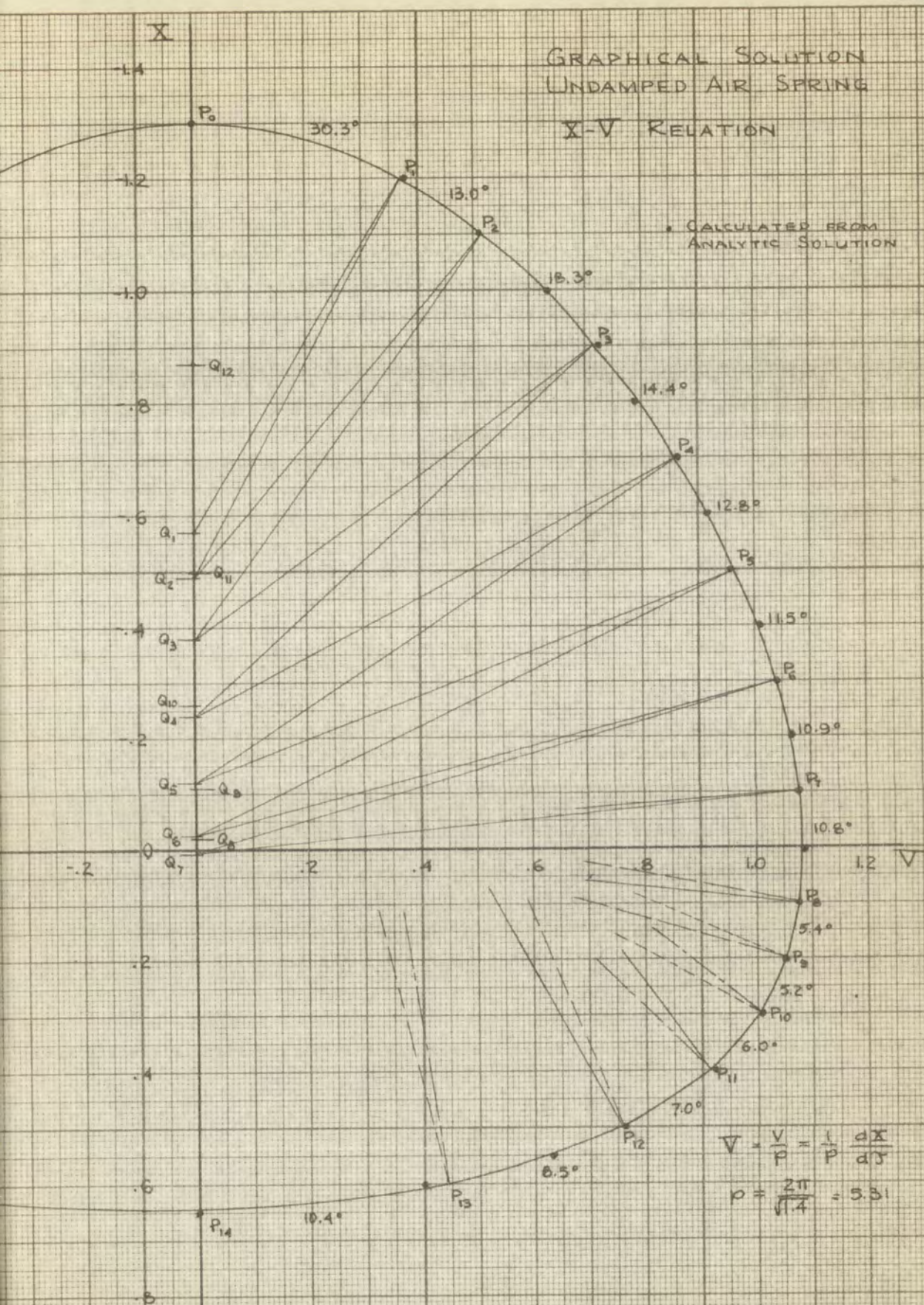
$$\delta = (1 - X)^{-\frac{1}{\gamma}} - 1 - X$$

$\gamma = 1.4$

GRAPH 34



GRAPHICAL SOLUTION UNDAMPED AIR SPRING X-V RELATION



GRAPH 35

35

X-T RELATION FOR FRICTIONLESS AIR SPRING
(From Graphic Solution)

	X	$\Delta\theta$	θ	θ	τ			X	$\Delta\theta$	θ	θ	τ
		DEGR.	DEGR.	RAD.					DEGR.	DEGR.	RAD.	
170												
160	-1.3		0	0	0			.5		183.4	3.301	.622
		30.3							7.0			
150	-1.2		30.3	.545	.103			.4		190.4	3.427	.645
		13.0							6.0			
140	-1.1		43.3	.779	.147			.3		196.4	3.535	.666
		18.3							5.2			
130	-.9		61.6	1.109	.209			.2		201.6	3.629	.683
		14.4							5.4			
120	-.7		76.0	1.368	.258			.1		207.0	3.726	.702
		12.8							10.8			
110	-.5		88.8	1.598	.301			-.1		217.8	3.920	.738
		11.5							10.9			
100	-.3		100.3	1.805	.340			-.3		228.7	4.117	.775
		10.9							11.5			
90	-.1		111.2	2.002	.377			-.5		240.2	4.324	.814
		10.8							12.8			
80	.1		122.0	2.196	.414			-.7		253.0	4.554	.858
		5.4							14.4			
70	.2		127.4	2.293	.432			-.9		267.4	4.813	.906
		5.2							18.3			
60	.3		132.6	2.387	.450			-1.1		285.7	5.143	.969
		6.0							13.0			
50	.4		138.6	2.495	.470			-1.2		298.7	5.377	1.013
		7.0							30.3			
40	.5		145.6	2.621	.494			-1.3		329.0	5.922	1.115
		8.5										
30	.6		154.1	2.774	.522							
		10.4										
20	.64		164.5	2.961	.558							
		10.4										
10	.6		174.9	3.148	.593							
		8.5										
0												
	JANUARY	FEBRUARY	MARCH	APRIL	MAY	JUNE	JULY	AUGUST	SEPTEMBER	OCTOBER	NOVEMBER	DECEMBER

and $\phi_0 = -\frac{\phi}{B}$ as before.

Then δ_0 is a function of X only, whose value corresponding to given values of X may be computed easily, and which may be plotted for convenient computation as in Graphs 33 and 34.

A convenient relation between Jacobsen's phase plane coordinate $\bar{V} = \frac{1}{p} \frac{dX}{d\tau}$ and the dimensional velocity $\frac{dx}{dt} = v$ may be found by applying the previously developed relation between $\frac{dX}{d\tau}$ and $\frac{dx}{dt}$:

$$\frac{dx}{dt} = \frac{dX}{d\tau} \frac{\sqrt{g \gamma \beta L}}{2\pi} .$$

Solving this for $\frac{dX}{d\tau}$ and substituting this and the value of p into the expression for \bar{V} , one finds

$$\bar{V} = \frac{\sqrt{\gamma}}{2\pi} \frac{2\pi}{\sqrt{g \gamma \beta L}} \frac{dx}{dt}$$

$$V = \frac{v}{\sqrt{g \beta L}}$$

It is seen then, that \bar{V} is proportional to v for any given air spring set-up, since g, β, L are all constant.

and

p.

Then δ is the angle of the cone, and withcorresponding to given values of δ and θ the angle α is

and which may be substituted in equation (1) to give

Equations 53 and 54 are the same as those given by

A convenient method for determining the angle α isplane coordinate $V = \frac{1}{2} \left(\frac{1}{\sin \theta} + \frac{1}{\sin \delta} \right)$ and the distancevelocity $\frac{dV}{dt} = \frac{1}{2} \left(\frac{1}{\sin^2 \theta} + \frac{1}{\sin^2 \delta} \right) \frac{d\theta}{dt}$ and the distancedeveloped relation between θ and δ is

$$\frac{d\theta}{dt} = \frac{d\delta}{dt} \frac{d\theta}{d\delta}$$

Solving this for $\frac{d\theta}{d\delta}$ and substituting in equation 54value of p into the expression for V gives

$$V = \frac{1}{2} \left(\frac{1}{\sin \theta} + \frac{1}{\sin \delta} \right)$$

EQUATION 55

$$\frac{dV}{d\delta} = \frac{1}{2} \left(\frac{1}{\sin^2 \theta} + \frac{1}{\sin^2 \delta} \right) \frac{d\theta}{d\delta}$$

It is seen then that V is a function of δ and θ andgiven any other relation between θ and δ the value of V is

The known function $\phi(v)$ may now be treated as a function of \bar{v} · (a constant) = v . Since ϕ may now be found corresponding to any given value of \bar{v} , the value of $\phi_0 = -\frac{\phi}{B}$ may be computed without difficulty, since B is constant for a given air spring set-up.

Now, Jacobsen's method may be applied to the experimental air spring in the following steps:

1. Calculate $B = AP_0 + W$ and $\sqrt{g \beta L}$
2. Assume a range of \bar{v} for first phase plane step. Find the mean value of $v = \bar{v} \sqrt{g \beta L}$ in this interval.
3. Read a mean value of ϕ from the friction curve, Graph 25. Calculate the corresponding value of $\phi_0 = -\frac{\phi}{B}$.
4. Estimate the range of X-values covered in the first phase plane step. Read a mean value of δ_0 corresponding to this range from Graph 33 or Graph 34.
5. Calculate $\delta = \delta_0 + \phi_0$.
6. Draw the first portion of the phase plane trajectory as a circular arc with center at $Q_0 (-\delta, 0)$ and starting at the point representing the initial conditions.
7. If the estimated range of X-values of step 4

The known function $\phi(v)$ may now be substituted in the function of \bar{V} (a constant) = v . Since ϕ may now be found corresponding to any given value of \bar{V} , the value of $\phi_0 = \frac{\phi}{\bar{V}}$ may be estimated without difficulty, since \bar{V} is constant for a given air column section.

Now, Jacobson's method may be applied to the experimental air spring in the following steps:

1. Calculate $\bar{V} = \bar{V}_0 + \sqrt{\frac{g}{\rho} L}$ and $\sqrt{\frac{g}{\rho} L}$.
2. Assume a range of \bar{V} for this phase plane map.
3. Find the mean value of $\bar{V} = \bar{V}_0$ in this interval.
4. Find a mean value of ϕ from the relation curve, Graph 25. Calculate the corresponding value of $\phi_0 = \frac{\phi}{\bar{V}}$.

4. Estimate the range of \bar{V} -values to be used in the first phase plane map. Find a mean value of \bar{V}_0 corresponding to this range from Graph 25 on Graph 25.

5. Calculate $\bar{V} = \bar{V}_0 + \sqrt{\frac{g}{\rho} L}$ and $\sqrt{\frac{g}{\rho} L}$.
6. Draw the first portion of the phase plane trajectory as a diagonal line with center at \bar{V}_0 (1-6, 2) and starting at the point representing the initial conditions.

7. If the estimated range of \bar{V} -values of step 4

is found to be in error appreciably, repeat steps 4 through 7 until results are satisfactory.

8. Repeat steps 2 to 7 for each subsequent step in the phase plane.

The value of acceleration $\frac{d^2x}{d\gamma^2}$ may be computed for any point on the phase plane trajectory by substitution of the phase plane coordinates in the original differential equation. For comparison with experimental data, however, it is more convenient to compute $\frac{1}{\beta} \frac{a}{g}$ instead of $\frac{d^2x}{d\gamma^2}$. Since it has been shown that $\frac{1}{\beta} \frac{a}{g} = \frac{\gamma}{4\pi^2} \frac{d^2x}{d\gamma^2}$,

the following equation applies:

$$\begin{aligned} \frac{1}{\beta} \frac{a}{g} &= \left[1 - (1 - x)^{-\gamma} \right] + \frac{\phi}{B} \\ &= \frac{E(x)}{B} + \frac{\phi}{B} \end{aligned}$$

The function $\frac{E(x)}{B}$ is plotted in Graphs 3, 4 and 5, and ϕ is plotted in Graph 25, so that computation of $\frac{1}{\beta} \frac{a}{g}$ becomes a simple matter.

It has been shown that for a step in the construction (for which δ is constant), the relation between the angle $\Delta\Theta$ subtended by the circular arc of the phase

is found to be in error...
 2. The value of α is found to be...
 in the phase plane.

The value of α is found to be...
 for any point on the phase plane...
 of the phase plane...
 equation. For comparison with...
 it is more convenient to use the...

the following equation holds:

$$\frac{1}{p} = \frac{1}{q} - \frac{1}{r}$$

The function $\frac{1}{p}$ is plotted in Graph 2, showing a single maximum...
 It has been shown that the function $\frac{1}{p}$ is plotted in Graph 2, showing a single maximum...
 for which α is constant, the value of α is found to be...
 angle α is constant, the value of α is found to be...

plane trajectory and the time increment for a phase point to traverse this arc is

$$\Delta T = \frac{\Delta \theta}{p}.$$

Here $p = \frac{2\pi}{\sqrt{g}}$ and $\gamma = 1.40$. In the actual construction $\Delta \theta$ is measured in degrees, whereas the above formula requires the value of $\Delta \theta$ in radians. Hence

$$\begin{aligned}\Delta T &= \frac{\sqrt{1.4}}{2\pi} \cdot \frac{\pi}{180} \quad (\Delta \theta \text{ in degrees}) \\ &= \frac{1}{340} \quad (\Delta \theta \text{ in degrees}).\end{aligned}$$

This formula may now be used to calculate time intervals between adjacent phase plane points.

As an illustration of the procedures outlined above, consider the application of Jacobsen's method to the air spring with $X_0 = -1.3$, $\beta = 9.04$, $L = 4.0$ in., $W = 7.40$ lb. (See Graph 35, and Table VI.) The steps outlined above are now followed.

$$1. \quad B = \beta W = (9.04)(7.40) = 66.9$$

$$\sqrt{g\beta L} = \sqrt{(386 \text{ in/sec}^2)(9.04)(4.0 \text{ in})} = 118 \text{ in/sec.}$$

where $\Delta\theta$ is the change in phase angle and ΔT is the time interval for a phase angle to traverse this arc.

$$\Delta T = \frac{\Delta\theta}{\omega}$$

Here $\omega = \frac{2\pi}{T}$ and $\Delta\theta = 1.57$ rad. In the general case, $\Delta\theta$ is measured in degrees, whereas the above formula requires the value of $\Delta\theta$ in radians. Hence

$$\Delta T = \frac{\Delta\theta}{\omega} = \frac{\Delta\theta}{2\pi} \cdot \frac{2\pi}{T} = \frac{\Delta\theta}{100} \cdot \frac{1}{T}$$

$$\Delta T = \frac{1}{3.6} \cdot \Delta\theta \quad (\Delta\theta \text{ in degrees})$$

This formula may now be used to calculate the interval between adjacent phase points.

As an illustration of the procedure outlined above,

consider the amplification of Jackson's method to the case

starting with $X_0 = -1.5$, $\theta = 0.04$, $L = 0.0$ in.

W. 7.40 in. (see Graph 35, and Table VI). The steps

outlined above are now followed.

$$1. \quad \theta = \theta_0 = (0.04) (7.40) = 0.296$$

$$2. \quad \theta = \theta_0 + \Delta\theta = (0.296) + (0.296) = 0.592$$

2. Assume $\bar{v}_{AV} = 0.2$. Then $v_{AV} = 118 (.2) = 23.6$

3. For this v_{AV} , read $\phi = -4.5$ from Graph 25.

$$\phi_o = \frac{-\phi}{B} = \frac{4.5}{66.9} = .067$$

4. Let X vary from -1.3 to -1.2 . Then $X_{AV} = -1.25$ for which $\delta_o = 0.58$.

$$5. \quad \delta = \delta_o + \phi_o = 0.58 + .07 = 0.65.$$

6. Locate center of circular arc at $X = -.65$ on X -axis. Draw arc $\widehat{P_o P_1}$. For this arc, $\bar{v}_{AV} = .17$.

7. Recalculate $v_{AV} = 118 (.17) = 20.0$,
 $\phi = -4.4$, $\phi_o = .066$, $\delta_o = 0.58$, $\delta = .58$
 $+ .07 = .65$. No change from Step 5. Note that the effect of small changes in v_{AV} on δ is very slight.

8. For Step 2, assume $\bar{v}_{AV} = .41$. Then $v_{AV} =$
 $(118) (.41) = 48.3$, $\phi = -7.5$, $\phi_o = .112$,
 $X_{AV} = -1.15$, $\delta_o = .49$, $\delta = .60$. Locate
 $\delta = .60$ on negative X -axis, draw $\widehat{P_1 P_2}$.

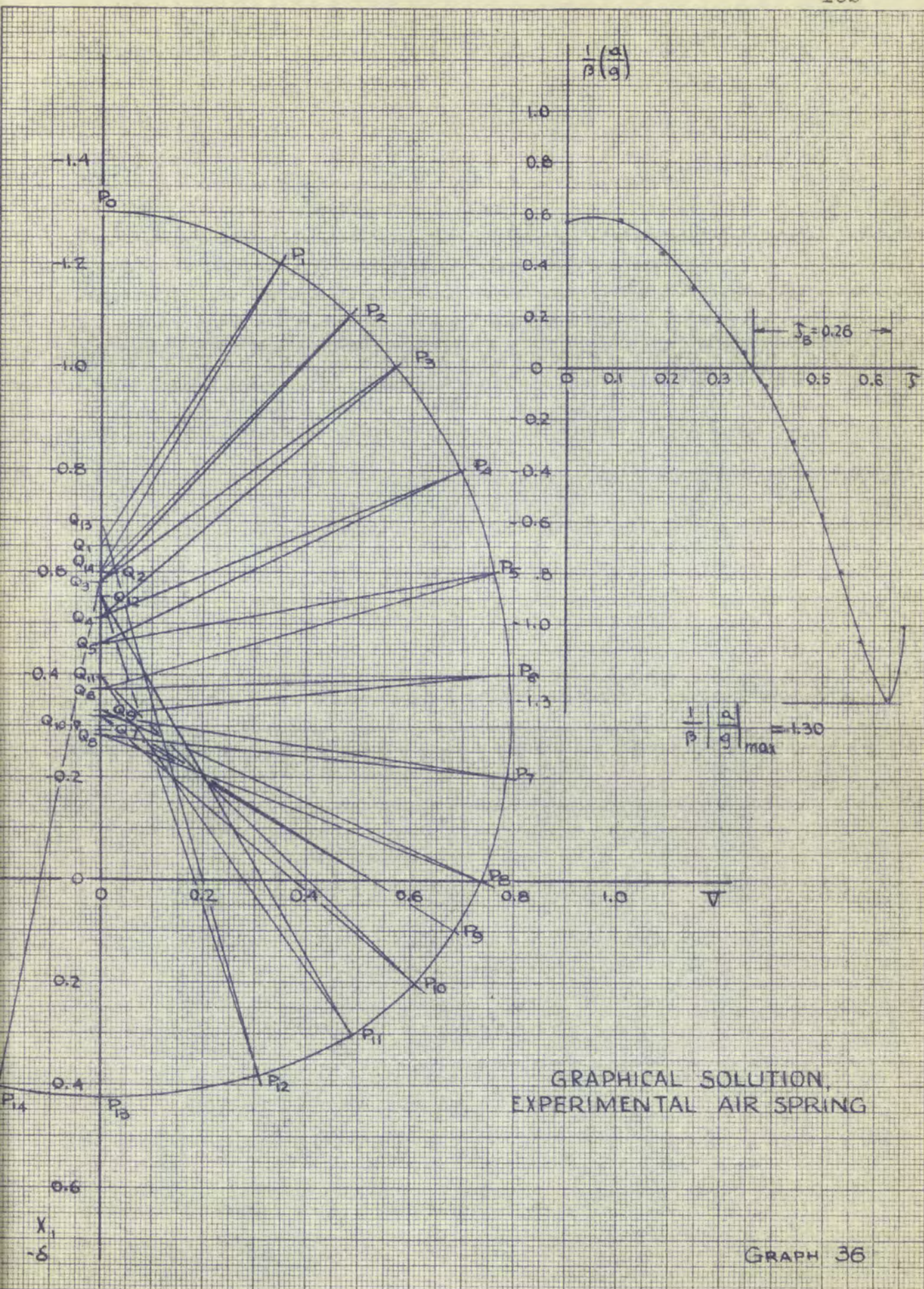
This procedure is then continued as indicated in Table VI.

1. Assumed $V_p = 1.0$	
2. For $V_p = 1.0$	
$\phi = 1.0$	
3. For $V_p = 1.0$	
$\phi = 1.0$	
4. For $V_p = 1.0$	
$\phi = 1.0$	
5. For $V_p = 1.0$	
$\phi = 1.0$	
6. For $V_p = 1.0$	
$\phi = 1.0$	
7. For $V_p = 1.0$	
$\phi = 1.0$	
8. For $V_p = 1.0$	
$\phi = 1.0$	
9. For $V_p = 1.0$	
$\phi = 1.0$	
10. For $V_p = 1.0$	
$\phi = 1.0$	
11. For $V_p = 1.0$	
$\phi = 1.0$	
12. For $V_p = 1.0$	
$\phi = 1.0$	
13. For $V_p = 1.0$	
$\phi = 1.0$	
14. For $V_p = 1.0$	
$\phi = 1.0$	
15. For $V_p = 1.0$	
$\phi = 1.0$	
16. For $V_p = 1.0$	
$\phi = 1.0$	
17. For $V_p = 1.0$	
$\phi = 1.0$	
18. For $V_p = 1.0$	
$\phi = 1.0$	
19. For $V_p = 1.0$	
$\phi = 1.0$	
20. For $V_p = 1.0$	
$\phi = 1.0$	
21. For $V_p = 1.0$	
$\phi = 1.0$	
22. For $V_p = 1.0$	
$\phi = 1.0$	
23. For $V_p = 1.0$	
$\phi = 1.0$	
24. For $V_p = 1.0$	
$\phi = 1.0$	
25. For $V_p = 1.0$	
$\phi = 1.0$	
26. For $V_p = 1.0$	
$\phi = 1.0$	
27. For $V_p = 1.0$	
$\phi = 1.0$	
28. For $V_p = 1.0$	
$\phi = 1.0$	
29. For $V_p = 1.0$	
$\phi = 1.0$	
30. For $V_p = 1.0$	
$\phi = 1.0$	
31. For $V_p = 1.0$	
$\phi = 1.0$	
32. For $V_p = 1.0$	
$\phi = 1.0$	
33. For $V_p = 1.0$	
$\phi = 1.0$	
34. For $V_p = 1.0$	
$\phi = 1.0$	
35. For $V_p = 1.0$	
$\phi = 1.0$	
36. For $V_p = 1.0$	
$\phi = 1.0$	
37. For $V_p = 1.0$	
$\phi = 1.0$	
38. For $V_p = 1.0$	
$\phi = 1.0$	
39. For $V_p = 1.0$	
$\phi = 1.0$	
40. For $V_p = 1.0$	
$\phi = 1.0$	
41. For $V_p = 1.0$	
$\phi = 1.0$	
42. For $V_p = 1.0$	
$\phi = 1.0$	
43. For $V_p = 1.0$	
$\phi = 1.0$	
44. For $V_p = 1.0$	
$\phi = 1.0$	
45. For $V_p = 1.0$	
$\phi = 1.0$	
46. For $V_p = 1.0$	
$\phi = 1.0$	
47. For $V_p = 1.0$	
$\phi = 1.0$	
48. For $V_p = 1.0$	
$\phi = 1.0$	
49. For $V_p = 1.0$	
$\phi = 1.0$	
50. For $V_p = 1.0$	
$\phi = 1.0$	

Table VI

Once the portion of the phase trajectory which yields the required information (i.e. the initial portion for positive \bar{V}) is completed, as in Graph 36, X and \bar{V} coordinates of points on the trajectory may be read off, and the angles subtended by the circular arcs may be measured. Then $\frac{a}{g\beta}$ values and values of τ may be computed by the means outlined in this appendix. The second portion of the tabulated calculations shows this procedure.

Finally, a graph of $\frac{a}{g\beta}$ vs. τ may be constructed, as in the upper right hand corner of the sample construction. From this graph maximum acceleration and build-up time may be read directly.



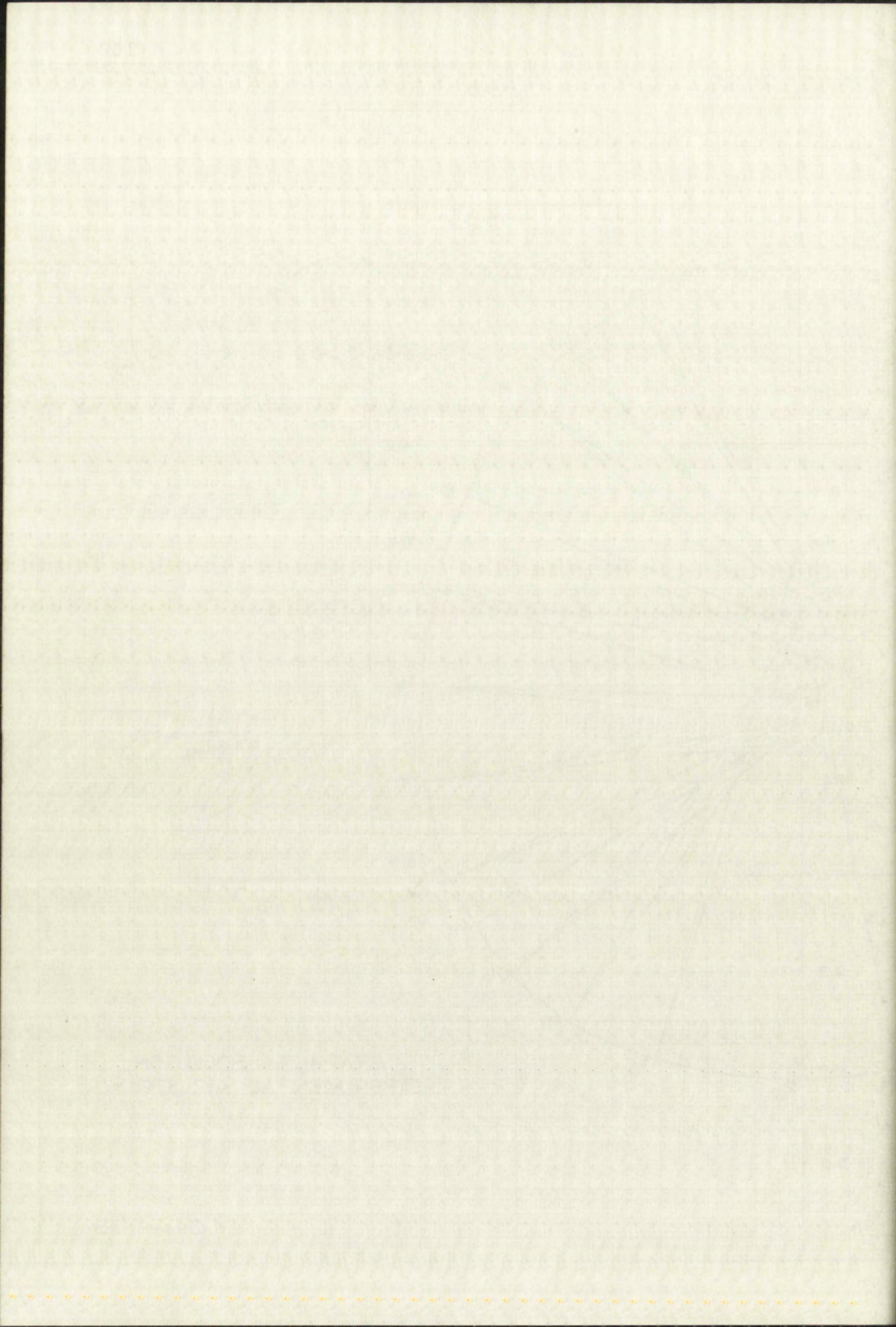


TABLE VI

CALCULATIONS FOR JACOBSEN'S CONSTRUCTION
AS APPLIED TO EXPERIMENTAL AIR SPRING

$$X_0 = -1.3, B = 66.9, \beta = 9.04, L = 4.0, \sqrt{g\beta L} = 118 \text{ in/sec.}$$

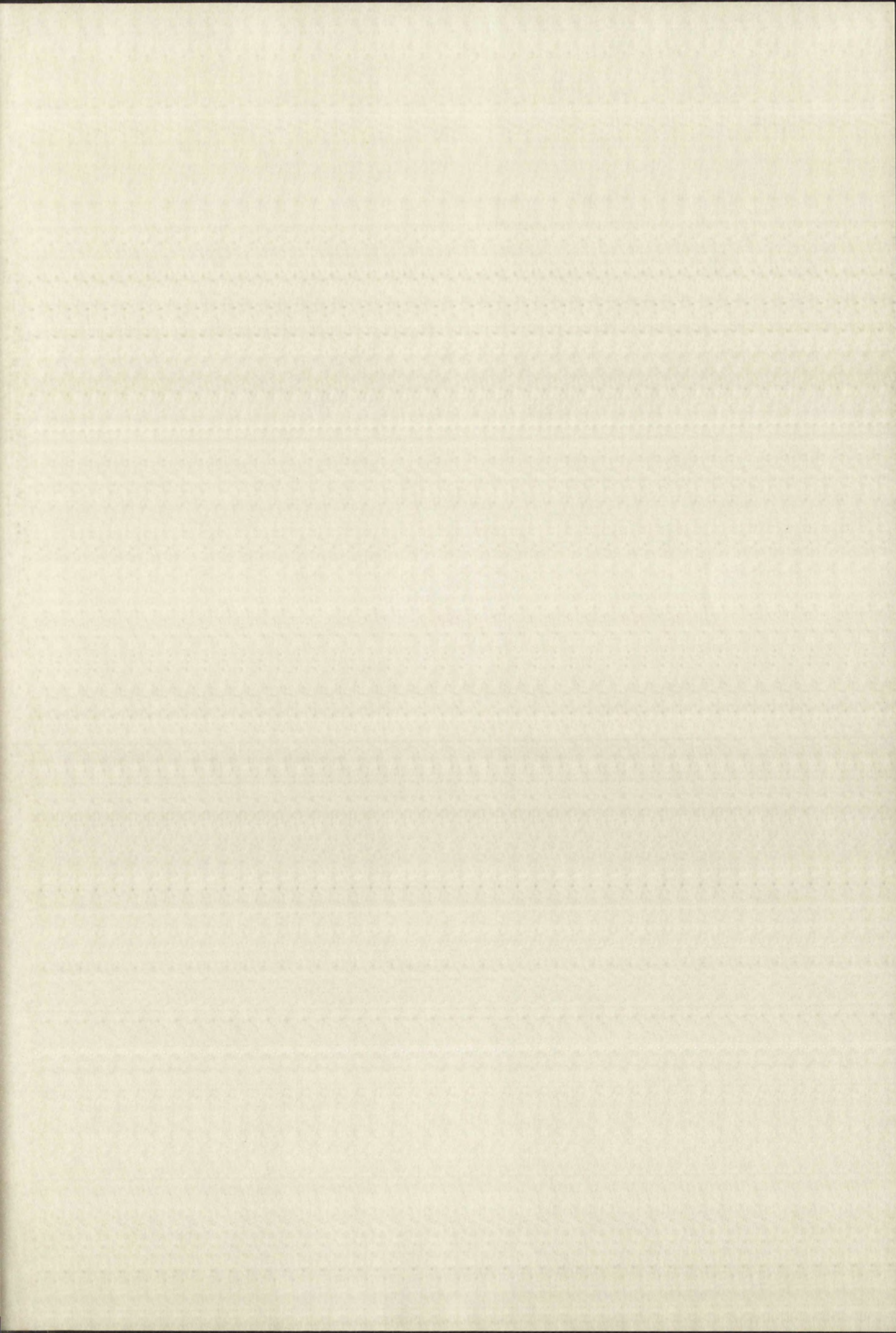
PHASE TRAJECTORY

PT.	\bar{V}_{av}	V_{av}	$-\phi$	ϕ_0	X_{av}	δ_0	δ	$(\Delta\theta)^\circ$	$\Delta\tau$
1	.17	20.0	44	.066	-1.25	.58	.65	32.3	.106
2	.41	48.3	7.5	.112	-1.15	.49	.60	14.0	.046
3	.53	62.5	10.7	.160	-1.05	.42	.58	10.9	.036
4	.61	71.8	13.4	.200	-.9	.31	.51	17.9	.059
5	.73	86	18.8	.280	-.7	.18	.46	15.7	.052
6	.76	90	20.3	.304	-.5	.07	.37	14.6	.048
7	.79	93	21.3	.32	-.3	0	.32	14.5	.047
8	.76	90	20.3	.304	-.1	-.02	.28	15.0	.049
9	.72	85	20.2	.30	.05	.03	.33	8.1	.027
10	.64	75	14.6	.22	.15	.10	.32	9.1	.030
11	.54	64	11.1	.166	.25	.23	.40	10.3	.034

PT.	\bar{V}_{av}	V_{av}	$-\phi$	ϕ_0	X_{av}	δ_0	δ	$(\Delta\theta)^\circ$	ΔT
12	.41	48.3	7.5	.112	.34	.44	.55	11.5	.038
13	.15	18	4.4	.07	.4	.63	.70	16.0	.053
14	-.1	12	-5	-.075	.41	.68	.61	11.1	.037

ACCELERATION-TIME CURVE

PT.	0	1	2	3	4	5	6	7	8	9	10	11	12	13	14
X	-1.3	-1.2	-1.0	-1.0	-.8	-.6	-.4	-.2	0	.1	.2	.3	.38	.42	.4
\bar{V}	0	.35	.48	.57	.69	.76	.79	.78	.74	.68	.61	.49	.31	0	-.20
V	0	41.3	56.7	67.3	81.4	89.7	93.2	92.2	87.3	80.3	72.0	57.8	36.6	0	-23.6
$-\phi$	8.0	6.3	9.2	12.1	17.1	20.1	21.4	21.0	19.3	16.6	13.5	9.4	5.6	8.0	-4.5
$-\frac{\phi}{B}$.12	.09	.14	.18	.26	.30	.32	.31	.29	.25	.20	.14	.08	.12	-.07
$\frac{E(x)}{B}$.69	.67	.65	.62	.55	.48	.38	.24	0	-.16	-.38	-.65	-.98	-1.16	-1.07
$\frac{a}{g\beta}$.57	.58	.51	.44	.30	.18	.06	-.07	-.29	-.41	-.58	-.79	-1.06	-1.28	-1.01
γ	0	.106	.152	.188	.247	.297	.345	.392	.441	.469	.499	.533	.571	.624	.661



IMPORTANT!
Special care should be taken to prevent loss or damage of this volume. If lost or damaged, it must be paid for at the current rate of typing.

Special care should be taken to prevent loss or damage of this volume. If lost or damaged, it must be paid for at the current rate of typing.

Date Due	
DEC 3 1954	
DEC 30 1960	
DEC 21 RECD	
FEB 10 1961	
MAR 30 RECD	
FEB 1 - 1965	
FEB 3 - RECD	
JUL 20 1962	
JUL 9 - 1961	

